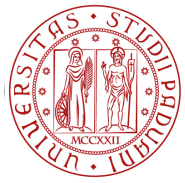

UNIVERSITÀ
DEGLI STUDI
DI PADOVA

Università degli Studi di Padova

Dipartimento di Biologia

SCUOLA DI DOTTORATO DI RICERCA IN : **Bioscienze e Biotecnologie**

INDIRIZZO: **Biochimica e Biofisica**

CICLO: **XXVIII**

Mitochondrial potassium homeostasis and its relevance in pathophysiological contexts

Direttore della Scuola : Ch.mo Prof. Paolo Bernardi

Coordinatore d'indirizzo: Ch.mo Prof. Fabio Di Lisa

Supervisore :Ch.ma Prof.ssa Ildikò Szabò

Dottoranda : Antonella Managò

Table of contents

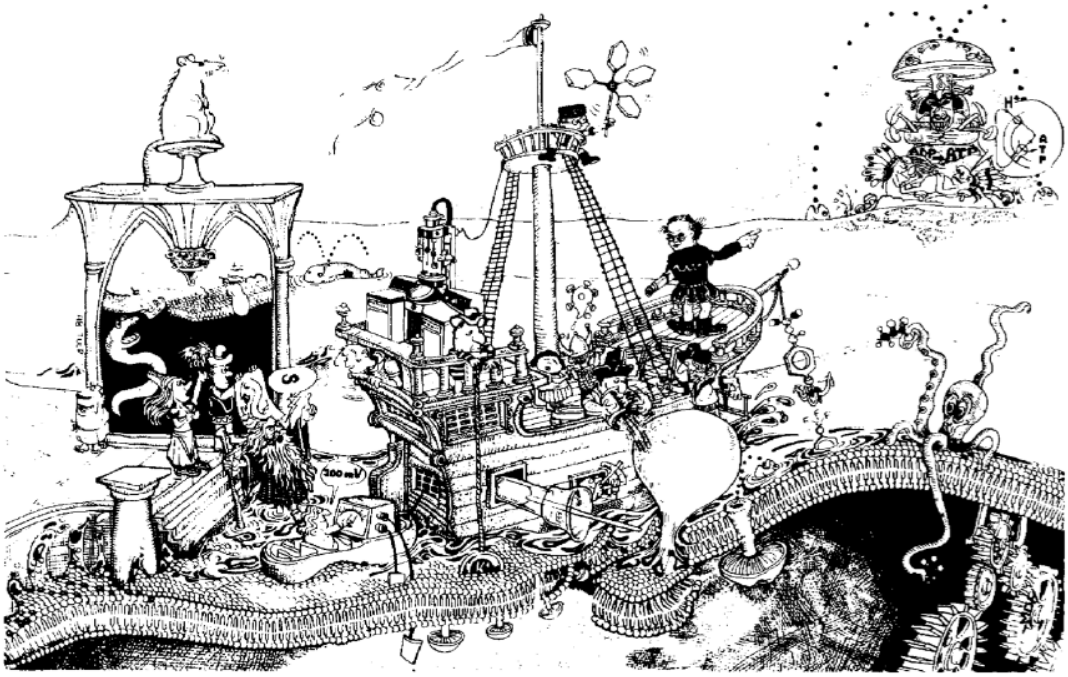

Mitchell sets sail for the Chemiosmotic New World, despite dire warnings that he will be consumed — Abraham Tulp's commentary on researcher Peter Mitchell (from Nicholls & Ferguson, Bioenergetics, Third edition, Elsevier)

Summary

1. Summary
1.1 English version

During my Ph.D., my research focused on the involvement and the role of mitochondrial potassium homeostasis in the context of pathophysiological processes. I have been working on three related projects, for which the common aspect is the study of the mitochondrial potassium homeostasis and its modulation by pharmacological tools. My thesis contains a general introduction, in order to give a general up-to-date overview covering all the topics treated during my Ph.D., followed by a collection of the papers where I gave my contribution.

Concerning the first project, my studies provided new insights into the mechanism of action of an emerging pro-apoptotic, oncologically relevant molecule, namely salinomycin. This molecule was considered a valinomycin-like K^+ ionophore. Its recent identification as a selective inducer of apoptosis in cancer stem cells (CSCs) and different types of non-stem cancer cells, together with the ability to spare healthy cells, led to an increased interest in unravelling its mechanism of action, poorly understood so far. Moreover, since salinomycin has been suggested to act as a K^+ ionophore, it is expected to impact mitochondrial function; however detailed information on its mitochondrial effects were not available from the literature. Therefore, I explored its early effects on mitochondrial bioenergetics. In order to do this, I compared its activity with that of valinomycin (K^+ ionophore) or of nigericin (K^+/H^+ exchanger), for which the action was already well defined by others in the past.
By using different approaches, ranging from classical bioenergetic studies on isolated mitochondria to more innovative measurement of bioenergetic parameters on intact cells, and of course by exploiting different cellular biology techniques, it has been concluded that salinomycin mediates K^+/H^+ exchange across the inner mitochondrial membrane, similarly to nigericin. It has been observed that salinomycin was also able to induce cell death of cells lacking some crucial actors of the apoptotic pathway (Bax/Bak-less double-knockout MEF cells). These results were compatible with the idea of direct modulation of mitochondrial function. At this point, the specificity of its action on pathologic B cells isolated from patients with chronic lymphocytic leukemia (CLL) versus B cells from healthy subjects has been investigated. The results indicated that salinomycin, when used above μM concentrations, exerts direct, mitochondrial effects, thus compromising cell survival, even in non-tumoral cells. These results were published in Managò *et al.*, Cell Death and Disease, 2015.

Having acquired the "know-how" to assess mitochondrial bioenergetic functions, I also actively contributed to a project carried out in collaboration with Prof. Erich Gulbins from University of Essen (Germany), where I also spent five months of my Ph.D. A strict collaboration between the lab where I did my Ph.D. and the lab of Prof. Gulbins led to the discovery of a

mitochondrial voltage-gated potassium channel, mtKv1.3 and to the clarification of its important role during apoptosis. Mechanistically, it has been demonstrated that the pro-apoptotic protein Bax directly interacts with and inhibits mtKv1.3, via a toxin-like mechanism. The direct inhibition of mtKv1.3 leads to hyperpolarization, mitochondrial ROS production, opening of the permeability transition pore (PTP), release of cytochrome c and finally to apoptosis. In accordance to this model, direct pharmacological inhibition of mtKv1.3 by using the membrane-permeant Kv1.3 inhibitors Psora-4, PAP-1 and clofazimine leads to cell death in different types of cancer, as demonstrated by our group.

The starting point of my second project was the fact that pyocyanin, a membrane-permeant toxin released by the Gram-negative bacterium *Pseudomonas aeruginosa* shows structural similarity to clofazimine, a membrane-permeant mtKv1.3 inhibitors. *P. aeruginosa* causes lung infections in immunocompromised patients and it is known that pyocyanin induces death of neutrophils, which plays an important role in the host's early acute defence against pulmonary *P. aeruginosa* infections. However the exact mechanism of action of pyocyanin is still unknown therefore we determined whether its effect is related to Kv1.3 expression, given the crucial role of mtKv1.3 in apoptosis and the structural similarity of pyocyanin to mtKv1.3 inhibitors. First of all, it was observed by patch clamp experiments that pyocyanin is able to inhibit Kv1.3 current. At low concentration (up to 10μM), pyocyanin induced cell death preferentially in cells expressing Kv1.3. However, in the literature pyocyanin was mostly used at higher concentrations (50-100 μM), since in the sputum of patients with *P. aeruginosa* infections it might reach such a high concentration. Moreover, data from the literature suggested that pyocyanin might have a mitochondrial action and is able to produce high amounts of reactive oxygen species (ROS). Therefore, it has been investigated how pyocyanin impacts on mitochondrial function on a short time scale when used at high concentration (at 50μM). Again, intact cells or isolated mitochondria were used to assay the effect of this compound. It has been shown that pyocyanin determines an instantaneous production of superoxide anion at mitochondrial sites and a rapid but incomplete dissipation of the mitochondrial membrane potential. Further, it has been observed that pyocyanin can replace the function of complex III, while it does not directly alter the function of complex I. Moreover, it has been shown that ROS production induced by pyocyanin activates the acid sphyngomyelinase, shown to be present in mitochondria. This event in turn leads to the formation of ceramide, induction of apoptosis and release of cytochrome c. Genetic deficiency of acid sphyngomyelinase or scavenging of ROS induced by pyocyanin prevented cell death in neutrophils, meaning that pyocyanin, at high concentrations, induces cell death via mitochondrial reactive oxygen species and mitochondrial acid sphyngomyelinase, independently of the expression of the voltage gated potassium channel Kv1.3. These results were published in Managò *et al.*, Antioxidant and redox signaling, 2015.

During the last period of my Ph.D, I also studied the effect of newly synthesized Psoralen derivatives and clofazimine for the treatment of cancer.

Concerning the first group, they are specific inhibitors of the voltage gated potassium channel Kv1.3; the second one is a molecule already in use in clinic to treat pathologies like leprosy, which also inhibits Kv1.3 current. Due to their lipophilic structure, they are all membrane-permeant, therefore able to reach intracellular membranes, like inner mitochondrial membrane where the voltage gated potassium channel Kv1.3 is also expressed and active. As mentioned above, the specific inhibition of mtKv1.3 triggers cell death. It has previously been demonstrated that Psora-4, PAP-1 (Psoralen derivatives) and clofazimine are able to specifically induce apoptosis in cancer cells *in vitro* on many cancer cell lines, *ex vivo* on B-CLL (chronic lymphocytic leukaemia) cells obtained from patients and *in vivo* on melanoma tumour model. Following these promising results, in collaboration with Professor Cristina Paradisi (Department of Chemical Sciences, University of Padova), PAP-1 and clofazimine derivatives have been synthesized in order to make these molecules more soluble and mitochondriotropic (i.e.: increased tendency to target mtKv1.3).
I tested the ability of these new compounds to induce cell death in cancer cells first *in vitro*. Since the results obtained on different cell lines *in vitro* were promising and death was strictly dependent on Kv1.3 expression, it has been decided to test these compounds also *in vivo* on a melanoma model and on a pancreatic cancer model. During my 2-month stay at the end of the first year of my Ph.D. at the Institute for Experimental Cancer Research, University of Kiel (Germany), I performed *in vivo* experiments, using PAP-1 derivatives and clofazimine on SCID mouse injected with Colo357, a human pancreas tumour Kv1.3 expressing cell line, obtaining a significant reduction of the mass of the tumour (Zaccagnino, Managò *et al.*, under submission to Oncotarget). Moreover, PAP-1 derivatives have been tested on a melanoma model *in vivo*, obtaining relevant results (Leanza, Romio, Becker, Azzolini, Trentin, Managò *et al.*, manuscript in preparation, not included in the present thesis). The treatment exerted an effect on cancer, without significant side effects on healthy tissues.
Some of the most promising clofazimine-derivatives have been selected to be tested on cells deriving from acute myeloid leukaemia (AML) patient. I carried out these experiments during my stay in Germany at the Department of Molecular Biology University of Duisburg-Essen. Blood samples came directly from the haematology ward of the university-hospital in Essen. So far, we obtained preliminary results which are however controversial, since different patients were diagnosed at different stage of the disease (i.e. have different levels of pathological cells) and AML itself is a heterogeneous disease at the molecular and cytogenetic level. Therefore this work has not been included in the thesis.

Furthermore, I took part in a project of the laboratory of Prof. Holger Kalthoff (University of Kiel, Germany), concerning the study of the mechanism of action of a seaweed extract, for which I performed the experiments of bioenergetics (Geisen , Zenthoefer , Peipp , Kerber , Plenge , Managò *et al.*, Marine drugs, 2015).

Beside the laboratory-based projects, I also contributed to the preparation of two reviews, one concerning intracellular ion channels and cancer (Leanza, Biasutto, Managò *et al.*, Frontiers on Physiology, 2013) and the other regarding *in vivo* pharmacological targeting of ion channels as possible therapeutic tool against cancer (Leanza, Managò *et al.*, BBA Mol. Cell Research, 2015).

1.2 Italian version

Durante il mio dottorato, la mia ricerca si è concentrata sul coinvolgimento e il ruolo dell'omeostasi mitocondriale di potassio (K^+) in processi fisiopatologici. Ho lavorato su tre progetti correlati, per cui l'aspetto comune è lo studio dell'omeostasi del potassio mitocondriale e la sua modulazione tramite strumenti farmacologici. La mia tesi contiene un'introduzione generale, al fine di dare una descrizione generale aggiornata di tutti gli argomenti trattati durante il mio dottorato di ricerca, seguiti da una raccolta di pubblicazioni scientifiche in cui ho dato il mio contributo.

Per quanto riguarda il primo progetto, i miei studi hanno fornito nuove informazioni sul meccanismo d'azione di una molecola pro-apoptotica emergente, rilevante dal punto di vista oncologico, nota come salinomicina. Questa molecola è stata considerata uno ionoforo di K^+ simile alla valinomicina. La sua recente identificazione come induttore selettivo di apoptosi in cellule staminali tumorali (CSCs) e diversi tipi di cellule tumorali non-staminali, insieme alla sua capacità di risparmiare le cellule sane, ha portato a un interesse crescente verso la comprensione del suo meccanismo d'azione, poco noto finora. Inoltre, poiché è stato suggerito che la salinomicina agisca come uno ionoforo di K^+, ci si aspetta un suo effetto sulla funzione mitocondriale. Tuttavia non erano disponibili in letteratura informazioni dettagliate sugli effetti mitocondriali di questa molecola. Pertanto, ho esplorato i suoi effetti istantanei sulla bioenergetica mitocondriale. Per fare questo, ho confrontato la sua attività con quella della valinomicina (ionoforo di K^+) e della nigericina (scambiatore K^+/H^+), l'azione delle quali era già stata ben definita da altri in passato.
Utilizzando diversi approcci, che vanno dagli studi bioenergetici classici su mitocondri isolati alla misurazione di parametri bioenergetici con strumenti più innovativi su cellule intatte, e, naturalmente, sfruttando diverse tecniche di biologia cellulare, si è concluso che la salinomicina media lo scambio K^+/H^+ attraverso la membrana mitocondriale interna , analogamente alla nigericina. Inoltre, è stato visto che la salinomicina è stata in grado di indurre la morte cellulare delle cellule prive di alcuni attori cruciali del processo apoptotico (doppio knock-out di Bax/Bak in cellule MEF). Questi risultati sono compatibili con l'idea di una modulazione diretta della funzione mitocondriale da parte della salinomicina. A questo punto, è stata studiata la specificità della sua azione su cellule B patologiche isolate da pazienti con leucemia linfatica cronica (CLL) *versus* cellule B di soggetti sani. I risultati hanno indicato che la salinomicina, quando usata sopra concentrazioni mM, esercita effetti mitocondriali diretti, compromettendo così la sopravvivenza delle cellule, anche di quelle non tumorali. Questi risultati sono stati pubblicati in Managò *et al*., *Cell Death and Disease*, 2015.

Avendo acquisito il "know-how" per valutare le funzioni bioenergetiche mitocondriali, ho anche contribuito attivamente a un progetto realizzato in collaborazione con il Prof. Erich Gulbins dell'Università di Essen (Germania),

dove ho anche trascorso cinque mesi del mio dottorato di ricerca. Una stretta collaborazione tra il laboratorio dove ho fatto il mio dottorato di ricerca e il laboratorio del Prof. Gulbins ha portato alla scoperta di un canale del potassio voltaggio-dipendente mitocondriale, mtKv1.3 e al chiarimento del suo importante ruolo durante l'apoptosi. Meccanicisticamente, è stato dimostrato che la proteina pro-apoptotica Bax interagisce direttamente con mtKv1.3 e lo inibisce, tramite un meccanismo simile a quello di alcune tossine. L'inibizione diretta di mtKv1.3 porta ad iperpolarizzazione, produzione di ROS a livello mitocondriale, apertura del poro di transizione di permeabilità (PTP), rilascio di citocromo c ed infine all'apoptosi. Secondo questo modello, l'inibizione farmacologica diretta di mtKv1.3 utilizzando inibitori di Kv1.3 permeanti la membrana come Psora-4, PAP-1 e clofazimina, porta alla morte cellulare in diversi tipi di cancro, come dimostrato dal nostro gruppo.

Il punto di partenza del mio secondo progetto è stato l'evidenza che la piocianina, una tossina permeante la membrana rilasciata dal batterio Gram-negativo *Pseudomonas aeruginosa* mostra somiglianza strutturale alla clofazimina, un inibitore di Kv1.3 permeante la membrana. *P. aeruginosa* provoca infezioni polmonari nei pazienti immunocompromessi ed è noto che la piocianina induce morte cellulare nei neutrofili, che svolgono un ruolo importante nella difesa precoce acuta dell'ospite contro infezioni polmonari da *P. aeruginosa*. Tuttavia l'esatto meccanismo d'azione della piocianina è ancora sconosciuta quindi abbiamo voluto studiare se il suo effetto è legato all'espressione di Kv1.3, dato il ruolo cruciale di mtKv1.3 nell'apoptosi e l'affinità strutturale della piocianina agli inibitori di Kv1.3. Prima di tutto, è stato osservato dagli esperimenti di patch-clamp che la piocianina è in grado di inibire la corrente di Kv1.3. A basse concentrazioni (fino a 10 μM), la piocianina induce morte cellulare preferenzialmente in cellule esprimenti Kv1.3. Tuttavia, in letteratura la piocianina è stata utilizzata principalmente a concentrazioni più elevate (50-100 μM), poiché nell'espettorato di pazienti con infezioni da *P. aeruginosa* potrebbe raggiungere tale concentrazioni. Inoltre, diversi dati in letteratura hanno suggerito che la piocianina potrebbe avere un'azione mitocondriale ed è in grado di produrre elevate quantità di specie reattive dell'ossigeno (ROS). Pertanto, è stato esaminato l'impatto della piocianina sulla funzione mitocondriale con cinetiche brevi, quando usata ad alta concentrazione (50 μM). Ancora una volta, cellule intatte o mitocondri isolati sono stati usati per saggiare l'effetto di questo composto. E 'stato osservato che la piocianina determina una produzione istantanea di anione superossido a livello di siti mitocondriali e una dissipazione rapida ma incompleta del potenziale di membrana mitocondriale. Inoltre, è stato visto che la piocianina può sostituire la funzione del complesso III, mentre non altera direttamente la funzione del complesso I. Infine, è stato dimostrato che la produzione di ROS indotta dalla piocianina attiva la sfingomielinasi acida, presente anche in mitocondri. Questo evento a sua volta porta alla formazione di ceramide, induzione di apoptosi e rilascio del citocromo c. La mancanza di espressione della sfingomielinasi acida o lo *scavenging* di ROS indotta dalla piocianina impedisce la morte cellulare in neutrofili, che indicando che la piocianina, ad alte concentrazioni, induce la morte cellulare attraverso specie reattive dell'ossigeno mitocondriali e

sfingomielinasi acida mitocondriale, indipendentemente dall'espressione del canale del potassio voltaggio dipendente Kv1.3. Questi risultati sono stati pubblicati in Managò *et al*., *Antioxidant and redox signaling*, 2015.

Durante l'ultimo periodo del mio dottorato di ricerca, ho anche studiato l'effetto di alcuni derivati di psoraleni di nuova sintesi e della clofazimina per il trattamento del cancro. Per quanto riguarda il primo gruppo, essi sono inibitori specifici del canale del potassio voltaggio dipendente Kv1.3; la seconda è una molecola già in uso in clinica per il trattamento di patologie come la lebbra, che agisce anche come inibitore della corrente di Kv1.3. Grazie alla loro struttura lipofila, sono tutti permeanti la membrana, quindi in grado di raggiungere le membrane intracellulari, come la membrana mitocondriale interna dove il canale del potassio voltaggio dipendente Kv1.3 è espresso e attivo. Come accennato in precedenza, l'inibizione specifica di mtKv1.3 innesca la morte cellulare. È stato dimostrato che Psora-4, PAP-1 e clofazimina sono in grado di indurre specificamente apoptosi nelle cellule tumorali *in vitro* su molte linee cellulari tumorali, *ex vivo* su cellule B ottenute da pazienti con leucemia linfatica cronica e *in vivo* su modello di melanoma. A seguito di questi risultati promettenti, in collaborazione con la Prof. Cristina Paradisi (Dipartimento di Scienze Chimiche, Università di Padova), sono stati sintetizzati derivati del PAP-1 e della clofazimina in modo da rendere queste molecole più solubili e mitocondriotropiche (i.e.: indirizzate al mitocondrio).
Ho testato prima la capacità di questi nuovi composti di indurre morte cellulare nelle cellule tumorali *in vitro*. Poiché i risultati ottenuti su diverse linee cellulari sono stati promettenti e l'induzione di morte cellulare era strettamente dipendente dalla espressione Kv1.3, si è deciso di testare questi composti anche *in vivo* in un modello di melanoma e di tumore pancreatico. Durante il mio soggiorno di due mesi al termine del primo anno di mio dottorato presso l'Istituto per la ricerca sperimentale sul cancro, Università di Kiel (Germania), ho eseguito esperimenti *in vivo*, usando derivati del PAP-1 e clofazimina su topi SCID iniettati con Colo357, una linea di cellule tumorali umane di pancreas esprimenti Kv1.3, ottenendo una riduzione significativa della massa del tumore (Zaccagnino, Managò *et al*., *under submission* alla rivista *Oncotarget*). Inoltre, i derivati del PAP-1 sono stati testati su un modello *in vivo* di melanoma, dando risultati rilevanti (Leanza, Romio, Becker, Azzolini, Trentin, Managò *et al*., manoscritto in preparazione, non incluso nella presente tesi). Il trattamento ha esercitato un effetto sul tumore, senza rilevanti effetti collaterali sui tessuti sani.
Alcuni dei più promettenti derivati della clofazimina sono stati selezionati per essere testati su cellule derivanti da pazienti con leucemia mieloide acuta (AML). Ho eseguito questi esperimenti durante il mio soggiorno in Germania presso il Dipartimento di Biologia Molecolare dell'Università di Duisburg-Essen. I campioni di sangue provenivano direttamente dal reparto di ematologia della clinica universitaria di Essen. Finora, abbiamo ottenuto risultati preliminari che sono però controversi, poiché i pazienti sono stati diagnosticati a diversi stadi della malattia (cioè hanno livelli differenti di cellule patologiche nel sangue) e poiché la leucemia mieloide acuta è di per sé una malattia eterogenea a livello molecolare e citogenetico. Questi studi non sono stati inclusi nella tesi.

Inoltre, ho partecipato a un progetto del laboratorio del Prof. Holger Kalthoff (Università di Kiel, Germania), riguardante lo studio del meccanismo d'azione di un estratto di alghe marine, per il quale ho eseguito gli esperimenti di bioenergetica (Geisen, Zenthoefer, Peipp, Kerber, Plenge, Managò et al., *Marine drugs*, 2015).
Oltre ai progetti basati sull'attività in laboratorio, ho anche contribuito alla preparazione di due review, una in materia di canali ionici intracellulare in relazione al cancro (Leanza, Biasutto, Managò et al., *Frontiers on Physiology*, 2013) e l'altra riguardante l'utilizzo *in vivo* di canali ionici come bersaglio farmacologico come possibile strumento terapeutico nella cura del cancro (Leanza, Managò *et al*., *BBA Mol Cell. Research*, 2015).

Introduction

2. Introduction

2.1 Mitochondrion

2.1.1 An overview on structure and function

Mitochondria derive from the engulfment of a proteobacterium by a precursor of an eukaryotic cell (Lane & Martin, 2010).
They are the organelles where the cellular energy production takes place, due to their ability to synthetize ATP by respiration. This unique feature represented a driving force in the evolution. However, mitochondria have acquired new functions in order to meet the demands of the cells, therefore evolving mechanisms for a constant dialogue between the organelle and the rest of the cellular systems, in many physiological processes.
As a consequence of their bacterial origin, mitochondria host a circular, double -stranded genome (mtDNA) of 16kb, present in multiple copies in each mitochondrion. This genome contains 37 genes encoding for ribosomal RNAs (2 genes), transfer-RNAs (22 genes) and protein of the core subunits of the respiratory chain complexes (13 genes). The quantity of genetic material has drastically became reduced throughout the evolution and, rapidly, part of it has been transferred to the nucleus.

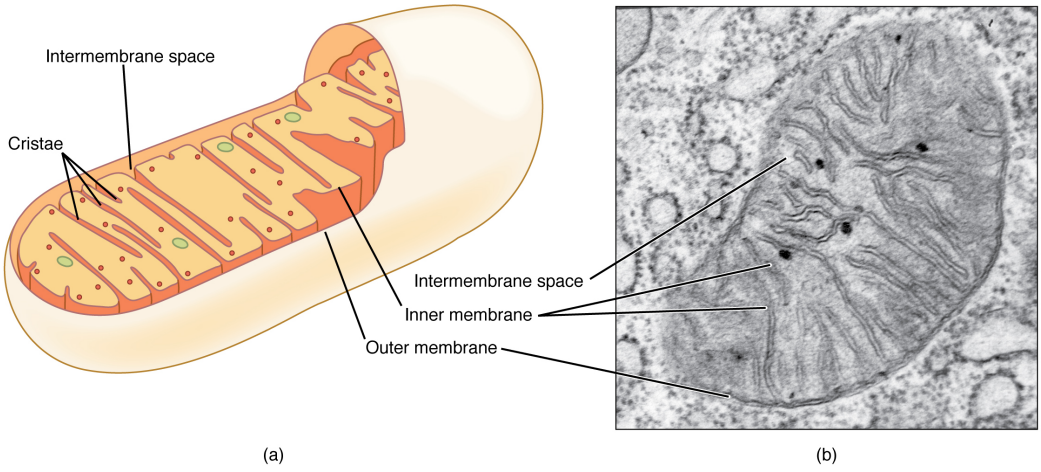

Figure 1: a): Schematic representation of mitochondria structure; **b):** TEM micrograph of a mitochondrion (https://commons.wikimedia.org/wiki/File:0315_Mitochondrion_new.jpg)

Mitochondria comprise over 1000 proteins, encoded by nuclear and mitochondrial genomes. Therefore the ones deriving from mitochondrial genome are translated inside the matrix, where mitochondrial translational machinery is assembled. The nucleus-encoded protein are translated on cytosolic ribosomes and further imported and sorted into mitochondrial sub-compartments by translocase machines present in both the inner and the outer mitochondrial membrane (IMM and OMM). In fact, mitochondria own

an outer mitochondrial membrane and inner mitochondrial membrane separated by the intermembrane space (IMS); inside in the mitochondria, the matrix is encapsulated. At the level of the membranes and in the matrix, the actors of the principal metabolic processes that sustain the survival of the cell and of the entire organism reside (Friedman & Nunnari, 2014).
Here I will first briefly describe the principal functions carried out by mitochondria or in which mitochondria take part, describing in more details only mitochondrial bioenergetics, since it is the object of my PhD work.
Mitochondria regulate several key metabolic processes: some processes entirely occur at the level of these organelles (Krebs cycle, oxidative phosphorylation, β-oxidation) while others find only some components of the pathway residing at the level of mitochondria (e.g.: in gluconeogenesis, glycolysis).

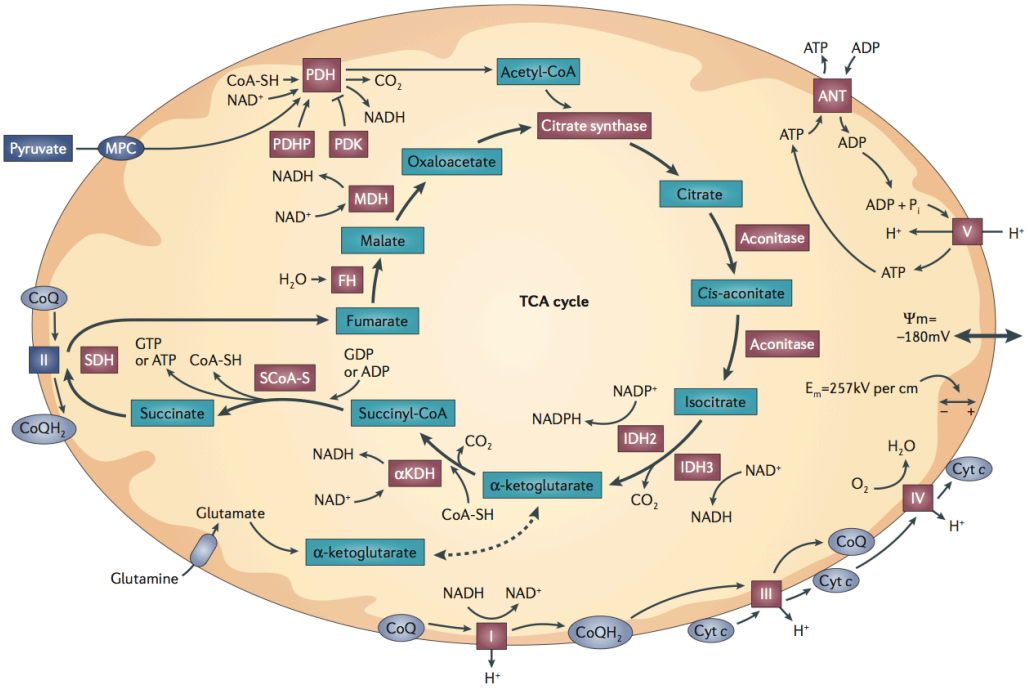

Figure 2: A scheme summarizing mitochondrial bioenergetic functions: Each pyruvate molecule produced by glycolysis is actively transported across the IMM and into the matrix via the mitochondria pyruvate carrier (MPC), where it is oxidized and combined with coenzyme A by pyruvate dehydrogenase (PDH) to form CO_2, acetyl-CoA, and NADH. The acetyl-CoA is the first molecule to enter the tricarbolixyc acid (TCA) cycle. The enzymes of the TCA cycle are located in the mitochondrial matrix, except for succinate dehydrogenase, which is bound to the IMM as part of complex II. During the TCA, acetyl-CoA is oxidized to CO2, through subsequent step; three molecules of NADH and one molecule of FADH2 are generated through the process. The redox energy from NADH and FADH2 is transferred to O2 in several steps via the electron transport along the respiratory complexes (i.e.: complexes I to IV plus ATPase). Complex I, complex III and complex IV perform the transfer, and the incremental release of energy is used to pump protons (H^+) into the IMS. As the proton concentration increases in the IMS, a strong electrochemical gradient is established across the IMM. The protons can return to the matrix through the ATP synthase complex, and their potential energy is used to synthesize ATP from ADP and inorganic phosphate (Pi). The adenine nucleotide transporter (ANT) mediates the exchange of ATP for ADP.

αKDH: α-ketoglutarate dehydrogenase; Em : electrical field within the membrane; FH: fumarate hydratase; IDH: isocitrate dehydrogenase; MDH: malate dehydrogenase; PDHP: pyruvate dehydrogenase phosphatase; PDK: pyruvate dehydrogenase kinase; Pi: inorganic phosphate; SCoA-S: succinyl-CoA synthase; SH: cysteine thiol (from Sabharwal and Schumacker, 2014).

Beside the main contribution given by mitochondria to cellular and organismal metabolism, they fulfil other functions in response to cellular demands. First of all they actively take part of cellular calcium homeostasis and they behave as cytosolic Ca^{2+} buffers. This is principally due to two conditions: first, the membrane potential established at the level of the IMM, negatively charged inside, represent a huge driving force for cation entry; second, mitochondria do posses Ca^{2+} channels and exchangers that allow this passage of charges, among them MCU plays key role in mitochondrial calcium signalling (Rizzuto, De Stefani, Raffaello, & Mammucari, 2012). Moreover, mitochondria take part in and regulate apoptosis, during which the opening of a mitochondria megachannel (i.e. the permability transition pore, PTP, see section 2.3.3) determine the disruption of mitochondrial transmembrane potential and the release of some IMS-located proteins such as cytochrome c (detailed description of apoptosis will be provided in section 2.5). Another important role of mitochondria is that they are a source of reactive oxygen species (ROS); ROS are considered important signalling molecules in many cellular responses (ROS are described in details in section 2.2). Finally they take part in cellular proliferation; this function is linked to mitochondrial ROS production, since ROS are able to regulate the transcription of some genes involved in proliferation, and to regulate production of other modulators of gene expression such as steroid hormones.
Subsequently, I will describe in details mitochondrial bioenergetics, where the term bioenergetics indicates the study of energy transformation in living organisms and systems (Nicholls & Ferguson 2002).

2.1.2 The chemiosmotic theory and the oxidative phosphorylation

The eukaryotic cells produce energy through the oxidative phosphorylation. The chemiosmotic theory, formulated by Mitchell in the 1965 describes the process by which electrons, deriving from the oxidation of organic nutrients, pass through a series of respiratory enzymes (I-IV) embedded in the IMM in a precise order (i.e. the respiratory chain complexes), finally providing the energy for the phosphorylation of ADP, leading to the production of ATP. Electrons derive from reducing equivalents produced during the oxidation phase of nutrients such as glucose or pyruvate, by glycolysis or Krebs cycle respectively, and are transferred by the respiratory chain complexes to the molecular oxygen. The passage of these electrons is coupled to the generation of an electrochemical proton gradient, composed of a membrane potential difference ($\Delta\Psi$) and a cation concentration difference (ΔpH), with the $\Delta\Psi$ representing the predominant component, because the electron transport reactions provide the energy for pumping protons (H^+) from the matrix to the intermembrane space. The electrochemical proton gradient

represents the driving force for H^+ re-entry and this powers the ATP synthase (complex V), which catalyse the synthesis of most cellular ATP (Mitchell, 1961; Mitchell & Moyle, 1967)

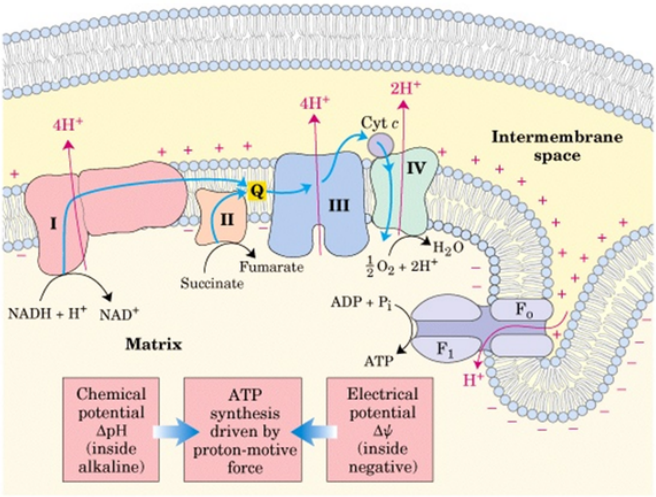

Figure 3: Schematic representation of the oxidative phosphorylation, with principal actors taking part to the process (http://www.notapositiva.com).

2.1.2.1 The respiratory chain complexes

The respiratory chain consists of four complexes (I-IV) and the ATP synthase (V), each composed by multiple subunits, located in the IMM in eukaryotic cells, together with two mobile carriers, i.e. ubiquinone (Q coenzyme, CoQ) and cytochrome c. Further, they form functionally relevant supercomplexes, i.e. structural association of different complexes, as demonstrated upon their isolation (Schägger, 2002). Both nuclear DNA and mitochondrial DNA encode these complexes (70 and 13 genes respectively), except for complex II, which is encoded only by the nuclear genome. Therefore genetic mutation of both genetic materials can lead to devastating pathologies. Since mitochondria must be able to continuously re-adapt their rate of activities in order to satisfy the needs of the entire cell, it is noteworthy to underline the plasticity in the organization of the electron transport chain (Acin-Perez & Enriquez, 2014; Nunnari & Suomalainen, 2012)

2.1.2.1.1 Complex I or NADH:ubiquinone oxidoreductase

The L-shaped complex I constitutes of protein (45 subunits, 7 from mitochondrial DNA) and non-protein components (i.e. coenzymes). Among the non-protein components are Q coenzyme (CoQ, ubiquinone), FMN (flavin mononucleotide), clusters Fe-S and phospholipid, all of which are necessary for the catalytic activity of this complex (Carroll et al., 2006). The reduction of CoQ is inhibited by rotenone. A water-soluble arm and a hydrophobic arm

compose complex I. The structure of the hydrophilic arm of complex I from *Thermus thermophilus* has been resolved and is likely to be very similar to that in mammals. It contains the NADH oxidation site, the primary electron acceptor FMN and a chain of Fe-S centres (Sazanov & Hinchliffe, 2006). Less is known about the hydrophobic arm where the CoQ reduction site is located. This respiratory enzyme catalyses the transfer of two electrons from NADH to ubiquinone, coupling this reaction to the vectorial pumping of four protons from the matrix to the IMM against electrochemical gradient. In detail, the electrons are first transferred to FMN, the non-covalently bound electrons acceptor of complex I. Subsequently, they are processed by the eight Fe-S clusters to reduce the final acceptor ubiquinone, now ubiquinol (QH2). The reaction catalysed by complex I is the following:

$$NADH + H^+ + Q + 4H^+_{matrix} \rightarrow NAD^+ + QH_2 + 4H^+_{IMS}$$

A 3-D high-resolution structure has not been solved for complex I, therefore the mechanism of proton pumping is uncertain. Two main models are suggested in the literature and shared in the scientific community: the coupling between electron transfer and proton translocation can be direct (redox-driven) or indirect (conformation-driven). In the first one (also defined Q-cycle mechanism) the membrane-located Q-binding sites and the proton translocation component are in close contact with the redox centres in the hydrophilic arm, therefore they can directly interact. Contrarily, in the second model the redox centres located on the water-soluble arm are coupled to distal proton-translocating components in the membrane domain, having an effect on them through long-range conformational changes (Holt, Morgan, & Sazanov, 2003). Further, in another model, redox-driven conformational changes can affect directly the Q-binding site, determining the proton pumping (Ohnishi & Salerno, 2005).

2.1.2.1.2 Complex II or succinate:ubiquinone oxidoreductase

Complex II or succinate:ubiquinone oxidoreductase (SQR), is the second entry point for the electrons to the respiratory chain. The resolution of the x-ray structure of the menaquinol fumarate-oxidoreductase (QFR) of *Escherichia coli*, an enzyme structurally and functionally related to SQR, has provided new insights into the function of this enzyme (Cecchini, Schröder, Gunsalus, & Maklashina, 2002). The whole complex is encoded by nuclear genes and it catalyses the oxidation of succinate to fumarate, during which electrons are carried from $FADH_2$ to ubiquinone. Its main component is succinate dehydrogenase (SDH), which is a membrane bound enzyme of the citric acid cycle. Two smaller subunits anchor SDH to the IMM, from the side of the matrix, and they carry cytochrome b_{556} and the Q-binding site. SDH itself shows a flavoprotein subunit and an iron-sulfur protein subunit. Genes encoding for this enzymes are considered housekeeping genes with ubiquitous expression (van den Heuvel & Smeitink, 2001)

2.1.2.1.3 Complex III or decylubiquinol:cytochrome c oxidoreductase

This complex, also called cytochrome *bc1*, catalyses the transfer of electrons from ubiquinol to cytochrome c. The reaction is coupled to the movement of protons from the matrix to the intermembrane space. Eleven components constitute the complex and nuclear DNA, except for the cytochrome b, encodes them all (van den Heuvel & Smeitink, 2001). Atomic models of most protein components of bovine cytochrome *bc1* have been provided (Xia et al., 1997), from which also the dimeric organization of complex III has emerged. Three of the eleven subunits carry a prosthetic group: heme c_1 for cytochrome c_1, heme b_H and b_L for cytochrome *b* and two Fe-S clusters on the Rieske iron-sulfur protein. All these prostetic groups take part to the proton motive Q cycle, which is the overall accepted mechanism underlying the proton pumping from the matrix side to the intermembrane space carried out by complex III.
The proton-motive Q cycle occurs in two steps. In the first step, ubiquinol (QH_2) is oxidized at the Q_0 site in a concerted reaction in which one electron is transferred to the Rieske iron-sulfur protein to form a ubisemiquinone anion ($Q^{\cdot-}$), which immediately reduces the b_L heme. This process deposits two protons on the positive side of the membrane. Later, the electron transferred to the Fe-S protein Rieske, moves to cytochrome c_1 and then to cytochrome c. The second electron from ubiquinol, transferred from the heme b_L to heme b_H. The latter then reduces ubiquinone (Q) to ubisemiquinone anion ($Q^{\cdot-}$) at the Q_i site. At this point only one electron from ubiquinol has been transferred to cytochrome c and only two protons have been deposited on the IMS, while the second electron from ubiquinol resides on the ubisemiquinone anion at the Q_i site. In the second step, a second molecule of ubiquinol is then oxidized by the Fe-S protein, transferring one electron to cytochrome c_1, to reduce a second molecule of cytochrome c. An ubisemiquinone anion is formed again and two more protons on are transferred on the positive side of the membrane. The $Q^{\cdot-}$ reacts as previously, transferring an electron from the heme b_L to heme b_H; the latter then reduces the previously formed ubisemiquinone anion to ubiquinol at the Q_i site, consuming two protons from the negative side of the membrane and completing the Q cycle (Trumpower, 1990; Nelson & Cox, 2006)
The general reaction catalysed by complex III is the following:

$$QH_2 + 2H^+_{\text{matrix}} + 2C_{ox} \rightarrow Q + 4H^+_{\text{IMS}} + 2C_{red}$$

Where C_{ox} and C_{red} indicate cytochrome c oxidized and reduced, respectively. Two inhibitors of complex III are known: antimycin A and myxothiazol. Antimycin A is a secondary metabolite produced by strains of *Streptomyces* bacteria, while myxothiazol is a molecule produced by the myxobacterium *Myxococcus fulvus*. From the crystal structure, the binding sites of these inhibitors have been identified. Antimycin A specifically blocks electron flow from heme b_H to ubiquinone at the Q_i site, while myxothiazol stops the electron flow from ubiquinol to the iron-sulfur center (Xia et al., 1997)

2.1.2.1.4 Complex IV or cytochrome c oxidase

Complex IV (COX) catalyses the last step of the electron transport respiratory chain, transferring electrons from reduced cytochrome c to oxygen, converting molecular oxygen in two molecules of water; simultaneously it moves protons across the IMM, contributing to the generation of the electrochemical gradient that drives the ATP synthesis at the level of complex V.
Complex IV is composed of 13 subunits, of which three are encoded by the mitochondrial DNA and are responsible of the protons transfer and the nuclear DNA encodes the other 10 subunits, for which the role is not completely clear (Grossman & Lomax, 1997; van den Heuvel & Smeitink, 2001). Two copper atoms form a complex with thiol group of some cysteines (Cu_A centre) and, together with two unique hemes, heme*a* and heme*a3*, that together with another cupper ion (Cu_B), they all participate in the electron transport (Nelson & Cox, 2006).
When four electrons are transferred through COX, four protons from the matrix are used to reduce molecular oxygen to water. Further, the energy deriving from the transfer of other four electrons is coupled with the moving of four protons from the matrix to the IMS, thus contributing to the generation of the proton gradient needed to drive ATP synthesis.
The general reaction is the following:

$$4C_{red} + 8H^+_{matrix} + O_2 \rightarrow 4C_{ox} + 4H^+_{IMS} + 2H_20$$

Where C_{ox} and C_{red} indicate cytochrome c oxidized and reduced, respectively. Complex IV is inhibited by cyanide, sulphide and azide; they bind to complex IV inhibiting its function, most likely inhibiting the hemes group.

2.1.2.1.5 Complex V or ATP synthase

Complex V catalyses the addition of one phosphate to a molecule of ADP forming ATP; the energy for this endergonic reaction is provided by the influx of protons from the mitochondrial intermembrane space to the matrix, because energy is conserved during the electron transport as a proton gradient (negative from the matrix side) and therefore provides the energy for ATP synthesis. Complex V also owns the ability to catalyse the reverse reaction, i.e. hydrolyse ATP to ADP and phosphate, linking this process to the opposite movement of protons, i.e. from the matrix to the intermembrane space. The structure of the ATP synthase allows these processes. It shows a feature that is in common with ATP synthases of bacteria and chloroplasts; it consists of two parts: the F_o (160 kDa), which crosses the inner mitochondrial membrane and functions as a proton conduction channel, and the $F_{1,}$ which is located into the matrix and connected to the F_0 by a short stalk; the stalk region is composed of subunits both from F_o and F_1. The passage of protons through the F_0 channel induces long-range conformational changes at the level of the stalk and of the F_1 subunit, allowing the formation of the ATP, which leaves the complex V from the matrix side (Nelson & Cox, 2006). The group of Walker identified in 1994 the crystal structure of bovine

mitochondrial F_1-ATPase, giving new insights in the understanding of the catalytic mechanism (Abrahams, Leslie, Lutter, & John E. Walker, 1994). Five different proteins constitute the F_1-ATPase, with the following stoichiometry: $\alpha_3\beta_3\gamma\delta\varepsilon$. Each β subunit contains the catalytic site for ATP synthesis. Concerning F_o, it results from the assembling of the subunits a,b and c, forming the proton channel, with the following stoichiometry: $ab_2c_{10\text{-}12}$. In the F1 subunit, α and β are organized like orange slices to create a sphere, with γ forming a central axis (see figure 3). The ATP catalysis is carried out by the β subunits. Even if their sequence is identical, they can assume three different conformations: β-ADP, binding ADP and P_i, β-ATP and β-empty. Switching from one conformation to another, they catalyse ATP synthesis. The conformational changes are induced by the passage of protons through the F_o subunit; this passage induces the rotation of the cylinder structure created by the c subunits and of γ subunit. These events determine the conformational changes affecting the β subunits and therefore the switching of the affinity for the substrate. For each complete γ rotation, each β subunit assumes all the possible conformations, leading to the formation of three ATP molecules for each rotational catalytic cycle. According to this model, three or four protons must be driven from the IMS to the matrix to synthesize one ATP molecule (Boyer, 1997).
Recently, the group of Bernardi proposed that dimers mitochondrial ATP synthase form the permeability transition pore, a mega-channel of the IMM whose molecular nature was not defined so far (Giorgio et al., 2013). (see section 2.3.3)

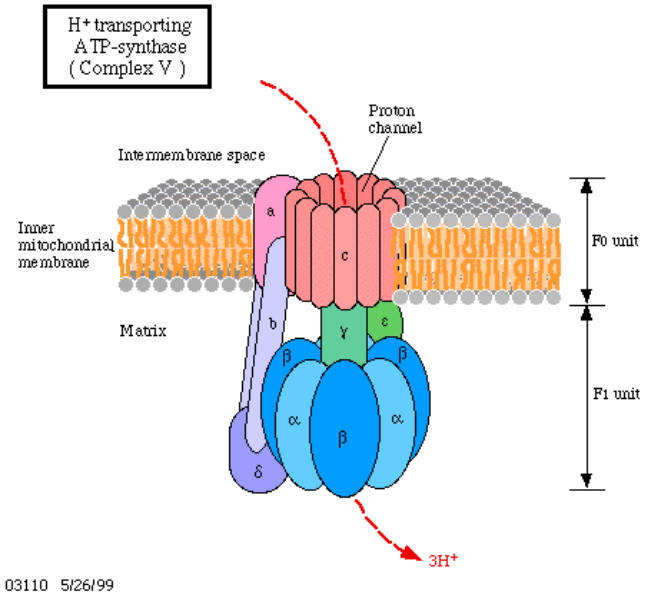

Figure 4: Schematic representation of the F_oF_1 structure of the ATP synthase. See text for a detailed description (http://acebiochemistry.yolasite.com/proton-gradient-and-atp-synthase.php)

2.2 Mitochondrial reactive oxygen species

2.2.1 Definition and roles

The term reactive oxygen species (ROS) includes oxygen free radicals such as superoxide anion ($O_2^{\cdot -}$) and hydroxyl ($^{\cdot}OH$) radicals and non-radical oxidants as hydrogen peroxide (H_2O_2) and singlet oxygen ($^1O_2$). ROS are produced at many sites within the cells (e.g: peroxisomes, endoplasmic reticulum, Golgi, mitochondria, nucleus, the cytosol). In the context of this dissertation, I will take into account only mitochondrial ROS (mROS) production.
Mitochondria are a notable source of ROS. They occur as natural byproducts of mitochondrial metabolism and posses a role in several physiological cellular responses, ranging from regulation of processes controlled by oxygen concentration such as adaptation to hypoxia (Bell et al., 2007), induction of autophagy under starvation (Scherz-Shouval et al., 2007), regulation of immune response to different infectious agents (Arsenijevic et al., 2000; Chaudhri, Clark, Hunt, Cowden, & Ceredig, 1986), differentiation of stem cells (Owusu-Ansah & Banerjee, 2009), aging (Liochev, 2013; Sena & Chandel, 2012) and, finally, control of oxidative stress responses that ensure the maintenance of redox homeostasis (Dröge, 2002). Indeed, redox homeostasis must be strictly regulated, because the presence of ROS becomes detrimental for the cells, over a certain threshold; in these conditions cells undergo a process called "oxidative stress", in which the level of ROS in the cells significantly exceed the "basal" level allowing the normal homeostatic function and in these conditions ROS can react with DNA, proteins and lipids, altering cellular structures and functions. In effect, they are involved in the mitochondrial damage observed in an extended range of pathologies such as cancer (Liou & Storz, 2010), diabetes mellitus (Nishikawa and Araki, 2007), atherosclerosis (Hulsmans, Van Dooren, & Holvoet, 2012), neurodegenerative diseases (Uttara, Singh, Zamboni, & Mahajan, 2009) and ischemia/reperfusion injury (Di Lisa & Bernardi, 2006).

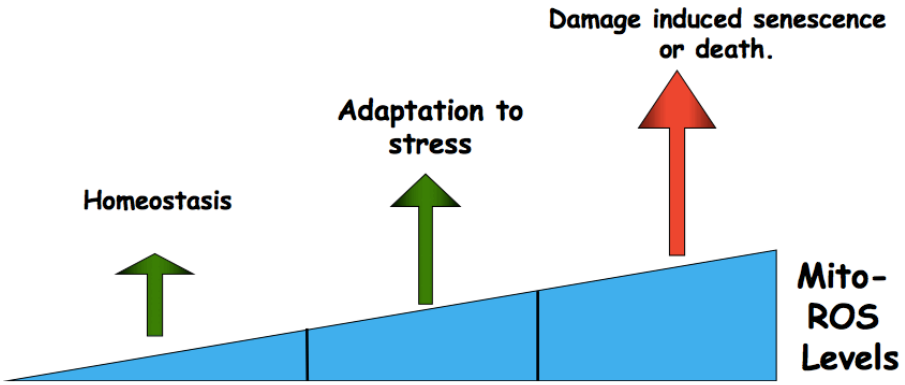

Figure 5: Mitochondria-derived ROS level determines their function in the cells (from Sena & Chandel 2012)

Summarizing, while very high quantities of mROS directly damage proteins, lipids, and nucleic acids, lower levels of ROS are needed for normal cell homeostasis and behave as signalling molecules in adaptation to stress processes. Even lower levels of mROS are required for normal cell homeostasis.
For all these reasons, the cells possess efficient mechanisms designated to balance ROS generation and ROS scavenging and avoid, in this way, oxidative stress.

2.2.2 Mechanisms of redox homeostasis maintenance

Redox homeostasis maintenance is controlled by several mechanisms. Among them, antioxidant enzymes play a major role.

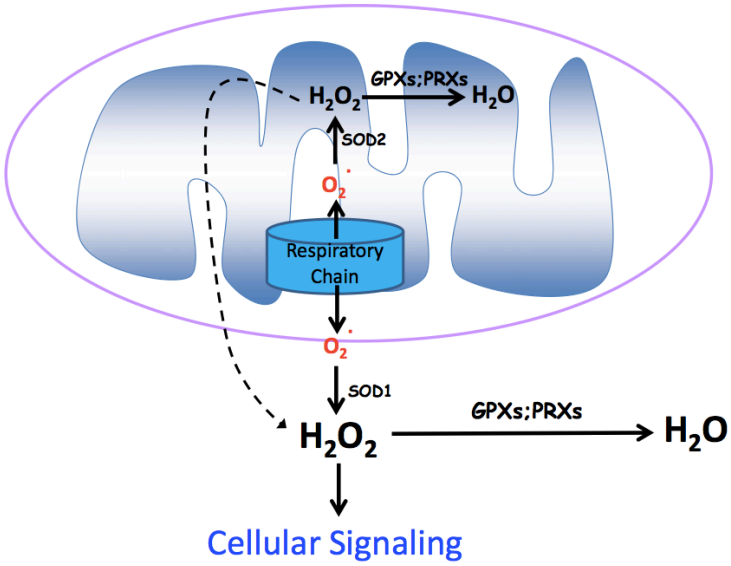

Figure 6: Representative figure depicting the most common mechanisms for superoxide dismutation within mitochondria (from Sena and Chandel 2012).

Superoxide anion is the proximal mitochondrial ROS and the enzymes superoxide dismutase (SODs) convert superoxide anion into hydrogen peroxide. Superoxide can either be emitted into the matrix either into the intermembrane space; the latter, can exit mitochondria through VDAC (voltage-dependent anion channel) present in the OMM. In mammals, the existence of three different isoforms of SOD with different cellular localization was found: the Cu,Zn SOD (SOD1, Fridovich I, 1974) located in the mitochondrial intermembrane space and cytosol; the Mn SOD (SOD2, Weisiger RA and Fridovich I, 1973), located in the mitochondrial matrix and Cu,Zn SOD (ecSOD, SOD3, Marklund SL, 1984) located in the extracellular space. Superoxide anion can also be non-enzymatically converted in the non-radical species singlet oxygen (Steinbeck, Khan, & Karnovsky, 1993). The fate of hydrogen peroxide is to be converted into the highly reactive hydroxyl

radical or, in the best case, in water by the enzymatic reaction catalysed by catalase or glutathione peroxidase (GPX) (Chance, Sies, & Boveris, 1979) or peroxiredoxins (PRX). In mammals there are 6 isoforms of PRXs and 8 of GPXs. Glutathione peroxidase determines the oxidation of glutathione (GSH) to glutathione disulphide (GSSG); glutathione reductase can catalyse the reverse reaction, in a NADPH consuming process. PRXs function reducing H_2O_2, leading to the formation of $2H_2O$, afterwards assuming again it reduced form, oxidizing a reduced thioredoxin molecule.

Beside the above mentioned enzymes with antioxidants activities, also non-enzymatic molecules such as vitamin E, β-caroten, glutathione and vitamin C show antioxidant capacities.

In general, antioxidants have been defined as molecules able to compete with other oxidizable substrates and, thus, to significantly delay or inhibit the oxidation of these substrates, when are present in the cells at relatively low concentrations (Dröge, 2002).

On the other hand, molecules with relatively low specific antioxidant activity, when present at high concentration (molar range), strongly contribute to the overall ROS scavenging and redox homeostasis maintenance. For example, free amino acids, peptides and proteins are among these low-efficiency antioxidants, that need to be present at high concentration within the cells to exert a certain antioxidant effect. All free amino acids are target of ROS; they are present at high concentration within the cells (10^{-1}M), therefore they are important ROS scavengers. In a relatively recent work, it has been demonstrated that the amino acid proline is a potent antioxidant, able to inhibit programmed cell death induced by high level of ROS in a fungal pathogen (Chen & Dickman, 2005). As mentioned above, proteins are damaged by ROS, which can induce oxidative modifications, leading to changes in protein function but also determine an increased susceptibility to proteasome with proteolysis as a consequence (Davies, 1987). This process further contributes to redox homeostasis, leading to the release of free amino acids in the cell. Moreover, redox homeostasis can be achieved by regulating antioxidant mechanisms at a transcriptional level. A major mechanism is the ROS-mediated induction of transcription of antioxidant enzymes. Redox regulation of transcription is an evolutionary conserved strategy in which alterations in intracellular ROS levels induce appreciable alterations in gene expression. The regulation of at least two transcription factors, nuclear factor (NF) KB and activator protein (AP)-1 depends on the intracellular redox state (Sen & Packer, 1996), and more recently p53 also joined this list (H. Liu, 2005). In general, the cellular response to an increase of reactive species involves the robust induction of numerous gene products that function both to inactivate ROS production and to restore homeostasis. Concerning the mechanisms regarding how ROS levels can regulate transcriptional activity, three manners have been identified: direct oxidation and reduction of transcription factors, changes in subcellular localization of the transcription factors and an alteration in ROS levels that can modulate the activity of chromatin-modifying enzymes as a consequence of changes of intracellular redox buffers (H. Liu, 2005).

2.2.3 Mitochondrial ROS production sites

Since mitochondria have been identified as source of ROS, several studies have been conducted to investigate the precise site of ROS production. The first evidence that mitochondrial ROS production is associated with the respiratory chain activity date back to the early '90s (Jensen, 1996). Since then, many details have been addressed and clarified. The two overall accepted main sources of ROS are complex I and complex III, principally producers of superoxide anion.

2.2.3.1 Complex I

Complex I tranfers electrons from NADH to CoQ. According to a recent work, two are the assigned sites for the reduction of O_2 to superoxide at the level of complex I: the NADH and the quinone-binding sites (Hirst, King, & Pryde, 2008). However, the role of the components of complex I involved in superoxide production is still debated. Some consider FMN (flavin mono-nucleotide), while others identified iron-sulfur clusters N1a and N2, or ubisemiquinone as responsible for superoxide generation in complex I (Zorov, Juhaszova, & Sollott, 2014). According to many scientists, the isolated complex produces superoxide from the reaction of O_2 with the fully reduced FMN. The limiting step of the formation of superoxide is the NADH/NAD+ ratio, which set the proportion of the FMN that is fully reduced (Hirst et al., 2008; Kussmaul & Hirst, 2006). Therefore, the processes determining the increase of NADH/NAD^+ ratio, such as respiratory chain damage, ischemia, low ATP demand/low respiration rate, will lead to the increase in O_2^- formation. In contrast, when mitochondria are respiring normally, consuming NADH and NADH/NAD+ ratio is relatively low, only small amounts of superoxide are produced from complex I (Votyakova & Reynolds, 2001). Seo and colleagues demonstrated that oxidative stress in rat and human cell lines was significantly reduced when cells were transfected with a vector expressing the gene of *Saccaromyces cerevisiae* for the NADH dehydrogenase, providing a clear evidence of the fundamental influence of the NADH/NAD^+ ratio in ROS production (Seo, Marella, Yagi, & Matsuno-Yagi, 2006) . However, an interesting work, using submitochondrial particles oxidizing NADH, showed that a significant amount of superoxide production occurred when micromolar concentrations of NADH were used (50 μM), while in a millimolar range, its production was suppressed (Grivennikova & Vinogradov, 2006). In the light of the fact that concentration of NADH in the cells, in physiological condition, reaches few millimolar concentrations (Yamada, Hara, Shibata, Osago, & Tsuchiya, 2006), the contribution of complex I to ROS generation should not be prevalent. Therefore, the contribution of complex I as source of ROS in physiological conditions remain unclear.

Nevertheless, the use of the inhibitor of complex I, rotenone, results in an increased ROS production; it probably diverts electrons onto FMN, blocking the reduction of ubiquinone and leading to production of superoxide. Some evidences attest how, by only the inhibition of complex I by rotenone, is

possible to trigger apoptotic cascade due to a burst in ROS production (Li, 2003). Most experimental data suggest that the complex I-produced superoxide anions are released into the matrix space (Kudin, Debska-vielhaber, & Kunz, 2005).

Among the events triggering superoxide production by mitochondria, there is also the reverse electron transport (RET), even if the site of superoxide production during RET is not known (Lambert & Brand, 2004). RET is a process by which, when ADP is absent and in presence of a significant $\Delta\psi$, electrons deriving from the oxidation of succinate move from $CoQH_2$ toward NAD^+ reducing it to NADH (Y. Liu, Fiskum, & Schubert, 2002). Addition of the uncoupler carbonyl cyanid-*4*-(trifluoromethoxy)phenylhydrazone (FCCP) and ADP to respiring mitochondria can inhibit RET; moreover the pathway of electron transfer from succinate to NAD^+ is inhibited by Antimycin A, meaning that it involves electron carriers up to antimycin A-sensitive site in complex III. Similarly, superoxide production by RET is inhibited by rotenone, confirming that during RET, an electron acceptor plays a role at the level of complex I. Interestingly, the rate of complex I-associated ROS production is higher during RET than during NADH-linked forward electron transport (Lambert & Brand, 2004; Murphy, 2009; Zorov et al., 2014). However, in presence of ATP, when inhibitors of the quinine-binding sites of complex I (e.g. rotenone) were added to mitochondria, leading to changes in the pH, this determined an increase in ROS production rate by forward electron flow higher than the rate observed wit RET at the same pH gradient, meaning that also pH gradient plays a role (Lambert & Brand, 2004).

As underlined above, ROS generation supported by RET is strongly dependent on membrane potential, since treatment of mitochondria with increasing doses of an uncoupler or of ADP progressively decreases ROS production, finally fully blocking it. On the other hand, mitochondria respiring on glutamate-malate are less sensitive to changes of membrane potential (Votyakova & Reynolds, 2001).

Moreover, the effect of mitochondrial potassium channel openers (KCOs) on ROS production has been investigated. When potassium channels of the IMM are activated, there is a huge driving force for potassium to enter mitochondria. Since the resting mitochondrial membrane potential is around 180-200 mV (negative inside), the net flux of potassium ions from the cytosol into the mitochondrial matrix space would lead to a 'mild uncoupling', therefore leading to mitochondrial membrane potential depolarization and consecutive stimulation of the respiration rate. This condition will decrease the $NADH/NAD^+$ ratio, leading to a diminished concentration of $FMNH_2$. This in turn would de- crease the production of reactive oxygen species by respiratory chain complex I. The decrease of mitochondrial membrane potential induced by treatment with KCOs would have the same effect on complex I producing ROS by forward or reverse electron transport, reducing the rate of superoxide production in both cases (Heinen et al., 2007; Kulawiak, Kudin, Szewczyk, & Kunz, 2008).

Summarizing, there are two different complex I-linked ways to produce ROS: when the ratio $NADH/NAD^+$ in the matrix is high, leading to the reduction of FMN site on complex I and the RET-associated superoxide production, occurring when $\Delta\psi$ is high and ADP is low.

It is noteworthy that ROS production at complex I depends on circumstances, that under healthy conditions should not occur. Consequently it seems that complex I becomes a major ROS source under pathological conditions rather than being under resting conditions (Murphy, 2009; Zorov et al., 2014).

2.2.3.2 Complex III

Complex III transfers electrons from the reduced form of CoQ pool to cytochrome c. This processes is carried out through the Q cycle. Complex III-linked superoxide formation is due to the reaction of O_2 with an ubisemiquinone ($Q_{\cdot-}$) bound to the Q_0 site (Murphy, 2009; Turrens et al. 1985; Cadenas et al, 1977). However, under physiological conditions, the probability of persistence of reactive ubisemiquinone at the Q_0 site together with the probability to give an electron to the molecular oxygen is quite low, since its fast oxidation occurs during the Q cycle. But in presence of antimycin A, an inhibitor of the Q_i site, complex III produces a large amount of ROS (Liu et al., 2002). This is apparently due to an increase in the basal level of ubisemiquinone, that in this conditions would accumulate at the Q_0 site (Zorov et al., 2014). Complex III-linked ROS production determines release superoxide towards the IMS (Kudin et al., 2005).

.

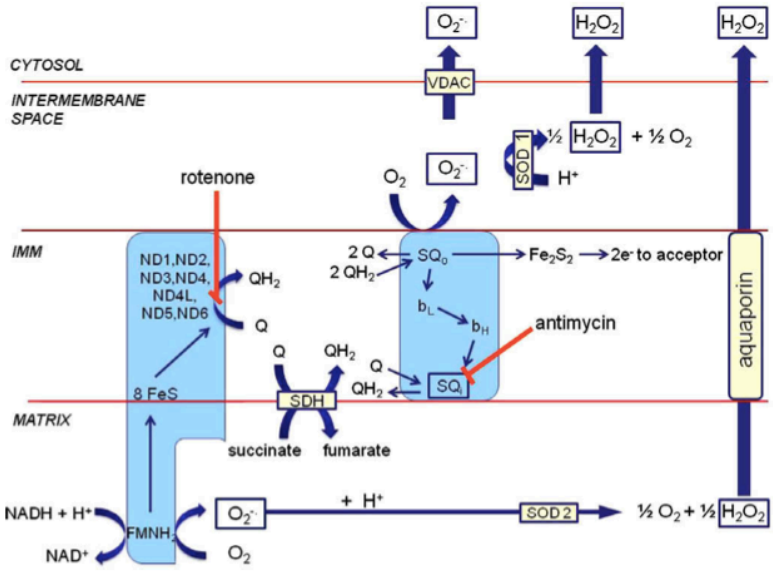

Figure 7: Scheme depicting the sites of ROS production at level of complex I and complex III in mitochondria and the mechanisms of dismutation (from Malinska et al., 2010)

The addition of a Q_0 site inhibitor is able to block the production of superoxide (Ksenzenko, Konstantinov, Khomutov, Tikhonov, & Ruuge, 1983). In particular, addition of two different inhibitors of the Q_0 site, causes slightly different effects: stigmatellin completely abolish superoxide production, while myxothiazol causes only partial reduction and when added alone, can

even induce low ROS production. Indeed it is clear that this two inhibitors bind to different portion (i.e. "proximal" and "distal") of the Q_0 site and this could explain the different effects (Muller, Roberts, Bowman, & Kramer, 2003; Starkov & Fiskum, 2001)
In an elegant work, Rottemberg and colleagues showed how complex III-linked superoxide production strongly depends on changes of mitochondrial membrane potential. The rate of superoxide generation increased exponentially with the hyperpolarization. This suggests that the membrane potential slows down electron transfer from heme b_L to heme b_H thereby promoting a more reduced state of heme b_L which then can react with molecular oxygen increasing superoxide generation (Rottenberg, Covian, & Trumpower, 2009). Contrarily, some other works attested an increasing effect in complex III-linked ROS production upon addition of potassium channel openers, able to determine a depolarization (Malinska, Mirandola, & Kunz, 2010).
Concluding, since complex III-linked ROS formation occurs only upon the addition of a drug (antimycin A) having no analogues in human physiology, it is reasonable to think that complex III contribution to the overall ROS production is reduced compared with that given by complex I during RET.
Many other sites within mitochondria are involved in ROS production (e.g: aconitase, monoaminoxidase, NADPH-oxidase, electron transfer flavoprotein, $p66^{shc}$), but they will not be taken into account in the context of this dissertation given that my works did not involve research in those directions.

2.3 Ion transport within mitochondria

2.3.1 General concepts

In general, any transport process across a membrane bilayer can be classified according to four criteria:

- The transport can be bilayer-mediated or be protein-mediated
- The transport can be passive or directly coupled to metabolism
- The transport can involve a single ion (or metabolite) or can mediate the flux of two or more species that are directly coupled
- The transport can determine net charge transfer across the membrane or be electroneutral

The bilayer-mediated permeability can occur naturally (when ions spontaneously move from one side of the membrane to the other, e.g.: membrane leakage) or can be mediate by ionophores (see below). The bilayer-mediated transport is always passive, while the protein-mediated ones can be directly coupled to a metabolite (very often ATP). A transport process involving one ion is called uniport (e.g. the mitochondrial calcium uniporter –MCU- in the IMM); when the transport process involves the obligatory coupling of two or more ions in parallel, this is called symport; when the transport is coupled to the movement of another species in the opposite direction, this is termed antiport. The movement of ions across a

membrane can be electrical, e.g.: when the transport process creates an electro-chemical gradient (electrogenic transport) or when the movement of ions occurs as a response of a pre-existing potential (electrophoretic transport). Finally, it can also be electroneutral, when no net charge transfer across the membrane occurs, e.g.: when a uniport transports un-charged species or when a symport carries a cation and an anion or an antiporter carries two species of equal charge.
However, membranes are very little permeable to ions, since lipids create a barrier to charged species. On the contrary, uncharged species like molecular oxygen and CO_2 can cross the membranes, and polar compounds like water can pass through the membranes thanks to the existence of acquaporines (Lodish et al., 2006). At the level of mitochondria, the low permeability of the IMM is a necessary prerequisite for the energy conservation (see section 2.3.3).
As already mentioned, ionophores can mediate movement of ions across the membranes. Ionophores are molecules able to delocalize or to shield the charge of an ion, increasing its permeability across the membrane and decreasing the energy activation necessary for this ion to insert into a hydrophobic region. They are able to carry ions through the membranes because they posses a hydrophobic outer component, to allow the passage through the lipid bilayer, and an hydrophilic interior to accommodate the ion. They can function in two manners: as mobile carrier or forming a channel within the membrane. In the first case they show high specificity among different ions, instead of pore forming ionophores, which poorly discriminate the different ionic species.
Channels and transporters are other actors mediating ion transport within mitochondria. A detailed description of ion channels will follow.

2.3.2 Mitochondrial membrane potential, energy conservation and cation distribution in mitochondria

As underlined above, at the level of the IMM an electrochemical gradient is established. The electrochemical gradient ($\Delta\mu$) is constituted by two components: the $\Delta\Psi m$, which is the voltage difference between the two sides of IMM, and the ΔpH, which is the different concentration of the distribution of the ions across the IMM. Under physiological conditions mitochondrial membrane potential is in between 160-200 mv, negative on the matrix side (Szabo & Zoratti, 2014).
Since in the IMM the passive permeability to H^+ (H^+ leak), ions and cations is very low, the pumping of protons by the respiratory chain complexes out from the matrix results in the establishment of a $\Delta\mu_H$; therefore the differential distribution of protons established by the respiratory chain complex activities represents the major component of the $\Delta\mu_H$. As stated by the chemiosmotic theory, this proton gradient is utilized for the ATP synthesis via the ATP synthase. Intrinsically, with this theory, the problem of the energy conservation arose. How mitochondria avoid the dissipation of the hyperpolarization created by the respiratory chain complexes, necessary for energy production? And do mitochondria lack any cation channel or do they posses them? The existence and maintenance of an opposite charge-

distribution at the level of the IMM, negative inside, supposes that mitochondrial cation distribution is regulated somehow (Azzone et al, 1977; Azzone et al., 1977; Bernardi, 1999). For many years, the low permeability of the IMM to monovalent cation has been explained by the absence of channels for them within mitochondria. The evidences that the electrophoretic uptake of K^+ and Na^+ in isolated mitochondria was very slow and that in KCl medium they did not swell, unless the K^+ ionophore valinomycin was added, supported this hypothesis. However, today we know that channels for cations do exist in mitochondria (Sorgato, Keller, & Stühmer, 1987) and that they are strictly regulated to limit energy dissipation.
Concerning energy dissipation and ions homeostasis, let's consider the case of potassium, which is the most abundant ion within the cells, in addition to being object of my studies reported in this thesis.
According to the Nernst equation, the K^+ electrochemical gradient through the membrane is defined as:

$$\Delta\mu_K = zF\Delta\Psi + RT \ln [K^+]_i/[K^+]_o$$

where $\Delta\Psi$ is the membrane potential, F defines the Faraday constant, R the gas constant and T is the absolute temperature. At the level of the mitochondrial membrane, we have that $[K^+]_o$ is extremely concentrated ($\approx$ 150 mM) and the $\Delta\Psi$, as described before, is around 180-200 mV, negative inside. Therefore, there would be a huge driving force for potassium influx; moreover, to reach the equilibrium potential for K^+ ion, $[K^+]_i$ should be very high. Actually, in the steady state K^+ ions are not distributed at electrochemical equilibrium, and even if a K^+ ion leak does exist, some system are designated to regulate mitochondrial K^+ concentration through a continuous equilibrium between K^+ infux and efflux, maintaining the mitochondrial volume homeostasis and sustaining membrane potential (Massari et al., 1972; Bernardi, 1999; Leanza et al., 2015). In physiological condition, K^+ electrochemical gradient would favour continuous K^+ uptake, leading to matrix swelling, rupture of OMM, release of cytochrome c and loss of mitochondrial functions. In order to maintain volume homeostasis, exchange-specific carrier systems that couple the exchange of cations with the re-entry of protons in the matrix do exist (Garlid, 1988; Brierley et al., 1994). It is evident that if these exchangers solved the problem of volume homeostasis and of cation distribution, on the other hand their activity would be responsible for the energy dissipation, because electrophoretic influx of cations followed by their extrusion via an electroneutral exchanger (H^+/K^+ exchanger) would result in a futile cycle dissipating the membrane potential. The high negative electrical membrane potential drives an electrophoretic K^+ influx, excess matrix K^+ is then exported by the electroneutral K^+/H^+ antiporter, i.e. potassium cycle (Garlid & Paucek, 2003; Leanza et al., 2015; Szabò et al, 2012). In order to maintain constant the mitochondrial membrane potential, the respiratory chain complexes must increase their activity, pumping protons from the matrix to the intermembrane space: when $\Delta\Psi$m decreases, ΔpH undergoes an increase, in order to maintain constant $\Delta\mu_H$.

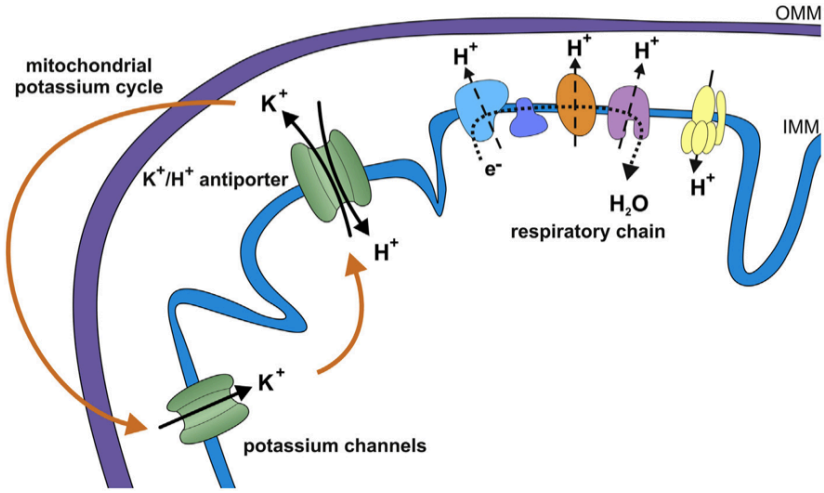

Figure 8: Mitochondrial potassium cycle. Inner mitochondrial membrane is not permeable to potassium ions (K^+), but they can enter mitochondria exclusively through potassium channels, even if a mild K^+ leakage does exist. A K^+/H^+ exchanger exploits the proton electrochemical gradient to extrude K+ ions from the matrix, in order to maintain constant mitochondrial ion homeostasis (from Leanza et al., 2015).

Summarizing, the chemiosmotic hypothesis of the energy conservation requests both the existence of cation-protons exchanger systems, which work at the expense of the energy, and the low permeability of the IMM to Na^+ and K^+, in order to limit the energy dissipation due to the activity of the antiporters.
Despite the low permeability represents a prerequisite for mitochondrial physiology and is central for mitochondrial functions, it is also true that, in precise conditions, mitochondria undergo a reversible permeability transition.

2.3.3 The permeability transition and the permeability transition pore

Following Ca^{2+} accumulation in the mitochondrial matrix, a sudden increase of permeability of the IMM to solutes of molecular mass up to 1,5 kDa occurs in energized mitochondria (Bernardi, 2013), defines as permeability transition (PT). It is inhibited by cyclosporine A (CsA), a cyclic immunosuppressant peptide (Broekemeier, Dempsey, & Pfeiffer, 1989). As a consequence of the PT, the mitochondrial electrochemical gradient dissipates, ATP synthesis stops, and substrates of different nature are lost from the mitochondrial matrix. Nowadays we know that PT is due to the reversible opening in the inner mitochondrial membrane of the permeability transition pore (PTP), but the physiological role of PT remains an outstanding question. If PTP opening is widespread and sustained, it causes cell death. Some features characterize the PTP, e.g.: a requirement for the presence of Ca^{2+} in the matrix, its inhibition induced by matrix pH acidification, the voltage dependence (i.e. the PTP opens upon depolarization if the mitochondria have been loaded with Ca^{2+} or other treatments) and

redox sensitivity (i.e. oxidative stress favours the PTP opening). Moreover, the pore is non-selective or at least poorly selective (Szabo & Zoratti, 2014).
Until a few years ago the molecular composition of the PTP comprised the participation of OMM and IMM proteins, such as: the adenine nucleotide translocator (ANT), the voltage-dependent anion channel (VDAC) of the OMM, the mitochondrial benzodiazepine receptor (TSPO), creatine kinase and cyclophilin D (CypD), a matrix peptidyl-prolyl cis,trans-isomerase (PPIase) (Beutner, Rück, Riede, & Brdiczka, 1998; Zamzami & Kroemer, 2001). The PTP inhibitor Cyclosporine A acts by binding CypD. All these components, when reconstructed in membranes, lead to the formation of a large pore (Beutner et al., 1998; Crompton, Virji, & Ward, 1998). However, since genetic evidences did not support this molecular composition, for many years the real molecular nature of the pore has been investigated.
Some recent findings pointed out the possibility that the ATP synthase might form the PTP. Indeed, initially it has been found the CypD interact with the lateral stalk of the F_0F_1 ATP synthase (Giorgio et al., 2009) and later it has been demonstrated that dimers of ATP synthase reconstructed in planar lipid membranes give rise to ion channel activities with characteristics that mimic those of the PTP (Giorgio et al., 2013). Moreover, more recently, it has been shown that another molecular actor actually is essential to the formation of the PTP: mitochondrial SPG7 (spastic paraplegia 7). It interacts with CypD and VDAC1 at the OMM/IMM contact sites and its ablation protect cells from PTP-dependent necrosis (Shanmughapriya et al., 2015).
As outlined above, the role of PT in pathophysiology is not clear. It might be that brief opening of the PTP acts as a Ca^{2+} release channel when mitochondria need to get rid of the excess of Ca^{2+} (Szabo & Zoratti, 2014). Moreover, the PT is a signal for induction of mitophagy (Kim, Rodriguez-Enriquez, & Lemasters, 2007). Following PT, mitochondria recruit Parkin, a key ubiquitin ligase whose loss-of-function mutations causes Parkinson's disease. In the course of the years, it has emerged that PTP principally exerts an effect in all degenerative, necrotic diseases. Among the most important pathologies in which PT exert a clear role is ischemia/reperfusion. During reperfusion, the conditions in the cell cytoplasm are nearly ideal for the induction of PT. Therefore, ablation of CypD or treatment with PTP inhibitors produces clear protective effects (Di Lisa & Bernardi, 2006).

2.4 Ion channels in mitochondria

Since my research has been focused, in general, on the modulation of potassium ion homeostasis at the level of the IMM, I will describe only potassium ion channels of the IMM, omitting any description of calcium, sodium and anion currents. Literature and information on these channels is quite vast, but the detailed description of all of them lies outside the scope of this dissertation. Therefore I will briefly give an up-to-date overview regarding mitochondrial inner membrane potassium channels and, later, I will reserve major relevance to the description of the general feature of the voltage gated potassium channels and in particular of mitochondrial Kv1.3 (mtKv1.3).

As pointed out in the previous paragraphs, the IMM has long been considered to be poorly permeable to cations and anions, since the strict control of inner mitochondrial membrane permeability is necessary for efficient mitochondrial energy production. Given the high driving force for cation influx, channels would be expected to be under tight control. It has become clear that various ion channels, along with exchangers and uniporters, are present in the mitochondrial inner membrane and that they are present in extremely low abundance and are open for very short times to maintain the low permeability to ions required to exploit the proton-motive force for ATP generation.
There are many proteins mediating ion fluxes in the inner mitochondrial membrane, as shown in figure 9. Concerning potassium fluxes, proteins known to mediate potassium ions are, so far: the ATP-dependent potassium channels (KATP), the big-conductance calcium-activated potassium channel (BKCa), the intermediate-conductance calcium-activated potassium channel (IKCa), the small-conductance calcium-activated potassium channel (SKCa), TASK-3 two-pore potassium channel, pH-sensitive potassium channel and finally the voltage-gated mitochondrial potassium channel Kv1.3. The above listed mitochondrial potassium channels are expressed also in the plasma membrane, in different types of tissues and cells, even if the mechanism mediating the dual targeting needs further investigation.

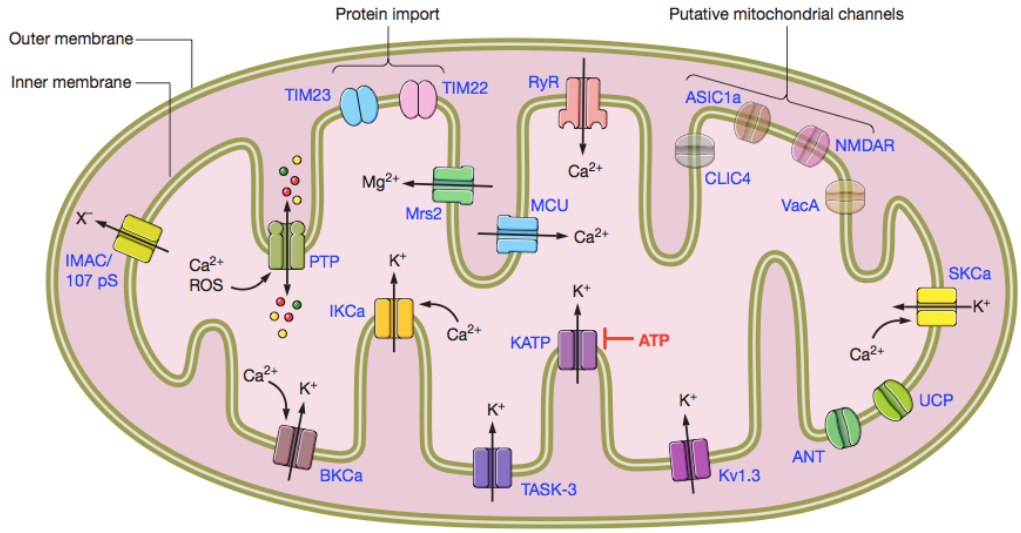

Figure 9: Picture showing proteins mediating ion fluxes in the IMM (from Szabò & Zoratti, 2014)

Even if the basic biophysical properties of IMM potassium channels have been found to be similar to those of the corresponding plasma membrane isoforms, their roles in the physiology are often different, because of the intrinsically unique nature of the mitochondrial organelle. In general, mitochondrial potassium channels are supposed to play a role in

mitochondrial respiration, establishment of membrane potential, mitochondrial matrix volume, regulation of energy demand of the cells, cardioprotection, protection of myocytes during "ischemic preconditioning", cell death and generation of reactive oxygen species, as already mentioned (Zoratti, De Marchi, Gulbins, & Szabò, 2009).
Molecular, electrophysiological and pharmacological characterization has made possible the elucidation of their pathophysiological role.
Mitochondrial swelling assays and later direct patch-clamp studies of mitoplasts (which are mitochondria stripped of their outer membranes) have identified a number of ion-conductive pores on the inner membrane (Zoratti & Szabó, 1994).
In order to better understand how this channels work, I will summarize the general features of ion channels. As a direct consequence of being an "open pore", the activity of K^+ channels can be directly measured using radioactive isotopes or electrophysiological techniques, such as patch-clamp and planar lipid bilayer. The electrophysiological techniques allow to describe the particular behaviour that distinguishes one channel from the other: for each one is possible, therefore, to evaluate conductance, selectivity, kinetics, mechanism of activation and pharmacology, as already mentioned.

2.4.1 General characteristic of ion channels

In general, ion channels are transmembrane proteins forming a hydrophilic pore allowing the passage of ions across the membrane. They permit specific inorganic ions to diffuse rapidly (more than one million ions per second) down their electrochemical gradient across the lipid membrane without energy consumption. Their omnipresence accounts for their fundamental role in cellular physiology of excitable and non-excitable cells, in all animals, plants and microorganism, included in their intracellular organelles.
Some specific characteristics differentiate ion channels from each other. First of all, the factors that can modulate their activity (i.e. the activation mechanisms). At least three types of activation mechanism can be distinguished: channels activated by changes of membrane potential (voltage-gated), channels modulated by ligands (ligand-gated) and channels that open following a tension on the membrane (stretch-activated). There are different types of ligand (neurotransmitters, ions, nucleotides, G proteins) that can exert an effect on the channels and they can bind the channel from the extra-cellular side or the intra-cellular one, or from one of the two sides of the membrane in the organelles. Moreover, ion channels are subject to the effect of a set of substances that are able to modulate their activity, reducing or increasing it. They are called inhibitors or activators. The term pharmacology refers to the activity of these molecules on the channels and they are used to modulate channels activity or even to identify a channel.
Another important characteristic that distinguish ion channels is their selectivity, given by the molecular properties of the selectivity filter (see next section). Indeed, ion channels preferentially carry some ionic species. Those selective for potassium, sodium, calcium and chloride are the most studied. Generally channels are not perfectly selective for a single ion and, on the other hand, there are some that are selective for diverse cations or anions.

Therefore, the ion selectivity, the activation mechanisms, the pharmacology together with the kinetic and the conductance, define the biophysical fingerprint of an ion channel, allowing its identification. In addition, channel activity is regulated by subcellular localization, post-translational modification, protein-protein and protein-lipid interaction (Lodish et al., 2006).
The most widely distributed types of ion channels are potassium channels and I will describe only voltage gated potassium channels.

2.4.2 Voltage gated potassium channels

The structures of K^+ channels share some features: a water-filled hole, the pore, which allows K^+ ions to flow across the cell membrane, a selectivity filter and a gating mechanism that serves to switch between open and close channel conformation. A prototypical K^+ channel has a trameric structure in which four identical subunits (α subunits, which are distinct from β and γ, that are accessory subunits, that regulate α subunits), associate to form a complex arranged around the central ion-conducting pore; however animal channels consisting of hetero-tetramers made of similar subunits exist. The canonical structure of a subunit consists of two TM α-helices (TM: transmembrane helical segment) traditionally called TM1 and TM2, with a short amino-acid segment between two transmembrane helices that dips into the membrane without fully crossing it, i.e. the P loop. The primary sequence of the P loop of K+ channels has the signature sequence Thr–Val–Gly–Tyr–Gly. This precise sequence at the level of the P-loop constitutes the selectivity filter. This structure referred to as TM1-P-TM2 structure (2TM/P) without additional peptide domains appears to be the minimum structure necessary for the permeation, the filtration and the opening, and represent a universal feature of potassium channel (Lu, Klem, & Ramu, 2001). The basic structure 2TM/P domain includes an amino-terminal tetramerization domain, which is conserved among voltage-gated K+ channels, and a carboxy-terminal, protein-interacting domain. The resolution of the crystal structure of KCsA channel encoded by a bacterial gene cloned from *Streptomyces lividans* was defined as shown in figure 11, confirming how trans-membrane helices and a short loop between them (which is the P-loop) are the principal characteristics of K^+ channels (Doyle, 1998). Other variations on the basic K^+ channel architecture include 4TM/P or 4TM/2P channels and 8TM/2P channels, which have two pores. Moreover, some variants can be added to the basic structure. Further, four transmembrane helices (S1–S4) precede the 2TM/P in voltage-gated K^+ channels (6TM/1P), including the positively charged S4 which confers to some of these channels the capability to sense and respond to the change in membrane potential, instead S5 and S6 which take part to the pore formation (see figure 10) This last structure is called Shaker, a name due to a mutant of *Drosophila melanogaster*, which corresponds to the first cloned gene for K^+ channels (Papazian et al., 1987; Tempel et al., 1987; Choe, 2002).
Voltage gated potassium channels (Kv) constitute the largest and most diverse family of potassium channels, comprising 40 of the 90 genes found in humans.

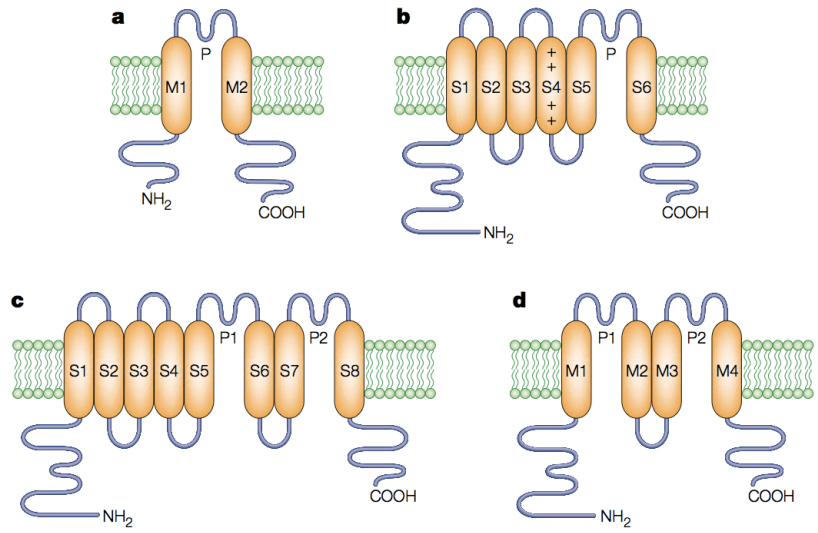

Figure 10: The four main classes of potassium channels (from Choe 2002)

According to the International Union of Pharmacology (IUPHAR), they are divided into 12 families (Kv1-12) (Gutman et al., 2005). For each family, the nomenclature refers to the homologous gene found in *Drosophila melanogaster.* The list of voltage gated K^+ channel comprise so far:

- Shaker Kv1: Kv1.1-Kv1.7
- Shab Kv2: Kv2.1-Kv2.2
- Shaw Kv3: Kv3.1-Kv3.4
- Shal Kv4: Kv4.1-Kv4.3
- KCNK/Kv7: Kv7.1-Kv7.5
- Eag-like: Kv10-Kv12
- Families Kv5, Kv6, Kv8 and Kv9 codify non-conducting subunits

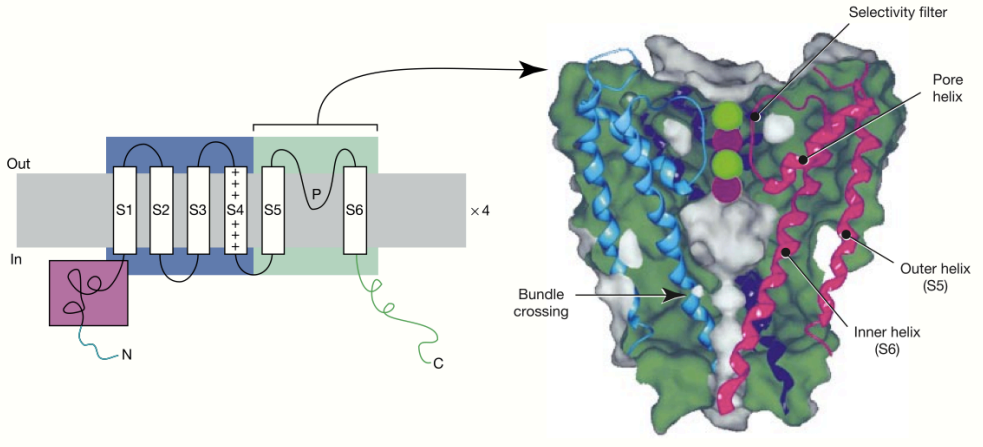

Figure 11: Typical structure of a voltage gated potassium channel (from Yellen 2002)

Beside the number of distinct encoding genes that distinguish Kv channels, other several factors add diversity among them.
First of all the heteromultimerization; each gene encode for a subunit, but the minimal number of subunit needed to create a functional Kv channel is four. Kv channels can be formed by subunit of the same types (homotetramers) but also by subunit of different type in the same families (heterotetramers). The heterotretamerization confers to the channels properties that are different from those of any hometratmer.
Another factor, which add diversity to the nature of the Kv channels, is alternative mRNA splicing. Many Kv channels gene contain intronless coding regions that undergo alternate splicing (all the members of the Kv1 family, except for Kv1.7, and Kv9.3). On the other hand other gene families (Kv3, 4, 6, 7, 9, 10 and 11) posses coding region made up of several exons that are alternately spliced, providing another source of diversity.
Then, post-translational modification: many Kv channels can be phosphorylated, ubiquitinated or palmitoylated.
"Modifier" subunits can further increase functional diversity within Kv families. Four Kv families (Kv5, 6, 8, and 9) encode subunits that do not generate functional channels on their own, but for heterotetramers with Kv2 subunits, increasing the functional Kv features.
Finally, accessory proteins can associate with Kv tetramers, modifying their properties. Among them, are peptide like calmodulin or Kvβ subunits, KCHIP1, mink, etc., (Gutman et al., 2005).
This huge diversity is aimed at the precise regulation of potassium ion channels, to fine-tune the cell homeostasis and the response during several pathophysiological processes.

2.4.2.1 Selectivity and gating mechanisms of voltage gated K^+ channels

In order to perform their functions in the best way, Kv channels have to be highly selective and fast. High flow rates are essential in many physiological processes in which ion channels in general are involved. Therefore they have to achieve a high throughput without using millions of proteins, while maintaining high selectivity. How do they achieve rapid permeation and selectivity? First of all, since ions have an extremely favourable interaction with water and not with lipids or proteins, the channel pores are filled with plenty of water, to make the ions stable and facilitate them to cross the lipid membranes. The molecules of water, in which the unequal sharing of electrons between the hydrogen atoms and the oxygen atom gives the water molecule a slight negative charge near its oxygen atom, reorients ion like K^+ with their negatively charged end towards a positively charged. Second, the K^+ channels achieve cations selectivity by electrostatic influence exploiting the fact that each helix possesses a negative side, therefore the intracellular vestibule of K^+ channels has the negative ends of four helix towards the pore of the channel, creating a negative intracellular vestibule. Moreover, the filter is characterized by the alignment of the carbonyl oxygens arranged horizontally, belonging to the canonical amino acid sequence Thr–Val–Gly–Tyr–Gly located in the S5-S6 linker, for each of the 4 subunits. Pairs of these quartets of oxygens partially surround K^+ ions with greater efficiency

compared to the eight oxygens of hydration of the sphere surrounding it in aqueous solution, providing an energetically favorable way for de-solvation of the ion. This also explains how the selectivity filter shows preference for potassium and not for sodium ion, since it precisely matches the configuration of oxygen atoms around a solvated potassium ion. Finally, the long-known feature that potassium ions cross the channel in single file gives the high throughput (Shieh, Coghlan, Sullivan, & Gopalakrishnan, 2000; Yellen, 2002).

Another characteristic of Kv channels is the presence of a vestibule, characterized by the presence of a set of negatively charged amino acids which impart an overall negative charge to the vestibule wall, which helps the transport of cations through the pore. These conserved residues can interact with a strategic conserved positive amino acid present in the peptide toxins of some venoms, such as ChTx, MgTx, IbTx, ShK, which can block the channel (Rauer et al., 1999).

The structural and architectural features of potassium channels are thus perfectly adapted to fit their function.

As mentioned before, the pore of Kv channels open in response to voltage changing. The S5-S6 transmembrane domains constitute the pore, while S1-S4 the voltage sensor. In particular S4 plays the major role in sensing variation in the voltage, owing a positively amino acids-enriched sequence (Papazian, Timpe, Jan, & Jan, 1991; Perozo, Santacruz-Toloza, Stefani, Bezanilla, & Papazian, 1994). Membrane depolarization is the conformational changes inducing factor, leading to channel opening and flowing of the ions. The transmembrane segment S4 displays a α-helix conformation with a positively charged amino acid residue (arginine or lysine) every three amino acid. Also the S2 and S3 segment contributes to the voltage sensing, because they stabilize the positively charged S4 segment with they negatively charged amino acid (Papazian et al., 1995; Seoh, Sigg, Papazian, & Bezanilla, 1996). During depolarization, this stability decreases and this accounts for the conformational changing occurring in response to voltage changing; indeed, during depolarization S4 is not more stabilized by S2-S3, and moving into the lipid membrane it drags S5-S6, via the S4-S5 linker, opening the pore (Choe et al., 2002)

However, during sustained depolarization, Kv channels can undergo inactivation, i.e. a closed, non-conducting state. Three types of inactivation exist, i.e N-, P- and C-type. The names derive from the distinct domain of the channel taking part to the process. For example, during the N-type inactivation (also known as “ball and chain” inactivation), the residues of the N-teriminal of the channel move into the channel vestibule to block the flow of ions, occluding the pore (Hoshi et al., 1990; Isacoff et al., 1991) This is a fast process, in contrast to the C- and P-type inactivation, in which are necessary specific rearrangements of some residues in the pore.

2.4.2.2 Kv1.3

The voltage gated potassium channel Kv1.3 is encoded by the intronless gene KCNA3, located on chromosome 1, p21-p13.3 and its product is 575 amino acids long protein (Folander K. et al., 1994).

The PM-located Kv1.3 channel displays an activation threshold between 50 mV and 60 mV, a single-channel conductance of 24 pS in T lymphocytes and, like the other voltage gated potassium channels, is activated by depolarization (Szabo & Zoratti, 2014).
Interestingly, Kv1.3 can undergo heterotetramerization with other *Shaker*-related members (Kv1.x). For example, in the human central nervous system, it has been shown that in grey matter Kv1.3 can form functional heterotetramers with Kv1.1, Kv1.2 and Kv1.4, contrarily to what happen in white matter or spinal cord where Kv1.3 is not found, demonstrating regional variation of its expression (Coleman, Newcombe, Pryke, & Dolly, 1999). Kv1.3 is also found assembled with Kv1.6 monomers in some other cases (Koch et al., 1997; Koschak et al., 1998).
Kv1.3 is the main potassium channel in T-lymphocytes were its function was first discovered (Chandy et al., 2004), but it is expressed also in other tissues, e.g. kidney (Yao, Chang, Boulpaep, Segal, & Desir, 1996), central nervous system (Mourre et al., 1999), in epithelia (Grunnet, Rasmussen, Hay-Schmidt, & Klaerke, 2003) and in brown and white fat (Xu et al., 2003). In T lymphocytes, during development and during activation of mature cells by mitogens, the surface density of K^+ channels is precisely regulated. When T cells are immature (thymocytes), they express hundreds of Kv1.3 per cell. As the developmental lineage diverges, Kv1.3 are downregulated. During activation, the abundance of Kv1.3 increases once again. This is well documented in murine T cells. In B-lymphocytes, stimulation through the antigen receptor increases expression of Kv1.3 channels (George Chandy et al., 2004). Moreover, Kv1.3 has been implicated in the regulation of cell proliferation; for example, in T-cells, antigen recognition leads to a molecular cascade which involves the activation of tyrosine kinases and phospholipase C, resulting in the generation of inositol(1,4,5)-triphosphate and diacylglycerol, which induce the release of calcium from the internal stores and activation of protein kinase C (PKC). Depletion of internal Ca^{2+} stores causes voltage-independent Ca^{2+} release-activated Ca^{2+} (CRAC) channels to open, determining calcium influx. Coordinated activity of Ca^{2+} and PKC-dependent signalling pathways culminates in cell proliferation (Chandy et al., 2009). In this contest, Kv1.3 regulates Ca^{2+} signalling. In particular, Ca^{2+} influx mediated by CRAC channels is reduced following membrane depolarization. The driving force for Ca^{2+} entry is restored by membrane hyperpolarization brought about by the opening of Kv1.3 potassium channels in the plasma membrane in response to membrane depolarization. Accordingly, inhibitors of Kv1.3 potently suppress effector memory T cell proliferation, making these blockers a promising tool for the therapy of autoimmune diseases, such as multiple sclerosis (Beeton et al., 2001). In addition, Kv1.3 together with other types of potassium channel participate to neurotransmitter release at the presynaptic nerve endings in different neuronal cells (Shoudai et al., 2007).
Furthermore, Kv1.3 channels are involved in volume regulatory mechanisms during apoptosis; following the induction of apoptosis by triggering of the CD95 receptor, activation of the cell volume regulatory anion channel ORCC occurs, but on the other hand this event is paralleled by inhibition of potassium channel Kvl.3, which exert a control on cell volume regulation as well. This latter event leads to shrinkage of the cell, which is one of the

principal hallmarks of apoptosis (Lang et al., 2004).
A central role of Kv1.3 in cell death was also highlighted by other studies. Cells genetically deficient for Kv1.3 expression did not undergo cell death when stimulated with cytostatic drugs like actinomycin D. Transfection of these cells with an expression vector for Kv1.3 rendered them sensitive to actinomycin D effects, and apoptotic hallmarks like DNA fragmentation, release of cytochrome C and loss of mitochondrial membrane potential ($\Delta\psi_m$) were observed (Bock, Szabó, Jekle, & Gulbins, 2002). In light of the fact that the lack of Kv1.3 determines resistance to apoptosis induced by cytostatic drugs and mitochondria-related apoptotic events are impaired, the subcellular localization of Kv1.3 was investigated. Interestingly, functionally active Kv channels have been identified in the IMM of T lymphocytes (mtKv1.3) (Szabò et al., 2005). First, its expression at the mitochondrial level was detected through immunogold electron microscopy on isolated human blood lymphocytes. Activity was observed with patch clamp experiments on mitochondria from human Jurkat leukemic T cells. To unambiguously identify mitoKv1.3, patch clamp experiments were performed on mitoplasts (mitochondria deprived of the OMM) isolated from cells lacking Kv1.3 expression and in parallel on the same cells stably transfected with an expression vector for Kv1.3. This allowed identifying precisely mitoKv1.3 current. Moreover mitoKv1.3 current colocalized with PTP current. The level of expression in lymphocytes was analyzed also by Western blot.
Subsequently, localization of Kv1.3 in the IMM has been demonstrated in other cell types beside lymphocytes by combining multiple techniques such as patch clamp, Western blot, in which isolated purified mitochondria were used with attention to different markers to assess contamination by ER and/or PM, and immunogold transmission electron microscopy. For example in macrophages (Vicente et al., 2006), in postsynaptic medial nucleus of the trapezoid body (MNTB) neurons (Gazula, Strumbos, & Mei, 2010), hippocampal neurons (Bednarczyk et al., 2010) and also in caner cells like PC-3 prostate cancer, MCF-7 breast adenocarcinoma, SAOS-2 osteosarcoma and B16F10 melanoma cells (Szabo & Zoratti, 2014), for all the cases revealed in genetically non-manipulated cell lines.
The channel is active at the resting negative mitochondrial potential, contrary to the plasma membrane Kv1.3 that do not mediate abundant flux at the resting potential. The functional expression of mtKv1.3 at the mitochondrial resting potential (-180, -200mV) is indicated by the fact that addition of specific Kv1.3 inhibitors to isolated mitochondria lead to hyperpolarization (Szabò et al., 2005). In fact, at resting condition potassium channel of the IMM are expected to drive an electrophoretic inward current since the entry of cation is thermodynamically favoured according to the electrochemical gradient established by the respiratory chin activity. As stressed in the previous paragraphs, entry of potassium must be compensated, otherwise this would lead to energy dissipation, volume changes and mitochondria depolarization; this job is carried out by the activity of the electroneutral K^+/H^+ antiporter and by the respiratory chain complexes.

If mtKv1.3 mediates the influx of K^+ across the IMM, plasma membrane Kv1.3 mediates the efflux of potassium ions from the cytoplasm, where K^+ ions are more concentrated towards the extracellular space, where K^+ ions is lower.
The mitochondria-located channel is a product of the Kv1.3 gene, since stable transfection of CTLL-2 lymphocytes (lacking Kv1.3 expression) with the Kv1.3 coding gene gave rise to active channel both in PM and in IMM, suggesting that the same gene generates the different located Kv1.3 channels. However, much less is known about the dual targeting of this channel. Alternative splicing or, more likely, posttranslational modifications could be possibilities.

2.4.2.2.1 Pharmacological features of Kv1.3

As mentioned above PM-located Kv1.3 opens in response to membrane depolarization at a voltage around 50-60 mV, instead of mtKv1.3, which results active at the extremely negative mitochondrial resting membrane potential.
Kv1.3 electrophysiological characteristics have been investigated mainly by exploiting the pharmacological features of kv1.3 channels. Kv1.3 pharmacology includes organic compounds or peptide inhibitors. Among the non-peptide inhibitors are general potassium channel blockers such as quinidine, tetraethylammonium (TEA), 4-aminopyridine (4-AP) (Grissmer et al., 1994), benzamide (Miao et al., 2003); but peptide inhibitors such as natural venoms appear as the most effective inhibitors and have been used for the electrophysiological characterization of this channel (Chandy et al., 2004). For example Margatoxin (MgTx) from the scorpion *Centuroides margaritatus,* exhibits an EC_{50} in the picomolar range; Charybdotoxin from *Leiurius quinquestriatus* (Quintero-Hernández, Jiménez-Vargas, Gurrola, Valdivia, & Possani, 2013) is also a scorpion venom effectively blocking Kv1.3. ShK, from the anemone *Stichodactyla helianthus*, block Kv1.3 at nanomolar concentration although some effect on Kv1.1, Kv1.4 and Kv1.6 have been described. The structure of the sea anemone toxin Shk is well characterized; it is a 35 amino-acid peptide. It has been demonstrated that Shk interacts with Kv1.3 by using positive residues (i.e. His^{19}, Ser^{20}, Lys^{22} Tyr^{23}) interacting with negative-charged residues (i.e. Asp^{386}) located at the level of the channel pore vestibule. The substitution of the critical Shk-Lys^{22} with neutral residues substantially reduce the affinity of the toxin for the channel, indicating that other residues are not binding efficiently to the channel pore vestibule (Rauer, Pennington, Cahalan, & Chandy, 1999). It binds to the channel with high affinity (K_d = 11pM) and shows 1000-fold higher selectivity with respect to other Kv and IK channels.
All the inhibitors described above are non permeable to the plasma membrane. However, a class of permeable Kv1.3 blockers also exists. These types of Kv1.3 inhibitors are able to enter the cytoplasm across the plasma membrane and to produce effects on mitochondrial K^+ channels. This class of Kv1.3 inhibitors includes Psora-4, PAP-1 and Clofazimine. Psora-4, a small molecule Kv1.3 blocker, is the most potent inhibitor (Chandy et al., 2004). It belongs to the family of natural products, called psoralens. Psoralens occur naturally in the seeds of *Psoralea corylifolia.* Psoralens are photosensitive

molecules used in the treatment of some skin disease like psoriasis. It has been shown that Psora-4 inhibits Kv1.3 (IC_{50} = 3 nM) (Vennekamp et al., 2004), but it inhibits to the same extent also Kv1.5 . For these reasons, the Wulff's group synthesized a derived inhibitor with the same potency but more selective called PAP-1 (IC_{50} = 2 nM) (Schmitz & Sankaranarayanan, 2005). Patch clamp experiments, however, demonstrated that both compounds, used at significantly higher concentration determine inhibition of other Kv family members as well.
Clofazimine (IC_{50}= 300nM), a fat-soluble riminophenazine compound, is currently used in the treatment of multi-bacillary leprosy. Moreover, its use in several infectious or non-infectious diseases, like antibiotic resistant tuberculosis, is under investigation. Clofazimine appears to preferentially bind to mycobacterial DNA, leading to disruption of the cell cycle and eventually kills the bacterium. It may also bind to bacterial potassium transporters, thereby inhibiting their function (Ren et al., 2008).
In the IMM, the roles played by mtKv1.3 are multiple, ranging from regulation of mitochondrial membrane potential, volume, ROS production. Interestingly, a crucial role for this channel in apoptosis became evident, first in lymphocytes and later in other systems as well.

2.5 Apoptosis

Apoptosis, also known as programmed cell death, is a complex and evolutionarily conserved physiological process. Programmed cell death allows the organism to tightly control cell number and tissue size, therefore to maintain tissue homeostasis and to remove cells that are in excess or potentially dangerous. It also plays an important role in the development and organogenesis. To this end, cells use a dedicated molecular program to regulate the destruction of the cell.
Mitochondria play an important role during apoptosis. In most pathways leading to apoptosis, permeability transition of the IMM and the consequence rapture of the OMM are critical.
I will describe the general aspects of this process, in order to contextualize the role of mitochondria

2.5.1 Pathways leading to apoptosis and molecular players

Programmed cell death was defined apoptosis and described for the first time in the early '70s (Kerr, Wyllie, & Currie, 1972). Nowadays we know in details the complex "death machinery" responsible for the execution of this "suicide", acting in a coordinated manner to regulate cell death.
There are two main pathways to induce apoptosis: the extrinsic pathway and the intrinsic one. Both pathways converge on mitochondria.
The extrinsic pathway, or death receptor pathway, is triggered by transmembrane receptors-mediated interactions. The death receptors (DR) are member of the tumour necrosis factors (TNF) receptors gene superfamily. A cysteine-rich extracellular domain and a cytoplasmic domain (the "death domain") characterize these receptors (Ashkenazi, 1998). One of the best-characterized ligands/receptors mechanisms is that involving

FasL/FasR. Binding of extrinsic ligands, such as CD95 ligand (also called FasL) to CD95 receptor (FasR), induces receptor clustering and formation of death inducing signalling complex (DISC). This complex recruits, via the adaptor molecule FADD (Fas-associated death domain protein) multiple procaspase-8 molecules, resulting in caspase-8 activation (Wajant, 2002). Following, other intracellular signals ultimately lead to the destruction of the cell. Other well-characterized death receptor ligands are TRAIL and TNF-α.
The intrinsic pathway, or mitochondrial pathway is extensively used in response to extracellular signals and internal insults. These stimuli that initiate the intrinsic apoptotic pathway can be positive or negative. The absence of certain growth factors, hormones and cytokines are considered negative stimuli that lead to apoptosis. On the other hand, radiation, toxins, hypoxia, hyperthermia, viral infections, free radicals and many others are stimuli that act in a positive fashion, leading to induction apoptosis as well. All of these stimuli affect mitochondria, causing changes in the inner mitochondrial membrane that results in an opening of the mitochondrial permeability transition pore (PTP), loss of the mitochondrial transmembrane potential and release of pro-apoptotic factors that reside in the mitochondrial intermembrane space. Pro- and anti-apoptotic Bcl-2 family proteins control the release of these factors from mitochondria (Saelens et al., 2004).
In some cases, the extrinsic and the intrinsic pathway can intersect, at the level of the caspase-8 mediated cleavage of the pro-apoptotic BH3-only protein Bid, member of the Bcl-2 family. After cleavage of the C-terminal portion, the truncated form of Bid (t-Bid) moves to mitochondria and determines the inhibition of the anti-apoptotic protein Bcl-2, determining the de-repression of pro-apoptotic proteins as Bax and Bak. These events lead to the permeabilization of the outer mitochondrial membrane (OMM), via the opening of the permeability transition pore (PTP) and/or the pores formed by the oligomerization of pro-apoptotic proteins (Wei et al., 2000). Once the OMM has been permeabilized, soluble protein diffuse from the inter-membrane space to the cytosol where they promote activation of the effector caspases caspase-3, -6, -7 and the capsase-9, by the formation of apoptosome (Cain, Brown, Langlais, & Cohen, 1999; Hengartner, 1997). Cytochrome c is released from mitochondria, as well as the protein Smac/Diablo which antagonize the action of the inhibitor of apoptosis proteins (IAPs). The release of cytochrome c is considered the non-return point of apoptosis.

2.5.1.1 The Bcl-2 family

The Bcl-2 family proteins (B-cell lymphoma-2, that are B-cells follicular lymphoma where the Bcl-2 gene was discovered) have either pro- or anti-apoptotic activity. These proteins are important not only in the regulation of apoptosis, but also in tumorigenesis and in the cellular responses to anti-cancer therapy.
Bcl-2 family members have been grouped in three classes: pro-survival family members (e.g. Bcl-2, Bcl-xL), the pro-apoptotic Bax/Bak family members and pro-apoptotic BH3-only proteins (e.g. Bim, Bid, PUMA, NOXA). The role of the anti-apoptotic members of this family is to inhibit the pro-apoptotic Bax/Bak family members. The BH3-only proteins, through their

BH3 conserved domain, bind and regulate the anti-apoptotic proteins, inhibiting their action and promoting apoptosis (Youle & Strasser, 2008).
The multi BH (Bcl-2 homology) domain Bcl-2 family members and the BH3-only proteins have conserved region of sequence homology. All members share at least one BH domain. Anti-apoptotic proteins like Bcl-2, Bcl-xL, Mcl-1, possess four BH domains. Members of the Bax pro-apoptotic family have sequences that are similar to those in Bcl-2, especially BH1, BH2, BH3. The other pro-apoptotic proteins share only the BH3 domain.
The pro-survival family members, in addition to their four BH domains, also have an hydrophobic carboxy-terminal domain, which helps to target them to the cytoplasmic face of three intracellular membranes: the outer mitochondrial membrane, the endoplasmic reticulum and the nuclear envelope. Bcl-2 is an integral membrane protein even in healthy cells, while other members like Bcl-xL and Bcl-w become associated to the membranes only after a cytotoxic signal. The three dimensional structure is well conserved among the members of this group of proteins. It is characterized by a globular bundle of five amphipathic α-helices located around two hydrophobic α-helices. Residues from BH1 to BH3 create a hydrophobic groove, which can bind the BH3 α-helix of a BH3-only relative. Every nucleated cell requires at least one Bcl-2 homologue because these proteins are "guardians" and are important in the regulation of tissue homeostasis (Cory & Adams, 2002).
Bax and Bak are the most abundant and widely distributed pro-apoptotic proteins. The absence of both these proteins dramatically impairs apoptosis. Bax is a cytosolic monomer in healthy cells, but its localization and conformation changes during apoptosis and it integrates into the outer mitochondrial membrane and it oligomerizes (Annis et al., 2005). On the contrary, Bak is located in the outer mitochondria membrane even in healthy cells, but apoptotic stimuli determine a conformational change also for this protein and the formation of aggregates. Bax and Bak oligomers are widely believed to provoke or contribute to the permeabilization of the OMM. The three-dimensional structure of Bax resembles that of its anti-apoptotic relatives.
The BH3 only proteins are subdivided in two subgroups, according to their mechanism of action. There are the "activators" (i.e. Bid, Bim, Puma), which directly engage Bax or Bak. The other subset of proteins is called the "sensitizers" (i.e. Bad and Noxa), which act only by displacing the pro-survival proteins, allowing to Bak and Bax to act. Thus, the apoptosis is triggered when BH3-only proteins engage the multiple pro-survival relatives, which normally inhibit Bax and Bak. Hence, the presence of Bax and Bak is however essential (Willis et al., 2007).
The precise way in which the anti-apoptotic Bcl-2 members prevent cell death is still debated. The widespread view is that the only function of Bcl-2 protein is to guard mitochondrial integrity, keeping enclosed, in this way, a number of factors involved in the induction of apoptosis. Despite this view, a central role for mitochondria destruction is difficult to reconcile with the lack of involvement of cytochrome C in cell death in other model organisms like *C. elegans* and *Drosophila* (Cory & Adams, 2002).

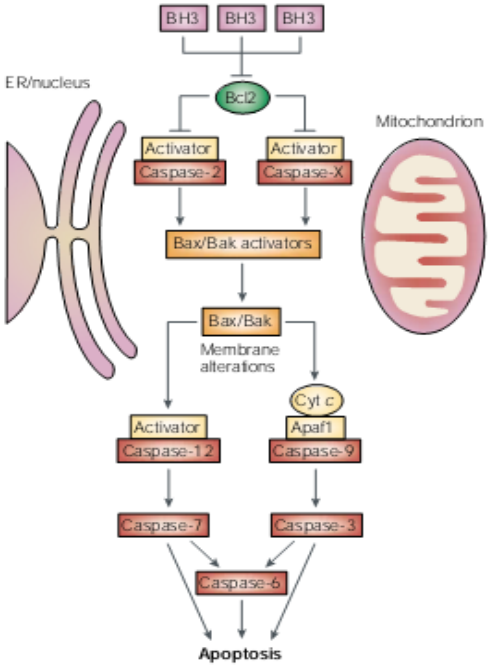

Figure 12. Bcl-2 family proteins regulate caspases activation both blocking or activating their functions (from Cory and Adams, 2002).

At the molecular level, Bcl-2 pro survival protein, acting at the mitochondrion, the endoplasmic reticulum and nuclear membrane, control the activation of several upstream initiator caspases, perhaps by sequestering their activators. Then, initiator caspases process proteins, for example Bid, those activate Bax and Bak. Bax and Bak form oligomers produce damage to the organelles and this event amplifies the proteolytic cascade. Furthermore, Bcl-2 might control apoptosis from the ER. The process is shown in Figure 12.
Alteration at the level of the Bcl-2 family repertoire of a cell has a determining role in tumorigenesis. Impaired apoptosis is one of the main characteristics in cancer development. In this scenario, all the Bcl-2 pro-survival family members are likely to be oncogenes. By contrast, members of both pro-apoptotic subfamilies are tumor suppressors. Both control of cell death and cell proliferation are important during cell cycle: in fact, cooperation between mutations those enforce proliferation and those that inhibit apoptosis has been observed in different type of cancers.

2.5.1.2 Caspases

Caspases, a large protein family, are a set of cysteine proteases activated in apoptotic cells, which determine most of the morphological changes observed during apoptosis.
Caspases are subdivided in two groups, according to their action: initiator caspases (2, 8, 9, 10) and effector caspases (3, 6, 7) (Alnemri et al., 1996).

All known caspases possess an active-site cysteine and cleave substrate specifically after an aspartic acid residues. The substrate specificity of caspases is determined by the four residues amino-terminal to the cleavage site. Therefore, caspases cleave a restricted set of target proteins (Thornberry et al., 1997).
Proteolytic cleavage by caspases not always lead to protein destruction and, hence, inactivation. The different results depend on the nature of the substrate. The simplest outcome is the loss of biological activity; in other case, cleavage by caspases can result in gain of biological activity; again, in other cases, cleavage of inhibitory domains lead to increased biological activity.
Caspases are synthesized as pro-enzymes, or zymogens. These inert pro-enzymes are constituted by an N-terminal pro-domain and by p10 and p20 domains. Therefore, caspases have to be activated by a proteolytic cleavage, which generally occurs between the p10 and p20 domains or between the pro-domain and the p20. These cleavage sites occur at Asp-X domain, suggesting the possibility of an autocatalytic activation (Hengartner, 2000).
Caspase-8 is the key initiator caspase in the dead receptor pathway. The interaction between the CD95 ligand and CD95 receptor determine the recruitment of several procaspase-8 molecules. The low intrinsic protease activity of procaspase-8 is sufficient to allow the pro-enzyme to cleave and activate each other. This mechanism is also called induced proximity model (Muzio, Stockwell, Stennicke, Salvesen, & Dixit, 1998). In the simplest case, caspases are activated by the proteolytic cleavage operated by an upstream-activated caspase. This is the case of caspase-3, an effector caspase.
The most complex mechanism described so far is that of activation of caspase-9. This event requires the association with the protein cofactor Apaf-1, which is not only necessary for caspase-9 activation, but also for its regulation. Together with other molecules, Apaf-1 and caspase-9 form a holoenzyme, called apoptosome. The ATP-dependent oligomerization of Apaf-1 allows the recruitment of procaspase-9 in the apoptosome complex, determining its activation.
In summary, effector caspase are usually activated proteolytically by an upstream caspase, while initiator caspases are activated through regulated protein-protein interaction (Youle & Strasser, 2008).

2.5.2 Kv1.3 in apoptosis

It is widely accepted that mitochondria have a central role in apoptosis since the release of cytochrome c and other proteins from the mitochondrial IMS and matrix mark the point of no return.
In cells lacking the expression of the potassium channel Kv1.3 (CTLL-2 lymphocytes), the expression of mitochondria-targeted Kv1.3 was sufficient to restore the response of these cells to several apoptotic stimuli. The mechanisms underlying these events have been completely elucidated. Indeed, mtKv1.3 has been identified as a target of the pro-apoptotic protein Bax, a member of the Bcl-2 family (details in the next section). Bax and mtKv1.3 physical interaction, occurring only upon induction of apoptosis, was demonstrated by co-immunoprecipitation experiments, confirmed both

in mouse and human cells. Moreover, incubation of isolated Kv1.3-positive mitochondria with recombinant Bax or toxins triggered hyperpolarization, due to the inhibition of the influx of positive charges mediated by Kv1.3, followed by a depolarization due to the opening of the PTP, formation of reactive oxygen species and release of cytochrome c, while deficient-Kv1.3 mitochondria were resistant (Szabó et al., 2008). A model of the structure of the membrane-integrated Bax monomer indicates that at least amino acids 127 and 128, located between the 5th and 6th helices of Bax, protrude from the outer mitochondrial membrane into the inter-membrane space (Annis et al., 2005). The amino acid in position 128 is a highly conserved, positively charged lysine, which mimics the action of the critical lysine in Kv1.3-blocking toxins by binding to the negative residues at the pore channel vestibule, which face the inter-membrane space in mitochondria. All toxins contained a positive residue, which is critical for interaction with Kv1.3. By contrast, anti-apoptotic proteins contain a negative charge in the corresponding position (Glu158 in Bcl-xL). Mutation of Bax at lysine 128 (K128E) abrogated its effects on Kv1.3 and the induction of apoptotic changes in mitochondria, while mutation of Bcl-xL at glutamic acid 158 to Lysine (E158K) rendered Bcl-xL pro-apoptotic when expressed in Bax/Bak-less MEF cells (Szabò et al, 2011). In the light of this, the mechanism of the inhibition exerted by Bax became delineated: Bax, after inserting as monomer, inhibits Kv1.3 via lysine 128 by interacting with the channel pore vestibule, inducing an increase of the electrochemical gradient (i.e. hyperpolarization) because of the block of the positive influx mediated by Kv1.3. Hyperpolarization interferes with respiration and triggers ROS release, favouring detachment of cytochrome c; ROS are also expected to prompt Bax migration to mitochondria (Ahmad, Iskandar, Hirpara, Clement, & Pervaiz, 2004); subsequent exit of cytochrome c through Bax oligomers in the outer membrane can occur. Activation of the PTP might be caused by oxidation of cysteine residues (Orrenius, Gogvadze, & Zhivotovsky, 2007). PTP opening determines membrane depolarization, and rupture of OMM, ultimately contributing to cytochrome C release.

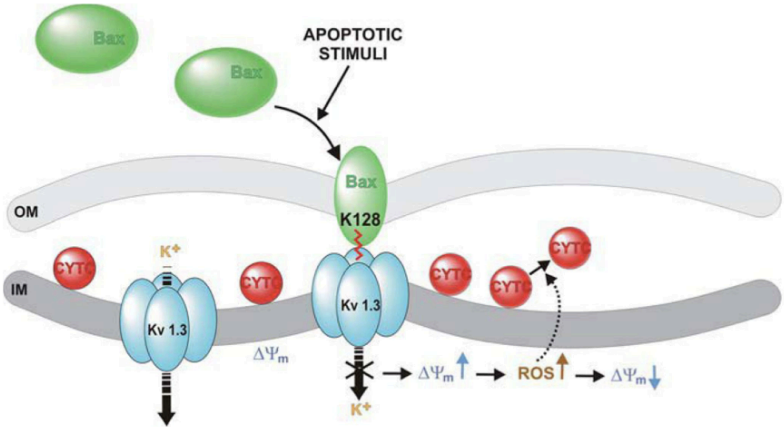

Figure 13: Mechanism of action of mtKv1.3 during apoptosis (from Szabò et al., 2008)

2.6 Potassium channels as therapeutic target in cancer

The involvement of ion channels in several cellular events and the evidence that many ion channel-related processes are altered in tumour biology makes them candidates as pharmacological target. In general, ion channels are virtually involved in all basic cellular processes, among them some of the most decisive such as proliferation and cell death (Lang et al., 2005). It dates back to the early 80s the first evidence that voltage gated potassium channels could have a role in mitogenesis (DeCoursey et al., 1984). Later, the oncogenic potential of EAG, a voltage gated potassium channel, was proved by the fact that transfection of EAG into mammalian cell led to transformed phenotype (Pardo et al 1999). Rapidly, the number of ion channels involved in tumorigenesis and progression of aggressive and metastatic cancers increased. Today we know that the vast group of ion channels involved in tumour biology includes plasma membrane ion channels (Prevarskaya, Skryma, & Shuba, 2010) and intracellular ion channels (Leanza et al., 2013), and that the pharmacological targeting *in vivo* for the treatment of tumour could be worthy of consideration (Leanza, Managò, Zoratti, Gulbins, & Szabo, 2015).

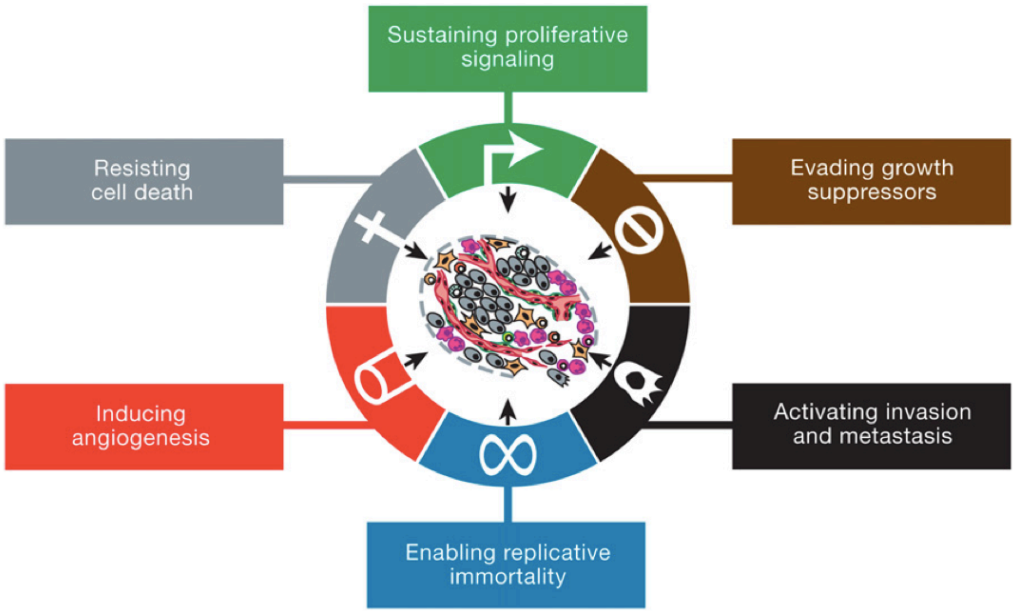

Figure 14: Acquired capabilities of cancer (from Hanahan and Weinberg, 2011).

In 2000, Hanahan and Weinberg (Hanahan & Weinberg, 2000) enumerated the typical features shared among all different types of cancer. Genome instability accounts for the impairment of tissues homeostasis and inflammation favours and sustains these altered functions. These hallmarks are six capabilities, acquired during the development of a tumour: 1) self-

sufficiency in growth signals, 2) insensitivity to growth-inhibitory (antigrowth) signals, 3) evasion of programmed cell death (apoptosis), 4) limitless replicative potential, 5) sustained angiogenesis, and 6) tissue invasion and metastasis (Hanahan et al., 2000). After a decade, the same authors added to the list two emerging hallmarks: reprogramming of energy metabolism and evading immune destruction. Further, they stressed on the role of normal cells, which contribute to the development of hallmarks trait by creating the ''tumor microenvironment.'' (Hanahan & Weinberg, 2011).

As stated above, since ion channels define cell volume, cellular proliferation rate, cell membrane potential and intra-cellular signalling events, it is predictable that genes encoding ion channels are affected during malignant transformation. Therefore the altered expression of different ion channels could account for one or more pathophysiological features that characterize malignant growth.

In the next figure are summarized the ion channels taking part to each cancer hallmarks. In 2008, the first international meeting of scientists, oncologists and representatives of the pharmaceutical industry interested made possible an up-to-date overview on the role of ion channels in the development and progression of cancer and the possibility of their exploitation for cancer diagnosis and treatment (Fraser & Pardo, 2008).

Among all ion channels, potassium channels represent the most heterogeneous group whit its huge structural and functional diversity. Moreover, potassium channels show the highest altered expression in tumours. As already mentioned and shown in figure 16, cell cycle and proliferation, cell migration, invasion and apoptosis are all processes that can be modified by the expression of potassium channels. They exert an effect on these processes by permeation-dependent and permeation-independent mechanisms. Potassium channels show cells and tissue specific expression; their activity can be modified by using synthetic blockers or natural peptides and this strategy is already in use in clinic for other pathologies such as cardiac diseases. For all these reasons targeting potassium channels in cancer therapy could give successful strategy (Pardo & Stühmer, 2013).

From the vast literature reporting dysregulated potassium channel expression in cancer, it is mostly about overexpression and potassium channels implicated in oncological processes belonging to all four main classes of potassium channels, i.e.: 2TM/P, 6TM/P, 8TM/2P, 4TM/2P. In the vast majority of cases, the abnormally expressed channel is wild type (Huang & Jan, 2014).

Changes in the expression levels of K^+ channels can occur in different ways: at the genomic level, at the transcriptional level, at the post-translational level or epigenetic levels, and in some cases an increase in channel activity can be explained by upstream changes such as interaction with non-channel molecules, often membrane proteins (such as β1 integrin) (Hofmann et al., 2001) or soluble ones (such as β-catenin) (Munoz et al., 2012).

Concerning the voltage gated potassium channel Kv1.3, epigenetic mechanisms regarding its gene KCNA3, such as DNA methylation, have been implicated in the altered expression of this channel in pancreatic (Brevet, Fucks, et al., 2009) and breast (Brevet, Haren, Sevestre, Merviel, & Ouadid-Ahidouch, 2009) cancer. Even if most of the mechanisms that lead to a loss of

controlled expression of potassium channels in tumours are not well understood, it is reasonable to think that the sustained expression of such a channels during tumour progression could give a selective advantage to cancer cells (Pardo & Stühmer, 2013).

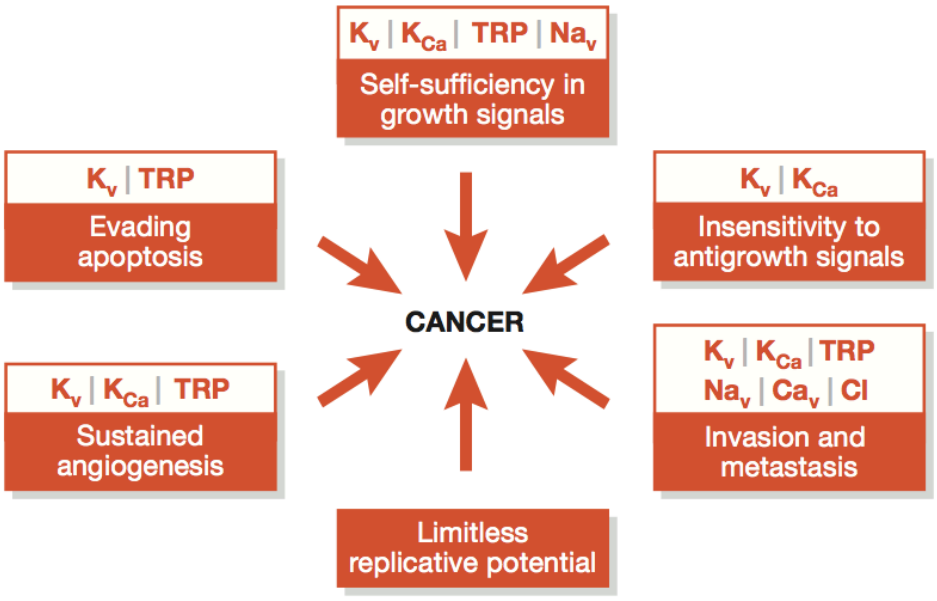

Figure 15: Ion channels linked to the six hallmarks of cancer proposed by Hanahan and Weinberg (from Fraser and Pardo, 2008)

Altogether, these observation led to the hypothesis that ion channel blockers, especially for potassium channels could impair tumour progression, especially in those cases where a different pattern of expression of ion channels in cancer with respect to healthy cells is found (Pardo 2004).
From a pharmacological point of view, ion channels offer several important benefits; for example, in the case of plasma membrane ion channels, they can be often accessed from the extracellular space, which allows reaching the range of concentration acting *in vitro* and the therapeutic doses in plasma. Another advantage of ion channels compared to other types of pharmaceutical targets is that by using patch-clamp techniques it is possible to elucidate the mechanism of drug action in a relatively easy manner because of the high sensitivity and kinetic insight offered by this method; with the same technique, the effect of newly synthetized compounds or derivatives of precursors of ion channels inhibitors can be studied and the electrophysiological properties can be defined in living cells. On the other hand, the fact that many potassium ion channels are expressed above all in excitable cells, carrying out fundamental function in the central nervous system (CNS), renders the use of ion channel blockers harmful for excitable tissue. An option to avoid side effect in central nervous system is to use molecules that are unable to cross the blood-brain barrier or limit the

therapeutic concentrations in order to limit the diffusion into the cerebrospinal fluid. However, emerging evidences suggest that the risk of causing side effect in peripheral tissues, e.g. inducing cardiotoxicity, is higher than that for the CNS (A. Arcangeli & Becchetti, 2015).

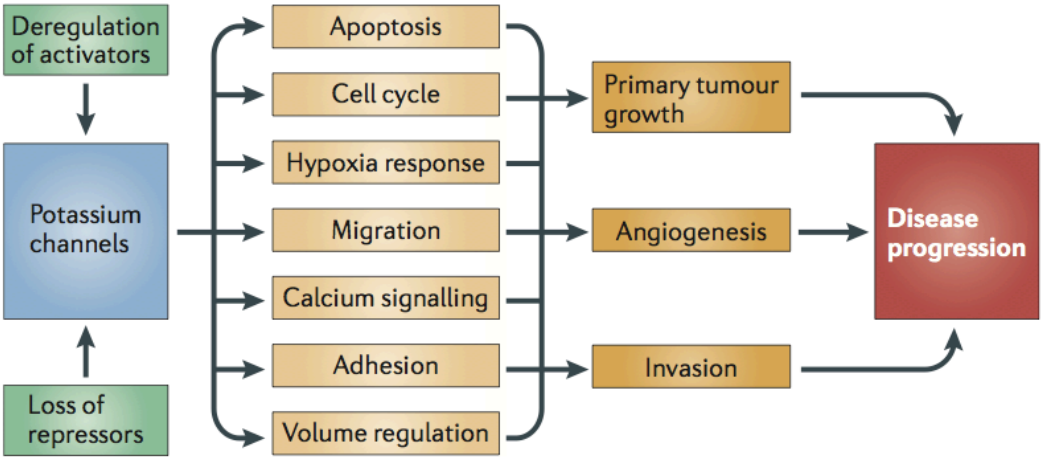

Figure 16: Summary of the process in which K^+ channels are involved in oncology. Changes in their expression level can influence precise steps of tumour progression (from Pardo & Stühmer, 2014)

There are several mechanisms by which an inhibitor can affect channel activity.
The simplest is by directly blocking the pore or preventing the agonist binding by occupying its binding site. Another way is by allosteric regulation; they can modify the conformational state of the channel interacting with allosteric sites. Composition and physical state of the plasma membrane also exert an effect on channel proteins. Several drugs can modify plasma membrane characteristics. Finally, ion channels form complexes with a variety of membrane proteins (e.g. the mentioned above β1 integrin and β catenin, and many others), which offers other possible ways for altering channel function (Andersen, 2008; A. Arcangeli & Becchetti, 2010).
The detailed understanding of the molecular mechanisms of the action of the drug and of its interaction with the channels allow to reach an high level of specificity, i.e. attack targeted cell types, without causing toxic effects in the healthy tissues. An example is exploiting the fact that cells not only have a different pattern of channels expression but also different proportion of channel in different states. The ion channel function is characterized by continuous transitions between three conformational states, such as open (active), closed (deactivated) and inactivated (or desensitized, in ligand-gated channels). If in pathological cells channels preferentially assume a precise conformational state, specificity can be obtained by using drugs that preferentially have more affinity for those states (Kaczorowski, McManus,

Priest, & Garcia, 2008). Indeed, membrane potential (and actually also organellar membrane potential) varies between healthy and pathological cells. Indeed, a specific conformational state of a voltage-dependent channel could predominate in a cancer type as compared to the normal tissue because of their different voltage dynamics (in the case of voltage-dependent channels) or different patterns of extracellular activators (for ligand-gated channels) of the different cell types.

2.6.1 Kv1.3 as oncological target

At this point, it is important to remind the crucial role of mtKV1.3 potassium channel in apoptosis. It is a direct target of the pro-apoptotic protein Bax and the inhibition exerted by this latter mimic the molecular mechanisms exerted by the toxins known to inhibit Kv1.3 currents (see above). The absence of Kv1.3 makes cells resistant to apoptotic stimuli of various nature (e.g.: TNFα, CD95, sphyngomielinase, staurosporine), underlining its crucial importance in programmed cell death. Moreover, Kv1.3 has been shown to be expressed in several tissues, such as brain, lung, thymus, spleen, lymph node, fibroblasts, lymphocytes (Szabò et al., 2005), tonsils, macrophages (Leanza, Zoratti, Gulbins, & Szabo, 2012), central nervous system (Mourre et al., 1999), brown and white fat, microglia, oligodendrocytes, osteoclasts, platelets, liver, skeletal muscle, in hippocampal neurons, astrocytes (Gutman et al., 2005). Interestingly, Kv1.3 was shown to be expressed in various types of cancer. In B-cells of lymphoma (Alizadeh et al., 2000), in melanoma cells in close proximity of β_1 integrin molecules (Artym & Petty, 2002), in human glioma together with Kv1.5 (Preußat et al., 2003) , in colon cancer (Abdul et al. 2002), in breast cancer (Abdul, Santo, & Hoosein, 2003; Jang, Kang, Ryu, & Lee, 2009) and gastric cancer (Lan & Shi, 2005). Moreover for some of these cancers, mitochondrial expression of Kv1.3 has been proven (Gulbins, Sassi, Grassmè, Zoratti, & Szabò, 2010; Leanza et al., 2013; Leanza et al., 2012). Moreover a slight increase of the transcripts of Kv1.3 has been highlighted in transformed hematopoietic cells (Smith et al., 2002), as well as its altered expression in various tumor cell lines was observed, such as in B-cells lymphoma, T-cell lymphoma, acute myeloid leukemia, breast cancer, prostate cancer and colon cancer (Arcangeli et al., 2009). Since Kv1.3 is involved in cell proliferation, its altered expression confers an advantage to cancer cells. On the other hand, mtKv1.3 is involved in apoptosis, leading its inhibition by Bax to a cascade of events culminating with cell death. As a consequence, exploiting its expression in cancer cells, sometimes even altered towards over-expression, mtKv1.3 became an oncological target of great interest.
In fact, in the light of the above-mentioned model (figure 13), by mimicking the action of the pro-apoptotic protein Bax it is possible to trigger cell death. Inhibition of mtKv1.3 is possible by using membrane permeant molecules, that are able to cross plasma membrane. As mentioned above, Psora-4, PAP-1 and clofazimine are selective membrane-permeant Kv1.3 inhibitors, representing potential therapeutic drugs. Actually, their ability to induce cell death in different types of cancer cells has been already demonstrated in vitro, in multiple human and mouse cancer cell lines, in vivo, in a melanoma mouse model and ex vivo on B-leukemic cells deriving from cronic

lymphocytic leukemia (CLL) patient (Leanza et al., 2013; Leanza et al., 2012). In order to prove the specificity of the action of the three inhibitors, experiments were carried out using a genetic model in which CTLL-2 lymphocytes, which normally lack Kv1.3 expression, were transfected with either an expression vector for Kv1.3 cells, *(pJK-Kv1.3)* (cells designated CTLL-2/Kv1.3), or control vector *(pJK)* (cells designated CTLL-2/pJK). It represents the same genetic model used to test the physiological processes linked to the activity of Kv1.3 (Szabó et al., 2008; Szabò et al., 2005). The experiments proved that only cells expressing Kv1.3 underwent cell death. To provide another level of specificity and clarify the contribute of mtKv1.3 to the whole process, cells were also treated with some non-permeant Kv1.3 inhibitors (e.g. MgTx). The results showed how membrane-impermeant Kv1.3 inhibitors did not affect cell viability, indicating that inhibition of mitochondrial but not plasma membrane Kv1.3 is necessary to induce cell death.

It is worth to underline that the inhibition of mtKv1.3 with membrane permeant inhibitors lead to apoptosis and not to other unspecific forms of necrosis. In fact, caspase-9 and caspase-3 activity was increased 25- and 30-fold respectively, in the Kv1.3 expressing cells upon 12 h of treatment with the three membrane permeant Kv1.3 inhibitors, while the drugs were without effect in CTLL-2/pJK cells. Moreover, Psora-4, PAP-1 and clofazimine induced poly (ADP-ribose) polymerase (PARP) cleavage, an event downstream of cytochrome C release and caspase-3 activation, only in cells expressing Kv1.3. PARP cleavage was more pronounced when these drugs were used in combination with multi-drug resistance pumps inhibitors (MDRi), since a typical feature of cancer cells is to extrude applied drugs. Mitochondrial cytochrome c release was also tested. It was observed only in Kv1.3-positive cells, upon treatment with the drugs. In contrast, MgTx and Shk did not induce caspase-9 or caspase-3 activation, cytochrome c release, mitochondrial depolarization or PARP cleavage neither in Kv1.3 negative cells nor in Kv1.3 positive ones (Leanza et al., 2012).

Two characteristic mitochondrial events occurring during cell death were observed after treatment CTLL-2 cells with Psora-4, PAP-1 and clofazimine: the increase of ROS production and the mitochondrial membrane depolarization. Both events were observed only in CTLL-2/Kv1.3 cells but not in CTLL-2/pJK cells, indicating that the three drugs did not induced oxidative stress *per se* and that ROS production is downstream of Kv1.3.

The molecular mechanism by which Kv1.3 induce apoptosis suggests that membrane permeant Kv1.3 inhibitors are able to induce cell death independently from Bax and Bak. This was demonstrated in Bax/Bak-double deficient human Jurkat leukemic T cells, where the three membrane permeant Kv1.3 inhibitors efficiently induced apoptosis. As expected, Bax/Bak deficient cells were resistant to staurosporine.

Further, the specificity of the action of the three membrane permeant inhibitors was proved by suppressing the Kv1.3 expression in human Jurkat leukemic T cells by transient transfection of siRNA targeting Kv1.3, which is the only potassium channel of the Kv family expressed in these cells and is active also in mitochondria (Szabò et al., 2005). Apoptosis induced by Psora-4, PAP 1 and clofazimine was significantly decreased in human Jurkat

leukemic T cells upon reduction of channel expression by siRNA. Cells transfected with control siRNA still underwent apoptosis to an extent similar to that observed in non-transfected cells.

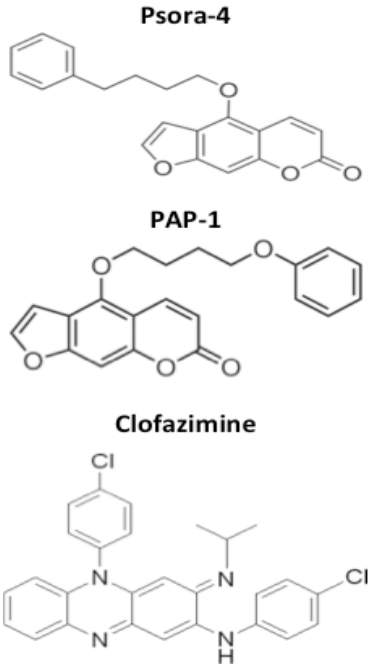

Figure 17: Structure of the three membrane-permeant Kv1.3 inhibitors Psora-4, PAP-1 and clofazimine

Altogether, the results suggested that the cytotoxic effect of Psora-4, PAP-1 and clofazimine was due to a specific action on mitoKv1.3.
The same results were obtained also in a variety of tumor cell lines by targeting mitoKv1.3, for example in B16F10 cells, which normally express Kv1.3. Transfection with siRNA prevent cell death upon treatment with Psora-4 PAP-1 and clofazimine.
Furthermore, the specificity of these compounds on mitoKv1.3 was demonstrated testing cell survival by the MTT assay on a variety of cancer cell lines. Psora-4, PAP-1 and clofazimine induced apoptosis only in Kv1.3-expressing cell lines, but not either in HEK293 cells, known to express low level of Kv potassium current (Yu & Kerchner, 1998), or in K562 human chronic myelogenous leukemia cell line, shown to lack Kv1.3 expression and current (Smith et al., 2002). Again, the non-permeant inhibitors, MgTx and Shk, did not have any effect both on expressing and not expressing Kv1.3 cell lines.
These results confirmed that cell death can be induced by these Kv1.3 membrane-permeant inhibitors downstream of Bax and Bak, offering in this way, novel treatment for chemotherapeutic drug-resistance malignancies, often expressing low level of these two pro-apoptotic proteins.

The significance of Kv1.3 inhibition mediated apoptosis was also tested *in vivo,* through the establishment of a melanoma model using B16F10 melanoma cells injected subcutaneously in a mouse. The tumor, after establishment and growth, was treated with intra-peritoneally injected clofazimine (at days 5, 7, 9 and 11 post cells injection). The tumors were removed and analyzed after 16 days: a 90% reduction of the volume was observed after treatment with clofazimine compare to the untreated (figure 19).

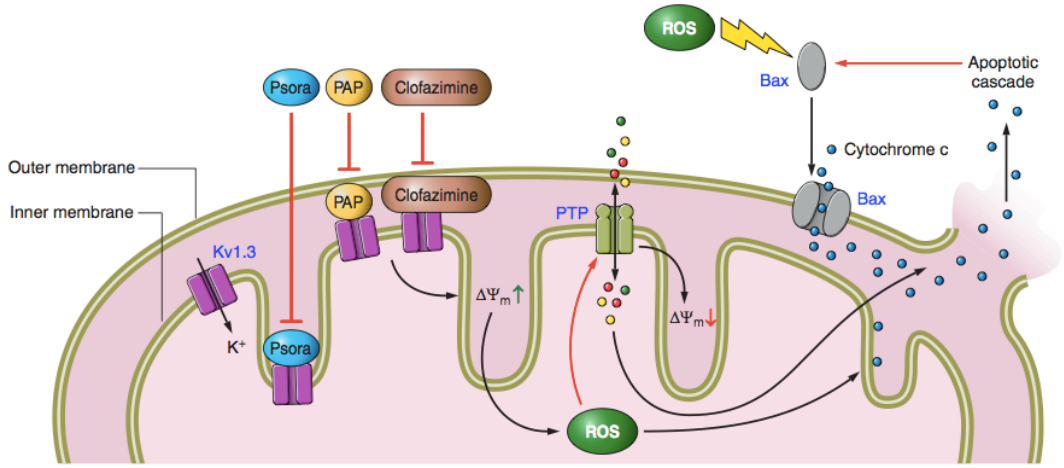

Figure 18: Scheme representing the events triggered by the use of membrane-permeant inhibitors Psora-4, PAP-1 and clofazimine , leading to apoptotic cascade (from Szabò and Zoratti 2014)

Moreover, no side effects were present in treated mice, as revealed by cytological analysis of the other tissues (Leanza et al., 2012).
The data by Leanza et al. provide a novel approach for the development of drugs that can induce apoptosis independently of Bax and Bak. The identification of molecules that mediate the death of cancer cells independent of Bax and Bak is a clinical challenge, because of the resistance of tumors to chemotherapy.
As already mentioned, the ability of membrane permeant Kv1.3 inhibitors to kill cancer cells was also demonstrated in an ex-vivo model.
Psora-4, PAP-1 and clofazimine were used against cancer cells deriving from chronic lymphocytic leukemia (CLL) patients.
B-CLL is a pathology characterized by a clonal accumulation of apoptosis-resistant mature neoplastic B-cells.
It has been demonstrated that cells from B-CLL patients show high expression and activity of Kv1.3 potassium channel compared with cells deriving from healthy subject (Leanza et al., 2013). Healthy B cells or pathologic B cells were purified from peripheral blood lymphocytes. By using FITC-labeled anti-Kv1.3, it was possible to assess the level of Kv1.3 proteins

in the two types of cells by fluorescence-activated cell sorting. Cells from B-CLL patients expressed higher levels of Kv1.3 than cells deriving from healthy subject. These results, together with the fact that Kv1.3 potassium channels are not only expressed but also active in these cells, were further confirmed by patch clamp experiments. Patch clamp experiments in the whole-cell configuration confirmed higher expression of functional Kv1.3: the peak current measured at +70mV was significantly higher in the B-CLL than in control B cells. Shk, a membrane-impermeant specific inhibitor, and clofazimine blocked Kv1.3 current (Szabo, Trentin, Trimarco, Semenzato, & Leanza, 2015). Moreover, biochemical assays revealed that subcellular fractions from B-CLL cells express Kv1.3 also in their mitochondria.

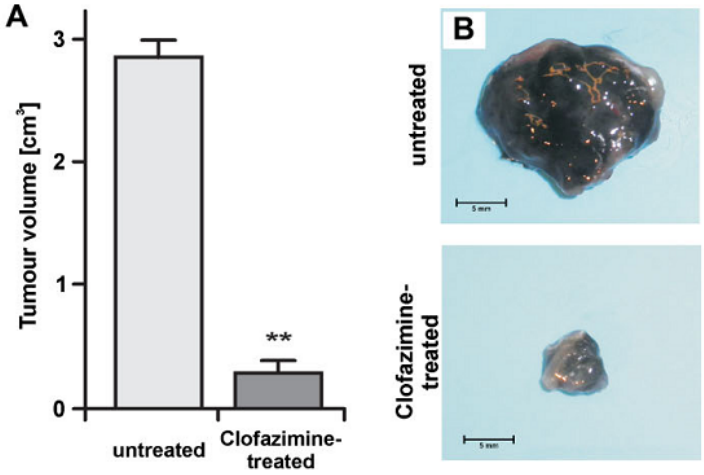

Figure 19: A) Average and SD of the volume of the melanoma tumors after 16 days of growth in untreated and clofazimine treated mice. **B)** Representative tumors from untreated and clofazimine treated mice (Leanza et al., 2012).

Given the fact that B-CLL cells expressed mtKv1.3, membrane permeant inhibitors activity was tested very efficiently induced apoptosis of B-CLL cells, in particular if administered in combination with inhibitors of the multidrug resistance pumps (MDRi). In contrast, the cells were resistant to the membrane-impermeant inhibitor ShK, clearly indicating that the PM-located Kv1.3 itself is not responsible for the apoptotic response. Interestingly, B or T cells isolated from healthy subjects were resistant to these stimuli. The same mechanisms observed from the in vitro experiments on cancer cells treated with the three membrane permeant Kv1.3 inhibitors were observed: an increased mtROS production and a marked depolarization in B-CLL cells after treatment with the drugs. Most importantly, residual T lymphocytes cells taken from a B-CLL patient did not undergo apoptosis when treated with Psora-4, PAP-1 and clofazimine; treatment induced

apoptosis only in the pathologic B cells, sparing the residual normal T cells. However, T lymphocytes from two B-CLL patients expressed relatively high levels of Kv1.3 but were resistant to treatment. This finding clearly suggested that specificity of the drugs towards pathologic cells is not merely due to higher expression of Kv1.3. A possibility could be the increase in mitochondrial ROS production, proposed to be involved in genesis and development of cancer (Ralph, Rodríguez-Enríquez, Neuzil, & Moreno-Sánchez, 2010). Indeed, a mild mitochondrial oxidative stress rendered healthy cells that express less Kv1.3 sensitive to permeant channel inhibitor-induced oxidative stress and death. Pre-incubation with a pro-oxidant stimulated mtROS production, but alone did not induce apoptosis. The subsequent addition of Kv1.3 inhibitors induced a rapid and significant increase in mtROS and subsequent apoptosis. On the other hand, pre-treatment of pathologic B cells with membrane-permeant catalase and superoxide dismutase abolished the apoptosis-inducing effect of Kv1.3 inhibitors. The same results were obtained also with residual T cells and pathologic B cells of the same patient.
These are clear evidences that mtKv1.3 inhibitors are potent and selective inducers of intrinsic apoptosis pathways in leukemic cells. Importantly, they kill B-CLL cells while sparing the residual T cells even of the same patient, and act on B-CLL cells independently of current prognostic factors. The selective effect seems to be given by the synergistic action of Kv1.3 expression level and of altered redox state in the malignant B-CLL cells.

2.7 Melanoma

Melanoma is a cancer that develops from the oncological transformation of melanocytes, the pigment-producing cells of the skin; however melanocytes are also found iris and rectum, where they can give rise to tumour as well. In the Western world, the majority of deaths related to skin cancer is caused by melanoma (Schadendorf & Hauschild, 2014).
In physiological conditions, melanocytes produce pigment that protects cells from sun-induced damages. However, sun exposure is the major risk factor. In fact, UV-light has a direct mutagenic role in melanoma pathogenesis and the mutational signature of UV-light induced mutation is cytosine to thymidine (C > T) transitions (induced by UVB) and guanine to thymidine (G > T) transitions (induced by UVA). Some mutations causing melanoma lack the typical UV signature; despite a causative role for UV-light cannot be excluded in these tumours. Also free radicals induced by UV-exposure can act as secondary mutagens (Hodis et al., 2012). However, like in all types of cancer, the transformation of melanocytes in malignant cells that give rise to melanoma is a set of exogenous and endogenous events.
A low percentage represents the familiar cases of melanoma tumour (~ 8%). In most of these cases (40%), mutation in cyclin-dependent kinase inhibitor 2A (CDKN2A) locus accounts for this familial predisposition (FitzGerald et al., 1996; Sheppard & McArthur, 2013). Inactivating mutations of the CDKN2A gene determine the loss of two important oncogenes: p53 and retinoblastoma associated protein (RB). In fact, this gene encodes two

distinct tumour suppressors p16INK4A and p14ARF. The first one maintains cell-cycle control by inhibiting inactivation of RB, while the second one prevents degradation of cellular tumour antigen p53. Thus the consequences of CDKN2A inactivating mutations lead to uncontrolled cell proliferation.

p53 is the most commonly mutated gene in human cancers (Kandoth et al., 2013). The p53 protein plays a central role in modulating cellular responses to diverse cellular stress signals (such as DNA damage, hypoxia and oncogenes activation) and contribute to cell-cycle arrest, senescence and apoptosis and other processes. Therefore, mutational loss of p53 function during carcinogenesis can lead to inappropriate cell growth, increased cell survival, and genetic instability (Bieging, Mello, & Attardi, 2014).

The higher percentage of melanomas (~90%) consists of sporadic cases. The genes responsible for these cases are several and their penetrance is a spectrum, ranging from high-risk allele to moderate risk alleles. The moderate risk alleles are more widespread in the population with mild effects while the high-risk alleles are less common but their effects arise almost always (Ward, Lazovich, & Hordinsky, 2012).

Common mutation giving rise to sporadic melanoma are those occurring at the level of genes such as BRAF (encoding for the proto-oncogene B-Raf) and NRAS (neuroblastoma RAS viral oncogene homologue, encoding for an enzyme).

The BRAF gene encodes a serine/threonine kinase implicated in the regulation of the signaling cascade and controlling cell proliferation, differentiation, migration and survival. NRAS is a member of the RAS gene family; they have GTPase activity and they are involved in the control of cell proliferation and cell growth. Other genes affected in melanoma are PTEN (encoding for the protein phosphatase and tensin homologue) and AKT (also known as protein kinase B) (Schadendorf & Hauschild, 2014).

In melanoma, metastatic progressions are also frequent, causing death in most cases. Metastasis can occur at late stage of the disease or be initiated already earlier (this last case is also called “parallel progression”). The mutational events described above (BRAF, NRAS etc.) are determinant not only for the driving the onset of melanoma but also for the development of metastases. Like in other types of cancers, metastatic events depend on secondary factors such as host defence, microenvironmental factors and survival of circulating cancer cells. It is still object of debate whether metastatic events depend on a population of cells deriving from a stem cell precursor. On the other hand it is clear that selected melanoma cell subpopulations are able to survive upon drug treatment and in adverse condition, accounting for the recurrence of cancer and for its spread in the body (Roesch et al., 2011).

Another feature conferring resistance to chemotherapeutic approaches and disease progression is the overexpression of anti-apoptotic proteins, like in several types of tumour. Moreover, melanoma cells probably use developmental programmes such as Notch or WNT signalling during metastasis to actively maintain their high mesenchymal cell-like plasticity.

The molecular understanding of genetic events leading to melanoma cancer and metastases, rapidly allowed the development of drugs targeting those protein involved in tumour progression. BRAF-inhibitors vemurafenib and

dabrafenib were used in clinical trials, determining survival benefit in patients and significantly improving prognosis for patients with advanced-stage metastatic disease.

2.8 Pancreatic ductal adenocarcinoma (PDAC)

Pancreatic ductal adenocarcinoma (PDAC) is the most common type of pancreatic cancer (90% of all pancreatic malignancies) and one of the most aggressive types of tumour.
It is relatively rare (about 2% of all cancer cases) and it is the fourth leading cause of cancer mortality in men and women. Life expectancy for patients affected by PDAC is at most five years after diagnosis, even if most of patients die within one year following cancer detection (Hariharan, Saied, & Kocher, 2008; Siegel, Miller, & Jemal, 2015). Due to the poor prognostic factor and due to the fact that pancreatic cancer usually has no symptoms, patients are diagnosed at late stage disease.
Several environmental factors account for the increase in predisposition to pancreatic cancer; among them smoking, obesity, chronic pancreatitis, diabetes mellitus and intake of alcohol have been reported. In patients with a PDAC family history genetic defects rather than environmental ones are the major cause. Some studies have shown an increased incidence of pancreatic cancer among patients with genetic mutations in *BRCA2, CDKN2A, PRSS1* and some other genes (Hidalgo, 2010).
Usually PDAC arises in the head of the pancreas, rapidly disseminating into surrounding tissues like spleen and peritoneal cavity and with metastasis to the liver and lungs. It evolves from precursors lesions present in pancreas. Precursors lesions mainly responsible for PDAC are three: pancreatic intraepithelial neoplasms (PanINs), mucinous cystic neoplasms (MCN), and intraductal papillary mucinous neoplasms (IPMN) (Hruban, Maitra, Kern, & Goggins, 2007). PanINs are the most common and well-characterized precursors.
The genetic causes leading to progression from precursors lesion to PDAC are several. Like in other types of cancer gene mutation, oncogene activation, inhibition of tumor suppressors and alteration in gene expression play a crucial role. Like in melanoma, the p16INK4A/CDKN2A gene show inactivating mutation very often (Caldas et al., 1994), as well as p53 (Kandoth et al., 2013).
Loss of function mutations have been identified also in p21, an important player in the control of cell cycle.
On the other hand, the activation/overexpression of oncogenes also accounts for tumor progression in PDAC. Among them, the member of the RAS family KRAS (V-Ki-ras2 Kirsten rat sarcoma viral oncogene homolog), represent the most frequent mutated oncogene in PDAC. Also BRAF is often expressed in PDAC, like in melanoma (see above) (Witkiewicz et al., 2015).
Moreover, several growth factor and the relative receptors have been reported to be overexpressed in PDAC, such as EGF (epidermal growth factors), IGF-I (insulin growth factor I), FGF (fibroblast growth factor) and

VEGF (vascular endothelial growth factor), together with their receptors (Ozawa, Friess, Tempia-Caliera, Kleeff, & Büchler, 2001).
Therapeutic options for pancreatic cancer are: surgery, chemotherapy, radiation therapy, targeted therapy, immune therapy, palliative therapy and personalized therapy. In order to choose which kind of therapy is the best for patients, the stage of pancreatic cancer is the most important factor. Unfortunately, only 20% of patients are candidates for surgery.
Concerning chemotherapy, it is the main treatment for metastatic unresectable pancreatic tumours. Chemotherapy is used as a neoadjuvant (before surgery) or as adjuvant (following surgery), but also when surgery is not an option. For about 20 years, the only option considered valid for the treatment of PDAC has been 5-fluorouracile (5-FU). Nowadays, the most diffused chemotherapy drug in clinical use is gemcitabine, administered alone or in combination with other chemotherapy such as 5-fluorouracile, capecitabine, platinum analogues and texane (Herreros-Villanueva, 2012). For all these molecules, the mechanism of action by which the cytotoxic effect is exerted is the block of DNA synthesis; therefore a lot of side effects are caused in the healthy tissues by these therapies.
We assessed whether PDAC cells express Kv1.3 and since it was the case, we addressed the effect of clofazimine in vitro and then in vivo (Zaccagnino, Managò et al, under submission, see attached manuscript).

2.9 Mitochondrial potassium homeostasis perturbing drug as antineoplastic agent: salinomycin

Salinomycin is a monocarboxyl polyether antibiotic obtained by isolation from fermentation products of *Streptomyces albus*. It is used commercially against coccidioisis, a gastrointestinal infection caused by a protozoan parasite, in poultry and as growth promoter for ruminants. In general, polyether antibiotic, also known as carboxyl ionophores, are broad spectrum antibiotics. They are active against a wide range of biological targets: bacterial, fungal, protozoan, viral, neoplastic, cardiovascular, immune system (Kevin II, Meujo, & Hamann, 2009) (a general description of ionophores can be found in section 2.3.1). They are effective even against many multi-drug resistant (MDR) pathological agents. Despite these characteristics and the fact that they are used at low doses in veterinary medicine, they have no use as clinical antibacterial agents in humans, due to their toxicity. The toxic effect in mammals is still not fully understood and it varies depending on the species, e.g. they are relatively less toxic for poultry, while horses and dogs are particularly sensitive to ionophores (Huczynski, 2012).
As well as other known carboxyl ionophores, salinomycin shows a typical structure characterized by a lipophilic outer part and an hydrophilic inner cavity; this latter contains oxygen atoms and carboxylic group which make possible the allocation of monovalent positively charged ions. Salinomycin shows preference for potassium ions but also Na^+ and H^+ can be carried by this ionophore. Obviously, this structure allows salinomycin to exert an effect at the plasma membrane and at the inner mitochondrial membrane whenever a K^+ gradient is present. The conformation of the ionophore-metal

complex between salinomycin and sodium was determined both by 2D-NMR spectroscopy in crystal structure, in organic solvent (Paulus, Kurz, Matter, & Vértesy, 1998) and in bicelles mimicking the membrane environment (Matsumori, Morooka, & Murata, 2007).

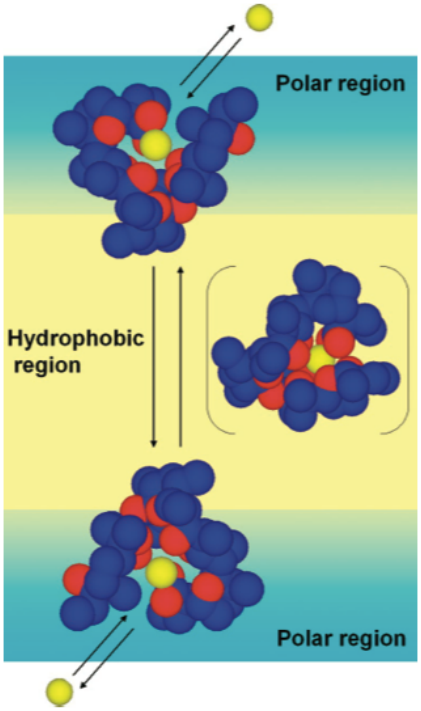

Figure 20: Model representing ion transport across lipid bilayer by salinomycin (from Matsumori et al., 2007)

Matsumori and colleagues proposed a working model of ion transport across biological membranes for salinomycin, on the basis of their work and of previous reports (Shown in figure 20). According to this model, salinomycin changes its conformation during its "trip" across biological lipid bilayers, assuming an open conformation in the polar region of the membrane, a closed conformation while diffusing into the hydrophobic region and then again an open conformation when it is on the other side of the membrane. The open conformation favours the association/dissociation of the ion, which in these conditions is weakly bound. Then the closed conformation ensures a strong bond of the ion to salinomycin and it is completely shielded from the non-polar lipid environment and can easily diffuse across the bilayer.
As described in the previous paragraphs ions are distributed in the cells at the steady state at precise concentrations in order to maintain cell homeostasis. The principal actors of this maintenance are ion channels. But, as explained above, other organic molecules (e.g. ionophores) can modify cell permeability. When this ion homeostasis is disrupted, cells activate some defence mechanisms (e.g.: apoptosis, necrosis). It is well known for example

that induction of volume loss in the cells (shrinkage) due for example to a massive efflux of potassium from the cytosol, where its concentration is higher than the extracellular space, leads to apoptosis; this event likely induces activation of caspases and endonucleases. On the contrary, apoptosis is prevented when potassium efflux is inhibited somehow (Bortner, Hughes, Cidlowski, & Carolina, 1997; Yu & Choi, 2000). Salinomycin exhibits several pharmacological effects acting on the alteration of ions balance across cell membranes, finally leading to cell death. Given its lipophilic structure, it is able to act also on intracellular membranes, disturbing also intracellular ion balance.

In 2009, the group of Weinberg announced that salinomycin, is a 100 times more effective killer of breast cancer stem-like cells than paclitaxel, a chemotherapeutic drug currently used to treat breast cancer. Salinomycin was selected following a screening of a library of 16000 natural and commercial chemical compounds for their ability to kill drug-resistant stem-like breast cancer cells. They found that only a small subset, including salinomycin and nigericin (known to be a H^+/K^+ exchanger), targeted cancer stem cells (CSCs) (Gupta et al., 2009). Nigericin, similarly to monensin, acts as an ionophore with a preference for potassium and mediates electroneutral exchange of potassium ions with protons at the level of the IMM. Notably, nigericin and monensin have been shown to induce apoptosis in human lung cancer and lymphoma cells(Andersson, Janson, Behnam-Motlagh, Henriksson, & Grankvist, 2006; Park, Kim, Kim, & Lee, 2003) suggesting that the common mechanism of polyether ionophore antibiotics to altering potassium homeostasis in the cytoplasm and mitochondria contributes to the induction of apoptosis in cancer cells. The work of Gupta and colleagues was really challenging since CSCs, integral to the development of tumour and responsible for the recurrence of cancer after remission, are very rare to find in a tumour cell population and is difficult to maintain them in culture. In this work, salinomycin was also administrated to mice and it was shown to decrease mammary tumour growth *in vivo*.

After the publication of this work, the interest around salinomycin has been growing. Indeed, its toxic effect towards cancer cells has been proved *in vitro* and *in vivo* also on various non-stem cancer cells like chronic lymphocytic leukemia (CLL) cells, colorectal cancer, hepatocellular carcinoma, lymphoma, human colon, breast, prostate, and lung (Kopp et al., 2014; D. Lu et al., 2011; Naujokat & Steinhart, 2012; Sánchez-Tilló et al., 2014; Verdoodt et al., 2012; Wang et al., 2012; Zhou et al., 2013).

On the other hand, the use of animal models revealed that salinomycin has a narrow therapeutic index. Daily salinomycin injection for 4 weeks at doses of 5mg/kg body weight was well tolerated, and no alterations on tissues and blood were revealed, but salinomycin induced neuropathy *in vivo* even at relatively low doses, such as sensory polyneuropathy with mechanical and cold allodynia, decreased sensory nerve action potential amplitudes, and loss of myelinated fibers in the sciatic nerve. However the treatment did not give rise to systemic toxicity Interestingly, it has been observed that inhibition of the mitochondrial Na^+/Ca^{2+} exchanger partially prevented the development of salinomycin-induced neuropathy *in vivo*, without reducing antineoplastic

efficacy of salinomycin (Boehmerle, Muenzfeld, Springer, Huehnchen, & Endres, 2014).

Extensive research has been undertaken to clarify the general mechanism(s) by which salinomycin induces apoptosis and blocks tumour growth. Several independent ways of action have been proposed to account for the cancer cell-killing ability of salinomycin. For example, it has been shown that salinomycin is able to inhibit proximal signalling; the Wnt/β-catenin transduction pathway plays a central role in the physiology of CSCs and undergoes aberrant activation during tumour development. It has been proposed that salinomycin acts blocking the phosphorylation of the Wnt coreceptor, lipoprotein receptor related protein 6 (LRP6), inducing its degradation. With the same mechanism nigericin exerts similar effects on CSCs (Lu et al., 2011). Another proposed mechanism is the induction of a marked increase in the expression of the pro-apoptotic protein NAG-1 upon salinomycin treatment (Arafat et al., 2013). Recent results point to salinomycin as a strong mTORC1 signaling antagonist, beside Wnt/β-catenin pathway inhibitor, in breast and prostate cancer cells, where mTORC1 is an essential effector in driving cell proliferation and oncogenic transformation (Lu & Li, 2014). Some opposing effects on autophagy have been proposed: salinomycin can be an initiator of autophagy in tumour cells (Reddy et al., 2013; Verdoodt et al., 2012), however it is also able to suppress late stages of autophagy, leading to accumulation of dysfunctional mitochondria with increased production of reactive oxygen species (ROS) (Klose et al., 2014).

Most important, salinomycin is expected to impact mitochondrial function thanks to its ability to act as an ionophore, but only few early studies addressed the direct effect of salinomycin on isolated mitochondria (Mitani, Yamanishi, Miyazaki, & Otake, 1976).

However, later works generally interpreted mitochondria-related effects of salinomycin in intact cells presuming that salinomycin acts similarly to valinomycin, a potassium selective ionophore mediating potassium influx into the mitochondria according to the electrochemical driving force. For example, effects like salinomycin-induced mitochondrial membrane potential depolarization and mitochondrial ROS production have been proposed to be compatible with influx of positively charged potassium ions (J. Kim, Choi, Kim, Kim, & Yoon, 2013; Verdoodt et al., 2012; Zhu et al., 2013). The chemical structure of salinomycin is however more similar to nigericin rather than to valinomycin; in fact, salinomycin structure shows a carboxyl group, which can act as the H+ carrier.

The mitochondrial effects of salinomycin have generally been addressed 12–48 h following addition of the drug, even though it is expected to reach quickly the IMM, as valinomycin and nigericin do when added to intact cells.

For all these reasons we decided to study the early effects of salinomycin on mitochondrial function as compared with valinomycin and nigericin, in primary human healthy cells, in cancer stem cell-like immortalized human mammary epithelial cells and in cancer cells. Our results reveal the short-term effects of salinomycin on mitochondrial function, contributing to the elucidation of its mechanism of action. The results indicate that salinomycin, when used above μM concentrations, exerts direct, mitochondrial effects, thus compromising cell survival (Managò et al., 2015).

2.10 A bacterial derived redox active compound as inducer of cell death

I previously described the principal features of apoptosis. The stimuli able to induce cell death are numerous and different and they can derive from inside the cells or be external. Many toxins existing in nature, clinically relevant because strongly pathogenic, lead to the induction of cell death when they come in contact with the host cells, therefore it is interesting to understand the mechanisms underlying these events in order to increase the therapeutic options.

One example is pyocyanin, a membrane-permeable pigment toxin released by the Gram-negative bacterium *Pseudomonas aeruginosa*. This bacterium has a ubiquitous nature and show ability to easily develop resistance to antibiotic. It is an important pathogen causing a wide range of acute and chronic infections, especially at the respiratory airways. *P. aeruginosa* rarely causes infection in the normal host, but its infections are clinically very serious for patients who are mechanically ventilated, immunosuppressed patients and for those with pneumonia, sepsis, or cystic fibrosis (Caldwell et al., 2009; Sadikot, Blackwell, Christman, & Prince, 2005).

It is therefore very important to define the first-line defence mechanisms of the immune system and their interaction with the pathogen.

A variety of factors accounts for the virulence of *P. aeruginosa,* including exoenzyme U (Exo U), a phospholipase A2, able to inhibit inflammasome activation by *P. aeruginosa*; pyocyanin, a heterocyclic nitrogen-containing phenazine, and rhamnolipid, another secreted small molecule, able to induce neutrophil necrosis; all these factors attack immune system cells and aim to establish a long-term lung infection (Lavoie, Wangdi, & Kazmierczak, 2012).

Pyocyanin is a redox-active compound capable of accepting and donating electrons. It was determined that in the sputum of patients with cystic fibrosis it is detected at concentrations till 100 μM (Wilson et al., 1988). In an *in vivo* model were mice were chronically exposed to pyocyanin it has been shown how it strongly contributes to oxidative stress and immunomodulation and how bacteria lacking pyocyanin are less pathogenic, a finding indicating that this factor plays an important role in *in vivo* infection. Moreover the solely chronic exposure to pyocyanin in mice can mimic the pulmonary pathophysiological phenotype observed in CF patients (Caldwell et al., 2009).

Due to its lipophilic structure, pyocyanin is able to cross biological membranes and this feature accounts for its role as a mobile electron carrier for *P. aeruginosa.* Under aerobic conditions, pyocyanin directly oxidizes reduced nicotinamide adenine dinucleotide phosphate (NADPH) in the host cell cytoplasm and donates accepted electrons to oxygen molecules to produce superoxide anions and reactive oxygen species (ROS). When pyocyanin is in its reduced state it is colourless; in this condition, it donates one electron to molecular oxygen thereby creating superoxide anion and turning into the blue, oxidized form (Rada, Lekstrom, Damian, Dupuy, & Leto, 2008).

Basically, pyocyanin shows to induce short-term effect and long-term effect when coming in contact with the respiratory epithelium. As soon as

pyocyanin is secreted by *P.aeruginosa,* it enters the cytosol of airway epithelial cells immediately determining production of oxygen species because of its direct interaction with NAD(P)H pool and molecular oxygen. Catalase, the enzyme responsible for the dismutation of superoxide to hydrogen peroxide, is inhibited by pyocyanin. These events in turn determine reduction of the level of reduced glutathione (GSH) and the level of ATP. The reduction of ATP levels has some consequence on energy metabolism of the cells, inhibiting for example ciliary beat frequency and CFTR (cystic fibrosis transmembrane conductance regulator) channel functions. Reduced NADPH levels inhibit antibacterial functions exerted by the enzymes dual oxidase 1 and 2 (Duox1 and Duox2), i.e. NADPH oxidases releasing hydrogen peroxide into the airway surface liquid, responsible for bacterial killing. Long-term effects of PYO manifest in transcriptional changes. Indeed, pyocyanin determines the inhibition of the transcription of genes acting as antioxidants and antimicrobial and enhances the transcription of the pro-inflammatory ones (Rada & Leto, 2013).

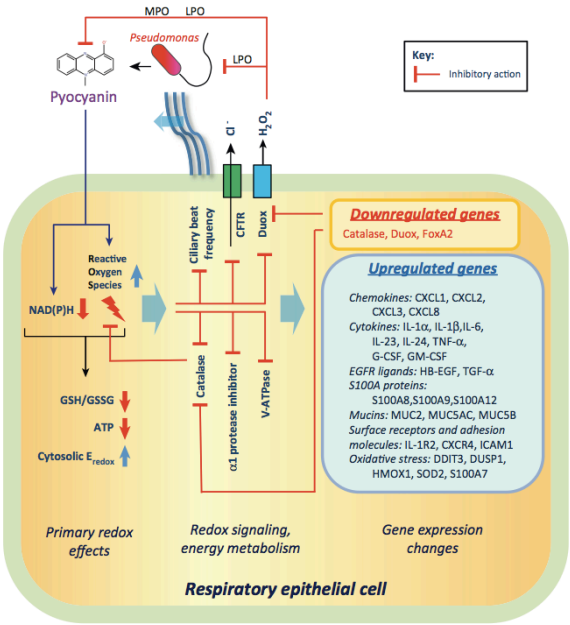

Figure 21: Model summarizing the several effects induced by pyocyanin produces by *Pseudomonas aeruginosa* in the respiratory epithelium (see text for details)(modified from Rada & Leto, 2013)
Abbreviations: CFTR, cystic fibrosis transmembrane conductance regulator; CXCL, chemokine (C-X-C motif) ligand; Duox, dual oxidase; E_{redox}, redox potential; EGFR, epidermal growth factor receptor; IL, interleukin; LPO, lactoperoxidase; MPO, myeloperoxidase; GSH, reduced glutathione; GSSG, oxidized glutathione

Given the fact that pyocyanin shows the ability to move electrons and to cross the biological membranes, it could have an effect also directly on intracellular component, for example mitochondria. Mitochondria are crucial for the production of ATP, the regulation of intracellular Ca^{2+} homeostasis,

and the production of ROS. They are also key participants in the regulation of cell death Indeed, it has been shown that pyocyanin determines mitochondrial ultra-structural changes, O_{2^-} and H_2O_2 formation at the level of mitochondria, time and concentration-dependent ATP cellular depletion upon treatment of the cells with pyocyanin and finally, to decease mitochondrial membrane potential, a finding suggesting a direct interaction between pyocyanin and mitochondria. Confocal microscopy studies indicated that extracellularly administered pyocyanin reaches mitochondria, where it may enhance the production of ROS and alter mitochondrial ultrastructure by mechanisms that are still poorly defined (O'Malley et al., 2003). One possibility could be that pyocyanin can directly interact with the respiratory chain complexes. Interestingly, Rho^0 yeast mutants, which are devoid of the mitochondrial respiratory chain, have been reported to be almost entirely resistant to pyocyanin under aerobic conditions (Barakat, Goubet, Manon, Berges, & Rosenfeld, 2014). Thus, elucidation of the mechanism by which pyocyanin affects mitochondrial functions in intact cells is an important but still largely unexplored topic.

The primary response of the lung during *P.aeruginosa* infection is carried out by macrophages and lymphocytes are involved in the primary response, but neutrophils are most important and absolutely necessary for the host's defence against the bacteria. This is also confirmed by the fact that in vivo, when mice are deprived of neutrophils (i.e. neutropenia), their lung are greatly sensitized to pulmonary *P. aeruginosa* infection, and the application of even very low numbers of bacteria to the lung is lethal for them (Koh, Priebe, Ray, Van Rooijen, & Pier, 2009). On the other hand, when mice are depleted of lymphocytes their mortality upon infection with *P. aeruginosa* increases only slightly (Dunkley, Clancy, Cripps, & Medicine, 1994), underling the critical role of neutrophils in the immune response against this bacterium. Therefore it is important to define the mechanism by which pyocyanin interacts with neutrophils of the host. Recently, new insights have been addressed, clarifying the effects of pyocyanin on mitochondria and identifying other molecular player involved in pyocyanin toxicity (Managò et al., 2015).

3. Bibliography

Abdul, M., Santo, A., & Hoosein, N. (2003). Activity of potassium channel-blockers in breast cancer. *Anticancer Research*, *23*(4), 3347–3351. Retrieved from http://eutils.ncbi.nlm.nih.gov/entrez/eutils/elink.fcgi?dbfrom=pubmed&id=12926074&retmode=ref&cmd=prlinks\npapers3://publication/uuid/61749EAC-21CA-485A-90C7-5771962F31C3

Abdul M, Hoosein N (2002) Voltage-gated potassium ion channels in colon cancer. Oncol. Rep. 9: 961-964

Abrahams, J. P., Leslie, An. G. W., Lutter, R., & John E. Walker. (1994). © 19 9 4 Nature Publishing Group. *Nature*, *370*, 621–628.

Acin-Perez, R., & Enriquez, J. a. (2014). The function of the respiratory supercomplexes: The plasticity model. *Biochimica et Biophysica Acta - Bioenergetics*, *1837*(4), 444–450. doi:10.1016/j.bbabio.2013.12.009

Ahmad, K. A., Iskandar, K. B., Hirpara, J. L., Clement, M. V, & Pervaiz, S. (2004). Hydrogen peroxide-mediated cytosolic acidification is a signal for mitochondrial translocation of Bax during drug-induced apoptosis of tumor cells. *Cancer Res*, *64*(21), 7867–7878. doi:10.1158/0008-5472.CAN-04-0648

Alizadeh, A. A., Eisen, M. B., Davis, R. E., Ma, C., Lossos, I. S., Rosenwald, A., … Staudt, L. M. (2000). Distinct types of diffuse large B-cell lymphoma identi ® ed by gene expression pro ® ling, *403*(February).

Alnemri, E. S., Livingston, D. J., Nicholson, D. W., Salvesen, G., Thornberry, N. A., Wong, W. W., & Yuan, J. (1996). Human ICE/CED-3 Protease Nomenclature. *Cell*, *87*(2), 171. doi:10.1016/S0092-8674(00)81334-3

Andersen, O. S. (2008). Perspectives on how to drug an ion channel. *The Journal of General Physiology*, *131*(5), 395–7. doi:10.1085/jgp.200810012

Andersson, B., Janson, V., Behnam-Motlagh, P., Henriksson, R., & Grankvist, K. (2006). Induction of apoptosis by intracellular potassium ion depletion: Using the fluorescent dye PBFI in a 96-well plate method in cultured lung cancer cells. *Toxicology in Vitro*, *20*(6), 986–994. doi:10.1016/j.tiv.2005.12.013

Annis, M. G., Soucie, E. L., Dlugosz, P. J., Cruz-Aguado, J. a, Penn, L. Z., Leber, B., & Andrews, D. W. (2005). Bax forms multispanning monomers that oligomerize to permeabilize membranes during apoptosis. *The EMBO Journal*, *24*(12), 2096–2103. doi:10.1038/sj.emboj.7600675

Arafat, K., Iratni, R., Takahashi, T., Parekh, K., Al Dhaheri, Y., Adrian, T. E., & Attoub, S. (2013). Inhibitory Effects of Salinomycin on Cell Survival, Colony Growth, Migration, and Invasion of Human Non-Small Cell Lung Cancer A549 and LNM35: Involvement of NAG-1. *PloS One*, *8*(6), e66931. doi:10.1371/journal.pone.0066931

Arcangeli, a, Crociani, O., Lastraioli, E., Masi, A., Pillozzi, S., & Becchetti, A. (2009). Targeting ion channels in cancer: a novel frontier in antineoplastic therapy. *Current Medicinal Chemistry*, *16*(1), 66–93. doi:10.2174/092986709787002835

Arcangeli, A., & Becchetti, A. (2010). New trends in cancer therapy: Targeting ion channels and transporters. *Pharmaceuticals*, *3*(2), 1202–1224. doi:10.3390/ph3041202

Arcangeli, A., & Becchetti, A. (2015). Novel perspectives in cancer therapy: Targeting ion channels. *Drug Resistance Updates*, *21-22*(4), 11–19. doi:10.1016/j.drup.2015.06.002

Arsenijevic, D., Onuma, H., Pecqueur, C., Raimbault, S., Manning, B. S., Miroux, B., … Ricquier, D. (2000). Disruption of the uncoupling protein-2 gene in mice reveals a role in immunity and reactive oxygen species production. *Nature Genetics*, *26*(4), 435–439. doi:10.1038/82565

Artym, V. V, & Petty, H. R. (2002). Molecular proximity of Kv1.3 voltage-gated potassium channels and beta(1)-integrins on the plasma membrane of melanoma cells: effects of cell adherence and channel blockers. *The Journal of General Physiology*, *120*(1), 29–37. doi:10.1085/jgp.20028607

Ashkenazi, A. (1998). Death Receptors: Signaling and Modulation. *Science*, *281*(5381), 1305–1308. doi:10.1126/science.281.5381.1305

Azzone, G. F., Pozzan, T., S. Massari, M. Bragadin, & Dell'antone, P. (1977). H^+/site ratio and steady state distribution of divalent cations in mitochondria. *FEBS Lett.* 78: 21–24.

Barakat, R., Goubet, I., Manon, S., Berges, T., & Rosenfeld, E. (2014). Unsuspected pyocyanin effect in yeast under anaerobiosis. *MicrobiologyOpen*, *3*(1), 1–14. doi:10.1002/mbo3.142

Bednarczyk, P., Kowalczyk, J. E., Beresewicz, M., Dolowy, K., Szewczyk, A., & Zablocka, B. (2010). Identification of a voltage-gated potassium channel in gerbil hippocampal mitochondria. *Biochem Biophys Res Commun*, *397*(3), 614–620. doi:10.1016/j.bbrc.2010.06.011

Beeton, C., Wulff, H., Barbaria, J., Clot-Faybesse, O., Pennington, M., Bernard, D., … Béraud, E. (2001). Selective blockade of T lymphocyte K(+) channels ameliorates experimental autoimmune encephalomyelitis, a model for multiple sclerosis. *Proceedings of the National Academy of Sciences of the United States of America*, *98*(24), 13942–13947. doi:10.1073/pnas.241497298

Bell, E. L., Klimova, T. a., Eisenbart, J., Moraes, C. T., Murphy, M. P., Budinger, G. R. S., & Chandel, N. S. (2007). The Qo site of the mitochondrial complex III is required for the transduction of hypoxic signaling via reactive oxygen species production. *The Journal of Cell Biology*, *177*(6), 1029–1036. doi:10.1083/jcb.200609074

Bernardi, P. (1999). Mitochondrial transport of cations: channels, exchangers, and permeability transition. *Physiological Reviews*, *79*(4), 1127–1155.

Bernardi, P. (2013). The mitochondrial permeability transition pore: a mystery solved? *Frontiers in Physiology*, *4*(May), 1–12. doi:10.3389/fphys.2013.00095

Beutner, G., Rück, A., Riede, B., & Brdiczka, D. (1998). Complexes between porin, hexokinase, mitochondrial creatine kinase and adenylate translocator display properties of the permeability transition pore. Implication for regulation of permeability transition by the kinases. *Biochimica et Biophysica Acta - Biomembranes*, *1368*(1), 7–18. doi:10.1016/S0005-2736(97)00175-2

Bieging, K. T., Mello, S. S., & Attardi, L. D. (2014). Unravelling mechanisms of p53-mediated tumour suppression. *Nature Reviews. Cancer*, *14*(5), 359–70. doi:10.1038/nrc3711

Boehmerle, W., Muenzfeld, H., Springer, A., Huehnchen, P., & Endres, M. (2014). Specific targeting of neurotoxic side effects and pharmacological profile of the novel cancer stem cell drug salinomycin in mice. *Journal of Molecular Medicine*, *92*(8), 889–900. doi:10.1007/s00109-014-1155-0

Bortner, C. D., Hughes, F. M., Cidlowski, J. A., & Carolina, N. (1997). A Primary Role for K and Na Efflux in the Activation of Apoptosis *, *272*(51), 32436–32442.

Boyer, P. D. (1997). the Atp Synthase — a Splendid. *Sites The Journal Of 20Th Century Contemporary French Studies*.

Brevet, M., Fucks, D., Chatelain, D., Regimbeau, J.-M., Delcenserie, R., Sevestre, H., & Ouadid-Ahidouch, H. (2009). Deregulation of 2 potassium channels in pancreas adenocarcinomas: implication of KV1.3 gene promoter methylation. *Pancreas*, *38*(6), 649–654. doi:10.1097/MPA.0b013e3181a56ebf

Brevet, M., Haren, N., Sevestre, H., Merviel, P., & Ouadid-Ahidouch, H. (2009). DNA Methylation of K_v1.3 Potassium Channel Gene Promoter is Associated with Poorly Differentiated Breast Adenocarcinoma. *Cellular Physiology and Biochemistry*, *24*(1-2), 25–32. doi:10.1159/000227810

Broekemeier, K. M., Dempsey, M. E., & Pfeiffer, D. R. (1989). Cyclosporin A is a potent inhibitor of the inner membrane permeability transition in liver mitochondria. *The Journal of Biological Chemistry*, *264*(14), 7826–7830.

Brierley, G.P., Baysal, K., Jung, D.W., (1994). Cation transport systems in mitochon- dria: Na+ and K+ uniports and exchangers. *J. Bioenerg. Biomembr.* 26 519–526.

Cain, K., Brown, D. G., Langlais, C., & Cohen, G. M. (1999). Caspase activation involves the formation of the aposome, a large (approximately 700 kDa) caspase-activating complex. *The Journal of Biological Chemistry*, *274*(32), 22686–92. doi:10.1074/jbc.274.32.22686

Caldas, C., Hahn, S. A., da Costa, L. T., Redston, M. S., Schutte, M., Seymour, A. B., … Kern, S. E. (1994). Frequent somatic mutations and homozygous deletions of the p16 (MTS1) gene in pancreatic adenocarcinoma. *Nature Genetics*, *8*(1), 27–32. doi:10.1038/ng0994-27

Caldwell, C. C., Chen, Y., Goetzmann, H. S., Hao, Y., Borchers, M. T., Hassett, D. J., … Lau, G. W. (2009). Pseudomonas aeruginosa Exotoxin Pyocyanin Causes Cystic Fibrosis Airway Pathogenesis. *The American Journal of Pathology*, *175*(6), 2473–2488. doi:10.2353/ajpath.2009.090166

Carroll, J., Fearnley, I. M., Skehel, J. M., Shannon, R. J., Hirst, J., & Walker, J. E. (2006). Bovine complex I is a complex of 45 different subunits. *Journal of Biological Chemistry*, *281*(43), 32724–32727. doi:10.1074/jbc.M607135200

Cecchini, G., Schröder, I., Gunsalus, R. P., & Maklashina, E. (2002). Succinate dehydrogenase and fumarate reductase from Escherichia coli. *Biochimica et Biophysica Acta*, *1553*(1-2), 140–157. doi:S0005272801002389 [pii]

Chance, B., Sies, H., & Boveris, a. (1979). Hydroperoxide metabolism in mammalian organs. *Physiological Reviews*, *59*(3), 527–605.

Chandy, K. G., Wulff, H., Beeton, C., Pennington, M., George, a, & Cahalan, M. D. (2009). NIH Public Access, *25*(5), 280–289. doi:10.1016/j.tips.2004.03.010.K

Chaudhri, G., Clark, I. a., Hunt, N. H., Cowden, W. B., & Ceredig, R. (1986). Effect of antioxidants on primary alloantigen-induced T cell activation and proliferation. *Journal of Immunology (Baltimore, Md. : 1950)*, *137*(8), 2646–2652.

Chen, C., & Dickman, M. B. (2005). Proline suppresses apoptosis in the fungal pathogen Colletotrichum trifolii. *Proceedings of the National Academy of Sciences of the United States of America*, *102*, 3459–3464. doi:10.1073/pnas.0407960102

Choe, S. (2002). Ion channel structurepotassium channel structures. *Nature Reviews Neuroscience*, *3*(2), 115–121. doi:10.1038/nrn727

Choe, S., Cushman, S., Baker, KA., Pfaffinger, P., Excitability is mediated by the T1 domain of the voltage-gated potassium channel (2002). *Novartis Found Symp.*;245:169–75; discussion 175–7, 261–4.

Coleman, S. K., Newcombe, J., Pryke, J., & Dolly, J. O. (1999). Subunit composition of Kv1 channels in human CNS. *Journal of Neurochemistry*, *73*(2), 849–58. doi:10.1046/j.1471-4159.1999.0730849.x

Cory, S., & Adams, J. M. (2002). The Bcl2 family: regulators of the cellular life-or-death switch. *Nature Reviews. Cancer*, *2*(9), 647–656. doi:10.1038/nrc883

Crompton, M., Virji, S., & Ward, J. M. (1998). Cyclophilin-D binds strongly to complexes of the voltage-dependent anion channel and the adenine nucleotide translocase to form the permeability transition pore. *European Journal of Biochemistry / FEBS*, *258*(2), 729–735. doi:10.1046/j.1432-1327.1998.2580729.x

Davies, K. J. (1987). Protein damage and degradation by oxygen radicals. I. general aspects. *The Journal of Biological Chemistry*, *262*(20), 9895–

9901. Retrieved from http://www.ncbi.nlm.nih.gov/pubmed/3036875

DeCoursey, T.E., Chandy, KG., Gupta, S., Cahalan, MD. (1984) Voltage-gated K+ channels in human T lymphocytes: a role in mitogenesis? *Nature* 307(5950):465-8

Dilisa, F., & Bernardi, P. (2006). Mitochondria and ischemia–reperfusion injury of the heart: Fixing a hole. *Cardiovascular Research*, *70*(2), 191–199. doi:10.1016/j.cardiores.2006.01.016

Doyle, D. a. (1998). The Structure of the Potassium Channel: Molecular Basis of K+ Conduction and Selectivity. *Science*, *280*(5360), 69–77. doi:10.1126/science.280.5360.69

Dröge, W. (2002). Free radicals in the physiological control of cell function. *Physiological Reviews*, *82*(1), 47–95. doi:10.1152/physrev.00018.2001

Dunkley, M. L., Clancy, R. L., Cripps, A. W., & Medicine, F. (1994). Pseudomonas aeruginosa from the lung, 362–369.

Folander K, Douglass J, Swanson R. (1994). Confirmation of the assignment of the gene encoding Kv1.3, a voltage-gated potassium channel (KCNA3) to the proximal short arm of human chromosome 1. *Genomics*.;23(1):295–6. doi:10.1006/geno.1994.1500.

FitzGerald, M. G., Harkin, D. P., Silva-Arrieta, S., MacDonald, D. J., Lucchina, L. C., Unsal, H., … Haber, D. a. (1996). Prevalence of germ-line mutations in p16, p19ARF, and CDK4 in familial melanoma: analysis of a clinic-based population. *Proceedings of the National Academy of Sciences of the United States of America*, *93*(16), 8541–5. doi:10.1073/pnas.93.16.8541

Fraser, S. P., & Pardo, L. A. (2008). Ion channels: functional expression and therapeutic potential in cancer. Colloquium on Ion Channels and Cancer. *EMBO Reports*, *9*(6), 512–5. doi:10.1038/embor.2008.75

Friedman, J. R., & Nunnari, J. (2014). Mitochondrial form and function. *Nature*, *505*(7483), 335–43. doi:10.1038/nature12985

Garlid, K. D., & Paucek, P. (2003). Mitochondrial potassium transport: the K+ cycle. *Biochimica et Biophysica Acta (BBA) - Bioenergetics*, *1606*(1-3), 23–41. doi:10.1016/S0005-2728(03)00108-7

Garlid, K.D., (1988). Sodium/proton antiporters in the mitochondrial inner membrane *Adv. Exp. Med. Biol*. 232 37–46.

Gazula, V., Strumbos, J., & Mei, X. (2010). Localization of Kv1. 3 channels in presynaptic terminals of brainstem auditory neurons. *Journal of …*, *518*(16), 3205–3220. doi:10.1002/cne.22393.Localization

George Chandy, K., Wulff, H., Beeton, C., Pennington, M., Gutman, G. A., & Cahalan, M. D. (2004). K+ channels as targets for specific immunomodulation. *Trends in Pharmacological Sciences*, *25*(5), 280–289. doi:10.1016/j.tips.2004.03.010

Giorgio, V., Bisetto, E., Soriano, M. E., Dabbeni-Sala, F., Basso, E., Petronilli, V., … Lippe, G. (2009). Cyclophilin D modulates mitochondrial F0F1-ATP

synthase by interacting with the lateral stalk of the complex. *The Journal of Biological Chemistry*, *284*(49), 33982–8. doi:10.1074/jbc.M109.020115

Giorgio, V., von Stockum, S., Antoniel, M., Fabbro, A., Fogolari, F., Forte, M., … Bernardi, P. (2013). Dimers of mitochondrial ATP synthase form the permeability transition pore. *Proceedings of the National Academy of Sciences*, *110*(15), 5887–5892. doi:10.1073/pnas.1217823110

Grissmer, S., Nguyen, A. N., Aiyar, J., Hanson, D. C., Mather, R. J., Gutman, G. A., … George Chandy, K. (1994). Pharmacological Characterization of Five Cloned Voltage-Gated Expressed in Mammalian Cell Lines. *Molecular Pharmacology*, *45*, 1227–1234.

Grivennikova, V. G., & Vinogradov, A. D. (2006). Generation of superoxide by the mitochondrial Complex I. *Biochimica et Biophysica Acta (BBA) - Bioenergetics*, *1757*(5-6), 553–561. doi:10.1016/j.bbabio.2006.03.013

Grossman, L. I., & Lomax, M. I. (1997). Nuclear genes for cytochrome c oxidase. *Biochimica Et Biophysica Acta-Gene Structure And Expression*, *1352*, 174. Retrieved from <Go to ISI>://A1997XC75900010

Grunnet, M., Rasmussen, H. B., Hay-Schmidt, A., & Klaerke, D. A. (2003). The voltage-gated potassium channel subunit, Kv1.3, is expressed in epithelia. *Biochimica et Biophysica Acta (BBA) - Biomembranes*, *1616*(1), 85–94. doi:10.1016/S0005-2736(03)00198-6

Gulbins, E., Sassi, N., Grassmè, H., Zoratti, M., & Szabò, I. (2010). Role of Kv1.3 mitochondrial potassium channel in apoptotic signalling in lymphocytes. *Biochimica et Biophysica Acta (BBA) - Bioenergetics*, *1797*(6-7), 1251–1259. doi:10.1016/j.bbabio.2010.01.018

Gupta, P. B., Onder, T. T., Jiang, G., Tao, K., Kuperwasser, C., Weinberg, R. a., & Lander, E. S. (2009). Identification of Selective Inhibitors of Cancer Stem Cells by High-Throughput Screening. *Cell*, *138*(4), 645–659. doi:10.1016/j.cell.2009.06.034

Gutman, G. A., Chandy, K. G., Grissmer, S., Lazdunski, M., McKinnon, D., Pardo, L. A., … Wang, X. (2005). International Union of Pharmacology. LIII. Nomenclature and molecular relationships of voltage-gated potassium channels. *Pharmacological Reviews*, *57*(4), 473–508. doi:10.1124/pr.57.4.10

Hanahan, D., & Weinberg, R. (2000). The Hallmarks of Cancer Review University of California at San Francisco, *100*, 57–70.

Hanahan, D., & Weinberg, R. A. (2011). Hallmarks of cancer: the next generation. *Cell*, *144*(5), 646–74. doi:10.1016/j.cell.2011.02.013

Hariharan, D., Saied, A., & Kocher, H. M. (2008). Analysis of mortality rates for pancreatic cancer across the world. *Hpb*, *10*(1), 58–62. doi:10.1080/13651820701883148

Heinen, A., Aldakkak, M., Stowe, D. F., Rhodes, S. S., Riess, M. L., Varadarajan, S. G., & Camara, A. K. S. (2007). Reverse electron flow-induced ROS

production is attenuated by activation of mitochondrial Ca2+-sensitive K+ channels. *American Journal of Physiology. Heart and Circulatory Physiology*, *293*(3), H1400–7. doi:10.1152/ajpheart.00198.2007

Hengartner. (1997). Apoptosis. CED-4 is a stranger no more. *Nature*, *388*(August), 728–729. doi:10.1038/41873

Hengartner, M. O. (2000). The biochemistry of apoptosis. *Nature*, *407*(6805), 770–776.

Herreros-Villanueva, M. (2012). Adjuvant and neoadjuvant treatment in pancreatic cancer. *World Journal of Gastroenterology*, *18*(14), 1565. doi:10.3748/wjg.v18.i14.1565

Hidalgo, M. (2010). Pancreatic Cancer. *New England Journal of Medicine*, *362*(17), 1605–1617. doi:10.1056/NEJMra0901557

Hirst, J., King, M. S., & Pryde, K. R. (2008). The production of reactive oxygen species by complex I. *Biochemical Society Transactions*, *36*(5), 976–980. doi:10.1042/BST0360976

Hodis, E., Watson, I. R., Kryukov, G. V, Arold, S. T., Imielinski, M., Theurillat, J.-P., … Chin, L. (2012). A landscape of driver mutations in melanoma. *Cell*, *150*(2), 251–63. doi:10.1016/j.cell.2012.06.024

Hofmann, G., Bernabei, P. A., Crociani, O., Cherubini, A., Guasti, L., Pillozzi, S., … Arcangeli, A. (2001). HERG K+ Channels Activation during 1Integrin-mediated Adhesion to Fibronectin Induces an Up-regulation of v 3 Integrin in the Preosteoclastic Leukemia Cell Line FLG 29.1. *Journal of Biological Chemistry*, *276*(7), 4923–4931. doi:10.1074/jbc.M005682200

Holt, P. J., Morgan, D. J., & Sazanov, L. a. (2003). The Location of NuoL and NuoM Subunits in the Membrane Domain of the Escherichia coli Complex I. *The Journal of Biological Chemistry*, *278*(44), 43114–43120. doi:10.1074/jbc.M308247200

Hoshi, T., Zagotta, WN., Aldrich, L.W. (1990) Biophysical and molecular mechanisms of Shaker potassium channel inactivation. *Science* 250(4980):533-8.

Hruban, R. H., Maitra, A., Kern, S. E., & Goggins, M. (2007). Precursors to pancreatic cancer. *Gastroenterology Clinics of North America*, *36*(4), 831–49, vi. doi:10.1016/j.gtc.2007.08.012

Huang, X., & Jan, L. Y. (2014). Targeting potassium channels in cancer. *The Journal of Cell Biology*, *206*(2), 151–162. doi:10.1083/jcb.201404136

Huczynski, A. (2012). Salinomycin: a new cancer drug candidate. *Chemical Biology & Drug Design*, *79*(3), 235–8. doi:10.1111/j.1747-0285.2011.01287.x

Hulsmans, M., Van Dooren, E., & Holvoet, P. (2012). Mitochondrial Reactive Oxygen Species and Risk of Atherosclerosis. *Current Atherosclerosis Reports*, *14*(3), 264–276. doi:10.1007/s11883-012-0237-0

Isacoff, E.Y, Jan, Y.N. & Jan, L.Y. (1991) Putative receptor for the cytoplasmic

inactivation gate in the Shaker K+ channel. *Nature* 353:86-90.

Jang, S. H., Kang, K.-S., Ryu, P. D., & Lee, S. Y. (2009). Kv1.3 voltage-gated K(+) channel subunit as a potential diagnostic marker and therapeutic target for breast cancer. *BMB Reports*, *42*(8), 535–539.

Jürgen, B., Szabó, I., Jekle, A., & Gulbins, E. (2002). Actinomycin D-induced apoptosis involves the potassium channel Kv1.3. *Biochemical and Biophysical Research Communications*, *295*(2), 526–531.

Kaczorowski, G. J., McManus, O. B., Priest, B. T., & Garcia, M. L. (2008). Ion channels as drug targets: the next GPCRs. *The Journal of General Physiology*, *131*(5), 399–405. doi:10.1085/jgp.200709946

Kandoth, C., McLellan, M. D., Vandin, F., Ye, K., Niu, B., Lu, C., … Ding, L. (2013). Mutational landscape and significance across 12 major cancer types. *Nature*, *502*(7471), 333–9. doi:10.1038/nature12634

Kerr, J. F., Wyllie, A. H., & Currie, A. R. (1972). Apoptosis: a basic biological phenomenon with wide-ranging implications in tissue kinetics. *British Journal of Cancer*, *26*(4), 239–57. doi:10.1111/j.1365-2796.2005.01570.x

Kevin II, D. a, Meujo, D. A., & Hamann, M. T. (2009). Polyether ionophores: broad-spectrum and promising biologically active molecules for the control of drug-resistant bacteria and parasites. *Expert Opinion on Drug Discovery*, *4*, 109–146. doi:10.1517/17460440802661443

Kim, I., Rodriguez-Enriquez, S., & Lemasters, J. J. (2007). Selective degradation of mitochondria by mitophagy. *Archives of Biochemistry and Biophysics*, *462*(2), 245–53. doi:10.1016/j.abb.2007.03.034

Kim, J., Choi, A., Kim, Y. K., Kim, H. S., & Yoon, S. (2013). Low Amount of Salinomycin Greatly Increases Akt Activation , but Reduces Activated p70S6K Levels, 17304–17318. doi:10.3390/ijms140917304

Klose, J., Stankov, M. V., Kleine, M., Ramackers, W., Panayotova-Dimitrova, D., Jäger, M. D., … Vondran, F. W. R. (2014). Inhibition of Autophagic Flux by Salinomycin Results in Anti-Cancer Effect in Hepatocellular Carcinoma Cells. *PLoS ONE*, *9*(5), e95970. doi:10.1371/journal.pone.0095970

Koch, R. O., Wanner, S. G., Koschak, A., Hanner, M., Schwarzer, C., Kaczorowski, G. J., … Knaus, H. G. (1997). Complex subunit assembly of neuronal voltage-gated K+ channels. Basis for high-affinity toxin interactions and pharmacology. *J Biol Chem*, *272*(44), 27577–27581. doi:10.1074/jbc.272.44.27577

Koh, A. Y., Priebe, G. P., Ray, C., Van Rooijen, N., & Pier, G. B. (2009). Inescapable need for neutrophils as mediators of cellular innate immunity to acute Pseudomonas aeruginosa pneumonia. *Infection and Immunity*, *77*(12), 5300–5310. doi:10.1128/IAI.00501-09

Kopp, F., Hermawan, A., Oak, P. S., Herrmann, A., Wagner, E., & Roidl, A. (2014). Salinomycin treatment reduces metastatic tumor burden by

hampering cancer cell migration. *Molecular Cancer*, *13*(1), 1–6. doi:10.1186/1476-4598-13-16

Koschak, a, Bugianesi, R. M., Mitterdorfer, J., Kaczorowski, G. J., Garcia, M. L., & Knaus, H. G. (1998). Subunit composition of brain voltage-gated potassium channels determined by hongotoxin-1, a novel peptide derived from Centruroides limbatus venom. *The Journal of Biological Chemistry*, *273*(5), 2639–2644. doi:10.1074/jbc.273.5.2639

Ksenzenko, M., Konstantinov, A. a., Khomutov, G. B., Tikhonov, A. N., & Ruuge, E. K. (1983). Effect of electron transfer inhibitors on superoxide generation in the cytochrome bc1 site of the mitochondrial respiratory chain. *FEBS Letters*, *155*(1), 19–24. doi:10.1016/0014-5793(83)80200-2

Kudin, A. P., Debska-vielhaber, G., & Kunz, W. S. (2005). Characterization of superoxide production sites in isolated rat brain and skeletal muscle mitochondria, *59*, 163–168. doi:10.1016/j.biopha.2005.03.012

Kulawiak, B., Kudin, A. P., Szewczyk, A., & Kunz, W. S. (2008). BK channel openers inhibit ROS production of isolated rat brain mitochondria. *Experimental Neurology*, *212*(2), 543–7. doi:10.1016/j.expneurol.2008.05.004

Kussmaul, L., & Hirst, J. (2006). The mechanism of superoxide production by NADH:ubiquinone oxidoreductase (complex I) from bovine heart mitochondria. *Proceedings of the National Academy of Sciences of the United States of America*, *103*(20), 7607–12. doi:10.1073/pnas.0510977103

Lambert, a. J., & Brand, M. D. (2004). Inhibitors of the Quinone-binding Site Allow Rapid Superoxide Production from Mitochondrial NADH:Ubiquinone Oxidoreductase (Complex I). *Journal of Biological Chemistry*, *279*(38), 39414–39420. doi:10.1074/jbc.M406576200

Lan, M., & Shi, Y. (2005). Expression of Delayed Rectifier Potassium Channels and Their Possible Roles in Proliferation of Human Gastric Cancer Cells ABBREVIATIONS KEY WORDS RIB, (December), 1342–1347.

Lane, N., & Martin, W. (2010). The energetics of genome complexity. *Nature*, *467*(7318), 929–934. doi:10.1038/nature09486

Lang, F., Föller, M., Lang, K. S., Lang, P. a., Ritter, M., Gulbins, E., … Huber, S. M. (2005). Ion channels in cell proliferation and apoptotic cell death. *Journal of Membrane Biology*, *205*(3), 147–157. doi:10.1007/s00232-005-0780-5

Lang, F., Gulbins, E., Szabo, I., Lepple-Wienhues, A., Huber, S. M., Duranton, C., … Wieder, T. (2004). Cell volume and the regulation of apoptotic cell death. *J Mol Recognit*, *17*(5), 473–480. doi:10.1002/jmr.705

Lavoie, E., Wangdi, T., & Kazmierczak, B. (2012). NIH Public Access, *13*, 1133–1145. doi:10.1016/j.micinf.2011.07.011.Innate

Leanza, L., Biasutto, L., Managò, A., Gulbins, E., Zoratti, M., & Szabò, I. (2013). Intracellular ion channels and cancer. *Frontiers in Physiology*, *4 SEP*.

doi:10.3389/fphys.2013.00227

Leanza, L., Henry, B., Sassi, N., Zoratti, M., Chandy, K. G., Gulbins, E., & Szabò, I. (2012). Inhibitors of mitochondrial Kv1.3 channels induce Bax/Bak-independent death of cancer cells. *EMBO Molecular Medicine*, *4*(7), 577–593. doi:10.1002/emmm.201200235

Leanza, L., Managò, A., Zoratti, M., Gulbins, E., & Szabo, I. (2015). Pharmacological targeting of ion channels for cancer therapy: In vivo evidences. *Biochimica et Biophysica Acta (BBA) - Molecular Cell Research*. doi:10.1016/j.bbamcr.2015.11.032

Leanza, L., Trentin, L., Becker, K. a, Frezzato, F., Zoratti, M., Semenzato, G., … Szabo, I. (2013). Clofazimine, Psora-4 and PAP-1, inhibitors of the potassium channel Kv1.3, as a new and selective therapeutic strategy in chronic lymphocytic leukemia. *Leukemia*, *27*(8), 1782–1785. doi:10.1038/leu.2013.56

Leanza, L., Venturini, E., Kadow, S., Carpinteiro, A., Gulbins, E., & Becker, K. A. (2015). Targeting a mitochondrial potassium channel to fight cancer. *Cell Calcium*, *58*(1), 131–8. doi:10.1016/j.ceca.2014.09.006

Leanza, L., Zoratti, M., Gulbins, E., & Szabo, I. (2012). Induction of apoptosis in macrophages via Kv1.3 and Kv1.5 potassium channels. *Curr Med Chem*, *19*(31), 5394–5404. doi:CMC-EPUB-20120801-11 [pii]

Li, N. (2003). Mitochondrial Complex I Inhibitor Rotenone Induces Apoptosis through Enhancing Mitochondrial Reactive Oxygen Species Production. *Journal of Biological Chemistry*, *278*(10), 8516–8525. doi:10.1074/jbc.M210432200

Liochev, S. I. (2013). Reactive oxygen species and the free radical theory of aging. *Free Radical Biology and Medicine*, *60*, 1–4. doi:10.1016/j.freeradbiomed.2013.02.011

Liou, M.-Y., & Storz, P. (2010). *Reactive oxygen species in cancer*. *Free Radic Res.* (Vol. 44). doi:10.3109/10715761003667554.Reactive

Liu, H. (2005). Redox-Dependent Transcriptional Regulation. *Circulation Research*, *97*(10), 967–974. doi:10.1161/01.RES.0000188210.72062.10

Liu, Y., Fiskum, G., & Schubert, D. (2002). Generation of reactive oxygen species by the mitochondrial electron transport chain. *J Neurochem*, *80*(5), 780–787. Retrieved from http://www.ncbi.nlm.nih.gov/pubmed/11948241

Lodish, H., Berk, A., Kaiser, C. A. & Krieger, M. (2006) Molecular cell biology, Sixth Edition, W.H. Freeman

Lu, D., Choi, M. Y., Yu, J., Castro, J. E., Kipps, T. J., & Carson, D. A. (2011). Salinomycin inhibits Wnt signaling and selectively induces apoptosis in chronic lymphocytic leukemia cells, *108*(32), 13253–13257. doi:10.1073/pnas.1110431108

Lu, W., & Li, Y. (2014). Salinomycin suppresses LRP6 expression and inhibits both Wnt/β-catenin and mTORC1 signaling in breast and prostate

cancer cells. *Journal of Cellular Biochemistry*, *115*(10), 1799–807. doi:10.1002/jcb.24850

Lu, Z., Klem, a M., & Ramu, Y. (2001). Ion conduction pore is conserved among potassium channels. *Nature*, *413*(6858), 809–813. doi:10.1038/35101535

Malinska, D., Mirandola, S. R., & Kunz, W. S. (2010). Mitochondrial potassium channels and reactive oxygen species. *FEBS Letters*, *584*(10), 2043–8. doi:10.1016/j.febslet.2010.01.013

Managò, A., Becker, K. A., Carpinteiro, A., Wilker, B., Soddemann, M., Seitz, A. P., … Gulbins, E. (2015). Pseudomonas aeruginosa Pyocyanin Induces Neutrophil Death via Mitochondrial Reactive Oxygen Species and Mitochondrial Acid Sphingomyelinase. *Antioxidants & Redox Signaling*, 150318122120006. doi:10.1089/ars.2014.5979

Managò, A., Leanza, L., Carraretto, L., Sassi, N., Grancara, S., Quintana-Cabrera, R., … Szabò, I. (2015). Early effects of the antineoplastic agent salinomycin on mitochondrial function. *Cell Death and Disease*, *6*(10), e1930. doi:10.1038/cddis.2015.263

Matsumori, N., Morooka, A., & Murata, M. (2007). Conformation and location of membrane-bound salinomycin-sodium complex deduced from NMR in isotropic bicelles. *Journal of the American Chemical Society*, *129*(48), 14989–14995.

Massari, S., Balboni, E. & Azzone, G. F. (1972). Distribution of permeant cations in rat liver mitochondria under steady-state conditions. *Biochim. Biophys. Acta* 283: 16–22.

Miao, S., Bao, J., Garcia, M. L., Goulet, J. L., Hong, X. J., Kaczorowski, G. J., … Rupprecht, K. M. (2003). Benzamide derivatives as blockers of Kv1.3 ion channel. *Bioorganic & Medicinal Chemistry Letters*, *13*(6), 1161–4. doi:10.1016/S0960-894X(03)00014-3

Mitani, M., Yamanishi, T., Miyazaki, Y., & Otake, N. (1976). Salinomycin Effects on Mitochondrial Ion Translocation and Respiration, *9*(4), 655–660.

Mitchell, P., & Moyle, J. (1967). Chemiosmotic Hypothesis of Oxidative Phosphorylation. *Nature*, *213*(5072), 137–139. doi:10.1038/213137a0

Mourre, C., Chernova, M. N., Martin-Eauclaire, M.-F., Bessone, R., Jacquet, G., Gola, M., … Crest, M. (1999). Distribution in rat brain of binding sites of kaliotoxin, a blocker of Kv1. 1 and Kv1. 3 α-subunits. *Journal of Pharmacology and Experimental Therapeutics*, *291*(3), 943–952.

Muller, F. L., Roberts, A. G., Bowman, M. K., & Kramer, D. M. (2003). Architecture of the Qo site of the cytochrome bc1 complex probed by superoxide production. *Biochemistry*, *42*(21), 6493–9. doi:10.1021/bi0342160

Munoz, C., Saxena, A., Pakladok, T., Bogatikov, E., Wilmes, J., Seebohm, G., … Lang, F. (2012). Stimulation of HERG channel activity by β-catenin. *PLoS ONE*, *7*(8), 3–7. doi:10.1371/journal.pone.0043353

Murphy, M. P. (2009). How mitochondria produce reactive oxygen species. *Biochemical Journal*, *417*(1), 1–13. doi:10.1042/BJ20081386

Muzio, M., Stockwell, B. R., Stennicke, H. R., Salvesen, G. S., & Dixit, V. M. (1998). An induced proximity model for caspase-8 activation. *Journal of Biological Chemistry*, *273*(5), 2926–2930. doi:10.1074/jbc.273.5.2926

Naujokat, C., & Steinhart, R. (2012). Salinomycin as a Drug for Targeting Human Cancer Stem Cells, *2012*, 44–46. doi:10.1155/2012/950658

Nelson, D.L. & Cox M. M. (2002) I princìpi di Biochimica di Lehninger, Third edition, Zanichelli

Nunnari, J., & Suomalainen, A. (2012). Mitochondria: In sickness and in health. *Cell*, *148*(6), 1145–1159. doi:10.1016/j.cell.2012.02.035

O'Malley, Y. Q., Abdalla, M. Y., McCormick, M. L., Reszka, K. J., Denning, G. M., & Britigan, B. E. (2003). Subcellular localization of Pseudomonas pyocyanin cytotoxicity in human lung epithelial cells. *American Journal of Physiology. Lung Cellular and Molecular Physiology*, *284*(2), L420–L430. doi:10.1152/ajplung.00316.2002

Ohnishi, T., & Salerno, J. C. (2005). Conformation-driven and semiquinone-gated proton-pump mechanism in the NADH-ubiquinone oxidoreductase (complex I). *FEBS Letters*, *579*(21), 4555–4561. doi:10.1016/j.febslet.2005.06.086

Orrenius, S., Gogvadze, V., & Zhivotovsky, B. (2007). Mitochondrial Oxidative Stress: Implications for Cell Death. *Annual Review of Pharmacology and Toxicology*, *47*(1), 143–183. doi:10.1146/annurev.pharmtox.47.120505.105122

Owusu-Ansah, E., & Banerjee, U. (2009). Reactive oxygen species prime Drosophila haematopoietic progenitors for differentiation. *Nature*, *461*(7263), 537–41. doi:10.1038/nature08313

Ozawa, F., Friess, H., Tempia-Caliera, A., Kleeff, J., & Büchler, M. W. (2001). Growth factors and their receptors in pancreatic cancer. *Teratogenesis, Carcinogenesis, and Mutagenesis*, *21*(1), 27–44. Retrieved from http://www.ncbi.nlm.nih.gov/pubmed/11135319

Papazian, D. M., Shao, X. M., Seoh, S. A., Mock, A. F., Huang, Y., & Wainstock, D. H. (1995). Electrostatic interactions of S4 voltage sensor in Shaker K+ channel. *Neuron*, *14*(6), 1293–301. doi:10.1016/0896-6273(95)90276-7

Papazian, D. M., Timpe, L. C., Jan, Y. N., & Jan, L. Y. (1991). Alteration of voltage-dependence of Shaker potassium channel by mutations in the S4 sequence. *Nature*, *349*(6307), 305–10. doi:10.1038/349305a0

Papazian, D.M., Schwarz, T.L., Tempel, B.L., Jan, Y.N., Jan, L.Y. (1987). Cloning of genomic and complementary DNA from Shaker, a putative potassium channel gene from Drosophila. *Science* 237, 749-753

Pardo, L. a, & Stühmer, W. (2013). The roles of K+ channels in cancer. *Nature Reviews Cancer*, *14*(1), 39–48. doi:10.1038/nrc3635

Pardo, L. A., Del Camino, D., Sanchez, A., Alves, F., Bruggemann, A., Beckh, S., & Stuhmer, W. (1999) Oncogenic role of EAG. *The EMBO Journal* 20:5540-5547

Park, W. O. O. H., Kim, E. U. N. S., Kim, B. K., & Lee, Y. Y. (2003). Monensin-mediated growth inhibition in NCI-H929 myeloma cells via cell cycle arrest and apoptosis, 197–204.

Paulus, E. F., Kurz, M., Matter, H., & Vértesy, L. (1998). Solid-state and solution structure of the salinomycin-sodium complex: Stabilization of different conformers for an ionophore in different environments. *Journal of the American Chemical Society*, *120*(4), 8209–8221. doi:10.1021/ja973607x

Perozo, E., Santacruz-Toloza, L., Stefani, E., Bezanilla, F., & Papazian, D. M. (1994). S4 mutations alter gating currents of Shaker K channels. *Biophysical Journal*, *66*(2), 345–354. doi:10.1016/S0006-3495(94)80783-0

Preußat, K., Beetz, C., Schrey, M., Kraft, R., Wölfl, S., Kalff, R., & Patt, S. (2003). Expression of voltage-gated potassium channels Kv1.3 and Kv1.5 in human gliomas. *Neuroscience Letters*, *346*, 33–36. doi:10.1016/S0304-3940(03)00562-7

Prevarskaya, N., Skryma, R., & Shuba, Y. (2010). Ion channels and the hallmarks of cancer. *Trends in Molecular Medicine*, *16*(3), 107–21. doi:10.1016/j.molmed.2010.01.005

Quintero-Hernández, V., Jiménez-Vargas, J. M., Gurrola, G. B., Valdivia, H. H., & Possani, L. D. (2013). Scorpion venom components that affect ion-channels function. *Toxicon*, *76*(9), 328–342. doi:10.1016/j.toxicon.2013.07.012

Rada, B., Lekstrom, K., Damian, S., Dupuy, C., & Leto, T. L. (2008). The Pseudomonas toxin pyocyanin inhibits the dual oxidase-based antimicrobial system as it imposes oxidative stress on airway epithelial cells. *Journal of Immunology (Baltimore, Md. : 1950)*, *181*(7), 4883–4893. doi:181/7/4883 [pii]

Rada, B., & Leto, T. L. (2013). Pyocyanin effects on respiratory epithelium: Relevance in Pseudomonas aeruginosa airway infections. *Trends in Microbiology*, *21*(2), 73–81. doi:10.1016/j.tim.2012.10.004

Ralph, S. J., Rodríguez-Enríquez, S., Neuzil, J., & Moreno-Sánchez, R. (2010). Bioenergetic pathways in tumor mitochondria as targets for cancer therapy and the importance of the ROS-induced apoptotic trigger. *Molecular Aspects of Medicine*, *31*(1), 29–59. doi:10.1016/j.mam.2009.12.006

Rauer, H., Pennington, M., Cahalan, M., & Chandy, K. G. (1999). Structural conservation of the pores of calcium-activated and voltage- gated potassium channels determined by a sea anemone toxin. *Journal of Biological Chemistry*, *274*(31), 21885–21892. doi:10.1074/jbc.274.31.21885

Reddy, J., Ghavami, S., Grabarek, J., Kratz, G., Wiechec, E., Fredriksson, B., …

Marek, J. Ł. (2013). Biochimica et Biophysica Acta Salinomycin induces activation of autophagy , mitophagy and affects mitochondrial polarity : Differences between primary and cancer cells ☆, *1833*, 2057–2069. doi:10.1016/j.bbamcr.2013.04.011

Ren, Y. R., Pan, F., Parvez, S., Fleig, A., Chong, C. R., Xu, J., … Liu, J. O. (2008). Clofazimine inhibits human Kv1.3 potassium channel by perturbing calcium oscillation in T lymphocytes. *PLoS ONE*, *3*(12), e4009. doi:10.1371/journal.pone.0004009

Rizzuto, R., De Stefani, D., Raffaello, A., & Mammucari, C. (2012). Mitochondria as sensors and regulators of calcium signalling. *Nature Reviews Molecular Cell Biology*, *13*(9), 566–578. doi:10.1038/nrm3412

Roesch, A., Fukunaga-kalabis, M., Schmidt, E. C., Susan, E., Brafford, P. A., Vultur, A., … Gimotty, P. (2011). NIH Public Access, *141*(4), 583–594. doi:10.1016/j.cell.2010.04.020.A

Rottenberg, H., Covian, R., & Trumpower, B. L. (2009). Membrane Potential Greatly Enhances Superoxide Generation by the Cytochrome bc1 Complex Reconstituted into Phospholipid Vesicles. *Journal of Biological Chemistry*, *284*(29), 19203–19210. doi:10.1074/jbc.M109.017376

Sadikot, R. T., Blackwell, T. S., Christman, J. W., & Prince, A. S. (2005). Pathogen–Host Interactions in *Pseudomonas aeruginosa* Pneumonia. *American Journal of Respiratory and Critical Care Medicine*, *171*(11), 1209–1223. doi:10.1164/rccm.200408-1044SO

Saelens, X., Festjens, N., Walle, L. Vande, Gurp, M. van, Loo, G. van, & Vandenabeele, P. (2004). Toxic proteins released from mitochondria in cell death. *Oncogene*, *23*(16), 2861–2874. doi:10.1038/sj.onc.1207523

Sánchez-Tilló, E., Fanlo, L., Siles, L., Montes-Moreno, S., Moros, a, Chiva-Blanch, G., … Postigo, a. (2014). The EMT activator ZEB1 promotes tumor growth and determines differential response to chemotherapy in mantle cell lymphoma. *Cell Death and Differentiation*, *21*(2), 247–57. doi:10.1038/cdd.2013.123

Sazanov, L. a, & Hinchliffe, P. (2006). Structure of the hydrophilic domain of respiratory complex I from Thermus thermophilus. *Science (New York, N.Y.)*, *311*(5766), 1430–1436. doi:10.1126/science.1123809

Schadendorf, D., & Hauschild, A. (2014). Melanoma in 2013: Melanoma—the run of success continues. *Nature Reviews Clinical Oncology*, *11*(2), 75–76. doi:10.1038/nrclinonc.2013.246

Schägger, H. (2002). Respiratory chain supercomplexes of mitochondria and bacteria. *Biochimica et Biophysica Acta - Bioenergetics*, *1555*(1-3), 154–159. doi:10.1016/S0005-2728(02)00271-2

Scherz-Shouval, R., Shvets, E., Fass, E., Shorer, H., Gil, L., & Elazar, Z. (2007). Reactive oxygen species are essential for autophagy and specifically regulate the activity of Atg4. *The EMBO Journal*, *26*(7), 1749–1760. doi:10.1038/sj.emboj.7601623

Schmitz, A., & Sankaranarayanan, A. (2005). Design of PAP-1, a selective small molecule Kv1. 3 blocker, for the suppression of effector memory T cells in autoimmune diseases. *Molecular …*, *68*(5), 1254–1270. doi:10.1124/mol.105.015669.nally

Sen, C. K., & Packer, L. (1996). Antioxidant and redox regulation of gene transcription. *FASEB Journal : Official Publication of the Federation of American Societies for Experimental Biology*, *10*(7), 709–20. Retrieved from http://www.ncbi.nlm.nih.gov/pubmed/8635688

Sena, L. A., & Chandel, N. S. (2012). Physiological Roles of Mitochondrial Reactive Oxygen Species. *Molecular Cell*, *48*(2), 158–167. doi:10.1016/j.molcel.2012.09.025

Seo, B. B., Marella, M., Yagi, T., & Matsuno-Yagi, A. (2006). The single subunit NADH dehydrogenase reduces generation of reactive oxygen species from complex I. *FEBS Letters*, *580*(26), 6105–6108. doi:10.1016/j.febslet.2006.10.008

Seoh, S. A., Sigg, D., Papazian, D. M., & Bezanilla, F. (1996). Voltage-sensing residues in the S2 and S4 segments of the Shaker K+ channel. *Neuron*, *16*(6), 1159–1167. doi:10.1016/S0896-6273(00)80142-7

Shanmughapriya, S., Rajan, S., Hoffman, N. E., Koch, W. J., Elrod, J. W., Shanmughapriya, S., … Higgins, A. M. (2015). SPG7 Is an Essential and Conserved Component of the Mitochondrial Permeability Transition Pore Article SPG7 Is an Essential and Conserved Component of the Mitochondrial Permeability Transition Pore, 1–16.

Sheppard, K. E., & McArthur, G. A. (2013). The Cell-Cycle Regulator CDK4: An Emerging Therapeutic Target in Melanoma. *Clinical Cancer Research*, *19*(19), 5320–5328. doi:10.1158/1078-0432.CCR-13-0259

Shieh, C. C., Coghlan, M., Sullivan, J. P., & Gopalakrishnan, M. (2000). Potassium channels: molecular defects, diseases, and therapeutic opportunities. *Pharmacological Reviews*, *52*(4), 557–594.

Shoudai, K., Nonaka, K., Maeda, M., Wang, Z.-M., Jeong, H.-J., Higashi, H., … Akaike, N. (2007). Effects of various K+ channel blockers on spontaneous glycine release at rat spinal neurons. *Brain Research*, *1157*, 11–22. doi:10.1016/j.brainres.2006.09.097

Siegel, R. L., Miller, K. D., & Jemal, A. (2015). Cancer statistics, 2015. *CA: A Cancer Journal for Clinicians*, *65*(1), 5–29. doi:10.3322/caac.21254

Smith, G. a M., Tsui, H. W., Newell, E. W., Jiang, X., Zhu, X. P., Tsui, F. W. L., & Schlichter, L. C. (2002). Functional up-regulation of HERG K+ channels in neoplastic hematopoietic cells. *Journal of Biological Chemistry*, *277*(21), 18528–18534. doi:10.1074/jbc.M200592200

Sorgato, M. C., Keller, B. U., & Stühmer, W. (1987). Patch-clamping of the inner mitochondrial membrane reveals a voltage-dependent ion channel. *Nature*, *330*(6147), 498–500. doi:10.1038/330498a0

Starkov, A. A., & Fiskum, G. (2001). Myxothiazol Induces H2O2 Production

from Mitochondrial Respiratory Chain. *Biochemical and Biophysical Research Communications*, *281*(3), 645–650. doi:10.1006/bbrc.2001.4409

Steinbeck, M. J., Khan, A. U., & Karnovsky, M. J. (1993). Extracellular production of singlet oxygen by stimulated macrophages quantified using 9,10-diphenylanthracene and perylene in a polystyrene film. *Journal of Biological Chemistry*, *268*(21), 15649–15654.

Szabó, I., Bock, J., Grassmé, H., Soddemann, M., Wilker, B., Lang, F., … Gulbins, E. (2008). Mitochondrial potassium channel Kv1.3 mediates Bax-induced apoptosis in lymphocytes. *Proceedings of the National Academy of Sciences of the United States of America*, *105*(39), 14861–14866. doi:10.1073/pnas.0804236105

Szabò, I., Bock, J., Jekle, A., Soddemann, M., Adams, C., Lang, F., … Gulbins, E. (2005). A novel potassium channel in lymphocyte mitochondria. *Journal of Biological Chemistry*, *280*(13), 12790–12798. doi:10.1074/jbc.M413548200

Szabò, I., Leanza, L., Gulbins, E., & Zoratti, M. (2012). Physiology of potassium channels in the inner membrane of mitochondria. *Pflugers Archiv European Journal of Physiology*, *463*(2), 231–246. doi:10.1007/s00424-011-1058-7

Szabò, I., Soddemann, M., Leanza, L., Zoratti, M., & Gulbins, E. (2011). Single-point mutations of a lysine residue change function of Bax and Bcl-xL expressed in Bax- and Bak-less mouse embryonic fibroblasts: novel insights into the molecular mechanisms of Bax-induced apoptosis. *Cell Death and Differentiation*, *18*(3), 427–438. doi:10.1038/cdd.2010.112

Szabo, I., Trentin, L., Trimarco, V., Semenzato, G., & Leanza, L. (2015). Biophysical Characterization and Expression Analysis of Kv1.3 Potassium Channel in Primary Human Leukemic B Cells. *Cellular Physiology and Biochemistry*, *37*(3), 965–978. doi:10.1159/000430223

Szabo, I., & Zoratti, M. (2014). Mitochondrial channels: ion fluxes and more. *Physiological Reviews*, *94*(2), 519–608. doi:10.1152/physrev.00021.2013

Tempel, B.L., Papazian, D.M., Schwarz, T.L., Jan, Y.N., Jan L.Y. (1987). Sequence of a probable potassium channel component encoded at Shaker locus of Drosophila. *Science* 237, 770-775

Thornberry, N. A., Rano, T. A., Peterson, E. P., Rasper, D. M., Timkey, T., Garcia-Calvo, M., … Nicholson, D. W. (1997). A combinatorial approach defines specificities of members of the caspase family and granzyme B. Functional relationships established for key mediators of apoptosis. *The Journal of Biological Chemistry*, *272*(29), 17907–17911.

Uttara, B., Singh, A. V, Zamboni, P., & Mahajan, R. T. (2009). Oxidative stress and neurodegenerative diseases: a review of upstream and downstream antioxidant therapeutic options. *Current Neuropharmacology*, *7*, 65–74. doi:10.2174/157015909787602823

van den Heuvel, L., & Smeitink, J. (2001). The oxidative phosphorylation

(OXPHOS) system: nuclear genes and human genetic diseases. *BioEssays : News and Reviews in Molecular, Cellular and Developmental Biology*, *23*(6), 518–525. doi:10.1002/bies.1071

Vennekamp, J., Wulff, H., Beeton, C., Calabresi, P. A., Grissmer, S., Wolfram, H., & Chandy, K. G. (2004). Kv1 . 3-Blocking 5-Phenylalkoxypsoralens : A New Class of Immunomodulators, *65*(6), 1364–1374.

Verdoodt, B., Vogt, M., Schmitz, I., Liffers, S., Tannapfel, A., & Mirmohammadsadegh, A. (2012). Salinomycin Induces Autophagy in Colon and Breast Cancer Cells with Concomitant Generation of Reactive Oxygen Species, *7*(9). doi:10.1371/journal.pone.0044132

Vicente, R., Escalada, A., Villalonga, N., Texido, L., Roura-Ferrer, M., Martín-Satué, M., … Felipe, A. (2006). Association of Kv1.5 and Kv1.3 contributes to the major voltage-dependent K+ channel in macrophages. *Journal of Biological Chemistry*, *281*(49), 37675–37685. doi:10.1074/jbc.M605617200

Votyakova, T. V, & Reynolds, I. J. (2001). DC m -Dependent and -independent production of reactive oxygen species by rat brain mitochondria. *Society*, 266–277.

Wajant, H. (2002). The Fas signaling pathway: more than a paradigm. *Science (New York, N.Y.)*, *296*(5573), 1635–1636. doi:10.1126/science.1071553

Wang, F., He, L., Dai, W., Xu, Y., Wu, D., Lin, C., … Xu, L. (2012). Salinomycin Inhibits Proliferation and Induces Apoptosis of Human Hepatocellular Carcinoma Cells In Vitro and In Vivo, *7*(12). doi:10.1371/journal.pone.0050638

Ward, K. A., Lazovich, D., & Hordinsky, M. K. (2012). Germline melanoma susceptibility and prognostic genes: A review of the literature. *Journal of the American Academy of Dermatology*, *67*(5), 1055–1067. doi:10.1016/j.jaad.2012.02.042

Wei, M. C., Lindsten, T., Mootha, V. K., Weiler, S., Gross, A., Ashiya, M., … Korsmeyer, S. J. (2000). tBID, a membrane-targeted death ligand, oligomerizes BAK to release cytochrome c. *Genes and Development*, *14*(16), 2060–2071. doi:10.1101/gad.14.16.2060

Willis, S. N., Fletcher, J. I., Kaufmann, T., van Delft, M. F., Chen, L., Czabotar, P. E., … Huang, D. C. S. (2007). Apoptosis initiated when BH3 ligands engage multiple Bcl-2 homologs, not Bax or Bak. *Science (New York, N.Y.)*, *315*(5813), 856–859. doi:10.1126/science.1133289

Wilson, R., Sykes, D. a., Watson, D., Rutman, a., Taylor, G. W., & Cole, P. J. (1988). Measurement of Pseudomonas aeruginosa phenazine pigments in sputum and assessment of their contribution to sputum sol toxicity for respiratory epithelium. *Infection and Immunity*, *56*(9), 2515–2517.

Witkiewicz, A. K., McMillan, E. A., Balaji, U., Baek, G., Lin, W.-C., Mansour, J., … Knudsen, E. S. (2015). Whole-exome sequencing of pancreatic cancer defines genetic diversity and therapeutic targets. *Nature Communications*, *6*, 6744. doi:10.1038/ncomms7744

Xia, D., Yu, C. a, Kim, H., Xia, J. Z., Kachurin, a M., Zhang, L., … Deisenhofer, J. (1997). Crystal structure of the cytochrome bc1 complex from bovine heart mitochondria. *Science (New York, N.Y.)*, *277*(5322), 60–66. doi:10.1126/science.277.5322.60

Xu, J., Koni, P. a., Wang, P., Li, G., Kaczmarek, L., Wu, Y., … Desir, G. V. (2003). The voltage-gated potassium channel Kv1.3 regulates energy homeostasis and body weight. *Human Molecular Genetics*, *12*(5), 551–559. doi:10.1093/hmg/ddg049

Yamada, K., Hara, N., Shibata, T., Osago, H., & Tsuchiya, M. (2006). The simultaneous measurement of nicotinamide adenine dinucleotide and related compounds by liquid chromatography/electrospray ionization tandem mass spectrometry. *Analytical Biochemistry*, *352*(2), 282–285. doi:10.1016/j.ab.2006.02.017

Yao, X., Chang, A. Y., Boulpaep, E. L., Segal, A. S., & Desir, G. V. (1996). Molecular cloning of a glibenclamide-sensitive, voltage-gated potassium channel expressed in rabbit kidney. *The Journal of Clinical Investigation*, *97*(11), 2525–33. doi:10.1172/JCI118700

Yellen, G. (2002). channels and their relatives, *419*(September).

Youle, R. J., & Strasser, A. (2008). The BCL-2 protein family: opposing activities that mediate cell death. *Nature Reviews. Molecular Cell Biology*, *9*(1), 47–59. doi:10.1038/nrm2308

Yu, S. P., & Choi, D. W. (2000). Ions , cell volume , and apoptosis, *97*(17), 9360–9362.

Yu, S. P., & Kerchner, G. a. (1998). Rapid Communication Endogenous Voltage-Gated Potassium Channels in Human Embryonic Kidney (HEK293) Cells. *Journal of Neuroscience Research*, *617*(January), 612–617. Retrieved from http://www.ncbi.nlm.nih.gov/entrez/query.fcgi?db=pubmed&cmd=Retrieve&dopt=AbstractPlus&list_uids=9632317

Zamzami, N., & Kroemer, G. (2001). The mitochondrion in apoptosis: how Pandora's box opens. *Nature Reviews. Molecular Cell Biology*, *2*(1), 67–71. doi:10.1038/35048073

Zhou, J., Li, P., Xue, X., He, S., Kuang, Y., Zhao, H., … Guo, X. (2013). Salinomycin induces apoptosis in cisplatin-resistant colorectal cancer cells by accumulation of reactive oxygen species. *Toxicology Letters*, *222*(2), 139–145. doi:10.1016/j.toxlet.2013.07.022

Zhu, L., Zhen, Y., Zhang, Y., Guo, Z., Dai, J., & Wang, X. (2013). Salinomycin Activates AMP-Activated Protein Kinase- Dependent Autophagy in Cultured Osteoblastoma Cells : A Negative Regulator against Cell Apoptosis, *8*(12), 1–11. doi:10.1371/journal.pone.0084175

Zoratti, M., De Marchi, U., Gulbins, E., & Szabò, I. (2009). Novel channels of the inner mitochondrial membrane. *Biochimica et Biophysica Acta (BBA) - Bioenergetics*, *1787*(5), 351–363. doi:10.1016/j.bbabio.2008.11.015

Zoratti, M., & Szabó, I. (1994). Electrophysiology of the inner mitochondrial membrane. *Journal of Bioenergetics and Biomembranes*, *26*(5), 543–553. doi:10.1007/BF00762739

Zorov, D. B., Juhaszova, M., & Sollott, S. J. (2014). Mitochondrial Reactive Oxygen Species (ROS) and ROS-Induced ROS Release. *Physiological Reviews*, *94*(3), 909–950. doi:10.1152/physrev.00026.2013

Collection of publications by the author

frontiers in
PHYSIOLOGY

MINI REVIEW ARTICLE
published: 03 September 2013
doi: 10.3389/fphys.2013.00227

Intracellular ion channels and cancer

*Luigi Leanza[1], Lucia Biasutto[2], Antonella Managò[1], Erich Gulbins[3], Mario Zoratti[2] and Ildikò Szabò[1]**

[1] Department of Biology, University of Padova, Padova, Italy
[2] CNR Institute of Neuroscience and Department of Biomedical Sciences of the University of Padova, Padova, Italy
[3] Department of Molecular Biology, University of Duisburg-Essen, Essen, Germany

Edited by:
Luca Munaron, University of Turin, Italy

Reviewed by:
Yong S. Song, Seoul National University College of Medicine, South Korea
Florian Lang, Eberhard-Karls-University of Tuebingen, Germany

***Correspondence:**
Ildikò Szabò, Department of Biology, University of Padova, Viale G. Colombo 3, 35131 Padova, Italy
e-mail: ildi@civ.bio.unipd.it

Several types of channels play a role in the maintenance of ion homeostasis in subcellular organelles including endoplasmatic reticulum, nucleus, lysosome, endosome, and mitochondria. Here we give a brief overview of the contribution of various mitochondrial and other organellar channels to cancer cell proliferation or death. Much attention is focused on channels involved in intracellular calcium signaling and on ion fluxes in the ATP-producing organelle mitochondria. Mitochondrial K^+ channels (Ca^{2+}-dependent BK_{Ca} and IK_{Ca}, ATP-dependent K_{ATP}, Kv1.3, two-pore TWIK-related Acid-Sensitive K^+ channel-3 (TASK-3)), Ca^{2+} uniporter MCU, Mg^{2+}-permeable Mrs2, anion channels (voltage-dependent chloride channel VDAC, intracellular chloride channel CLIC) and the Permeability Transition Pore (MPTP) contribute importantly to the regulation of function in this organelle. Since mitochondria play a central role in apoptosis, modulation of their ion channels by pharmacological means may lead to death of cancer cells. The nuclear potassium channel Kv10.1 and the nuclear chloride channel CLIC4 as well as the endoplasmatic reticulum (ER)-located inositol 1,4,5-trisphosphate (IP_3) receptor, the ER-located Ca^{2+} depletion sensor STIM1 (stromal interaction molecule 1), a component of the store-operated Ca^{2+} channel and the ER-resident TRPM8 are also mentioned. Furthermore, pharmacological tools affecting organellar channels and modulating cancer cell survival are discussed. The channels described in this review are summarized on **Figure 1**. Overall, the view is emerging that intracellular ion channels may represent a promising target for cancer treatment.

Keywords: cancer, organelles, ion channel, apoptosis, pharmacology

MITOCHONDRIA

The "impermeable" mitochondrial inner membrane (IMM) allows the formation of an electrochemical proton gradient which drives the aerobic synthesis of ATP. The "semipermeable" outer membrane (OMM) encloses a periplasmic space where proteins with fundamental roles in cell death are stored until a sufficiently strong pro-apoptotic signal arrives. Mitochondria have assumed a peculiar role in cancer cell physiology (Ralph and Neuzil, 2009). They are crucial for the control of intracellular Ca^{2+} homeostasis, and produce reactive oxygen species (ROS). ROS are involved in the regulation of physiological processes, but may also be harmful if produced excessively. Mitochondria are the checkpoint of the intrinsic pathway of apoptosis: the release of caspase cofactors, such as cytochrome c (cyt c) and SMAC/Diablo, results in the assembly of the apoptosome and in commitment of the cell to apoptosis. In cancer cells mitochondrial metabolism is deregulated to optimize the production of glycolytic intermediates for anabolic reactions. Much effort has been devoted to discover drugs inducing cancer cell death by targeting tumor-specific alterations of mitochondrial metabolism or by stimulating OMM permeabilization and thus, allowing the release of apoptotic cofactors (Fulda et al., 2010). Mitochondrial ion channels play a role in this process by influencing organellar membrane potential, ROS production, volume, calcium homeostasis, and possibly morphology. The mitochondrial channels characterized over the last two decades include outer membrane-located VDAC and MAC in the IMM, potassium channels mtK_{ATP}, $mtBK_{Ca}$, $mtIK_{Ca}$, mtKv1.3, TASK-3, the non-selective permeability transition pore PTP, chloride channels, and the calcium uniporter (e.g., Zoratti et al., 2009; Shoshan-Barmatz et al., 2010; Rizzuto et al., 2012; Szabò et al., 2012).

CHANNELS OF THE OUTER MITOCHONDRIAL MEMBRANE INVOLVED IN APOPTOSIS/CANCER

Mitochondrial apoptosis-induced channel (MAC)

OMM permeabilization has been proposed to involve oligomers of pro-apoptotic Bax, which display ion channel activity in phospholipid bilayers (e.g., Tait and Green, 2010). However, the hypothesis that Bax alone is sufficient to induce cyt c release has been challenged, given that a single point mutant of Bax did not mediate cell death in Bax/Bak-less mouse embryonic fibroblasts despite forming channels with properties similar to WT Bax (Brustovetsky et al., 2010; Szabò et al., 2011). A pore (mitochondrial apoptosis-induced channel, MAC) with an estimated diameter sufficient to allow the passage of cyt c was detected by patch clamp (Martinez-Caballero et al., 2009). The timing of cyt c release in apoptotic cells correlated with the onset of MAC activity and with the translocation of Bax to mitochondrial membranes. MAC, whose formation requires Bim-induced activation of Bax and a still unidentified protein, is considered as a target for novel

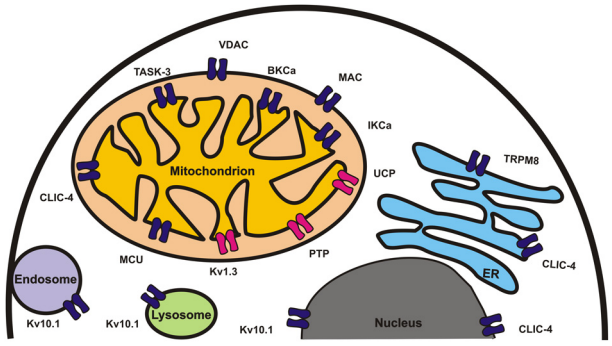

FIGURE 1 | Ion channels involved in regulation of apoptosis and/or tumorigenesis are shown in different organelles. Channels for whose crucial role pharmacological and/or genetic *in vivo* evidence is available are shown in red.

cancer therapies (Peixoto et al., 2012) but specific MAC activators are not available yet. The BH3 mimetic ABT-737, an efficient anticancer agent *in vivo*, activates MAC by disrupting Bcl-2/Bax/Bim complexes (Dejean et al., 2010).

Mitochondrial voltage dependent anion channel (VDAC)

The major protein of the OMM, porin or VDAC is deeply involved in apoptosis. The role of VDAC1 and of the other isoforms VDAC2 and VDAC3 in cell death is multi-faceted and complex (e.g., McCommis and Baines, 2012; Shoshan-Barmatz and Golan, 2012; Shoshan-Barmatz and Mizrachi, 2012). Formation of a large pore comprising VDAC and Bax/Bak was proposed to account for cyt c release (Tsujimoto and Shimizu, 2000; but see Martinez-Caballero et al., 2009). Alternatively, dimers and higher oligomers of VDAC1 might form the conduit for the efflux of cyt c (Shoshan-Barmatz et al., 2010). Binding of anti-apoptotic Bcl-2 and BclxL to VDAC1 (with resulting inhibition of porin) (Shimizu et al., 2000) has an anti-apoptotic action (e.g., Arbel et al., 2012). In contrast, block of VDAC1 by the phosphorothioate oligonucleotide G3139 (Tan, 2012) or by avicins (plant saponins with anticancer activity) is pro-apoptotic, presumably by reducing flux of metabolites across the OMM (Haridas et al., 2007). VDAC2 inhibits Bak activation and apoptosis (Cheng et al., 2003), and Bak reportedly relocates from the OMM to the ER in the absence of VDAC2 (Raghavan et al., 2012). In contrast, Bax-induced cyt c release from mitochondria isolated from WT or VDAC1^{-}, VDAC3^{-} and VDAC1/VDAC3-null cells was reported to be the same (Baines et al., 2007).

VDAC may inhibit apoptosis and promote tumorigenesis through specific interactions with enzymes favoring glycolysis. It is being examined as a cancer-specific target since tumor cells have elevated glycolysis and increased expression of VDACs (Grills et al., 2011). Overexpression of Hexokinase-2 (HK2) and its association with VDAC are key features of glycolytic cancers (e.g., Wolf et al., 2011). HK2 binding to the conduit channeling ATP out of mitochondria provides a metabolic benefit to cancer cells (Warburg effect) and it antagonizes cell death via inhibition of Bax-induced cyt c release (Pastorino et al., 2002; Gall et al., 2011) and/or inhibition of the Mitochondrial Permeability Transition (MPT) (Chiara et al., 2008). HK detachment seems to favor cell death by disruption of aerobic glycolysis and of the energy balance of the cell, regulation of ROS production, altered interaction of Bcl2 family proteins with mitochondria, facilitation of VDAC oligomer formation (e.g., Shoshan-Barmatz et al., 2010; Shoshan-Barmatz and Golan, 2012). Therefore, a major oncological target is the HK-VDAC complex (e.g., Galluzzi et al., 2008; Simamura et al., 2008; Fulda et al., 2010; Mathupala and Pedersen, 2010). HK2 can be dissociated from mitochondria by peptides interfering with HK-VDAC association, by erastin (Yagoda et al., 2007) and by 3-bromopyruvate (e.g., Cardaci et al., 2012; Ko et al., 2012; Pedersen, 2012; Shoshan, 2012). Antifungal drugs clotrimazole and bifonazole and the plant hormone methyl jasmonate (MJ) are also effective. MJ is particularly promising since it has selective anticancer activity in preclinical studies (Fulda et al., 2010). Finally, the anti-cancer agent furanonaphthoquinone (FNQ) induces caspase-dependent apoptosis via the production of ROS, which is enhanced by VDAC1 overexpression (Simamura et al., 2008). A systematic search for compounds acting at the level of VDAC to antagonize cancer remains to be performed.

ION CHANNELS OF THE INNER MITOCHONDRIAL MEMBRANE INVOLVED IN APOPTOSIS/CANCER

Permeability transition pore (MPTP)

When the IMM becomes freely permeable to solutes, the consequences for the cell can be catastrophic. Thus, the selective induction of IMM permeabilization in cancer cells is a strategy worth pursuing in oncotherapy. A number of cellular stresses and cytotoxic agents trigger the prime example of such a catastrophe, i.e., the mitochondrial permeability transition (MPT), considered as a final common pathway of cell death (Brenner and Grimm, 2006; Bernardi, 2013). The MPT is caused by the opening of a large Ca^{2+}- and oxidative stress-activated pore [the mitochondrial megachannel, MMC, with a conductance of up to 1.5 nS (Szabó and Zoratti, 1991)] which makes the IMM permeable to ions and solutes up to about 1500 Da MW, leading to matrix swelling.

MPT is considered to bear substantial responsibilities in the tissue damage caused by, e.g., ischemia/reperfusion and oxidative stress. In cancer cells, instead, signaling pathways are activated which desensitize the mitochondria to MPT induction (Rasola et al., 2010; Matassa et al., 2012; Traba et al., 2012), while chemotherapeutic agents causing oxidative stress may activate signals causing death via the MPT (Chiara et al., 2012). Cyclosporin A (CSA), a cyclic endecapeptide, is a powerful inhibitor of the MPTP (Fournier et al., 1987; Crompton et al., 1988; Broekemeier et al., 1989) (and also of calcineurin and thus is a widely used immunosuppressant). CSA inhibits the MPTP via its binding to matrix cyclophilin (CyP) D, a peptidyl-prolyl cis-trans isomerase (PPIase). Patients treated with CSA to prevent transplant rejection have a high incidence of cancer not only because of the drug's immunosuppressive action, but also because CSA inhibits the MPTP (Norman et al., 2010). The molecular nature of the MPTP is being finally delineated: the dimeric form of ATP synthase and CypD as regulator are currently proposed as components (Baines et al., 2005; Bernardi, 2013; Giorgio et al., 2013).

For oncological applications MPT inducers are relevant, despite the likelihood of noxious side-effects, for example on the nervous system. A large number of compounds, often used at relatively high concentrations, have been shown to induce

the MPT in cultured cells, often as a consequence of oxidative stress and/or disruption of Ca^{2+} homeostasis. Some MPTP-targeting molecules such as 4-(N-(S-glutathionylacetyl) amino) phenylarsenoxide are currently being evaluated in clinical trials for cancer treatment of refractory tumors (Brenner and Moulin, 2012; Elliott et al., 2012).

Signaling pathways which modulate occurrence of the MPT have been elucidated, a key component being GSK3α/β whose activation, e.g., by induction of oxidative stress by gold complex AUL12, favors MPTP opening (Chiara and Rasola, 2013). A large portion of MPTP openers are natural compounds like jasmonates (e.g., Raviv et al., 2013), betulinic acid, the synthetic retinoid CD437 (Lena et al., 2009; Javadov et al., 2011), berberine (Pereira et al., 2007, 2008), honokiol (Li et al., 2007), α-bisabolol (Cavalieri et al., 2009) and shikonin (Han et al., 2007), just to name a few. Data on *in vivo* anti-tumor activities are available for all these compounds (Fulda et al., 2010). Mitochondria-penetrating peptides, such as mastoparan-like sequences, peptides of the innate immunity systems, or the molecules developed by Kelley's group (e.g., Risso et al., 2002; Jones et al., 2008; Horton et al., 2012) also induce MPT. Some MPTP-targeting molecules such as 4-(N-(S-glutathionylacetyl) amino) phenylarsenoxide are currently being evaluated in clinical trials for cancer treatment of refractory tumors (Brenner and Moulin, 2012; Elliott et al., 2012).

IMM potassium channels Kv1.3, BKca, IKca, and TASK-3 in the regulation of apoptosis/cancer

A functional mitochondrial counterpart of the potassium channel Kv1.3 has been identified in the IMM of several cell types (mtKv1.3) (Szabò et al., 2005; Gulbins et al., 2010). It is expected to participate in regulation of mitochondrial membrane potential, volume, and ROS production. A crucial role of mtKv1.3 in apoptosis became evident since expression of a mitochondria-targeted Kv1.3 construct was sufficient to sensitize apoptosis-resistant CTLL-2 T lymphocytes, which lack Kv channels. MtKv1.3 has been identified as a target of Bax and physical interaction between the two proteins in apoptotic cells has been demonstrated (Szabó et al., 2008; Szabò et al., 2011). Incubating Kv1.3-positive isolated mitochondria with Bax triggered apoptotic events including membrane potential changes (hyperpolarization followed by depolarization due to the opening of MPTP), ROS production and cyt c release, whereas Kv1.3-deficient mitochondria were resistant. Highly conserved Bax lysine 128 protrudes into the intermembrane space (Annis et al., 2005) and mimics a crucial lysine in Kv1.3-blocking peptide toxins. Mutation of Bax at K128 (BaxK128E) abrogated its effects on Kv1.3 and mitochondria, as well as in Bax/Bak-less double knockout (DKO) mouse embryonic fibroblasts, indicating a toxin-like action of Bax on Kv1.3 to trigger mitochondrial phenomena.

Psora-4, PAP-1 and clofazimine, three membrane-permeant inhibitors of Kv1.3, can induce death by directly targeting the mitochondrial channel, while membrane-impermeant Kv1.3 inhibitors ShK or Margatoxin did not induce apoptosis (Leanza et al., 2012a,b). Importantly, the membrane-permeant drugs killed cells also in the absence of Bax and Bak, in agreement with the above model. Genetic deficiency or siRNA-mediated downregulation of Kv1.3 abrogated the effects of the drugs. Intraperitoneal injection of clofazimine reduced tumor size by 90% in an orthotopic melanoma B16F10 mouse model *in vivo*, while no adverse effects were observed in several healthy tissues. Similar results were obtained with primary human cancer cells from patients with chronic lymphocytic leukemia (Leanza et al., 2013). The selective action of these drugs on tumor cells is related to a synergistic effect of a higher expression of Kv1.3 and of an altered redox state of cancer cells. The fact that clofazimine is already used in the clinic for the treatment of e.g., leprosis (Ren et al., 2008) and shows an excellent safety profile supports the feasibility of targeting mtKv1.3 for therapy.

The large conductance calcium- and voltage-activated K^+ channel BK_{Ca} (KCa1.1) has been revealed also in intracellular membranes, including nuclear membrane, ER, Golgi and mitochondria (Xu et al., 2002; O'Rourke, 2007; Singh et al., 2012). Patch clamp experiments with recombinant Bax showed an inhibition of BK_{Ca}, which might contribute to opening of the MPTP during cell death (Cheng et al., 2011).

The intermediate conductance potassium channel (IK_{Ca}; KCa3.1), selectively inhibited by clotrimazole and TRAM-34, has been recorded from the inner mitochondrial membranes of human cancer cells (De Marchi et al., 2009; Sassi et al., 2010). TRAM-34 used alone did not induce apoptosis (Sassi et al., 2010; Quast et al., 2012), but it synergistically increased sensitivity to the death receptor ligand TRAIL in melanoma cells (Quast et al., 2012). Given that both TRAM-34 and TRAIL have a relatively good safety profile, co-administration of the two drugs might be exploited for melanoma treatment.

Recently TASK-3 (KCNK9), a two-pore potassium channel, was identified in mitochondria of melanoma and keratinocyte (Rusznák et al., 2008) as well as healthy intestinal epithelial cells (Kovács et al., 2005). Reduced expression of TASK-3 resulted in compromised mitochondrial function and cell survival in WM35 melanoma cells (Kosztka et al., 2011). Whether TASK-3 protein gives rise to a functional channel in the IMM and whether it will become an oncological target remain to be determined.

OTHER IMM CHANNELS LINKED TO TUMORIGENESIS: UNCOUPLING PROTEIN UCP, Mg^{2+} CHANNEL Mrs-2 AND CALCIUM UNIPORTER MCU

Uncoupling protein-2 (UCP-2), which mediates proton leak (Cannon and Nedergaard, 2004; Fedorenko et al., 2012), has been proposed to regulate cell survival by decreasing mitochondrial ROS, since a depolarizing proton leak is expected to diminish superoxide production (Baffy et al., 2011). UCP2 overexpression reportedly prevents oxidative injury, thereby possibly contributing to a higher apoptotic threshold assisting survival of cancer cells. Over-expression of UCP2 was found in numerous types of tumors and has been shown to protect cells from oxidative stress (Arsenijevic et al., 2000; Zhang et al., 2007) and even to abolish chemotherapeutic agent- induced apoptosis (Derdak et al., 2008). Ectopic expression of UCP2 in MCF7 breast cancer cells leads to a decreased mitochondrial membrane potential and increased tumorigenic properties as measured by cell migration, *in vitro* invasion, and anchorage independent growth. Interestingly, UCP2 over-expression has also been proposed to directly contribute to the Warburg phenotype (Samudio et al., 2008) and to development of tumors in an orthotopic model of breast cancer (Ayyasamy et al., 2011). Cisplatin downregulated the expression of UCP2 in colon cancer

cells (Santandreu et al., 2010), suggesting that UCP2 overexpression is involved in the development of a variety of cancers. UCP2 can be considered as a promising oncological target.

Mitochondria accumulate Mg^{2+} via Mrs2, a Mg^{2+}–selective channel of the IMM (Kolisek et al., 2003). An early increase in cytosolic Mg^{2+} occurs during apoptosis (Chien et al., 1999) and this ion seems to be required for cytochrome c release (Kim et al., 2000). Long-lasting knock-down of Mrs2 caused cell death by inducing loss of respiratory complex I and mitochondrial membrane depolarization (Piskacek et al., 2009). A subtractive hybridization method applied on vincristine or adriamycin resistant and parental human gastric adenocarcinoma cell lines highlighted upregulation of Mrs2 (Chen et al., 2009), suggesting that high expression of Mrs2 may protect against death (Wolf and Trapani, 2009).

The molecular identification of the mitochondrial Ca^{2+} "uniporter" (MCU), responsible for the low-affinity uptake of calcium into the mitochondrial matrix (Kirichok et al., 2004), has recently been achieved (Baughman et al., 2011; De Stefani et al., 2011). MCU participates in the control of Ca^{2+} signaling in the whole cell, and may thus be a very useful tool to influence the myriad cellular calcium-dependent processes, including cell death (Rizzuto et al., 2012). Subthreshold apoptotic signals were shown to synergize with cytosolic Ca^{2+} waves (Pinton et al., 2001) resulting in opening of MPTP. Cells overexpressing MCU underwent more pronounced apoptosis upon challenging with H_2O_2 and C2-ceramide (De Stefani et al., 2011). Overexpression of an MCU-targeting microRNA, miR-25, in colon cancer cells resulted in MCU downregulation, impaired calcium uptake and increased resistance to apoptosis (Marchi et al., 2013). Thus, MCU seems to be a crucial protein for tumorigenesis and its specific pharmacological activators, if identified, might become useful tools.

ION CHANNELS IN OTHER ORGANELLES WITH A ROLE IN APOPTOSIS/TUMORIGENESIS

The intracellular chloride channel CLIC4/mtCLIC has both a soluble and a membrane-inserted form and can be localized to the mitochondrial inner membrane (Fernández-Salas et al., 1999), cytoplasm, ER membrane, and the nucleus. CLIC4 overexpression induced apoptosis associated with loss of mitochondrial membrane potential, cytochrome c release, and caspase activation (Fernández-Salas et al., 2002). On the other hand, inhibition of CLIC4 expression triggered mitochondrial apoptosis under starvation and enhanced autophagy in glioma cells (Zhong et al., 2012). Marked changes in expression and subcellular localization of CLIC4 occur early in tumorigenesis. In particular, reduced CLIC4 expression and nuclear localization in cancer cells is associated with the altered redox state and CLIC4 acts as an important suppressor of squamous tumor development and progression (Suh et al., 2012).

A functional "oncogenic" potassium channel, Kv10.1 has been described in the nuclear inner membrane (Chen et al., 2011) where it might participate in setting nuclear $[K^+]$ thereby affecting gene expression. The PM Kv10.1 is also rapidly internalized to lysosomes (Kohl et al., 2011), whose patch clamping has been achieved (Wang et al., 2012). The possible influence of these channels on cancer cell survival remains to be determined.

Finally, we should briefly mention other intracellular channels involved in Ca^{2+} signaling, (Ca^{2+} permeable channels are discussed in detail by other contributions in this special issue). For example the calcium-permeable ion channel TRPM8, overexpressed in several tumors, has been located to the ER (Zhang and Barritt, 2004), resulting in decreased ER $[Ca^{2+}]$ and increased resistance to apoptosis (Bidaux et al., 2007). Patients suffering of breast cancers with high ER-located STIM1 levels have significantly reduced survival (McAndrew et al., 2011). The PM-located other component, ORAi1 contributes to altered calcium homeostasis as well (Monteith et al., 2012). Expression of ER-resident IP_3 receptors acting as Ca^{2+} store release channels is altered in glioblastoma (Kang et al., 2010). Repression of IP_3- mediated Ca^{2+} elevation by Bcl-2 has been proposed to contribute to the pathophysiology of chronic lymphocytic leukemia (Zhong et al., 2011).

In summary, while considerable further work is required to clarify the mechanisms by which intracellular channels contribute to tumorigenesis and tumor progression, or intervene in cell death, a few *in vivo* studies targeting these channels underline the importance of pursuing this line of research.

ACKNOWLEDGMENTS

Senior post-doc fellowship and Young Investigator grant of the University of Padova to Luigi Leanza is acknowledged. The authors are grateful for funding to the Italian Association for Cancer Research (AIRC) (grant 5118 to Ildikò Szabò), the Progetti di Rilevante Interesse Nazionale (PRIN) program (2010CSJX4F to Ildikò Szabò and 20107Z8XBW to Mario Zoratti), by DFG-grant Gu 335/13–3 (Erich Gulbins), the International Association for Cancer Research (Erich Gulbins); the EMBO Young Investigator Program grant (Ildikò Szabò), the Fondazione Cassa di Risparmio di Padova e Rovigo (to Mario Zoratti); the CNR Project of Special Interest on Aging (Mario Zoratti).

REFERENCES

Annis, M. G., Soucie, E. L., Dlugosz, P. J., Cruz-Aguado, J. A., Penn, L. Z., Leber, B., et al. (2005). Bax forms multispanning monomers that oligomerize to permeabilize membranes during apoptosis. *EMBO J.* 24, 2096–2103. doi: 10.1038/sj.emboj.7600675

Arbel, N., Ben-Hail, D., and Shoshan-Barmatz, V. (2012). Mediation of the antiapoptotic activity of Bcl-xL protein upon interaction with VDAC1 protein. *J. Biol. Chem.* 287, 23152–23161. doi: 10.1074/jbc.M112.345918

Arsenijevic, D., Onuma, H., Pecqueur, C., Raimbault, S., Manning, B. S., Miroux, B., et al. (2000). Disruption of the uncoupling protein-2 gene in mice reveals a role in immunity and reactive oxygen species production. *Nat. Genet.* 26, 435–439. doi: 10.1038/82565

Ayyasamy, V., Owens, K. M., Desouki, M. M., Liang, P., Bakin, A., Thangaraj, K., et al. (2011). Cellular model of Warburg effect identifies tumor promoting function of UCP2 in breast cancer and its suppression by genipin. *PLoS ONE* 6:e24792. doi: 10.1371/journal.pone.0024792

Baffy, G., Derdak, Z., and Robson, S. C. (2011). Mitochondrial recoupling: a novel therapeutic strategy for cancer. *Br. J. Cancer* 105, 469–474. doi: 10.1038/bjc.2011.245

Baines, C. P., Kaiser, R. A., Purcell, N. H., Blair, N. S., Osinska, H., Hambleton, M. A., et al. (2005). Loss of cyclophilin D reveals a critical role for mitochondrial permeability transition in cell death. *Nature* 434, 658–662. doi: 10.1038/nature03434

Baines, C. P., Kaiser, R. A., Sheiko, T., Craigen, W. J., and Molkentin,

J. D. (2007). Voltage-dependent anion channels are dispensable for mitochondrial-dependent cell death. *Nat. Cell Biol.* 9, 550–555. doi: 10.1038/ncb1575

Baughman, J. M., Perocchi, F., Girgis, H. S., Plovanich, M., Belcher-Timme, C. A., Sancak, Y., et al. (2011). Integrative genomics identifies MCU as an essential component of the mitochondrial calcium uniporter. *Nature* 476, 341–345. doi: 10.1038/nature10234

Bernardi, P. (2013). The mitochondrial permeability transition pore: a mystery solved. *Front. Physiol.* 4:95. doi: 10.3389/fphys.2013.00095

Bidaux, G., Flourakis, M., Thebault, S., Zholos, A., Beck, B., Gkika, D., et al. (2007). Prostate cell differentiation status determines transient receptor potential melastatin member 8 channel subcellular localization and function. *J. Clin. Invest.* 117, 1647–1657. doi: 10.1172/JCI30168

Brenner, C., and Grimm, S. (2006). The permeability transition pore complex in cancer cell death. *Oncogene* 25, 4744–4756. doi: 10.1038/sj.onc.1209609

Brenner, C., and Moulin, M. (2012). Physiological roles of the permeability transition pore. *Circ. Res.* 111, 1237–1247. doi: 10.1161/CIRCRESAHA.112.265942

Broekemeier, K. M., Dempsey, M. E., and Pfeiffer, D. R. (1989). Cyclosporin A is a potent inhibitor of the inner membrane permeability transition in liver mitochondria. *J. Biol. Chem.* 264, 7826–7830.

Brustovetsky, T., Li, T., Yang, Y., Zhang, J. T., Antonsson, B., and Brustovetsky, N. (2010). BAX insertion, oligomerization, and outer membrane permeabilization in brain mitochondria: role of permeability transition and SH-redox regulation. *Biochim. Biophys. Acta* 1797, 1795–1806. doi: 10.1016/j.bbabio.2010.07.006

Cannon, B., and Nedergaard, J. (2004). Brown adipose tissue: function and physiological significance. *Physiol. Rev.* 84, 277–359. doi: 10.1152/physrev.00015.2003

Cardaci, S., Desideri, E., and Ciriolo, M. R. (2012). Targeting aerobic glycolysis: 3-bromopyruvate as a promising anticancer drug. *J. Bioenerg. Biomembr.* 44, 17–29. doi: 10.1007/s10863-012-9422-7

Cavalieri, E., Bergamini, C., Mariotto, S., Leoni, S., Perbellini, L., Darra, E., et al. (2009). Involvement of mitochondrial permeability transition pore opening in alpha-bisabolol induced apoptosis. *FEBS J.* 276, 3990–4000. doi: 10.1111/j.1742-4658.2009.07108.x

Chen, Y., Sánchez, A., Rubio, M. E., Kohl, T., Pardo, L. A., and Stühmer, W. (2011). Functional K(v)10.1 channels localize to the inner nuclear membrane. *PLoS ONE* 6:e19257. doi: 10.1371/journal.pone.0019257

Chen, Y., Wei, X., Yan, P., Han, Y., Sun, S., Wu, K., et al. (2009). Human mitochondrial Mrs2 protein promotes multidrug resistance in gastric cancer cells by regulating p27, cyclin D1 expression and cytochrome C release. *Cancer Biol. Ther.* 8, 607–614. doi: 10.4161/cbt.8.7.7920

Cheng, E. H., Sheiko, T. V., Fisher, J. K., Craigen, W. J., and Korsmeyer, S. J. (2003). VDAC2 inhibits BAK activation and mitochondrial apoptosis. *Science* 301, 513–517. doi: 10.1126/science.1083995

Cheng, Y., Gulbins, E., and Siemen, D. (2011). Activation of the permeability transition pore by Bax via inhibition of the mitochondrial BK channel. *Cell. Physiol. Biochem.* 27, 191–200. doi: 10.1159/000327944

Chiara, F., Castellaro, D., Marin, O., Petronilli, V., Brusilow, W. S., Juhaszova, M., et al. (2008). Hexokinase II detachment from mitochondria triggers apoptosis through the permeability transition pore independent of voltage-dependent anion channels. *PLoS ONE* 3:e1852. doi: 10.1371/journal.pone.0001852

Chiara, F., Gambalunga, A., Sciacovelli, M., Nicolli, A., Ronconi, L., Fregona, D., et al. (2012). Chemotherapeutic induction of mitochondrial oxidative stress activates GSK-3α/β and Bax, leading to permeability transition pore opening and tumor cell death. *Cell Death Dis.* 3:e444. doi: 10.1038/cddis.2012.184

Chiara, F., and Rasola, A. (2013). GSK-3 and mitochondria in cancer cells. *Front. Oncol.* 3:16. doi: 10.3389/fonc.2013.00016

Chien, M. M., Zahradka, K. E., Newell, M. K., and Freed, J. H. (1999). Fas-induced B cell apoptosis requires an increase in free cytosolic magnesium as an early event. *J. Biol. Chem.* 274, 7059–7066. doi: 10.1074/jbc.274.11.7059

Crompton, M., Ellinger, H., and Costi, A. (1988). Inhibition by cyclosporin A of a Ca^{2+}-dependent pore in heart mitochondria activated by inorganic phosphate and oxidative stress. *Biochem. J.* 255, 357–360.

Dejean, L. M., Ryu, S. Y., Martinez-Caballero, S., Teijido, O., Peixoto, P. M., and Kinnally, K. W. (2010). MAC and Bcl-2 family proteins conspire in a deadly plot. *Biochim Biophys Acta* 1797, 1231–1238. doi: 10.1016/j.bbabio.2010.01.007

De Marchi, U., Sassi, N., Fioretti, B., Catacuzzeno, L., Cereghetti, G. M., Szabò, I., et al. (2009). Intermediate conductance Ca^{2+}-activated potassium channel (KCa3.1) in the inner mitochondrial membrane of human colon cancer cells. *Cell Calcium* 45, 509–516. doi: 10.1016/j.ceca.2009.03.014

Derdak, Z., Mark, N. M., Beldi, G., Robson, S. C., Wands, J. R., and Baffy, G. (2008). The mitochondrial uncoupling protein-2 promotes chemoresistance in cancer cells. *Cancer Res.* 68, 2813–2819. doi: 10.1158/0008-5472.CAN-08-0053

De Stefani, D., Raffaello, A., Teardo, E., Szabò, I., and Rizzuto, R. (2011). A forty-kilodalton protein of the inner membrane is the mitochondrial calcium uniporter. *Nature* 476, 336–340. doi: 10.1038/nature10230

Elliott, M. A., Ford, S. J., Prasad, E., Dick, L. J., Farmer, H., Hogg, P. J., et al. (2012). Pharmaceutical development of the novel arsenical based cancer therapeutic GSAO for Phase I clinical trial. *Int. J. Pharm.* 426, 67–75. doi: 10.1016/j.ijpharm.2012.01.024

Fedorenko, A., Lishko, P. V., and Kirichok, Y. (2012). Mechanism of fatty-acid-dependent UCP1 uncoupling in brown fat mitochondria. *Cell* 151, 400–413. doi: 10.1016/j.cell.2012.09.010

Fernández-Salas, E., Sagar, M., Cheng, C., Yuspa, S. H., and Weinberg, W. C. (1999). p53 and tumor necrosis factor alpha regulate the expression of a mitochondrial chloride channel protein. *J Biol Chem.* 274, 36488–36497. doi: 10.1074/jbc.274.51.36488

Fernández-Salas, E., Suh, K. S., Speransky, V. V., Bowers, W. L., Levy, J. M., Adams, T., et al. (2002). mtCLIC/CLIC4, an organellular chloride channel protein, is increased by DNA damage and participates in the apoptotic response to p53. *Mol Cell Biol.* 22, 3610–3620. doi: 10.1128/MCB.22.11.3610-3620.2002

Fournier, N., Ducet, G., and Crevat, A. (1987). Action of cyclosporine on mitochondrial calcium fluxes. *J. Bioenerg. Biomembr.* 19, 297–303. doi: 10.1007/BF00762419

Fulda, S., Galluzzi, L., and Kroemer, G. (2010). Targeting mitochondria for cancer therapy. *Nat. Rev. Drug Discov.* 9, 447–464. doi: 10.1038/nrd3137

Gall, J. M., Wong, V., Pimental, D. R., Havasi, A., Wang, Z., Pastorino, J. G., et al. (2011). Hexokinase regulates Bax-mediated mitochondrial membrane injury following ischemic stress. *Kidney Int.* 79, 1207–1216. doi: 10.1038/ki.2010.532

Galluzzi, L., Kepp, O., Tajeddine, N., and Kroemer, G. (2008). Disruption of the hexokinase-VDAC complex for tumor therapy. *Oncogene* 27, 4633–4635. doi: 10.1038/onc.2008.114

Giorgio, V., von Stockum, S., Antoniel, M., Fabbro, A., Fogolari, F., Forte, M., et al. (2013). Dimers of mitochondrial ATP synthase form the permeability transition pore. *Proc. Natl. Acad. Sci. U.S.A.* 110, 5887–5892. doi: 10.1073/pnas.1217823110

Grills, C., Jithesh, P. V., Blayney, J., Zhang, S. D., and Fennell, D. A. (2011). Gene expression meta-analysis identifies VDAC1 as a predictor of poor outcome in early stage non-small cell lung cancer. *PLoS ONE* 6:e14635. doi: 10.1371/journal.pone.0014635

Gulbins, E., Sassi, N., Grassmè, H., Zoratti, M., and Szabò, I. (2010). Role of Kv1.3 mitochondrial potassium channel in apoptotic signalling in lymphocytes. *Biochim. Biophys. Acta* 1797, 1251–1259. doi: 10.1016/j.bbabio.2010.01.018

Han, W., Li, L., Qiu, S., Lu, Q., Pan, Q., Gu, Y., et al. (2007). Shikonin circumvents cancer drug resistance by induction of a necroptotic death. *Mol. Cancer Ther.* 6, 1641–1649. doi: 10.1158/1535-7163.MCT-06-0511

Haridas, V., Li, X., Mizumachi, T., Higuchi, M., Lemeshko, V. V., Colombini, M., et al. (2007). Avicins, a novel plant-derived metabolite lowers energy metabolism in tumor cells by targeting the outer mitochondrial membrane. *Mitochondrion* 7, 234–240. doi: 10.1016/j.mito.2006.12.005

Horton, K. L., Pereira, M. P., Stewart, K. M., Fonseca, S. B., and Kelley, S. O. (2012). Tuning the activity of mitochondria-penetrating peptides for delivery or disruption. *Chembiochem.* 13, 476–485. doi: 10.1002/cbic.201100415

Javadov, S., Hunter, J. C., Barreto-Torres, G., and Parodi-Rullan, R. (2011). Targeting the mitochondrial permeability transition: cardiac ischemia-reperfusion versus carcinogenesis. *Cell Physiol. Biochem.* 27, 179–190. doi: 10.1159/000327943

Jones, S., Martel, C., Belzacq-Casagrande, A. S., Brenner, C., and Howl, J. (2008). Mitoparan and target-selective chimeric analogues: membrane translocation and intracellular redistribution induces mitochondrial apoptosis. *Biochim. Biophys. Acta* 1783, 849–863. doi: 10.1016/j.bbamcr.2008.01.009

Kang, S. S., Han, K. S., Ku, B. M., Lee, Y. K., Hong, J., Shin, H. Y., et al. (2010). Caffeine-mediated inhibition of calcium release channel inositol 1 4, 5-trisphosphate receptor subtype 3 blocks glioblastoma invasion and extends survival. *Cancer Res.* 70, 1173–1183. doi: 10.1158/0008-5472.CAN-09-2886

Kim, T. H., Zhao, Y., Barber, M. J., Kuharsky, D. K., and Yin, X. M. (2000). Bid-induced cytochrome c release is mediated by a pathway independent of mitochondrial permeability transition pore and Bax. *J Biol Chem*.275, 39474–39481. doi: 10.1074/jbc.M003370200

Kirichok, Y., Krapivinsky, G., and Clapham, D. E. (2004). The mitochondrial calcium uniporter is a highly selective ion channel. *Nature* 427, 360–364. doi: 10.1038/nature02246

Ko, Y. H., Verhoeven, H. A., Lee, M. J., Corbin, D. J., Vogl, T. J., and Pedersen, P. L. (2012). A translational study "case report" on the small molecule "energy blocke" 3-bromopyruvate (3BP) as a potent anticancer agent: from bench side to bedside. *J. Bioenerg. Biomembr.* 44, 163–170. doi: 10.1007/s10863-012-9417-4

Kohl, T., Lörinczi, E., Pardo, L. A., and Stühmer, W. (2011). Rapid internalization of the oncogenic K^+ channel K(V)10.1. *PLoS ONE* 6:e26329. doi: 10.1371/journal.pone.0026329

Kolisek, M., Zsurka, G., Samaj, J., Weghuber, J., Schweyen, R. J., and Schweigel, M. (2003). Mrs2p is an essential component of the major electrophoretic Mg^{2+} influx system in mitochondria. *EMBO J.* 22, 1235–1244. doi: 10.1093/emboj/cdg122

Kosztka, L., Rusznák, Z., Nagy, D., Nagy, Z., Fodor, J., Szucs, G., et al. (2011). Inhibition of TASK-3 (KCNK9) channel biosynthesis changes cell morphology and decreases both DNA content and mitochondrial function of melanoma cells maintained in cell culture. *Melanoma Res.* 21, 308–322. doi: 10.1097/CMR.0b013e3283462713

Kovács, I., Pocsai, K., Czifra, G., Sarkadi, L., Szücs, G., Nemes, Z., et al. (2005). TASK-3 immunoreactivity is present but shows differential distribution in the human gastrointestinal tract. *Virchows Arch.* 446, 402–410. doi: 10.1007/s00428-005-1205-7

Leanza, L., Zoratti, M., Gulbins, E., and Szabò, I. (2012a). Induction of apoptosis in macrophages via Kv1.3 and Kv1.5 potassium channels. *Curr. Med. Chem.* 19, 5394–5404. doi: 10.2174/092986712803833281

Leanza, L., Henry, B., Sassi, N., Zoratti, M., Chandy, K. G., Gulbins, E., et al. (2012b). Inhibitors of mitochondrial Kv1.3 channels induce Bax/Bak-independent death of cancer cells. *EMBO Mol. Med.* 4, 577–593. doi: 10.1002/emmm.201200235

Leanza, L., Trentin, L., Becker, K. A., Frezzato, F., Zoratti, M., Semenzato, G., et al. (2013). Clofazimine, Psora-4 and PAP-1, inhibitors of the potassium channel Kv1.3, as a new and selective therapeutic strategy in chronic lymphocytic leukemia. *Leukemia* 27, 1782–1785. doi: 10.1038/leu.2013.56

Lena, A., Rechichi, M., Salvetti, A., Bartoli, B., Vecchio, D., Scarcelli, V., et al. (2009). Drugs targeting the mitochondrial pore act as cytotoxic and cytostatic agents in temozolomide-resistant glioma cells. *J. Transl. Med.* 7:13. doi: 10.1186/1479-5876-7-13

Li, L., Han, W., Gu, Y., Qiu, S., Lu, Q., Jin, J., et al. (2007). Honokiol induces a necrotic cell death through the mitochondrial permeability transition pore. *Cancer Res.* 67, 4894–4903. doi: 10.1158/0008-5472.CAN-06-3818

Marchi, S., Lupini, L., Patergnani, S., Rimessi, A., Missiroli, S., Bonora, M., et al. (2013). Downregulation of the mitochondrial calcium uniporter by cancer-related miR-25. *Curr. Biol.* 23, 58–63. doi: 10.1016/j.cub.2012.11.026

Martinez-Caballero, S., Dejean, L. M., Kinnally, M. S., Oh, K. J., Mannella, C. A., and Kinnally, K. W. (2009). Assembly of the mitochondrial apoptosis-induced channel, MAC. *J. Biol. Chem.* 284, 12235–12245. doi: 10.1074/jbc.M806610200

Matassa, D. S., Amoroso, M. R., Maddalena, F., Landriscina, M., and Esposito, F. (2012). New insights into TRAP1 pathway. *Am. J. Cancer Res.* 2, 235–248.

Mathupala, S. P., and Pedersen, P. L. (2010). Voltage dependent anion channel-1 (VDAC-1) as an anti-cancer target. *Cancer Biol. Ther.* 9, 1053–1056. doi: 10.4161/cbt.9.12.12451

McAndrew, D., Grice, D. M., Peters, A. A., Davis, F. M., Stewart, T., Rice, M., et al. (2011). ORAI1-mediated calcium influx in lactation and in breast cancer. *Mol. Cancer Ther.* 10, 448–460. doi: 10.1158/1535-7163.MCT-10-0923

McCommis, K. S., and Baines, C. P. (2012). The role of VDAC in cell death: friend or foe. *Biochim. Biophys. Acta* 1818, 1444–1450. doi: 10.1016/j.bbamem.2011.10.025

Monteith, G. R., Davis, F. M., and Roberts-Thomson, S. J. (2012). Calcium channels and pumps in cancer: changes and consequences. *J. Biol. Chem.* 287, 31666–31673. doi: 10.1074/jbc.R112.343061

Norman, K. G., Canter, J. A., Shi, M., Milne, G. L., Morrow, J. D., and Sligh, J. E. (2010). Cyclosporine A suppresses keratinocyte cell death through MPTP inhibition in a model for skin cancer in organ transplant recipients. *Mitochondrion* 10, 94–101. doi: 10.1016/j.mito.2009.10.001

O'Rourke, B. (2007). Mitochondrial ion channels. *Annu. Rev. Physiol.* 69, 19–49. doi: 10.1146/annurev.physiol.69.031905.163804

Pastorino, J. G., Shulga, N., and Hoek, J. B. (2002). Mitochondrial binding of hexokinase II inhibits Bax-induced cytochrome c release and apoptosis. *J. Biol. Chem.* 277, 7610–7618. doi: 10.1074/jbc.M109950200

Pedersen, P. L. (2012). 3-Bromopyruvate (3BP) a fast acting, promising, powerful, specific, and effective "small molecule" anti-cancer agent taken from labside to bedside: introduction to a special issue. *J. Bioenerg. Biomembr.* 44, 1–6. doi: 10.1007/s10863-012-9425-4

Peixoto, P. M., Dejean, L. M., and Kinnally, K. W. (2012). The therapeutic potential of mitochondrial channels in cancer, ischemia-reperfusion injury, and neurodegeneration. *Mitochondrion* 12, 14–23. doi: 10.1016/j.mito.2011.03.003

Pereira, G. C., Branco, A. F., Matos, J. A., Pereira, S. L., Parke, D., Perkins, E. L., et al. (2007). Mitochondrially targeted effects of berberine [Natural Yellow 18 5,6-dihydro-9,10-dimethoxybenzo(g)-1,3-benzodioxolo(5,6-a) quinolizinium] on K1735-M2 mouse melanoma cells: comparison with direct effects on isolated mitochondrial fractions. *J. Pharmacol. Exp. Ther.* 323, 636–649. doi: 10.1124/jpet.107.128017

Pereira, C. V., Machado, N. G., and Oliveira, P. J. (2008). Mechanisms of berberine (natural yellow 18)-induced mitochondrial dysfunction: interaction with the adenine nucleotide translocator. *Toxicol. Sci.* 105, 408–417. doi: 10.1093/toxsci/kfn131

Pinton, P., Ferrari, D., Rapizzi, E., Di Virgilio, F., Pozzan, T., Rizzuto, R. (2001). The Ca2+ concentration of the endoplasmic reticulum is a key determinant of ceramide-induced apoptosis: significance for the molecular mechanism of Bcl-2 action. *EMBO J.* 20, 2690–2701. doi: 10.1093/emboj/20.11.2690

Piskacek, M., Zotova, L., Zsurka, G., and Schweyen, R. J. (2009). Conditional knockdown of hMRS2 results in loss of mitochondrial $Mg^{(2+)}$ uptake and cell death. *J. Cell Mol. Med.* 13, 693–700. doi: 10.1111/j.1582-4934.2008.00328.x

Quast, S. A., Berger, A., Buttstädt, N., Friebel, K., Schönherr, R., and Eberle, J. (2012). General Sensitization of melanoma cells for TRAIL-induced apoptosis by the potassium channel inhibitor TRAM-34 depends on release of SMAC. *PLoS ONE* 7:e39290. doi: 10.1371/journal.pone.0039290

Raghavan, A., Sheiko, T., Graham, B. H., and Craigen, W. J. (2012). Voltage-dependant anion channels: novel insights into isoform function through genetic models. *Biochim. Biophys. Acta* 1818, 1477–1485. doi: 10.1016/j.bbamem.2011.10.019

Ralph, S. J., and Neuzil, J. (2009). Mitochondria as targets for cancer therapy. *Mol. Nutr. Food Res.* 53, 9–28. doi: 10.1002/mnfr.200800044

Rasola, A., Sciacovelli, M., Pantic, B., and Bernardi, P. (2010). Signal transduction to the permeability transition pore. *FEBS Lett.* 584, 1989–1996. doi: 10.1016/j.febslet.2010.02.022

Raviv, Z., Cohen, S., and Reischer-Pelech, D. (2013). The anti-cancer activities of jasmonates. *Cancer Chemother. Pharmacol.* 71, 275–285. doi: 10.1007/s00280-012-2039-z

Ren, Y. R., Pan, F., Parvez, S., Fleig, A., Chong, C. R., Xu, J., et al. (2008). Clofazimine inhibits human Kv1.3 potassium channel by perturbing calcium oscillation in T lymphocytes. *PLoS ONE* 3:e4009. doi: 10.1371/journal.pone.0004009

Risso, A., Braidot, E., Sordano, M. C., Vianello, A., Macrì, F., Skerlavaj, B., et al. (2002). BMAP-28, an antibiotic peptide of innate immunity, induces cell death through opening of the mitochondrial permeability transition pore. *Mol Cell Biol.* 22, 1926–1935. doi: 10.1128/MCB.22.6.1926-1935.2002

Rizzuto, R., De Stefani, D., Raffaello, A., and Mammucari, C. (2012). Mitochondria as sensors and regulators of calcium signalling. *Nat. Rev. Mol. Cell Biol.* 13, 566–578. doi: 10.1038/nrm3412

Rusznák, Z., Bakondi, G., Kosztka, L., Pocsai, K., Dienes, B., Fodor, J., et al. (2008). Mitochondrial expression of the two-pore domain TASK-3 channels in malignantly transformed and non-malignant human cells. *Virchows Arch.* 452, 415–426. doi: 10.1007/s00428-007-0545-x

Samudio, I., Fiegl, M., McQueen, T., Clise-Dwyer, K., and Andreeff, M. (2008). The Warburg effect in leukemia-stroma cocultures is mediated by mitochondrial uncoupling associated with uncoupling protein 2 activation. *Cancer Res.* 68, 5198–5205. doi: 10.1158/0008-5472.CAN-08-0555

Santandreu, F. M., Roca, P., and Oliver, J. (2010). Uncoupling protein-2 knockdown mediates the cytotoxic effects of cisplatin. *Free Radic. Biol. Med.* 49, 658–666. doi: 10.1016/j.freeradbiomed.2010.05.031

Sassi, N., De Marchi, U., Fioretti, B., Biasutto, L., Gulbins, E., Francolini, F., et al. (2010). An investigation of the occurrence and properties of the mitochondrial intermediate-conductance Ca^{2+}-activated K^+ channel mtKCa3.1. *Biochim. Biophys. Acta* 1797, 1260–1267. doi: 10.1016/j.bbabio.2009.12.015

Shimizu, S., Ide, T., Yanagida, T., and Tsujimoto, Y. (2000). Electrophysiological study of a novel large pore formed by Bax and the voltage-dependent anion channel that is permeable to cytochrome c. *J. Biol. Chem.* 275, 12321–12325. doi: 10.1074/jbc.275.16.12321

Shoshan, M. C. (2012). 3-Bromopyruvate: targets and outcomes. *J. Bioenerg. Biomembr.* 44, 7–15. doi: 10.1007/s10863-012-9419-2

Shoshan-Barmatz, V., Keinan, N., Abu-Hamad, S., Tyomkin, D., and Aram, L. (2010). Apoptosis is regulated by the VDAC1 N-terminal region and by VDAC oligomerization: release of cytochrome c, AIF and Smac/Diablo. *Biochim. Biophys. Acta* 1797, 1281–1291. doi: 10.1016/j.bbabio.2010.03.003

Shoshan-Barmatz, V., and Golan, M. (2012). Mitochondrial VDAC1: function in cell life and death and a target for cancer therapy. *Curr. Med. Chem.* 19, 714–735.

Shoshan-Barmatz, V., and Mizrachi, D. (2012). VDAC1: from structure to cancer therapy. *Front. Oncol.* 2:164. doi: 10.3389/fonc.2012.00164

Simamura, E., Shimada, H., Hatta, T., and Hirai, K. (2008). Mitochondrial voltage-dependent anion channels (VDACs) as novel pharmacological targets for anti-cancer agents. *J. Bioenerg. Biomembr.* 40, 213–217. doi: 10.1007/s10863-008-9158-6

Singh, H., Stefani, E., and Toro, L. (2012). Intracellular BKCa (iBKCa) channels. *J. Physiol.* 590, 5937–5947. doi: 10.1113/jphysiol.2011.215533

Suh, K. S., Malik, M., Shukla, A., Ryscavage, A., Wright, L., Jividen, K., et al. (2012). CLIC4 is a tumor suppressor for cutaneous squamous cell cancer. *Carcinogenesis.* 33, 986–995. doi: 10.1093/carcin/bgs115

Szabó, I., Bock, J., Grassmé, H., Soddemann, M., Wilker, B., Lang, F., et al. (2008). Mitochondrial potassium channel Kv1.3 mediates Bax-induced apoptosis in lymphocytes. *Proc. Natl. Acad. Sci. U.S.A.* 105, 14861–14866. doi: 10.1073/pnas.0804236105

Szabò, I., Bock, J., Jekle, A., Soddemann, M., Adams, C., Lang, F., et al. (2005). A novel potassium channel in lymphocyte mitochondria. *J. Biol. Chem.* 280, 12790–12798. doi: 10.1074/jbc.M413548200

Szabò, I., Leanza, L., Gulbins, E., and Zoratti, M. (2012). Physiology of potassium channels in the inner membrane of mitochondria. *Pflugers Arch.* 463, 231–246. doi: 10.1007/s00424-011-1058-7

Szabò, I., Soddemann, M., Leanza, L., Zoratti, M., and Gulbins, E. (2011). Single-point mutations of a lysine residue change function of Bax and Bcl-xL expressed in Bax- and Bak-less mouse embryonic fibroblasts: novel insights into the molecular mechanisms of Bax-induced apoptosis. *Cell Death Differ.* 18, 427–438. doi: 10.1038/cdd.2010.112

Szabó, I., and Zoratti, M. (1991). The giant channel of the inner mitochondrial membrane is inhibited by cyclosporin A. *J. Biol. Chem.* 266, 3376–3379.

Tait, S. W., and Green, D. R. (2010). Mitochondria and cell death: outer membrane permeabilization and beyond. *Nat. Rev. Mol. Cell Biol.* 11, 621–632. doi: 10.1038/nrm2952

Tan, W. (2012). VDAC blockage by phosphorothioate oligonucleotides and its implication in apoptosis. *Biochim. Biophys. Acta* 1818, 1555–1561. doi: 10.1016/j.bbamem.2011.12.032

Traba, J., Del Arco, A., Duchen, M. R., Szabadkai, G., and Satrústegui, J. (2012). SCaMC-1 promotes cancer cell survival by desensitizing mitochondrial permeability transition via ATP/ADP-mediated matrix $Ca(^{2+})$ buffering. *Cell Death Differ.*19, 650–660. doi: 10.1038/cdd.2011.139

Tsujimoto, Y., and Shimizu, S. (2000). VDAC regulation by the Bcl-2 family of proteins. *Cell Death Differ.* 7, 1174–1181. doi: 10.1038/sj.cdd.4400780

Wang, X., Zhang, X., Dong, X. P., Samie, M., Li, X., Cheng, X., et al. (2012). TPC proteins are phosphoinositide- activated sodium-selective ion channels in endosomes and lysosomes. *Cell* 151, 372–383. doi: 10.1016/j.cell.2012.08.036

Wolf, A., Agnihotri, S., Micallef, J., Mukherjee, J., Sabha, N., Cairns, R., et al. (2011). Hexokinase 2 is a key mediator of aerobic glycolysis and promotes tumor growth in human glioblastoma multiforme. *J. Exp. Med.* 208, 313–326. doi: 10.1084/jem.20101470

Wolf, F. I., and Trapani, V. (2009). Multidrug resistance phenotypes and MRS2 mitochondrial magnesium channel: two players from one stemness. *Cancer Biol. Ther.* 8, 615–617. doi: 10.4161/cbt.8.7.8152

Xu, W., Liu, Y., Wang, S., McDonald, T., Van Eyk, J. E., Sidor, A., et al. (2002). Cytoprotective role of Ca^{2+}-activated K^+ channels in the cardiac inner mitochondrial membrane. *Science* 298, 1029–1033. doi: 10.1126/science.1074360

Yagoda, N., von Rechenberg, M., Zaganjor, E., Bauer, A. J., Yang, W. S., Fridman, D. J., et al. (2007). RAS-RAF-MEK-dependent oxidative cell death involving voltage-dependent anion channels. *Nature* 447, 864–868. doi: 10.1038/nature05859

Zhang, K., Shang, Y., Liao, S., Zhang, W., Nian, H., Liu, Y., et al. (2007). Uncoupling protein 2 protects testicular germ cells from hyperthermia-induced apoptosis. *Biochem. Biophys. Res. Commun.* 360, 327–332. doi: 10.1016/j.bbrc.2007.06.071

Zhang, L., and Barritt, G. J. (2004). Evidence that TRPM8 is an androgendependent Ca^{2+} channel required for the survival of prostate cancer cells. *Cancer Res.* 64, 8365–8373. doi: 10.1158/0008-5472.CAN-04-2146

Zhong, F., Harr, M. W., Bultynck, G., Monaco, G., Parys, J. B., DeSmedt, H., et al. (2011). Induction of Ca^{2+}-driven apoptosis in chronic lymphocytic leukemia cells by peptide-mediated disruption of Bcl-2–IP3 receptor interaction. *Blood* 117, 2924–2934. doi: 10.1182/blood-2010-09-307405

Zhong, J., Kong, X., Zhang, H., Yu, C., Xu, Y., Kang, J., et al. (2012). Inhibition of CLIC4 enhances autophagy and triggers mitochondrial and ER stress-induced apoptosis in human glioma U251 cells under starvation. *PLoS ONE* 7:e39378. doi: 10.1371/journal.pone.0039378

Zoratti, M., De Marchi, U., Gulbins, E., and Szabò, I. (2009). Novel channels of the inner mitochondrial membrane. *Biochim. Biophys. Acta* 1787, 351–363. doi: 10.1016/j.bbabio.2008.11.015

Conflict of Interest Statement: The authors declare that the research was conducted in the absence of any commercial or financial relationships that could be construed as a potential conflict of interest.

Received: 17 May 2013; accepted: 05 August 2013; published online: 03 September 2013.

*Citation: Leanza L, Biasutto L, Managò A, Gulbins E, Zoratti M and Szabò I (2013) Intracellular ion channels and cancer. Front. Physiol. **4**:227. doi: 10.3389/fphys.2013.00227*

This article was submitted to Membrane Physiology and Membrane Biophysics, a section of the journal Frontiers in Physiology.

ANTIOXIDANTS & REDOX SIGNALING
Volume 22, Number 13, 2015
Mary Ann Liebert, Inc.
DOI: 10.1089/ars.2014.5979

FORUM ORIGINAL RESEARCH COMMUNICATION

Pseudomonas aeruginosa Pyocyanin Induces Neutrophil Death *via* Mitochondrial Reactive Oxygen Species and Mitochondrial Acid Sphingomyelinase

Antonella Managò,[1,*] Katrin Anne Becker,[2,*] Alexander Carpinteiro,[2] Barbara Wilker,[2] Matthias Soddemann,[2] Aaron P. Seitz,[3] Michael J. Edwards,[3] Heike Grassmé,[2] Ildiko Szabò,[1,†] and Erich Gulbins[2,3,†]

Abstract

Aims: Pulmonary infections with *Pseudomonas aeruginosa* are a serious clinical problem and are often lethal. Because many strains of *P. aeruginosa* are resistant to antibiotics, therapeutic options are limited. Neutrophils play an important role in the host's early acute defense against pulmonary *P. aeruginosa*. Therefore, it is important to define the mechanisms by which *P. aeruginosa* interacts with host cells, particularly neutrophils. ***Results:*** Here, we report that pyocyanin, a membrane-permeable pigment and toxin released by *P. aeruginosa*, induces the death of wild-type neutrophils; its interaction with the mitochondrial respiratory chain results in the release of reactive oxygen species (ROS), the activation of mitochondrial acid sphingomyelinase, the formation of mitochondrial ceramide, and the release of cytochrome *c* from mitochondria. A genetic deficiency in acid sphingomyelinase prevents both the activation of this pathway and pyocyanin-induced neutrophil death. This reduced death, on the other hand, is associated with an increase in the release of interleukin-8 from pyocyanin-activated acid sphingomyelinase-deficient neutrophils but not from wild-type cells. ***Innovation:*** These studies identified the mechanisms by which pyocyanin induces the release of mitochondrial ROS and by which ROS induce neutrophil death *via* mitochondrial acid sphingomyelinase. ***Conclusion:*** These findings demonstrate a novel mechanism of pyocyanin-induced death of neutrophils and show how this apoptosis balances innate immune reactions. *Antioxid. Redox Signal.* 22, 1097–1110.

Introduction

PSEUDOMONAS AERUGINOSA INFECTIONS are clinically very serious for immunosuppressed patients and for those with trauma, burn wounds, ventilator-associated pneumonia, sepsis, or cystic fibrosis (30). It is therefore very important to define the first-line defense mechanisms of the immune system and their interaction with the pathogen. Previous studies have shown that macrophages and lymphocytes are involved in the primary response of the lung to *P. aeruginosa*, but neutrophils are most important and are absolutely necessary for the host's defense against the bacteria (5, 16). It has been reported that mortality rates of mice depleted of lymphocytes increase only slightly (5) and, surprisingly, that the depletion of macrophages does not affect mortality rates at all (16). In marked contrast, neutropenia or the inhibition of neutrophil migration to the lung greatly sensitizes mice to pulmonary *P. aeruginosa* infection, and the application of even very low numbers of bacteria to the lung is lethal for neutropenic mice (5, 16). Although the induction of proinflammatory mediators and the activation of neutrophils are required for an efficient innate immune response to pathogens, this activation must be carefully balanced and turned off, because overshooting immune activation may result in a cytokine storm and a lethal shock syndrome.

[1]Department of Biology, University of Padova, Padova, Italy.
[2]Department of Molecular Biology, University Hospital, University of Duisburg-Essen, Essen, Germany.
[3]Department of Surgery, University of Cincinnati College of Medicine, Cincinnati, Ohio.
*The first two authors contributed equally to this article and share first authorship.
†The last two authors share senior authorship.

Innovation

The studies described here identified the mechanisms of mitochondrial reactive oxygen species (ROS) release by *Pseudomonas aeruginosa* pyocyanin. The Asm/ceramide system is functional in mitochondria and is activated by ROS. Mitochondrial Asm mediates both cytochrome *c* release from mitochondria and cell death. Induction of cell death not only is a part of the method by which *P. aeruginosa* attack the host, but it also prevents an overshooting inflammatory reaction, which is observed in Asm-deficient cells. The results of these studies may be important for understanding sepsis and the often-lethal cytokine storm, as well as for defining molecular events involved in the interaction between pyocyanin and neutrophils in *P. aeruginosa* infections.

We have previously shown that a deficiency in acid sphingomyelinase (human protein, ASM; EC 3.1.4.12, sphingomyelin phosphodiesterase; optimal pH 5.0; murine protein, Asm; gene symbol, *Smpd1*) overshoots the activation of the immune system after pulmonary infection with *P. aeruginosa* (9). At present, the mechanisms by which a deficiency in Asm disturbs the balance of innate immune activation are unknown. Asm is ubiquitously expressed and releases ceramide from sphingomyelin, predominantly not only in lysosomes but also in secretory lysosomes and on the plasma membrane (7, 13, 25). The ceramide molecules generated by Asm spontaneously associate to form ceramide-enriched membrane domains that serve to trap and cluster receptor and signaling molecules (8, 11, 12, 25). This spatial organization of receptors and signaling molecules seems to mediate many of the signaling effects of Asm and ceramide (11). This general function in the organization of cellular signaling explains the involvement of Asm in many forms of cellular stress.

ASM is also present in mitochondria (21). However, its physiological function and significance in these organelles are unknown.

P. aeruginosa can induce neutrophil death by a variety of factors, including exoenzyme U (Exo U), a phospholipase A_2; pyocyanin, a phenazine; and rhamnolipids (17, 26). Bacteria that lack pyocyanin are less pathogenic *in vivo* (3), a finding indicating that this factor plays an important role in *in vivo* infection.

Pyocyanin is a redox-active compound capable of accepting and donating electrons. It has been detected at concentrations till 100 μM in the sputum of patients with cystic fibrosis (36). Because pyocyanin can cross biological membranes, it serves as a mobile electron carrier for *P. aeruginosa* (29). Under aerobic conditions, pyocyanin directly oxidizes reduced nicotinamide adenine dinucleotide phosphate (NADPH) in the host cell cytoplasm and donates accepted electrons to oxygen molecules to produce superoxide anions and reactive oxygen species (ROS) (29). Pyocyanin, however, has been also shown to decrease both cellular adenosine trisphosphate (ATP) levels and the mitochondrial membrane potential (MMP), a finding suggesting a direct interaction between pyocyanin and mitochondria (15, 22). Mitochondria are crucial for the production of ATP, the regulation of intracellular Ca^{2+} homeostasis, and the production of ROS. They are also key participants in the regulation of cell death.

Confocal microscopy studies indicate that extracellularly administered pyocyanin reaches mitochondria, where it may enhance the production of ROS and alter mitochondrial ultrastructure by mechanisms that are still poorly defined (22). Rho^0 cells, which are devoid of the mitochondrial respiratory chain, have been reported to be almost entirely resistant to pyocyanin under aerobic conditions (1). Thus, elucidation of the mechanism by which pyocyanin affects mitochondrial functions in intact cells is an important but still largely unexplored topic.

The studies reported here focused on the molecular mechanisms that determine the balance between the proinflammatory and proapoptotic effects of pyocyanin in neutrophils. In particular, we investigated a possible effect of pyocyanin on mitochondria. Indeed, not only mitochondria are the checkpoint for the release of procaspases and caspase cofactors such as cytochrome *c* during cell death (6), but also they coordinate the inflammasome and inflammatory pathways (38).

We found that bacterial pyocyanin interferes with mitochondrial respiration and that this interference results in the formation of ROS and in the loss of MMP within a few minutes, even in intact cells. ROS then activate mitochondrial Asm, trigger the release of mitochondrial ceramide and the release of cytochrome *c* from mitochondria, and induce cell death. A deficiency in Asm prevents the pyocyanin-induced release of cytochrome *c* from isolated mitochondria, thereby preventing cell death. This reduced cell death, on the other hand, is associated with an increase in the release of interleukin-8 (IL-8) from pyocyanin-activated cystic fibrosis neutrophils but not from wild-type cells.

Results

Pseudomonas aeruginosa *induces the death of neutrophils* via *acid sphingomyelinase*

Neutrophils not only are key cells of the innate immune system but also play an important role in cystic fibrosis and its associated lung changes. To define the molecular mechanisms of the interaction between neutrophils and *P. aeruginosa*, we tested whether the *P. aeruginosa* strain ATCC 27853 induces the death of cultured and *ex vivo* neutrophils. We stimulated HL-60 cells with retinoic acid to induce their maturation to neutrophils and then determined cell death 8 h after infection with *P. aeruginosa* by staining the cells with Cy3-labeled annexin V and analyzing them by fluorescence-activated cell sorting (FACS). Furthermore, we isolated peritoneal neutrophils from wild-type and Asm-deficient mice and infected them with *P. aeruginosa*. The results showed that neutrophils lacking Asm are resistant to *P. aeruginosa*-induced death, whereas wild-type neutrophils rapidly undergo apoptosis after infection with *P. aeruginosa* strain ATCC 27853 (Fig. 1A). Similar findings were obtained with a second *P. aeruginosa* strain, 762 (not shown).

P. aeruginosa releases soluble toxins that are very important for the infection of mammalian hosts. To gain insight into the mechanism of *P. aeruginosa*-induced cell death, we incubated the pathogen directly with isolated mitochondria, key organelles in many forms of cell death. We determined cytochrome *c* release as a measurement for apoptotic changes in isolated mitochondria. Because it has been previously shown that Asm is present in the mitochondrial intermembrane space and that it associates with procaspase 3 and nitrous oxide (NO) synthases (21), we also tested the effect of *P. aeruginosa* on Asm-deficient mitochondria. The results

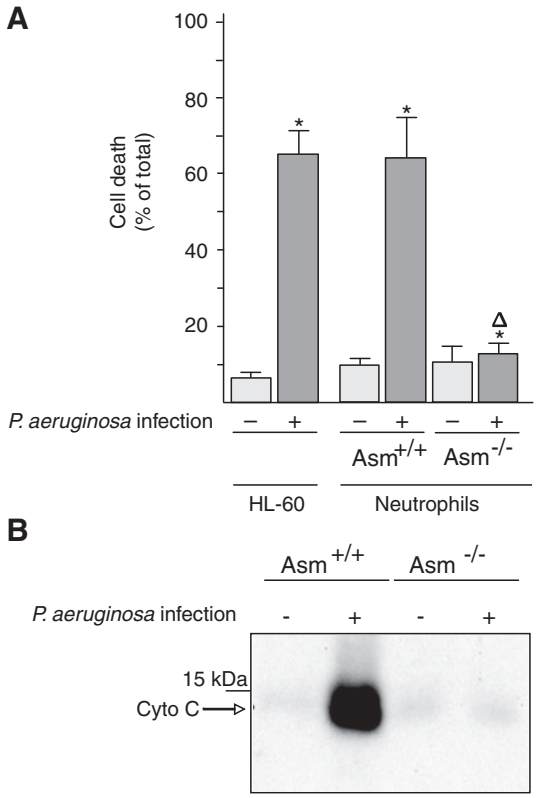

FIG. 1. Acid sphingomyelinase expression is required for cell death and the release of cytochrome *c* from mitochondria upon infection with *Pseudomonas aeruginosa.* **(A)** HL-60 neutrophils or freshly isolated wild-type and Asm-deficient peritoneal neutrophils were infected for 8 h with *P. aeruginosa* strain ATCC 27853. Apoptosis was determined by staining with FITC-annexin V. Displayed are the means ± SD, $n = 4$; $^{*}p < 0.05$ compared with uninfected and $^{\Delta}p < 0.05$ compared with infected Asm-positive cells by ANOVA. **(B)** Mitochondria were isolated from splenic neutrophils expressing or lacking Asm. Isolated mitochondria were infected with *P. aeruginosa* strain ATCC 27853 at a MOI of 10 bacteria/1 mitochondrium for 15 min. Expression of Asm is required for the release of Cyto c from mitochondria by *P. aeruginosa*. Shown are representative data from three independent experiments. Asm, acid sphingomyelinase; Cyto c, cytochrome *c*; FITC, fluorescein isothiocyanate; MOI, multiplicity of infection; SD, standard deviation.

showed that incubating isolated mitochondria from wild-type neutrophils with *P. aeruginosa* strains 762 or ATCC 27853 results in the release of cytochrome *c*, an effect that is abrogated by a deficiency of Asm in mitochondria isolated from Asm-deficient neutrophils (Fig. 1B). Control studies confirmed that the mitochondrial preparations did not contain lysosome-associated membrane protein 2 (LAMP-2) and cathepsin D but were very highly enriched in cytochrome *c* and in Tim and Tom proteins, findings that exclude contamination with lysosomes that also contain Asm (not shown).

To gain insight into the mechanisms by which *P. aeruginosa* kill neutrophils, we determined whether the bacterial product, pyocyanin, is involved in this process and whether pyocyanin acts in mitochondria by stimulating mitochondrial Asm and releasing ceramide.

Pyocyanin induces ROS in mitochondria

To gain in-depth insight into the possible interaction between pyocyanin and mitochondria, we first determined the short-term effects of pyocyanin on mitochondrial function in intact cells. The addition of 50 μM pyocyanin, a concentration that has been measured in the sputum of patients (36) and, thus, is pathophysiologically relevant, to Jurkat lymphocytes or neutrophils resulted in an immediate increase in superoxide anion production at the level of the mitochondria (Fig. 2A, B). This increase was assessed with MitoSOX Red, a mitochondria-targeted fluorogenic dye that can directly measure the superoxide generated in the mitochondria of live cells. Superoxide anion ($O_2^{-\bullet}$), the product of reducing oxygen by one electron (produced by various respiratory complexes that leak electrons to oxygen, producing primarily superoxide anions), is the precursor of most ROS. We used antimycin A, an inhibitor of complex III activity, as a positive control to force electrons to leak outside of the tight single-electron transfer mechanism, causing the production of superoxide anions. Dismutation of $O_2^{-\bullet}$ produces hydrogen peroxide (H_2O_2), which, in turn, may be fully reduced to H_2O or partially reduced to hydroxyl radical ($OH^{\bullet}$), one of the strongest oxidants. Although pyocyanin has been reported to directly interact with 2′,7′-dichlorodihydrofluorescein and dihydrorhodamine, which are commonly used to detect ROS (22), it did not oxidize MitoSOX (not shown). Incubation of cells with Mito-TEMPO, a mitochondria-targeted antioxidant with superoxide and alkyl-scavenging properties, significantly reduced pyocyanin-induced ROS production (Fig. 2C). These results suggest that a considerable portion of the pyocyanin-induced ROS production occurs at the level of mitochondria, although some pyocyanin-induced ROS production may also take place in the cytosol, mediated by the ability of pyocyanin to oxidize NADPH and to reduce cellular oxygen concentrations (29).

The addition of pyocyanin to intact cells not only led to ROS production but also resulted in a very rapid but incomplete dissipation of the MMP, $\Delta\psi m$ (Fig. 3A). This change in $\Delta\psi m$ was independent of the opening of the permeability transition pore (PTP) (34), because it also occurred in the presence of cyclosporin A, a potent PTP inhibitor (Fig. 3B). Next, we used an extracellular flux analyzer to determine the effects of pyocyanin on respiration in intact adherent mouse embryonic fibroblasts. The addition of pyocyanin to these cells immediately increased oxygen consumption (Fig. 3C). This apparent increase in respiration was only partially reversible by oligomycin, which blocks ATP synthase (Fig. 3C). The subsequent addition of the uncoupler carbonylcyanide-p-trifluoromethoxyphenyl-hydrazone (FCCP) did not restore respiration, whereas the addition of antimycin A, an inhibitor of complex III, further reduced but did not completely abolish oxygen consumption (Fig. 3C). Antimycin A, by binding to the Qi site of cytochrome *c* reductase, inhibits the oxidation of ubiquinol in the electron transport chain of oxidative phosphorylation. The inhibition of this reaction disrupts respiration and prevents the formation of the proton gradient across the inner membrane. Thus, pyocyanin drastically reduced the respiratory response to the

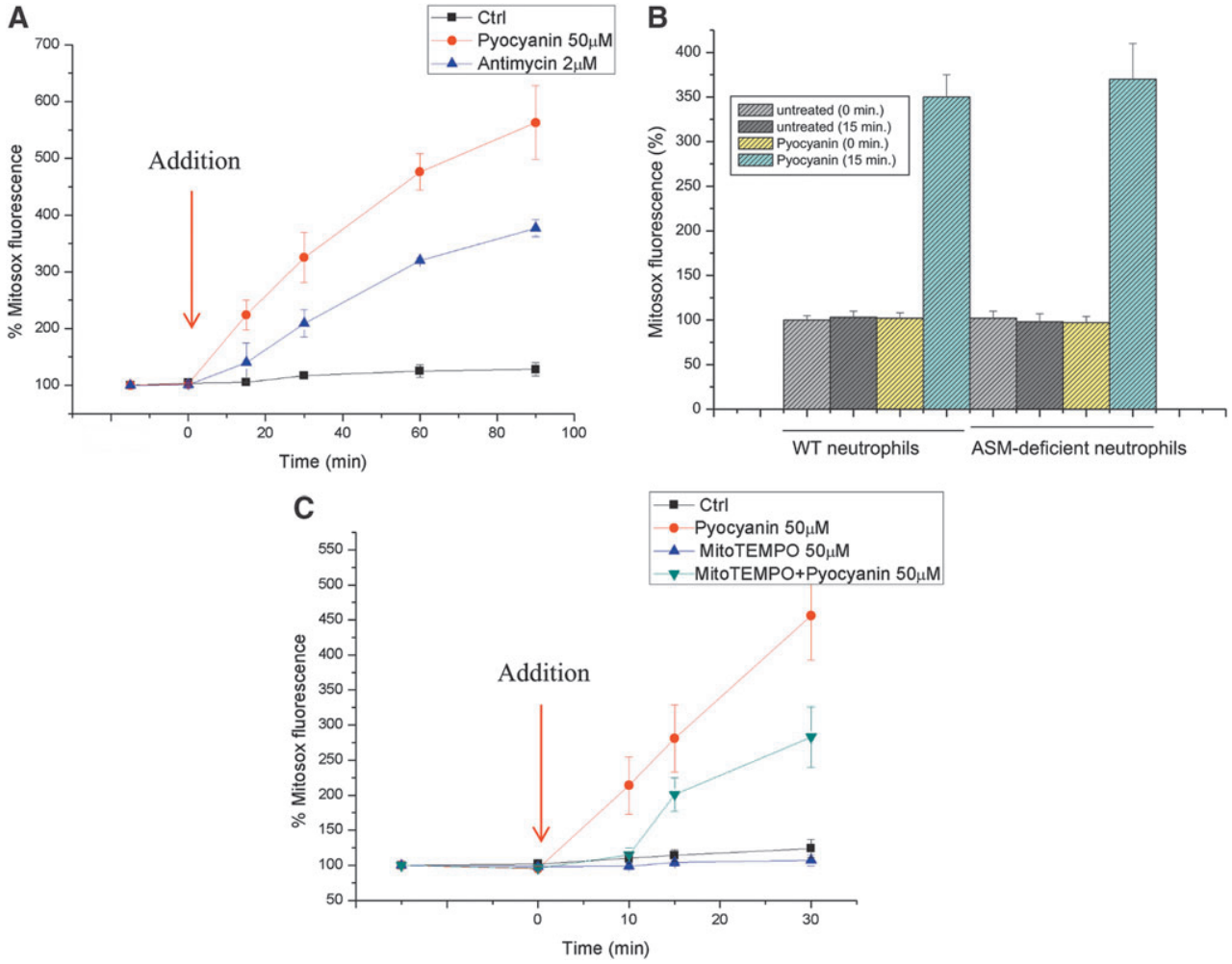

FIG. 2. Pyocyanin-induced production of mitochondrial ROS in intact cells. **(A)** Production of mitochondrial ROS was assayed with MitoSOX in intact Jurkat cells. Pyocyanin was added at the zero time point. **(B)** ROS production in peritoneal neutrophils using MitoSOX. **(C)** Jurkat cells were preincubated with MitoTEMPO for 1 h before the addition of pyocyanin. Shown are means ± SD, $n = 3$. ROS, reactive oxygen species. To see this illustration in color, the reader is referred to the web version of this article at www.liebertpub.com/ars

subsequent addition of oligomycin and FCCP. A massive loss of cells because of death and detachment was excluded by direct microscopic observation of the cells at the end of the experiments. In contrast, if cellular respiration was depressed by oligomycin, the addition of pyocyanin induced a recovery of the respiratory rate (Fig. 3D). This recovery may be simply a reflection of the loss of $\Delta\psi$m induced by pyocyanin: According to the chemiosmotic model, depolarization with associated respiratory stimulation is likely to reflect the appearance of a $\Delta\psi$m-dissipating proton leak. Again, the subsequent addition of FCCP had no effect, whereas antimycin A reduced respiration (Fig. 3D). Similar effects were observed in both settings with 25 μM pyocyanin (not shown). These results suggest that the pyocyanin-induced increase in oxygen consumption is only partially caused by an increase in respiration, given the lack of full reversal by antimycin A. Alternatively, respiration may be increased bypassing complex III. Oxygen consumption is probably also enhanced by the involvement of molecular oxygen as an acceptor of electrons directly from pyocyanin, independent of the respiratory chain.

However, these experiments also point to a possible interaction between pyocyanin and the respiratory chain complexes. One possible explanation of the generation of mitochondrial superoxide by pyocyanin is the direct interference of the toxin with respiration, diverting a part of the electron flow to superoxide production. To test this hypothesis, we used the well-established method of alamethicin-permeabilized rat liver mitochondria (RLM). We addressed the function of complexes I and III, the main sites of ROS production, after the addition of pyocyanin. Pyocyanin did not alter the function of complex I (Fig. 4A). We assessed the function of complex III by measuring the reduction of cytochrome *c* concentrations in mitochondria in which the function of complex I was inhibited by rotenone. An increase in absorbance measured at 550 nm corresponds with the chemical reduction of this mobile electron carrier. On the addition of decylubiquinol, cytochrome *c* reduction occurred; this reduction was further stimulated by the addition of pyocyanin. Reduced cytochrome *c* is then reoxidized by complex IV. Adding the complex III inhibitor antimycin A during the reoxidation phase did not drastically change the rate of

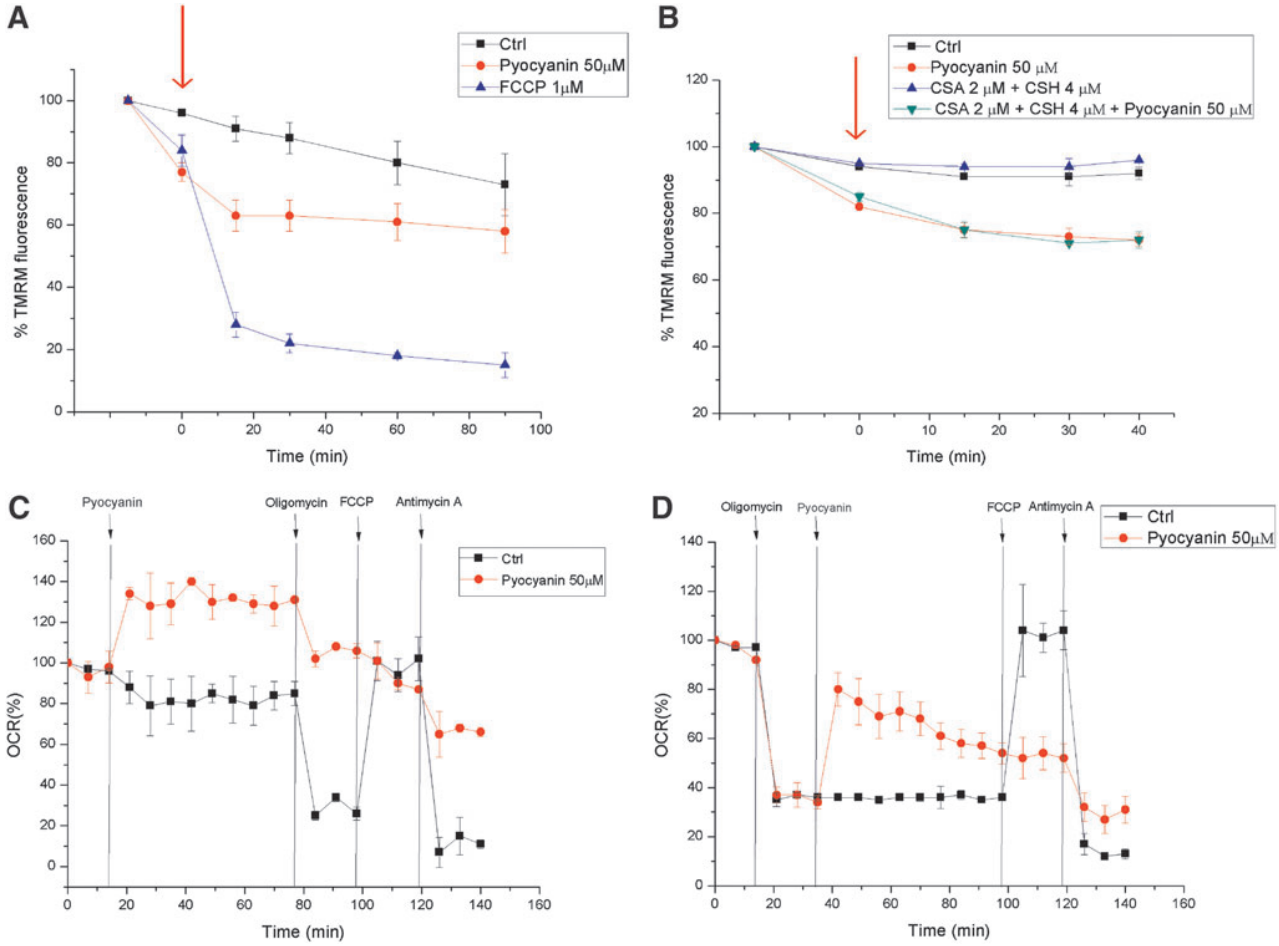

FIG. 3. Short-term bioenergetic effects of pyocyanin in intact cells. (A) Mitochondrial membrane potential was measured in Jurkat lymphocytes using TMRM under control conditions and on treatment with pyocyanin or uncoupler FCCP. Mean values ± SD are shown ($n = 3$). **(B)** As in **(A)**, but after preincubation of the cells for 30 min with CSA, an inhibitor of the PTP. The *arrows* in panels **(A)** and **(B)** indicate addition of drugs as outlined. **(C, D)** OCR measured in intact cells on addition of the indicated compounds. Results shown are representative of three independent experiments. CSA, cyclosporine A; FCCP, carbonylcyanide-p-trifluoromethoxyphenyl-hydrazone; OCR, oxygen consumption rate; PTP, permeability transition pore; TMRM, tetramethylrhodamine, methyl ester. To see this illustration in color, the reader is referred to the web version of this article at www.liebertpub.com/ars

reoxidation. The subsequent addition of sodium azide (NaN_3), which inhibits complex IV activity, increased cytochrome *c* reduction (Fig. 4B). These results indicate that pyocyanin accepts electrons from decylubiquinol and reduces cytochrome *c*, thus replacing the function of complex III. Indeed, pyocyanin reduced cytochrome *c* even in the presence of the complex III inhibitor antimycin A (Fig. 4C). Reduction also occured when all complexes were inhibited (Fig. 4D) and even in the absence of mitochondria, provided an electron donor was present (Fig. 4E). The rate of cytochrome c reduction induced by pyocyanin was slightly lower when antimycin A was added after NaN_3 than when NaN_3 was used alone (Fig. 4F), a finding suggesting that maximal reduction of cytochrome c by pyocyanin is partially dependent on complex III activity.

ROS activate mitochondrial acid sphingomyelinase

Next, we tested whether the Asm/ceramide system functions as a downstream target of pyocyanin and ROS, because oxygen radicals have been shown to activate Asm (27), which, in turn, releases ceramide, a proapoptotic molecule. To this end, we purified mitochondria from freshly isolated peritoneal neutrophils and determined the activity of Asm after treatment with pyocyanin or H_2O_2. The results (Fig. 5A, B) demonstrate a rapid activation of mitochondrial Asm activity by pyocyanin or H_2O_2. The addition of Tiron, an antioxidant, to isolated mitochondria prevented the activation of Asm by pyocyanin (Fig. 5A), a finding demonstrating the crucial role of ROS in Asm stimulation by pyocyanin in mitochondria.

Activation of Asm in isolated mitochondria on treatment with pyocyanin or H_2O_2 resulted in a ceramide release that was abrogated in Asm-deficient peritoneal neutrophils (Fig. 5C). Confocal microscopy confirmed the increase in ceramide concentrations in wild-type mitochondria after treatment with pycoyanin; this increase did not occur in Asm-deficient cells (Fig. 5D, E). This finding indicates that Asm is necessary for the release of ceramide from isolated mitochondria after treatment with pyocyanin or H_2O_2.

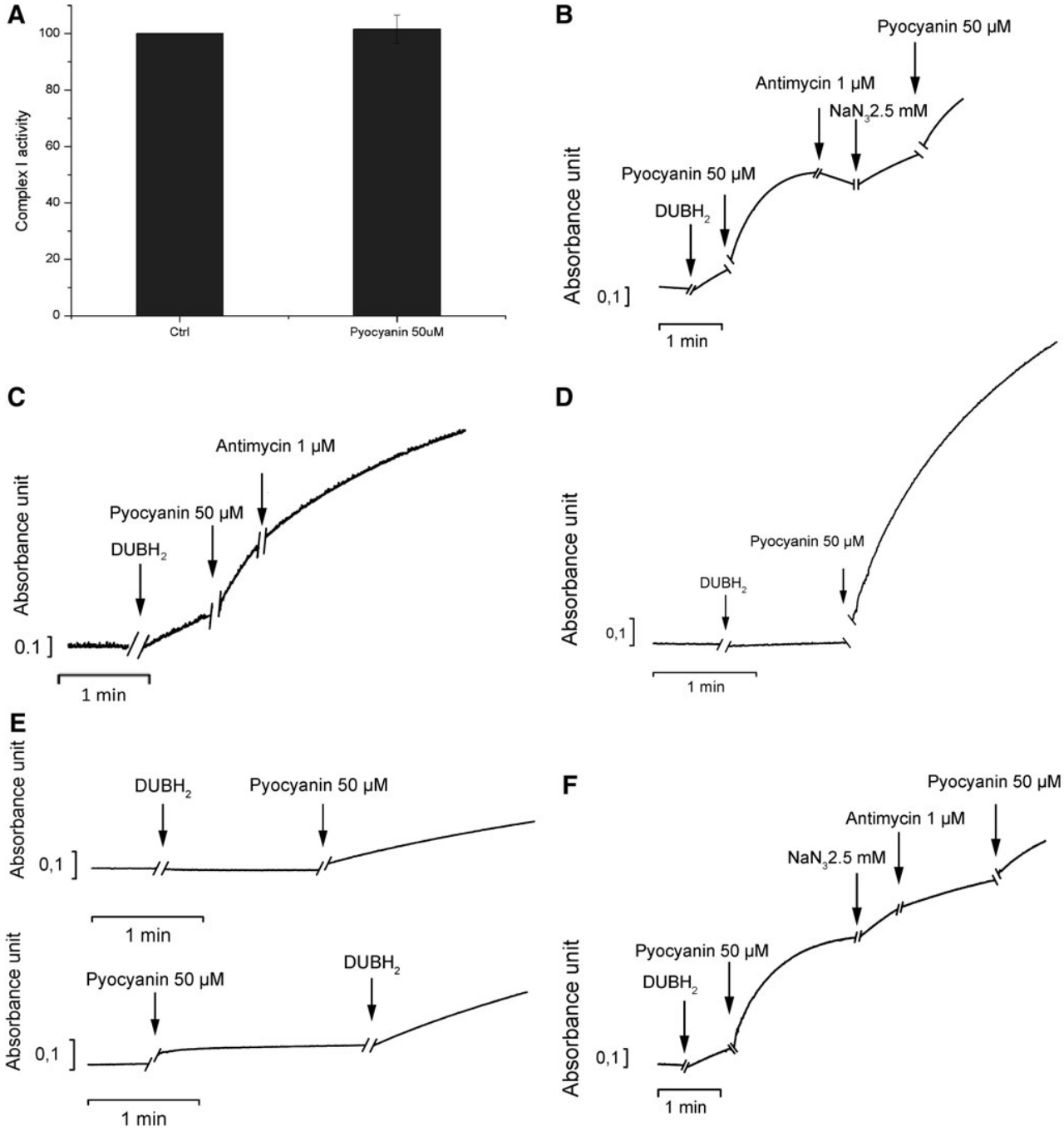

FIG. 4. Function of respiratory chain complexes in isolated mitochondria on addition of pyocyanin. **(A)** Complex I activity was assayed as described in the Materials and Methods section, taking into account the direct oxidation of the complex I substrate NADH by pyocyanin ($n = 5$). **(B–D)** Cytochrome *c* reduction after addition of the indicated substances in the presence of permeabilized mitochondria. Pyocyanin was added in all experiments in its oxidized state as deduced from the measured absorption spectra (not shown). In **(B)**, only the complex I inhibitor rotenone was present; whereas in **(C)**, complex I and complex IV were inhibited with rotenone and NaN_3. **(D)** Cytochrome *c* was reduced after the addition of the indicated substances in the presence of permeabilized mitochondria, whereas complexes I, III, and IV were inhibited by rotenone, antimycin, and NaN_3, respectively. **(E)** Experiments were performed as in **(B–D)**, but without addition of mitochondria. Pyocyanin itself does not reduce cytochrome *c* unless the electron donor decylubiquinol is added. **(F)** The experiment was performed as in **(B)**. Results shown are representative of three experiments or conditions. NaN_3, sodium azide; NADH, nicotinamide adenine dinucleotide.

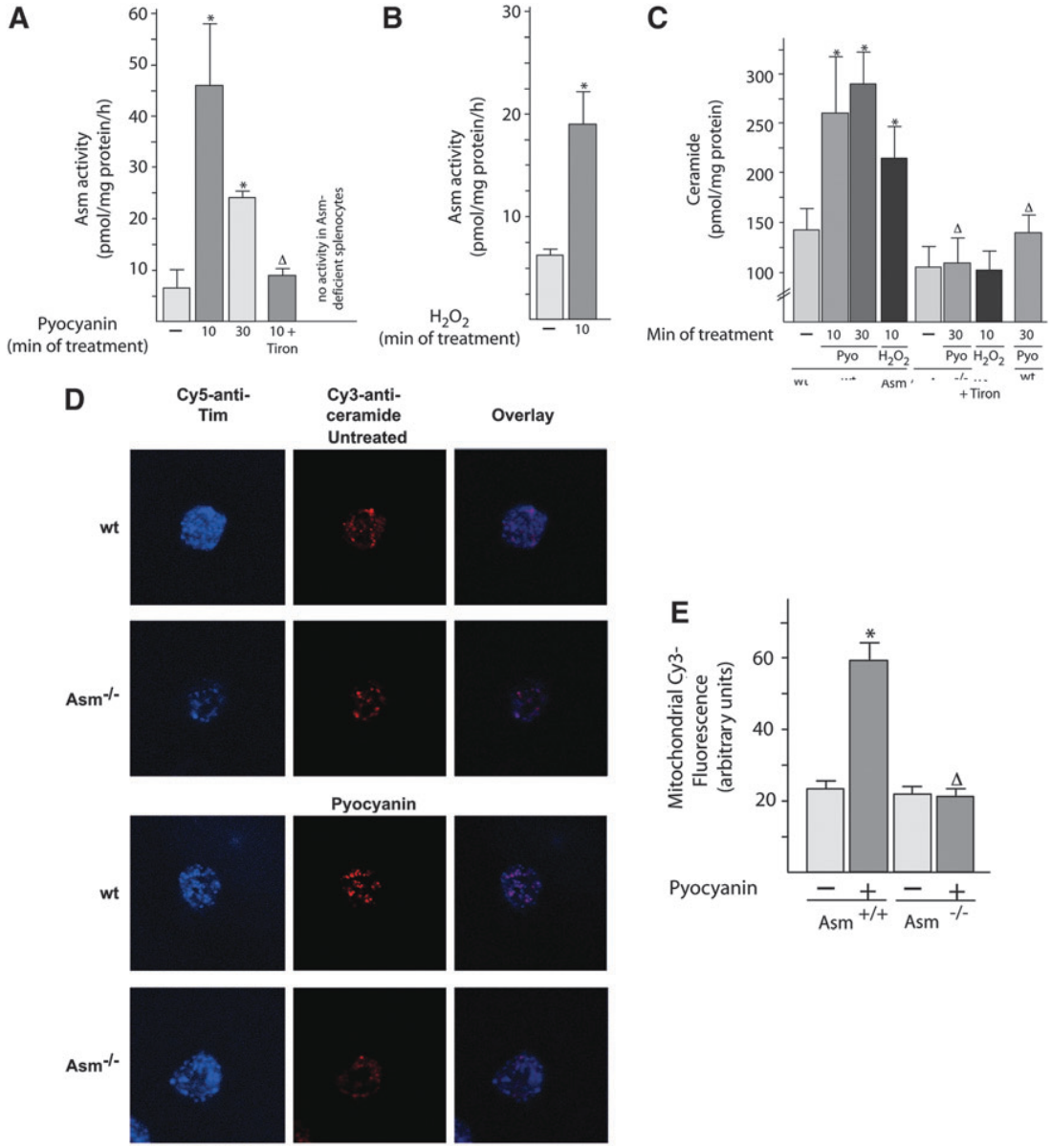

FIG. 5. ***Pseudomonas aeruginosa*** **pyocyanin activates the acid sphingomyelinase/ceramide system in mitochondria.** **(A–C)** Mitochondria were isolated from wt or Asm-deficient neutrophils. Aliquots were stimulated with 50 μM pyocyanin for 10 or 30 min or with H_2O_2 for 10 min or left unstimulated. They were then lysed, and Asm activity **(A, B)** or mitochondrial ceramide concentrations **(C)** were determined. If indicated, 10 mM Tiron was added during the stimulations. Shown are the means ± SD from four independent experiments; $^{*}p < 0.05$ compared with untreated samples, $^{\Delta}p < 0.05$ compared with treated wild-type cells, by ANOVA. **(D, E)** Wild-type or Asm-deficient peritoneal neutrophils were cultured on glass cover slips for 15 min, stimulated with 50 μM pyocyanin for 10 min, or left unstimulated. They were then fixed, permeabilized, stained with Cy3-coupled anti-ceramide and Cy5-coupled anti-Tim 23 antibodies, and analyzed by confocal microscopy. Shown are representative results from five independent experiments **(D)** and mean ± SD ($n = 5$) **(E)** of the fluorescence intensity in the Cy3 channel representing ceramide levels in mitochondria as defined by staining with Cy5-coupled anti-Tim antibodies. Fluorescence was quantified in at least 100 mitochondria per group, that is, 500 mitochondria total. The *blue* color represents Cy5, the *red* Cy3. $^{*}p < 0.05$ compared with untreated samples, $^{\Delta}p < 0.05$ compared with treated wild-type cells, ANOVA. H_2O_2, hydrogen peroxide; wt, wild-type.

Acid sphingomyelinase negatively regulates pyocyanin-induced production of IL-8

Mitochondria have been shown to be crucial in the activation of inflammasomes by recruiting and activating proinflammatory caspases; they are also crucial in the induction of cell death by the release of cytochrome *c* (6, 38). Therefore, we tested the effect of pyocyanin on the release of IL-8 and on the induction of death in freshly isolated neutrophils from wild-type and Asm-deficient

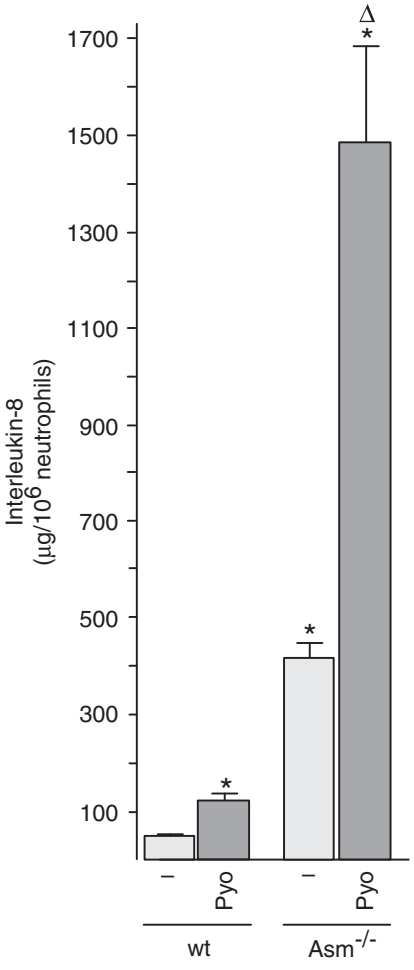

FIG. 6. Pyocyanin-induced interleukin-8 is negatively regulated by acid sphingomyelinase. Peritoneal neutrophils were obtained from wt or Asm-deficient mice and stimulated with 50 μM Pyo for 8 h. Interleukin-8 levels were determined by ELISA. Shown are the means ± SD of four independent experiments; $^{*}p < 0.05$ compared with untreated, $^{\Delta}p < 0.05$ compared with treated wild-type cells, by ANOVA. ELISA, enzyme-linked immunosorbent assay; Pyo, pyocyanin.

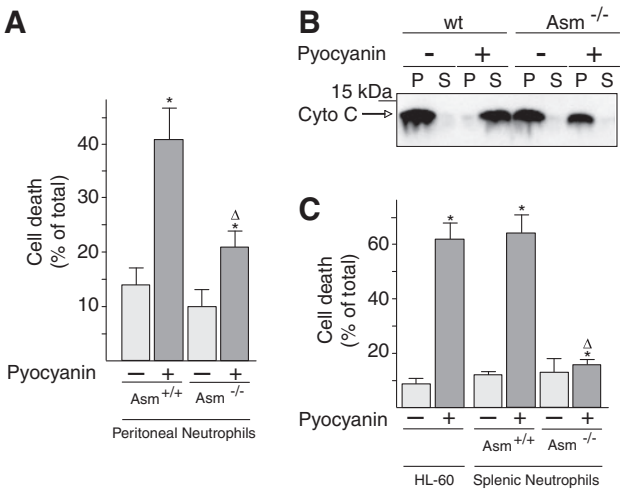

FIG. 7. Pyocyanin-induced cell death and mitochondrial cytochrome *c* release require mitochondrial acid sphingomyelinase. (A, C) Peritoneal neutrophils or splenic neutrophils were obtained from wt or Asm-deficient mice. Cells were stimulated for 8 h with 50 μM pyocyanin, and apoptosis was analyzed by FITC-annexin V staining followed by flow cytometry. Shown are mean ± SD, $n = 4$; $^{*}p < 0.05$ compared with untreated, $^{\Delta}p < 0.05$ compared with treated wild-type cells, by ANOVA. **(B)** Wild-type or Asm-deficient mitochondria were incubated with 50 μM pyocyanin for 15 min and centrifuged. The pellets and the supernatants were subjected to Western blot analysis for cytochrome *c*. Cyochrome *c* in the pellet (P) of each sample represents mitochondrial cytochrome *c*; cytochrome *c* in the supernatant (S) of the same sample represents cyctochrome *c* released from mitochondria on induction of apoptosis. The sum equals total cytochrome *c*. Results are representative of six independent experiments.

neutrophils. The results demonstrate that pyocyanin induces the release of a higher amount of IL-8 from Asm-deficient neutrophils than from wild-type cells (Fig. 6). Basal levels of IL-8 were also higher in Asm-deficient neutrophils than in wild-type neutrophils. These findings indicate a negative regulation of IL-8 release from neutrophils by Asm and ceramide.

Pyocyanin induces the death of neutrophils via *mitochondrial acid sphingomyelinase*

Pyocyanin-induced cell death in wild-type neutrophils was determined by fluorescein isothiocyanate (FITC)-annexin V staining of intact peritoneal neutrophils. Asm-deficient neutrophils resisted the toxin and exhibited significantly less apoptosis than wild-type neutrophils after treatment with pyocyanin (Fig. 7A). In accordance, only isolated mitochondria from wild-type peritoneal neutrophils, not those from Asm neutrophils, released cytochrome *c* after treatment with pyocyanin (Fig. 7B). Similar results were obtained with neutrophils isolated from the spleen and with HL-60 cells (Fig. 7C).

These results indicate that pyocyanin requires the expression of Asm if it is to mediate the mitochondrial release of cytochrome *c* and to trigger neutrophil death.

Discussion

Neutrophils are key elements of the host defense against infection with *P. aeruginosa* (16). Neutropenia greatly sensitizes mice to *P. aeruginosa* infections, with the result that neutropenic mice cannot eliminate the pathogens from the lung; they experience severe pneumonia and finally lethal sepsis (16). It is therefore of great clinical importance to understand the molecular mechanisms of the interaction between *P. aeruginosa* and neutrophils and, in particular, the mechanisms that allow the pathogen to escape the neutrophil attack.

Previous studies demonstrated that pyocyanin-induced death of neutrophils is an important element in the strategies used by *P. aeruginosa* as protection against the host defense (3). On the other hand, it is important for the host immune system to prevent overactivation, which may result in a very harmful destruction of parenchyma or even a lethal cytokine

storm. Thus, the induction of neutrophil apoptosis may also contribute to the prevention of such an overactivation of the immune system and may balance the proinflammatory response. In this study, we tested this novel concept of a balance between immune activation and apoptosis.

We found that pyocyanin induces rapid death of wild-type neutrophils and that this death depends on the activation of Asm. We report a novel mechanism for this pyocyanin action, that is, activation of Asm in mitochondria on the generation of ROS induced by pyocyanin in mitochondria. At present, the function and regulation of mitochondrial Asm have not been elucidated, athough previous studies clearly showed mitochondrial expression of the enzyme and its association with pro-caspase 3, a protein involved in the induction of apoptosis on its release from mitochondria (21). Our studies of isolated mitochondria indicate that the release of cytochrome *c* as a prototypic event for the induction of mitochondrial changes during apoptosis is induced by pyocyanin *via* activation of Asm and is mediated by locally produced ROS. At present, it is unknown how ceramide mediates this proapoptotic effect. Several studies have shown that ceramide can form large pores that may allow proteins such as cytochrome *c* and proapoptotic caspases to be released from mitochondria (32). Ceramide may also interfere with the binding of cytochrome *c* to cardiolipin and may trigger the release of cytochrome *c* from this lipid (14, 24); such a release is an initial and necessary event in the induction of mitochondrial changes during apoptosis. Furthermore, ceramide has been shown to regulate several ion channels, including Ca^{2+} and K^{+} channels (2, 10, 20). C6 ceramide has been recently suggested to trigger PTP opening (28), and it may be possible that endogenous ceramide mediates death by a similar effect. Furthermore, ceramide has been shown to trigger the integration of Bax and Bak into mitochondrial membranes (19). Therefore, the generation of ceramide may allow these proteins, which are cytoplasmic or loosely associated with the outer mitochondrial membrane in viable cells, to change their conformation, integrate into the membrane, and cause apoptosis. It is certainly possible that ceramide activates several of these events that may act in concert. Finally, it is possible that ceramide is converted to proapoptotic sphingosine (for a recent review see Ref. 35), which may also permeabilize mitochondrial membranes, interfere with cytochrome *c* binding to cardiolipin, or both.

The molecular mechanisms of Asm activation have been only partially characterized. *In vitro* studies used purified Asm and demonstrated direct oxidation of Asm at cysteine residue 629, resulting in enzyme dimerization and activation (27). Our studies suggest a similar mechanism of mitochondrial Asm activation, because the effects of pyocyanin on Asm in isolated mitochondria were prevented by preincubation with the antioxidant Tiron. However, at present, it is unknown whether Asm dimerization occurs in mitochondria after stimulation. It is also possible that ROS regulate some yet unknown intermediates that transmit the signal to Asm.

In addition, Asm has been shown to be regulated by the lipid composition of membranes (23). Thus, anionic phospholipids, as well as diacylglycerol, ceramide itself, and free fatty acids, stimulate Asm activity (23). Whether pyocyanin induces a change in mitochondrial membrane lipids, for instance by oxidation, and thereby stimulates Asm has not yet been determined.

Finally, Asm is a pH-sensitive enzyme, and the activation of redox processes by pyocyanin may trigger a change in pH, in particular an acidification of the matrix that increases the activity of Asm and the generation of ceramide.

We found that pyocyanin increases the concentration of IL-8 in neutrophils from wild-type mice. To understand whether this increase depends on Asm, possibly by recruitment of inflammasome proteins to mitochondria (38), we tested whether an Asm deficiency impairs the release of IL-8 by neutrophils. Our findings demonstrate that Asm-deficient neutrophils respond to pyocyanin by releasing IL-8, the concentration of which is much higher in these neutrophils than in wild-type cells. These findings suggest that the release of IL-8 from neutrophils is negatively regulated by Asm. This conclusion is consistent with the findings of Yu *et al.* (37), who reported that a deletion of Asm results in an increase in IL-8 concentrations on infection with *P. aeruginosa*. A simple explanation for the enhanced production of IL-8 by cells lacking Asm on treatment with pyocyanin is the resistance of these cells to pyocyanin-induced death, whereas wild-type cells die on treatment with pyocyanin. However, it is also possible that mitochondrial ceramide serves to trap proinflammatory molecules, downregulating their activity or preventing them from their proper interactions with other molecules of the respective inflammasome. In this scenario, the absence of Asm and ceramide abrogates this inhibitory effect, resulting in a marked overactivation of neutrophils. Thus, the proinflammatory activity of neutrophils caused by pyocyanin is regulated by the balance between stimulation and ceramide-mediated death, downregulation of inflammation, or both. The observed form of death is most likely classical apoptosis brought about by changes in mitochondrial functions and not caused by pyroptosis, because Asm-deficient cells release massive amounts of cytokines but do not die.

Finally, because ROS activates death and it may also trigger the induction of cytokines, for instance by activation of an inflammasome, on treatment of neutrophils with pyocyanin, the absence of one pathway may shunt ROS to the other, resulting in an overactivation of this pathway.

These findings suggest that the induction of apoptosis in neutrophils is not only a part of the pathogen's attack against the host but also serves to balance the innate immune response and prevent an overshooting reaction.

Our studies further demonstrate that pyocyanin directly affects mitochondrial functions in intact cells. In particular, pyocyanin seems to have multiple effects within the cells and can provide an electron shunt pathway at various respiratory chain sites. Pyocyanin can accept electrons from both nicotinamide adenine dinucleotide (NADH) and ubiquinol; its measured electrochemical redox potential (0.045 mV; not shown) is higher than that of ubiquinol (-0.034 mV; see also results of experiments depicted in Fig. 4). In turn, pyocyanin can donate electrons not only to cytochrome *c*, as shown in this study, but also to molecular oxygen (29). As a redox cycler, pyocyanin can oxidize mitochondrial NADH, thereby decreasing proton export from the matrix through respiratory complexes and causing a significant depolarization and presumably a decrease in the pH of the matrix. Indeed, such a decrease in the MMP can be seen in intact cells within a few minutes of pyocyanin treatment (25% decrease within 30 min). Such a change is not related to the opening of the

PTP, because this change also occurs in the presence of cyclosporin A, an inhibitor of the PTP. A recent study obtained a similar result with pancreatic acinar cells: 50 μM of pyocyanin decreased tetramethylrhodamine, methyl ester (TMRM) fluorescence by 18% within 40 min (4). The observed depolarization explains the ATP depletion of the cells, which has also been observed by several other groups (15, 22).

With regard to changes in the respiration of intact cells, pyocyanin increased their oxygen consumption, which was only partially sensitive to antimycin A, a finding suggesting that increases in these parameters are independent of complex III. Our interpretation is that this higher oxygen consumption occurs because of the conversion of molecular oxygen into superoxide radicals, a conversion that is not detected by the extracellular flux analyzer used in this study. Indeed, the addition of pyocyanin to intact cells immediately induces a substantially increased production of mitochondrial superoxide. The question arose as to whether mitochondrial ROS production is linked to a direct effect of pyocyanin on respiratory chain complexes. We found that pyocyanin does not affect complex I function but can ''replace'' complex III by draining electrons from ubiquinol and donating them to cytochrome *c*. These results suggest, first, that pyocyanin-induced superoxide production can be observed in mitochondria, primarily because NADH is the most concentrated in mitochondria and, second, that pyocyanin can provide an electron shunt pathway at various respiratory chain sites.

In summary, we found that the high concentrations of *P. aeruginosa* pyocyanin that are present in the lungs of patients infected with *P. aeruginosa* directly interfere with mitochondrial functions. This interference results in depolarization, release of ROS, activation of Asm, and formation of ceramide; this pathway triggers the release of cytochrome *c* and, finally, causes cell death, whereas it negatively regulates the induction of the proinflammatory cytokine IL-8. This pathway constitutes a novel pathway of host-pathogen interactions and serves to balance immune reactions.

Materials and Methods

Mice

Asm-deficient mice were in a C57BL/6 background, and littermates were used as controls. Mice were housed in isolated ventilated cages while providing a pathogen-free environment. The mice were routinely tested for microbial infections by bacterial culturing and serology; test results were negative before and during the study period. The hygienic status of the mice was repeatedly tested by a panel of common mouse pathogens according to the 2002 Federation of Laboratory Animal Science Associations (FELASA) recommendations.

Cells

To obtain mature primary neutrophils, we infected mice intraperitoneally for 3 h with 5×10^7 colony-forming units (CFU) of the clinical *P. aeruginosa* strain 762 (9). We then performed a lavage followed by Percoll purification of the cells. The identity of neutrophils was determined by staining with FITC-coupled anti-Gr1 antibodies followed by flow cytometric analysis. Isolated cells were cultured for 8 h in RPMI 1640 medium supplemented with 10% fetal calf serum (FCS), 10 m*M* HEPES (pH 7.4), 2 m*M* L-glutamine, 1 m*M* sodium pyruvate, 100 μM nonessential amino acids, 100 units/ml penicillin, 100 μg/ml streptomycin (all Life Technologies), and 50 μM β-mercaptoethanol. The data were confirmed by the use of primary splenic or peripheral blood neutrophils. To this end, blood was taken or spleens were homogenized, and cells were subjected to a discontinuous density gradient composed of Histopaque 1077 and 1119 (Sigma-Aldrich). Samples were centrifuged for 30 min at 700 *g* at room temperature with no brake. Neutrophils were collected from the interface of Histopaque 1077 and 1119, washed thrice, and resuspended in Dulbecco's modified Eagle's medium (DMEM) supplemented with 10% mouse serum.

Jurkat T cells and HL-60 neutrophils were grown in RPMI 1640 supplemented as described earlier. HL-60 cells were differentiated for 36 h with 2 μM retinoic acid.

Mouse embryonic fibroblasts were grown in DMEM medium supplemented as previously described (18).

Bacterial cultures

P. aeruginosa strains 762 or ATCC 27853 were grown on tryptic soy agar plates (Becton Dickinson Biosciences). Bacteria were removed from the plate and suspended in 40 ml of prewarmed, sterile tryptic soy broth (Becton Dickinson Biosciences) in Erlenmeyer flasks. The optical density of the bacterial culture was adjusted to 0.225, and the bacteria were grown for 60 min at 37°C with shaking at 125 rpm. This procedure resulted in a culture in which the bacteria were in the early log phase. The bacteria were pelleted by centrifugation for 10 min at 1600 *g* and were then resuspended in prewarmed RPMI medium buffered with 10 m*M* HEPES. Aliquots were added to the cells or the mitochondria at a multiplicity of infection (MOI) of 10 bacteria per cell or mitochondrium.

Mice were infected by an intraperitoneal injection of 5×10^7 CFU *P. aeruginosa* strain 762 suspended in HEPES/saline (H/S; 132 m*M* NaCl, 20 m*M* HEPES, pH 7.4; 5 m*M* KCl, 1 m*M* $CaCl_2$, 0.7 m*M* $MgCl_2$, and 0.8 m*M* $MgSO_4$) and were put to death after 3 h so that we could obtain mature peritoneal neutrophils.

Stimulations and infections

Cells or mitochondria were incubated with 50 μM pyocyanin or 10 μM H_2O_2 or were infected with *P. aeruginosa* at an MOI of 10 bacteria per cell for the indicated time.

Cell death

Cells were infected with *P. aeruginosa* at an MOI of 10 bacteria per cell or treated with 50 μM pyocyanin for 8 h. Cell death was determined by staining cells with FITC-coupled annexin V, followed by FACS analysis or by trypan blue staining and microscopic analysis of at least 200 cells per sample.

Isolation of mitochondria

Cells were incubated for 30 min at 4°C in buffer A, consisting of 0.3 *M* sucrose, 10 m*M* TES (pH 7.4), and 0.5 m*M* ethylene glycol tetraacetic acid (EGTA) (33). Cells were then

disintegrated with a Dounce homogenizer with 40 strokes of the tight pestle. Nuclei and unbroken cells were pelleted by centrifugation for 5 min at 600 *g* and 4°C. Mitochondria in the supernatants were pelleted at 6000 *g* for 10 min at 4°C and resuspended in 50 m*M* PIPES-KOH (pH 7.4), 50 m*M* KCl, 2 m*M* $MgCl_2$, 2 m*M* EGTA, 10 μg/ml aprotinin/leupeptin (A/L), 2 m*M* ATP, 10 m*M* phosphocreatine, 5 m*M* succinate, and 50 μg/ml creatine kinase. This buffer is slightly hyperosmotic to protect the mitochondria from swelling. Mitochondria were then incubated with the indicated doses of H_2O_2 or pyocyanin. The purity of the mitochondrial preparations was confirmed by Western blot analysis for the mitochondrial marker proteins cytochrome *c*, Tom, and Tim 23 and for proteins that are not present in mitochondria, in particular LAMP-1 and cathepsin D.

Cytochrome c *release from isolated mitochondria*

Isolated mitochondria were incubated with 50 μM pyocyanin for 15 min or with 10 μM H_2O_2 for 10 min. Stimulation was terminated by centrifugation at 4°C, after which supernatants were added to 5 × sodium dodecyl sulfate (SDS) sample buffer. The pellets were resuspended in 1 × SDS sample buffer. Samples were boiled, and proteins were separated on 12.5% sodium dodecyl sulfate–polyacrylamide gel electrophoresis (SDS-PAGE), eletrophoretically transferred onto nitrocellulose membranes, incubated with anti-cytochrome *c* antibodies (Becton Dickinson Biosciences), and developed with the Tropix electrochemoluminescence system.

Asm activity

Isolated mitochondria were stimulated with 50 μM pyocyanin for 10 or 30 min or with 10 μM H_2O_2 for 10 min. Samples were lysed in 250 m*M* sodium acetate (pH 5.0) and 1% NP40 for 10 min and homogenized by three rounds of sonication (10 s each) with a tip sonicator. The lysates were diluted to 250 m*M* sodium acetate (pH 5.0) and 0.1% NP40 and incubated with 50 nCi per sample [^{14}C]sphingomyelin for 60 min at 37°C. The substrate was dried before use and resuspended in 250 m*M* sodium acetate (pH 5.0) and 0.1% NP40. Micelles were obtained by a 10-min bath sonication. The enzymatic reaction was stopped by the addition of 800 μl chloroform/methanol (2:1, v/v), phases were separated by centrifugation, and radioactivity of an aliquot of the aqueous phase was measured by liquid scintillation counting to determine the release of [^{14}C]phosphorylcholine from [^{14}C]sphingomyelin as a measure of acid sphingomyelinase activity.

Ceramide measurements

Mitochondria were stimulated as described earlier. Stimulation was terminated by lysis in 200 μl H_2O and extraction in $CHCl_3$:CH_3OH:1 N HCl (100:100:1, v/v/v). The lower phase was collected, dried, and resuspended in 20 μl of a detergent solution consisting of 7.5% (w/v) n-octyl glucopyranoside and 5 m*M* cardiolipin in 1 m*M* diethylenetriaminepentaacetic acid (DTPA). Samples were sonicated for 10 min, and the kinase reaction was performed for 45 min at room temperature by the addition of 70 μl of a reaction mixture containing 10 μl diacylglycerol kinase (GE Healthcare Europe), 0.1 *M* imidazole/HCl (pH 6.6), 0.2 m*M* DTPA (pH 6.6), 70 m*M* NaCl, 17 m*M* $MgCl_2$, 1.4 m*M* EGTA, 2 m*M* dithiothreitol, 1 μM ATP, and 10 μCi [^{32}P]γATP. The kinase reaction was terminated by extraction of the samples in 1 ml $CHCl_3$:CH_3OH:1 N HCl (100:100:1, v/v/v), 170 μl buffered saline solution (135 m*M* NaCl, 1.5 m*M* $CaCl_2$, 0.5 m*M* $MgCl_2$, 5.6 m*M* glucose, 10 m*M* HEPES [pH 7.2]), and 30 μl of a 100 m*M* EDTA solution. The lower phase was collected and dried, and the samples were spotted onto Silica G60 thin-layer chromatography (TLC) plates and developed with chloroform/acetone/methanol/acetic acid/H_2O (50:20:15:10:5, v/v/v/v/v). The TLC plates were exposed to radiography films, the spots were removed from the plates, and the incorporation of [^{32}P] into ceramide was measured with a phosphoimager (Fuji). Ceramide amounts were determined by comparison with a standard curve with C16 to C24 ceramides used as substrates.

Interleukin-8 measurements

IL-8 was measured by enzyme-linked immunosorbent assay according to the manufacturer's instructions (R&D).

Immunostaining of neutrophils

Neutrophils were cultured on glass cover slips and treated with pyocyanin for 6 h, fixed for 15 min in 1% paraformaldehyde, washed in phosphate-buffered saline (PBS), permeabilized for 10 min in 0.1% Triton X-100 in PBS, washed, blocked with 5% FCS and 0.025% Tween 20 in PBS, washed again in PBS, and stained with anti-ceramide (clone MAB 011, diluted 1:250; Glycobiotech) and anti-Tim 23 (#611223, diluted 1:200; Becton Dickinson Biosciences) for 45 min in H/S supplemented with 1% FCS. Cells were washed thrice for 5 min each with PBS plus 0.025% Tween 20 and once in PBS; they were then stained for 45 min at room temperature with Cy3-coupled anti-mouse immunoglobulin M (1:250 dilution) and DyLight 649 goat anti-mouse IgG antibodies (dilution, 1:500; all from Jackson ImmunoResearch). Cells were washed again thrice for 5 min each with PBS plus 0.025% Tween 20 and once in PBS; they were then embedded in Mowiol and analyzed by confocal microscopy. Cy3-fluorescence intensity, as a measurement for ceramide in mitochondria, was quantified with Photoshop.

Mitochondrial membrane potential and ROS production

MMP and ROS production were measured as reported by Leanza *et al.* (18). Briefly, MMP was monitored with TMRM (20 n*M*), whereas ROS production was measured with MitoSOX (1 μM). Jurkat cells were incubated for 20 min at 37°C in Hank's balanced saline solution. After incubation, the indicated compounds were added, and the decrease in TMRM fluorescence or the increase in MitoSOX fluorescence was measured by FACS.

Oxygen consumption assay

Oxygen consumption by adherent cells was measured with an XF24 Extracellular Flux Analyzer (Seahorse Bioscience). Wild-type mouse embryonic fibroblasts cells were seeded at 3×10^4 cells per well in 200 μl of supplemented culture medium (DMEM; Sigma-Aldrich). Oxygen consumption rate

was measured at preset time intervals, and the instrument automatically carried out the preprogrammed additions of the various compounds (oligomycin, 1 μg/ml final concentration; FCCP, 400 n*M*; antimycin A, 1 μM), added as a solution in 70 μl of DMEM.

Isolation of RLM

After rats were sacrificied, the liver was removed and immediately immersed in an ice-cold isolation medium (250 m*M* sucrose, 5 m*M* HEPES, 2 m*M* EGTA; pH 7.5). The liver tissue was minced, thoroughly rinsed several times with ice-cold medium, and finally homogenized in the same solution with a glass Teflon Potter homogenizer. Mitochondria were then isolated by conventional differential centrifugation, as described by Schneider *et al.* (31). The protein content was measured by the biuret method, with bovine serum albumin (BSA) as a standard.

Activity of mitochondrial respiratory chain complexes

Complex activity was extrapolated from the slope of absorbance decrease; data are expressed as a percentage of the control (*i.e.*, the activity without the addition of any derivative).

Complex I activity. To measure NADH-coenzyme Q (CoQ) oxidoreductase (complex I) activity, we incubated RLMs (50 μg of protein per ml) with 10 μM alamethicin, 3 mg/ml BSA, 10 m*M* Tris-HCl (pH 8.0), 2.5 m*M* NaN_3, and 65 μM CoQ_1. The reaction was started by the addition of 100 μM NADH. Changes in absorbance (340 nm) were monitored at 37°C with an Agilent Technologies Cary 100 UV-Vis spectrophotometer. Rotenone 2 μM was added to assess the rotenone-independent (and thus complex I-independent) activity to be subtracted.

Complex III activity. To measure CoQ cytochrome *c* oxidoreductase (complex III) activity, we added RLMs (10 μg protein per ml) to a cuvette containing 50 m*M* potassium phosphate buffer, pH 7.5, supplemented with 10 μM alamethicin, 3 mg/ml BSA, 2.5 m*M* NaN_3, 2 μM rotenone, 0.025% Tween, and 75 μM oxidized cytochrome *c*. The reaction was started by the addition of 75 μM reduced decylubiquinol (produced by reduction of decylubiquinone in ethanol with $NaBH_4$ shortly before use); changes in absorbance were monitored at 550 nm and 37°C. We added 2 μg/ml antimycin to assess the activity of the antimycin-dependent complex III enzyme.

Statistical analysis

All data are displayed as mean ± standard deviation. All data were tested for normal distribution with the David–Pearson–Stephens test. Statistical analysis was performed with Student's *t*-test for single comparisons and ANOVA for multiple comparisons. The sample size planning was based on two-sided Wilcoxon–Mann–Whitney tests using the free software G*Power Version 3.1.7 of the University of Duesseldorf, Germany. Statistical significance was set at the level of $p < 0.05$.

Acknowledgments

This study was supported by DFG grants GU 335/13-3 and GU 335/30-1 to E.G. and AIRC IG11814 to I.S. The authors thank Dr. Andrea Mattarei for measurement of the electrochemical redox potential of pyocyanin and Dr. Mario Zoratti for useful discussion.

Author Disclosure Statement

No competing financial interests exist.

References

1. Barakat R, Goubet I, Manon S, Berges T, and Rosenfeld E. Unsuspected pyocyanin effect in yeast under anaerobiosis. *Microbiologyopen* 3: 1–14, 2014.
2. Bock J, Szabó I, Gamper N, Adams C, and Gulbins E. Ceramide inhibits the potassium channel Kv1.3 by the formation of membrane platforms. *Biochem Biophys Res Commun* 305: 890–897, 2003.
3. Caldwell CC, Chen Y, Goetzmann HS, Hao Y, Borchers MT, Hassett DJ, Young LR, Mavrodi D, Thomashow L, and Lau GW. *Pseudomonas aeruginosa* exotoxin pyocyanin causes cystic fibrosis airway pathogenesis. *Am J Pathol* 175: 2473–2488, 2009.
4. Chvanov M, Huang W, Jin T, Wen L, Armstrong J, Elliot V, Alston B, Burdyga A, Criddle DN, Sutton R, and Tepikin AV. Novel lipophilic probe for detecting near-membrane reactive oxygen species responses and its application for studies of pancreatic acinar cells: effects of pyocyanin and L-ornithine. *Antioxid Redox Signal* 22: 451–464, 2015.
5. Dunkley ML, Clancy RL, and Cripps AW. A role for CD4+ T cells from orally immunized rats in enhanced clearance of *Pseudomonas aeruginosa* from the lung. *Immunology* 83: 362–369, 1994.
6. Fulda S, Galluzzi L, and Kroemer G. Targeting mitochondria for cancer therapy. *Nat Rev Drug Discov* 9: 447–464, 2010.
7. Grassmé H, Jekle A, Riehle A, Schwarz H, Berger J, Sandhoff K, Kolesnick R, and Gulbins E. CD95 signaling *via* ceramide-rich membrane rafts. *J Biol Chem* 276: 20589–20596, 2001.
8. Grassmé H, Cremesti A, Kolesnick R, and Gulbins E. Ceramide-mediated clustering is required for CD95-DISC formation. *Oncogene* 22: 5457–5470, 2003.
9. Grassmé H, Jendrossek V, Riehle A, von Kürthy G, Berger J, Schwarz H, Weller M, Kolesnick R, and Gulbins E. Host defense against *Pseudomonas aeruginosa* requires ceramide-rich membrane rafts. *Nat Med* 9:322–330, 2003.
10. Gulbins E, Szabo I, Baltzer K, and Lang F. Ceramide-induced inhibition of T lymphocyte voltage-gated potassium channel is mediated by tyrosine kinases. *Proc Natl Acad Sci U S A* 94: 7661–7666, 1997.
11. Gulbins E and Kolesnick R. Raft ceramide in molecular medicine. *Oncogene* 22: 7070–7077, 2003.
12. Holopainen JM, Subramanian M, and Kinnunen PK. Sphingomyelinase induces lipid microdomain formation in a fluid phosphatidylcholine/sphingomyelin membrane. *Biochemistry* 37: 17562–17570, 1998.
13. Horinouchi K, Erlich S, Perl DP, Ferlinz K, Bisgaier CL, Sandhoff K, Desnick RJ, Stewart CL, and Schuchman EH. Acid sphingomyelinase deficient mice: a model of types A and B Niemann-Pick disease. *Nat Genet* 10: 288–293, 1995.
14. Iverson SL and Orrenius S. The cardiolipin-cytochrome c interaction and the mitochondrial regulation of apoptosis. *Arch Biochem Biophys* 423: 37–46, 2004.
15. Kanthakumar K, Taylor G, Tsang KW, Cundell DR, Rutman A, Smith S, Jeffery PK, Cole PJ, and Wilson R. Mechanisms of action of *Pseudomonas aeruginosa* pyocyanin on human ciliary beat in vitro. *Infect Immun* 61: 2848–2853, 1993.

16. Koh AY, Priebe GP, Ray C, Van Rooijen N, and Pier GB. Inescapable need for neutrophils as mediators of cellular innate immunity to acute *Pseudomonas aeruginosa* pneumonia. *Infect Immun* 77: 5300–5310, 2009.
17. Lavoie EG, Wandi T, and Kazmierczak BI. Innate immune responses to *Pseudomonas aeruginosa* infection. *Microbes Infect* 13:1133–1145, 2011.
18. Leanza L, Trentin L, Becker KA, Frezzato F, Zoratti M, Semenzato G, Gulbins E, and Szabo I. Clofazimine, Psora-4 and PAP-1, inhibitors of the potassium channel Kv1.3, as a new and selective therapeutic strategy in chronic lymphocytic leukemia. *Leukemia* 27: 1782–1785, 2013.
19. Lee H, Rotolo JA, Mesicek J, Penate-Medina T, Rimner A, Liao WC, Yin X, Ragupathi G, Ehleiter D, Gulbins E, Zhai D, Reed JC, Haimovitz-Friedman A, Fuks Z, and Kolesnick R. Mitochondrial ceramide-rich macrodomains functionalize Bax upon irradiation. *PLoS One* 6: e19783, 2011.
20. Lepple-Wienhues A, Belka C, Laun T, Jekle A, Walter B, Wieland U, Welz M, Heil L, Kun J, Busch G, Weller M, Bamberg M, Gulbins E, and Lang F. Stimulation of CD95 (Fas) blocks T lymphocyte calcium channels through sphingomyelinase and sphingolipids. *Proc Natl Acad Sci U S A* 96: 13795–13800, 1999.
21. Matsumoto A, Comatas KE, Liu L, and Stamler JS. Screening for nitric oxide-dependent protein-protein interactions. *Science* 301: 657–661, 2003.
22. O'Malley YQ, Abdalla MY, McCormick ML, Reszka KJ, Denning GM, and Britigan BE. Subcellular localization of Pseudomonas pyocyanin cytotoxicity in human lung epithelial cells. *Am J Physiol Lung Cell Mol Physiol* 284: L420–L430, 2003.
23. Oninla VO, Breiden B, Babalola JO, and Sandhoff K. Acid sphingomyelinase activity is regulated by membrane lipids and facilitates cholesterol transfer by NPC2. *J Lipid Res* 55: 2606–2619, 2014.
24. Ott M, Robertson JD, Gogvadze V, Zhivotovsky B, and Orrenius S. Cytochrome c release from mitochondria proceeds by a two-step process. *Proc Natl Acad Sci U S A* 99: 1259–1263, 2002.
25. Perrotta C, Bizzozero L, Cazzato D, Morlacchi S, Assi E, Simbari F, Zhang Y, Gulbins E, Bassi MT, Rosa P, and Clementi E. Syntaxin 4 is required for acid sphingomyelinase activity and apoptotic function. *J Biol Chem* 285: 40240–40251, 2010.
26. Prince LR, Bianchi SM, Vaughan KM, Bewley MA, Marriott HM, Walmsley SR, Taylor GW, Buttle DJ, Sabroe I, Dockrell DH, and Whyte MK. Subversion of a lysosomal pathway regulating neutrophil apoptosis by a major bacterial toxin, pyocyanin. *J Immunol* 180: 3502–3511, 2008.
27. Qiu H, Edmunds T, Baker-Malcolm J, Karey KP, Estes S, Schwarz C, Hughes H, and Van Patten SM. Activation of human acid sphingomyelinase through modification or deletion of C-terminal cysteine. *J Biol Chem* 278: 32744–32752, 2003.
28. Qiu Y, Yu T, Wang W, Pan K, Shi D, and Sun H. Curcumin-induced melanoma cell death is associated with mitochondrial permeability transition pore (mPTP) opening. *Biochem Biophys Res Commun* 448: 15–21, 2014.
29. Rada B and Leto TL. Pyocyanin effects on respiratory epithelium: relevance in *Pseudomonas aeruginosa* airway infections. *Trends Microbiol* 21: 73–81, 2013.
30. Sadikot RT, Blackwell TS, Christman JW, and Prince AS. Pathogen-host interactions in *Pseudomonas aeruginosa* pneumonia. *Am J Respir Crit Care Med* 171: 1209–1223, 2005.
31. Schneider WC, Hogeboom GH, Shelton E, and Striebich MJ. Enzymatic and chemical studies on the livers and liver mitochondria of rats fed 2-methyl- or 3-methyl-4-dimethylaminoazobenzene. *Cancer Res* 13: 285–288, 1953.
32. Siskind LJ, Kolesnick RN, and Colombini M. Ceramide channels increase the permeability of the mitochondrial outer membrane to small proteins. *J Biol Chem* 277: 26796–26803, 2002.
33. Szabò I, Soddemann M, Leanza L, Zoratti M, and Gulbins E. Single-point mutations of a lysine residue change function of Bax and Bcl-xL expressed in Bax- and Bak-less mouse embryonic fibroblasts: novel insights into the molecular mechanisms of Bax-induced apoptosis. *Cell Death Differ* 18: 427–438, 2011.
34. Szabo I and Zoratti M. Mitochondrial channels: ion fluxes and more. *Physiol Rev* 94: 519–608, 2014.
35. Villamil Giraldo AM, Appelqvist H, Ederth T, and Öllinger K. Lysosomotropic agents: impact on lysosomal membrane permeabilization and cell death. *Biochem Soc Trans* 42: 1460–1464, 2014.
36. Wilson R, Sykes DA, Watson D, Rutman A, Taylor GW, and Cole PJ. Measurement of *Pseudomonas aeruginosa* phenazine pigments in sputum and assessment of their contribution to sputum sol toxicity for respiratory epithelium. *Infect Immun* 56: 2515–2517, 1988.
37. Yu H, Zeidan YH, Wu BX, Jenkins RW, Flotte TR, Hannun YA, and Virella-Lowell I. Defective acid sphingomyelinase pathway with *Pseudomonas aeruginosa* infection in cystic fibrosis. *Am J Respir Cell Mol Biol* 41: 367–375, 2009.
38. Zhou R, Yazdi AS, Menu P, and Tschopp J. A role for mitochondria in NLRP3 inflammasome activation. *Nature* 469: 221–225, 2011.

Address correspondence to:
Dr. Erich Gulbins
Department of Molecular Biology
University Hospital
University of Duisburg-Essen
Hufelandstrasse 55
Essen 45122
Germany

E-mail: erich.gulbins@uni-due.de

Dr. Ildiko Szabò
Department of Biology
University of Padova
Viale G. Colombo 3
Padova 35131
Italy

E-mail: ildi@civ.bio.unipd.it

Date of first submission to ARS Central, May 2, 2014; date of final revised submission, January 12, 2015; date of acceptance, February 9, 2015.

Abbreviations Used

ANOVA = analysis of variance
Asm = acid sphingomyelinase
ATP = adenosine trisphosphate
BSA = bovine serum albumin
CFU = colony-forming units
CoQ = coenzyme Q

Abbreviations Used (Cont.)

DMEM = Dulbecco's modified Eagle's medium
DTPA = diethylenetriamine-pentaacetic acid
EGTA = ethylene glycol tetraacetic acid
ELISA = enzyme-linked immunosorbent assay
FACS = fluorescence-activated cell sorting
FCCP = carbonylcyanide-p-trifluoromethoxyphenyl-hydrazone
FCS = fetal calf serum
FITC = fluorescein isothiocyanate
H_2O_2 = hydrogen peroxide
IL-8 = interleukin 8
LAMP-2 = lysosome-associated membrane protein 2
MMP = mitochondrial membrane potential
MOI = multiplicity of infection
NADH = nicotinamide adenine dinucleotide
NADPH = nicotinamide adenine dinucleotide phosphate
NaN_3 = sodium azide
NO = nitrous oxide
OCR = oxygen consumption rate
OD = optical density
PBS = phosphate-buffered saline
PTP = permeability transition pore
RLM = rat liver mitochondria
ROS = reactive oxygen species
SD = standard deviation
SDS = sodium dodecyl sulfate
SDS-PAGE = sodium dodecyl sulfate–polyacrylamide gel electrophoresis
TLC = thin-layer chromatography
TMRM = tetramethylrhodamine, methyl ester
wt = wild type

Mar. Drugs **2015**, *13*, 4470-4491; doi:10.3390/md13074470

OPEN ACCESS

marine drugs

ISSN 1660-3397

www.mdpi.com/journal/marinedrugs

Article

Molecular Mechanisms by Which a *Fucus vesiculosus* Extract Mediates Cell Cycle Inhibition and Cell Death in Pancreatic Cancer Cells

Ulf Geisen [1], Marion Zenthoefer [2], Matthias Peipp [3], Jannik Kerber [1], Johannes Plenge [4], Antonella Managò [5], Markus Fuhrmann [6], Roland Geyer [6], Steffen Hennig [2], Dieter Adam [4], Levent Piker [2], Gerald Rimbach [7] and Holger Kalthoff [1,*]

[1] Division of Molecular Oncology, Institute for Experimental Cancer Research, Medical Faculty, CAU, University Hospital Schleswig-Holstein, 24105 Kiel, Germany; E-Mails: ugeisen@email.uni-kiel.de (U.G.); jannik-kerber@t-online.de (J.K.)

[2] CRM, Coastal Research & Management, 24159 Kiel, Germany; E-Mails: m.zenthoefer@web.de (M.Z.); steffen.hennig@crm-online.de (S.H.); lpiker@oceanbasis.de (L.P.)

[3] Division of Stem Cell Transplantation and Immunotherapy, Department of Internal Medicine II, University Hospital Schleswig-Holstein, 24105 Kiel, Germany; E-Mail: m.peipp@med2.uni-kiel.de

[4] Institute of Immunology, University Hospital Schleswig-Holstein, 24105 Kiel, Germany; E-Mails: Johannes.plenge@gmx.de (J.P.); dadam@email.uni-kiel.de (D.A.)

[5] Department of Biology, University of Padua, 35131 Padua, Italy; E-Mail: manago.antonella@gmail.com

[6] Numares AG, 93053 Regensburg, Germany; E-Mails: markus.fuhrmann@numares.com (M.F.); Roland.Geyer@numares.com (R.G.)

[7] Institute of Human Nutrition and Food Science, Christian-Albrechts University of Kiel, 24118 Kiel, Germany; E-Mail: rimbach@foodsci.uni-kiel.de

* Author to whom correspondence should be addressed; E-Mail: hkalthoff@email.uni-kiel.de; Tel.: +49-431-597-1937.

Academic Editor: Peer B. Jacobson

Received: 4 June 2015 / Accepted: 8 July 2015 / Published: 20 July 2015

Abstract: Pancreatic cancer is one of the most aggressive cancer entities, with an extremely poor 5-year survival rate. Therefore, novel therapeutic agents with specific modes of action are urgently needed. Marine organisms represent a promising source to identify new pharmacologically active substances. Secondary metabolites derived from marine algae are

of particular interest. The present work describes cellular and molecular mechanisms induced by an HPLC-fractionated, hydrophilic extract derived from the Baltic brown seaweed *Fucus vesiculosus* (Fv1). Treatment with Fv1 resulted in a strong inhibition of viability in various pancreatic cancer cell lines. This extract inhibited the cell cycle of proliferating cells due to the up-regulation of cell cycle inhibitors, shown on the mRNA (microarray data) and protein level. As a result, cells were dying in a caspase-independent manner. Experiments with non-dividing cells showed that proliferation is a prerequisite for the effectiveness of Fv1. Importantly, Fv1 showed low cytotoxic activity against non-malignant resting T cells and terminally differentiated cells like erythrocytes. Interestingly, accelerated killing effects were observed in combination with inhibitors of autophagy. Our *in vitro* data suggest that Fv1 may represent a promising new agent that deserves further development towards clinical application.

Keywords: algae; *Fucus vesiculosus*; pancreatic; cancer; cell cycle inhibitors; autophagy; proliferation

1. Introduction

Pancreatic cancer has an overall five-year survival rate of 7.2% (in 2010) [1] and the only curative treatment option—being limited to less than 20% of the patients—is resection of the tumor by surgery. However, also patients with resection are dying because of tumor recurrence or metastasis development [2]. Pancreatic cancer is one of the few tumor entities for which the incidence and mortality rate is even predicted to increase in the next years [1,3]. Chemotherapeutic treatment regimens for pancreatic cancer have improved within the last years, but prolonged lifetime is limited to only a few months [2]. New therapeutic options are urgently needed.

Brown algae might represent an invaluable source for identifying new therapy agents since they are rich in sulfated polysaccharides and secondary plant metabolites like fucoidans, fucoxanthin or phlorotannins [4–6]. Besides antioxidant activity and beneficial effects on cardiovascular disease, these substances were shown to exhibit anti-cancerous properties [4,5,7–10]. Fucoidans are known to inhibit proliferation in tumor cells [11,12]. For fucoxanthin and phlorotannins, anti-proliferative and apoptotic effects are known [13–16]. However, the particular mechanisms are not yet unraveled.

In the present work, we systematically investigated the effect of a purified acetonic extract of the Baltic brown seaweed *Fucus vesiculosus* (called Fv1) on human cancer and non-malignant cell lines. We studied its effects on the gene expression and protein level and our analyses suggest cell cycle control mechanisms as the major mode of action.

2. Results

2.1. Influence of Fv1 on Viability of Cancer Cells

First, we analyzed the effect of Fv1 on the viability of tumor cells. Fv1 inhibited the growth of different tumor cell lines significantly (Figure 1). The EC50 (effective half maximal concentration) values of Fv1 range between 17.35 µg/mL for PancTU1 (95% CI: 16.74–17.99), 17.5 µg/mL for Panc89 (95% CI: 17.24–17.77), 19.23 µg/mL for Panc1 (95% CI: 18.52–19.98) and 28.9 µg/mL for Colo357 (95% CI: 22.71–32.11). Morphologically, Fv1-treated cells exhibited more spindle-like cells, observed with staining of actin and tubulin (Figure 2). Treated cells changed their microfilamental structures. Moreover, they rather grew in a solitary way and did not form dense epithelial structures like untreated cells do. Figure 2 shows one representative experiment with Panc89 pancreatic ductal adenocarcinoma (PDAC) cells.

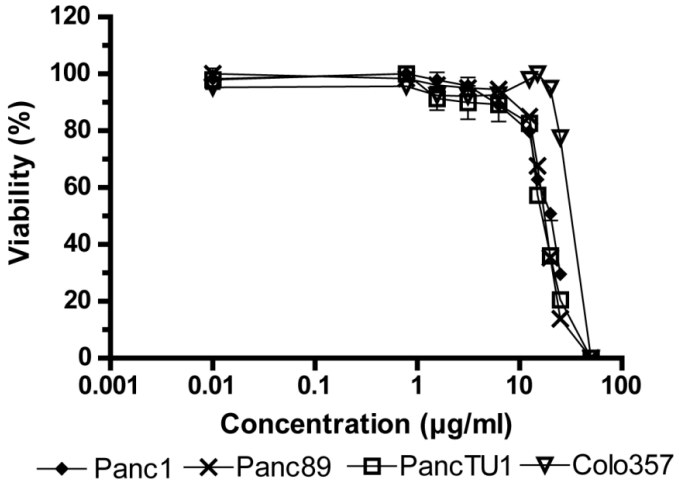

Figure 1. Inhibition of cell viability by *Fucus vesiculosus* (Fv1) in different cancer cell lines. 5×10^3 cells were seeded in 96 well plates and treated with Fv1 or dimethyl sulfoxide (DMSO) as control (0.15%) after 24 h. After 72 h treatment, an AlamarBlue viability assay was performed. Values are presented as % of control; concentrations are shown using a logarithmic scale. Raw data are shown in Supplementary Table S1. $n = 4$.

To get more insight into the time-dependent morphological changes induced by Fv1, live cell imaging was performed by taking microscopic images every 15 min. While untreated cells divided normally, we observed many Fv1-treated cells entering mitosis, showing a cleaving furrow but then the cells rounded up and died. Often, cell fragmentation was observed several hours later. Representative images of this process are given in Figure 3.

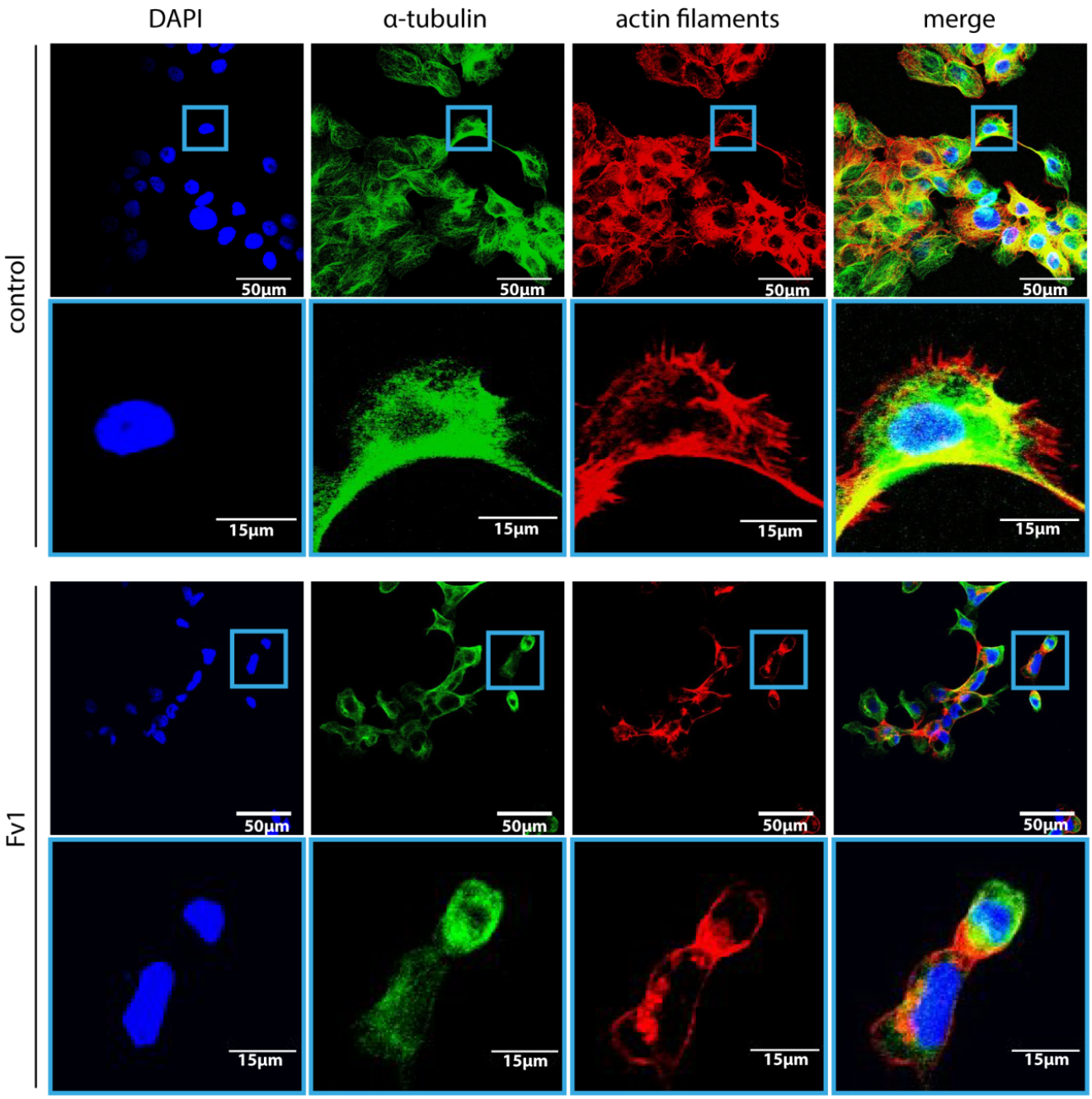

Figure 2. Fv1 leads to decreased cell numbers and to morphological alterations. Panc89 cells were seeded on coverslips and treated with Fv1 (10 µg/mL) or DMSO (0.125%)-containing cell culture medium. After 24 h, the cells were stained with an α-Tubulin antibody (2nd antibody: α-mouse, Alexa 488-coupled) and with phalloidin (Alexa 546-coupled) for actin cytoskeleton staining. The coverslips were mounted using a DAPI-containing mounting medium. Representative pictures were taken with a Zeiss CLSM. Two magnifications are shown.

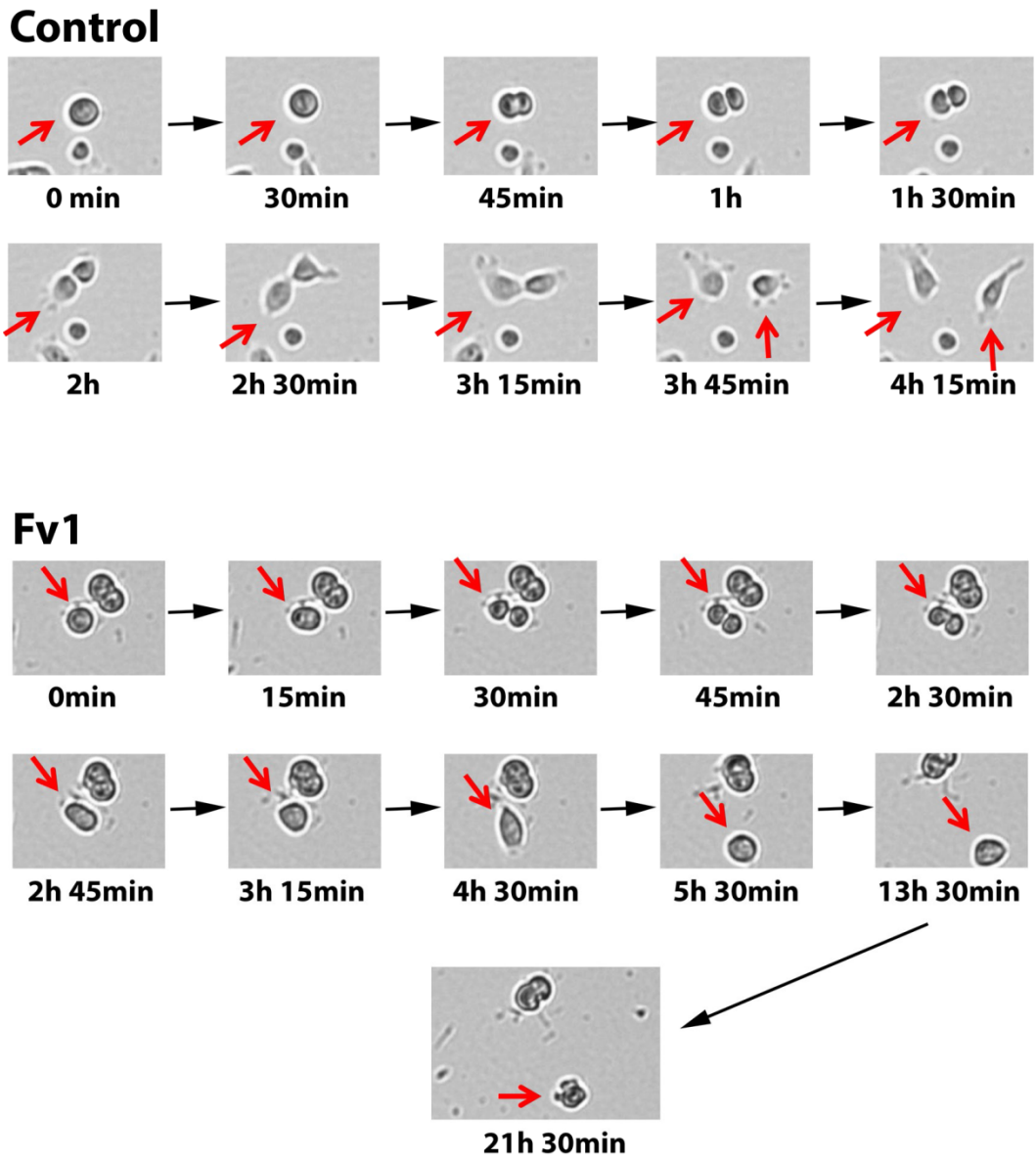

Figure 3. Fv1 inhibits mitosis. Human pancreatic ductal epithelial (HPDE) cells were treated with Fv1 in a lethal dose (50 µg/mL) and observed using the JuLI Br Live Cell Analyzer. Pictures were taken every 15 min automatically for 24 h. Representative pictures show one single cell undergoing mitosis.

2.2. Effect of Fv1 on Cell Cycle and Cell Cycle Inhibitors

To elucidate the molecular mechanism mediated by Fv1 in more detail, we performed large scale gene expression profiling on over 40,000 transcripts using Agilent arrays, comparing Fv1-treated with untreated cells. The expression of many genes was significantly changed (Table 1A). Fv1 regulated about 10-fold less genes in Colo357 cells than in the cell lines Panc1, Panc89, PancTU1 and HPDE. 157 genes were found to be commonly deregulated in the treated cell lines Panc89, Panc1 and PancTU1. Many of these genes are involved in cell cycle control, DNA repair and also in inflammation and cancer (Table 1B). Because of these findings, we focused on cell cycle regulating pathways. Interestingly, the cell cycle inhibitor p57 was induced in three cancer cell lines (Panc1, Panc89, PancTU1). Accordingly,

some downstream targets that are inhibited by p57 were suppressed (Cyclin E2, CDC45, CDC7, CDC25A, E2F1, PCNA, see Table 1C and Supplementary Figure S1 for the pathway graphic). Furthermore, the expression of the upstream regulator "tumor protein 53 inducible protein" TP53INP1 was increased. In addition, the expression of cell division cycle protein 20 (CDC20) which activates the anaphase promoting complex (APC) [17], was decreased in three cell lines (Panc1, PancTU1, Panc89, see Table 1C). This led us to the suggestion that Fv1 induces a cell cycle arrest.

Table 1. Fv1 regulates pathways involved in DNA-replication and cell cycle cells were cultured and incubated with Fv1 for 24 h. Whole cell lysates were produced by pooling attached cells and detached cells in the supernatant. RNA was isolated, reverse-transcribed and hybridized to Agilent 40K chips. After hybridization, data were normalized according to the analysis standards of SourceBioscience (Berlin). (**A**) Number of significantly regulated genes after Fv1 treatment. Criteria of significance were a p-value < 0.05 and a log fold change (lfc) >1 or <−1; (**B**) Collectively regulated genes of the cell lines Panc1, PancTU1 and Panc89 were analyzed using the DAVID (Database for Annotation, Visualization and Integrated Discovery) functional annotation clustering tool and KEGG (Kyoto Encyclopedia of Genes and Genomes) pathway. The most probable pathways, according to DAVID analysis, are shown. All experiments were performed in biological triplicates; (**C**) Gene expression data of single genes which are involved in the KEGG pathway of cell cycle regulation are shown with log fold changes (log 2) and bonferroni-corrected p-values.

A

Cell Line	Number of Regulated Genes
Panc1	3951
Panc89	3909
HPDE	2614
Colo357	200
PancTU1 6 h	340
PancTU1 24 h	2930

B

Term	Count	% of Pathway Genes	p-Value (Benjamini-Hochberg-Corrected)
DNA replication	8	6.25	0.0000012
Cell cycle	11	8.59	0.0000034
Base excision repair	5	3.91	0.0045238
Terpenoid backbone biosynthesis	4	3.13	0.0038877
Oocyte meiosis	5	3.91	0.1670225
Lysosome	5	3.91	0.1705743
Pyrimidine metabolism	4	3.13	0.3412000
Nucleotide excision repair	3	2.34	0.3292213

Table 1. *Cont.*

C								
Target ID	**Panc1**		**PancTU1**		**Panc89**		**Gene Symbol**	**Gene Name**
	Lfc	***p*-Value**	**Lfc**	***p*-Value**	**Lfc**	***p*-Value**		
NM_000076	2.0364	0.0326	1.0465	0.0261	2.7013	0.0347	CDKN1C	cyclin-dependent kinase inhibitor 1C (p57, Kip2)
NM_057749	−1.9238	0.0470	−1.9484	0.0003	−4.3172	0.0050	CCNE2	cyclin E2
NM_003504	−1.5647	0.0243	−1.3113	0.0054	−3.5616	0.0005	CDC45	cell division cycle 45 homolog (*S. cerevisiae*)
NM_003503	−1.3615	0.0132	−1.5369	0.0012	−3.7463	0.0081	CDC7	cell division cycle 7 homolog (*S. cerevisiae*)
NM_001789	−1.9897	0.0263	−1.8791	0.0001	−4.5741	0.0359	CDC25A	cell division cycle 25 homolog A (*S. pombe*)
NM_005225	−1.3352	0.0197	−1.3330	0.0004	−3.2981	0.0415	E2F1	E2F transcription factor 1
NM_002592	−1.3851	0.0047	−1.1083	0.0018	−2.9858	0.0056	PCNA	proliferating cell nuclear antigen
NM_033285	2.2445	0.0023	3.9746	0.0052	5.6604	0.0427	TP53INP1	tumor protein p53 inducible nuclear protein 1
NM_001255	−1.1762	0.0036	−1.0547	0.0160	−3.2856	0.0221	CDC20	cell division cycle 20 homolog (*S. cerevisiae*)

To confirm this hypothesis, we examined changes in cell cycle by propidium iodide staining. Treatment with Fv1 led to an elevated number of cells in G2 phase and a decrease of cells in G1 and S phase (Figure 4). This suggests a cell cycle inhibition in the G2 phase, which was also observed in Panc89 cells (see Supplementary Figures S12 and S13).

In addition, we analyzed some of the de-regulated genes on the protein level by Western blotting. The cell cycle inhibitors p21 and p27 were induced by Fv1 after 4 to 24 h as shown for the PDAC cell line Panc89 (Figure 5A). These findings support our hypothesis of a cell cycle affecting mechanism induced by Fv1. Analysis of cyclin D3, cyclin E1, p15 and p16 showed no differences compared to β-Actin or α-Tubulin as reference controls (see Supplementary Figures S2 and S3).

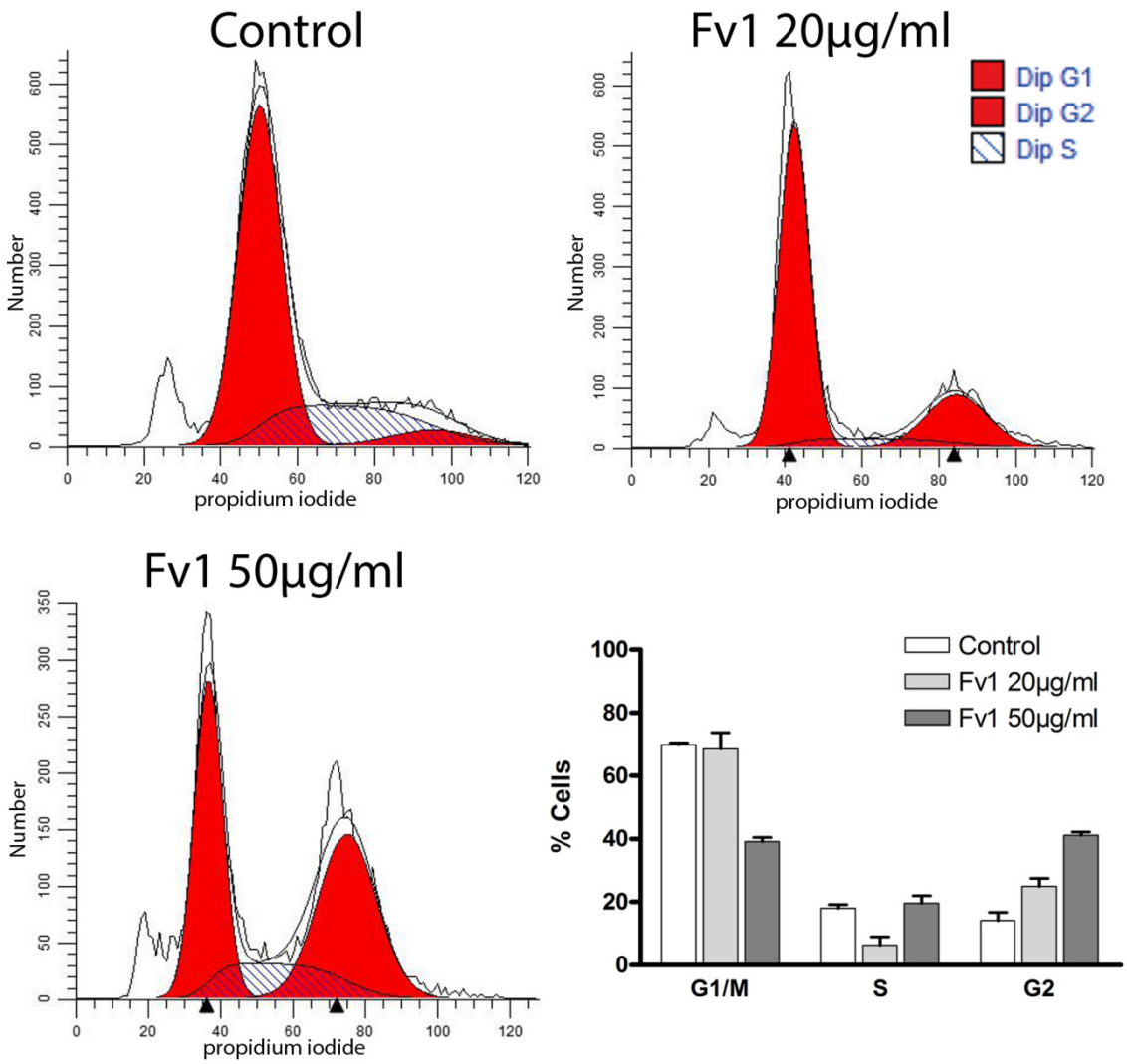

Figure 4. Fv1 induces a cell cycle arrest in pancreatic cancer cells. Colo357 cells were treated with Fv1 24 h after seeding and detached after 24 h of treatment. The detached cells were stained with hypotonic propidium iodide staining and measured by flow cytometry. The data were analyzed with Modfit and presented as percentage of cells for each cell cycle phase. One representative of two replicates is shown. See Supplementary Figures S11–S13 for a 4 h time point and the corresponding experiments with the cell line Panc89. The sub-G1 peak was not considered, because only cells with a cell-like FSC and SSC were taken into account.

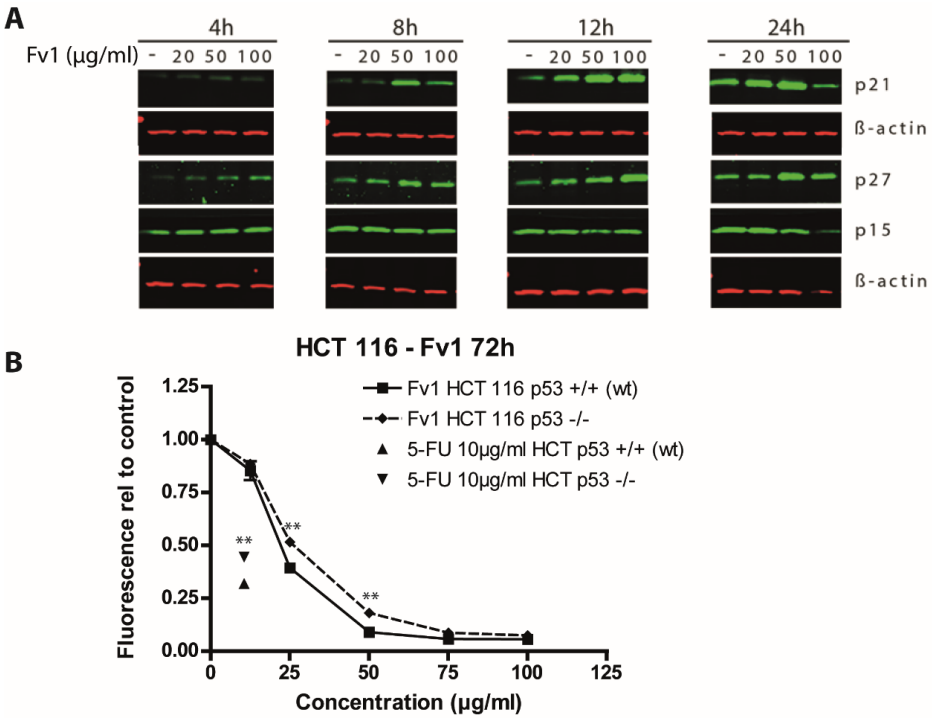

Figure 5. Effect of Fv1 on cell cycle regulating proteins. (**A**) Panc89 cells were grown for 24 h in 6 well plates and treated with different concentrations of Fv1. At the indicated time points, cells were lysed and lysates were analyzed by Western blotting. Proteins were detected using fluorescence-labeled secondary antibodies and an infrared scanner (Odyssey, LICOR); (**B**) HCT 116 cells with wild-type p53 or loss of p53 were treated with different concentrations of Fv1 for 72 h. 5-Fluorouracil at 10 µg/mL was used as control. Viability was measured with AlamarBlue. The experiment was performed in biological triplicates. Significance was calculated using students *t*-test. Differences with a *p*-value <0.001 are indicated with **. One of 3 replicates is shown as representative experiment.

The upstream regulator and one of the most important cell cycle regulators is p53. We analyzed its role in response to Fv1 using a p53 knockout model generated with the cell line HCT 116. The p53-inducing drug 5-Fluorouracil was used as control. The effect of Fv1 was significantly lower in the p53-lacking (−/−) cells than in the p53 wild-type variant (Figure 5B).

2.3. Impact of Caspase Activity and Autophagy

Analysis of PARP via Western blot showed a cleavage when high concentrations of Fv1 were applied (Figure 6A). Analysis of cell death via co-staining with Annexin V and propidium iodide showed no clear differentiation between apoptosis and necrosis, but a general dose-dependent cell death after 24 h of treatment (Figure 6B). Treated cells were larger in size (FSC) and more granulated (SSC) than normal cells. While the caspase inhibitor zVAD-fmk inhibited the cytotoxic effect of the prototypical member of the death ligand family, TRAIL, it had no impact on the Fv1 activity (Figure 6B). In addition, zVAD-fmk did not inhibit the anti-proliferative effect as observed by AlamarBlue assays (see Supplementary Figure S4).

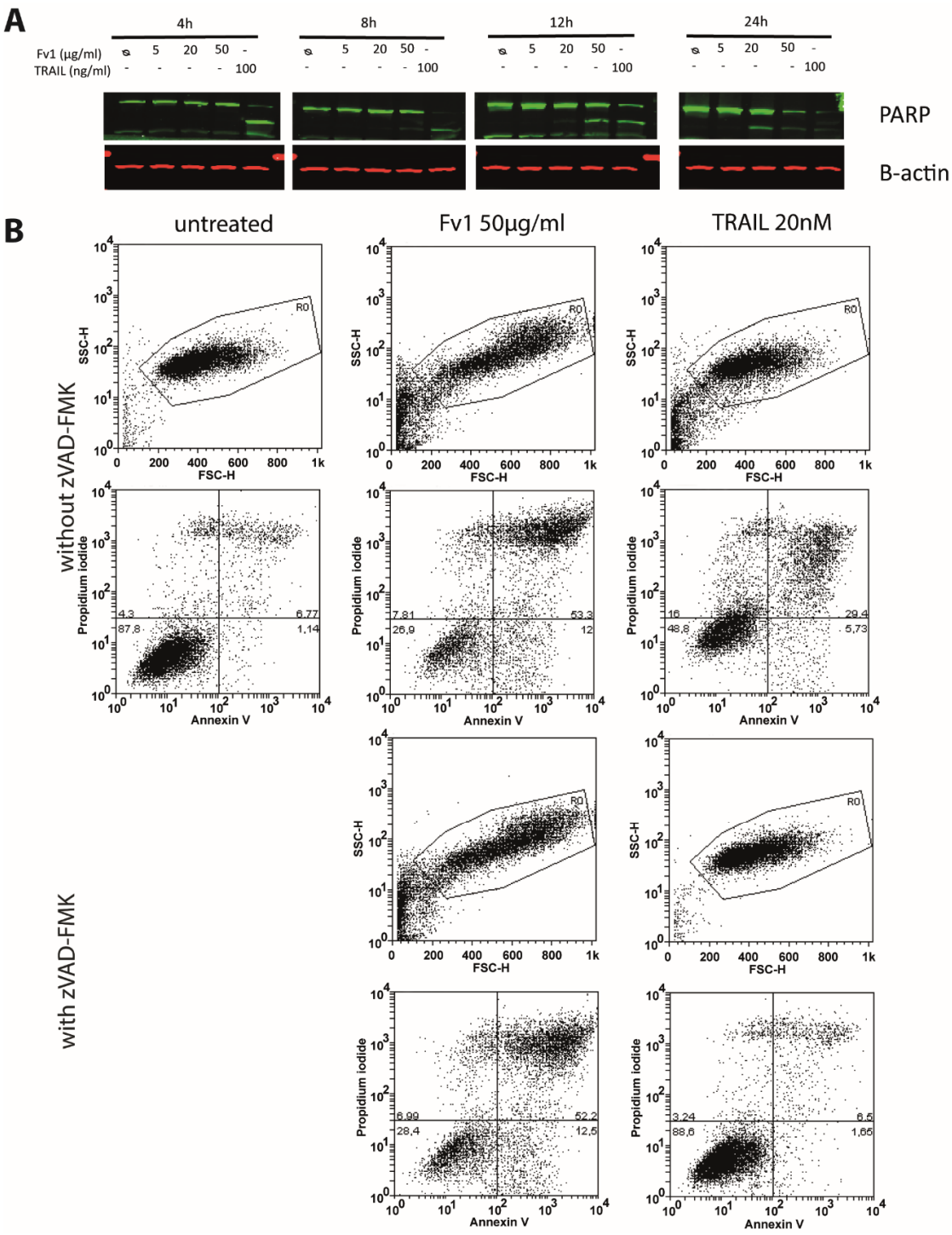

Figure 6. Fv1 induces cleavage of Poly ADP ribose polymerase 1 (PARP), but cell death is not blocked by the caspase inhibitor zVAD-fmk. (**A**) 24 h after seeding, Panc89 cells were treated with Fv1. At the indicated time points, whole cell lysates were analyzed by Western blotting for the cleavage of PARP; (**B**) Panc89 cells were treated with Fv1 as described above, but in combination with zVAD-fmk for 24 h. Afterwards, cells were stained with Annexin V and propidium iodide and measured by flow cytometry. Viability of Panc89 cells treated with Fv1 and zVAD-fmk was observed by AlamarBlue staining after 72 h of treatment (see Supplementary Figure S4).

Cell death is often mediated through the mitochondrial pathway. The production of reactive oxygen species (ROS) and mitochondrial swelling were not induced when Colo357 cells were treated with Fv1 for up to 60 min. Moreover, the membrane potential of isolated rat liver mitochondria was not influenced by Fv1 treatment (Supplementary Figures S5–S8).

Another mechanism possibly involved in cell death is autophagy. The dependency of Fv1 on autophagy was analyzed using three different inhibitors of autophagy pathways (Figure 7). Interestingly, the effect of Fv1 was increased when autophagy was blocked by each of the three inhibitors.

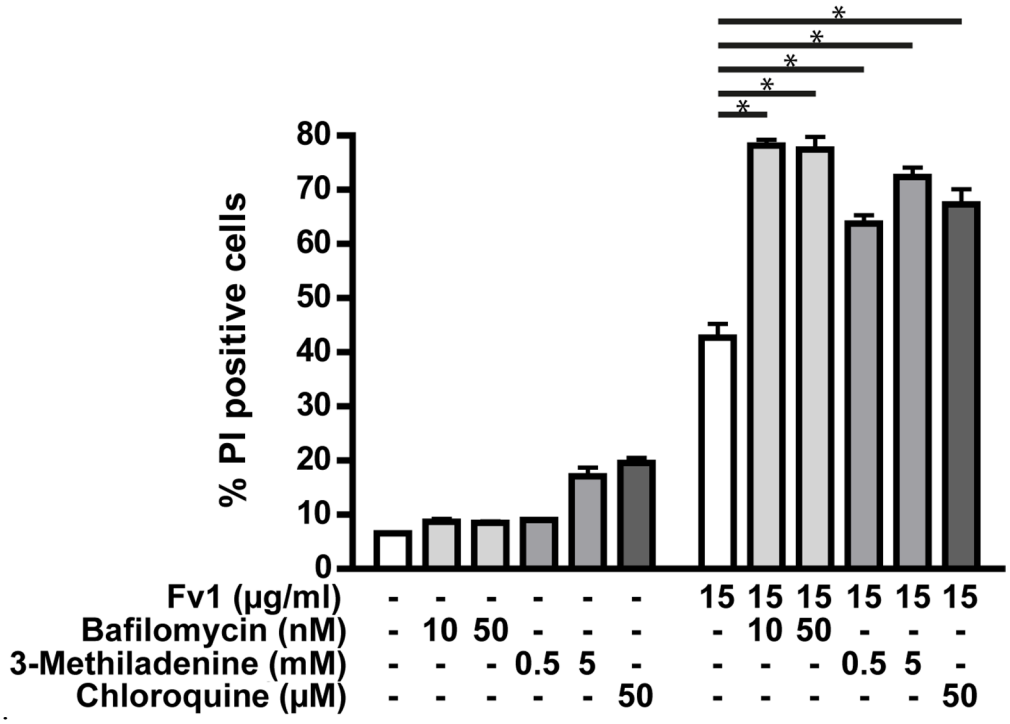

Figure 7. Autophagy inhibitors increase the effect of Fv1. Colo357 cells were prestimulated 23 h after seeding with chloroquine (50 µM), bafilomycin (10 nM, 50 nM) or 3-methyladenine (0.5 mM, 5 mM). One hour later, they were treated with Fv1 (15 µg/mL). After 24 h of Fv1 treatment, cells were detached with accutase, stained with propidium iodide and measured by FACS. Single inhibitor treatments were subtracted from the combination treatments before calculating significances with *t*-tests. $n = 2$.

2.4. Analysis of the Fv1 Effect on Non-Dividing Cells

As many chemotherapeutics depend on cell proliferation, we analyzed the effect of Fv1 on non-proliferating cells. To do so, we used the PDAC A818-4 cell line model [18]. These cells can be transferred into a quiescent state by contact inhibition (previous unpublished data of our group). Panc89 cells were used as a negative control, representing a common type of cancer cell line that is not influenced by contact inhibition. Accordingly, Panc89 cells incorporated more BrdU when they were seeded at higher numbers, while the incorporation of BrdU in A818-4 cells did not increase with the higher seeding density (Figure 8A).

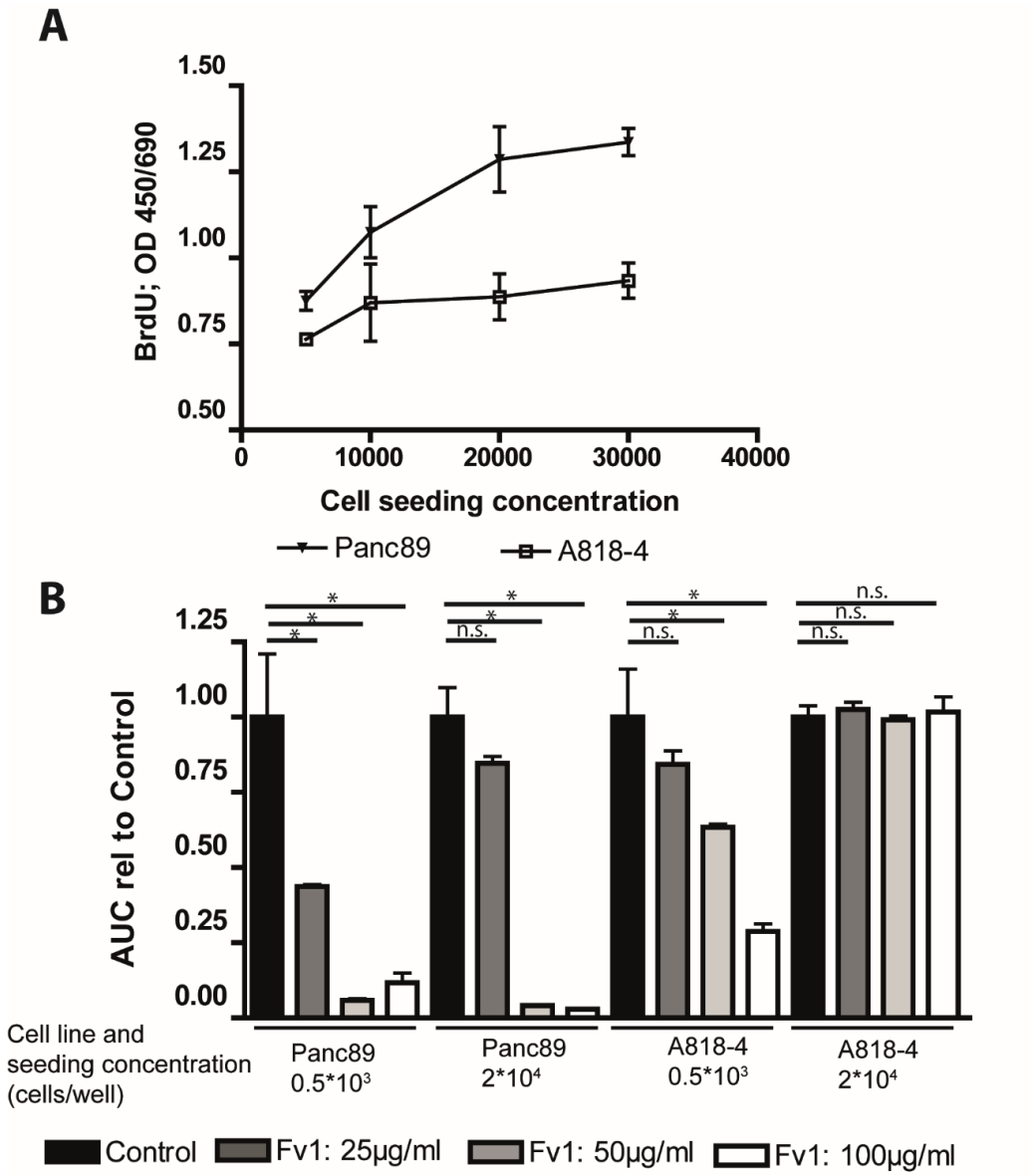

Figure 8. Fv1 preferentially inhibits proliferating cells. (**A**) The PDAC cell lines A818-4 and Panc89 were seeded at different densities. After 24 h, the cells were incubated with BrdU for 4 h. Subsequently, a BrdU ELISA was performed, and the BrdU incorporation was analyzed by measuring the absorbance at 450 nm. The slopes of the curves are significantly different ($p = 0.000315$); (**B**) A818-4 and Panc89 cells were seeded in a CIM 16 plates. After 24 h, they were incubated with different concentrations of Fv1. For 72 h, the cell impedance was monitored in intervals of 15 min by the Roche XCelligence RTCA system. The cell number is represented by the area under the curve (AUC) which is presented as bar chart. $n = 2$. The experiment was validated with an AlamarBlue viability assay which shows the endpoint situation after 72 h of treatment (Supplementary Figure S9). $n = 2$.

To analyze the effect of Fv1 on these non-proliferating cells, we monitored them in real-time by the XCelligence RTCA system. Fv1 dose-dependently decreased the cell numbers of A818-4 cells when the seeding density was low. In contrast, Fv1 had no effect upon growth-arrested cells (Figure 8B). Cell numbers are represented as area under the curve (AUC).

Panc89 cells, on the other hand, were inhibited at both seeding densities (Figure 8B). This finding was confirmed with a viability endpoint measurement after 72 h (Supplementary Figure S9).

For toxicity analysis against sensitive non-malignant body cells, we tested the hemoglobin release of fresh red blood cells derived from healthy donors (Figure 9A). We did not see hemolysis in Fv1-treated red blood cells after 1–4 h of treatment, indicating that Fv1 does not destroy terminally differentiated, non-dividing cells (Supplementary Table S2). Quiescent peripheral blood mononuclear cells (PBMC) were also not affected, while activated proliferating PBMCs showed a reduced viability after 24 h of Fv1 treatment (Figure 9B).

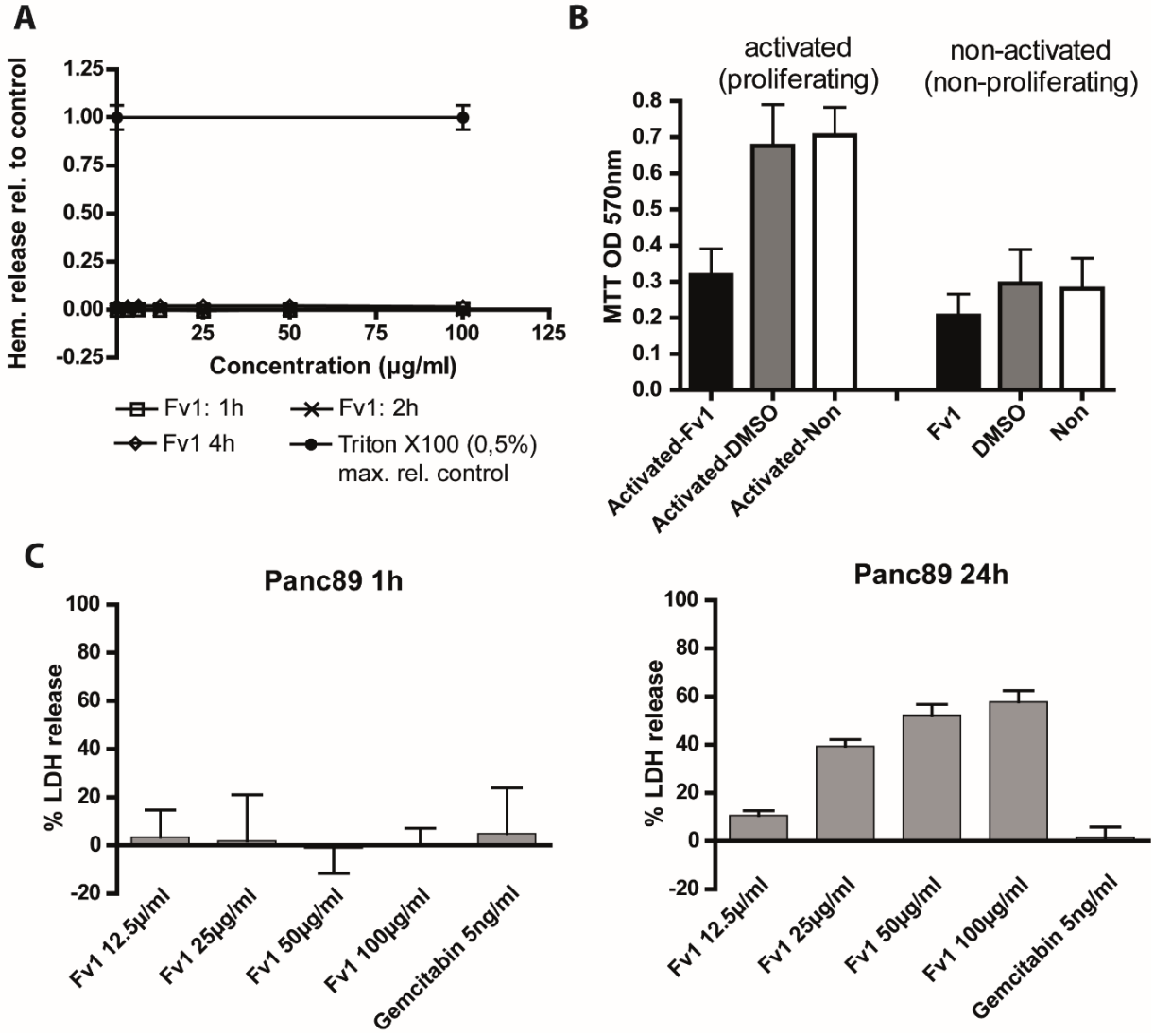

Figure 9. *Cont.*

D

	Fv1 (HPLC fraction, µg/ml))		
Cell line	**5000 cells**	**10000 cells**	**20000 cells**
HUVEC	4.89	7.75	9.48
NHDF	25.75*	30.15*	32.28*
KIF5eGFP	17.94*	22.31*	25.25*
HPDE	4.19	6.31	13.85
Panc89	13.16	19.31	29.43
A818-4	48.81	>100	>100

* fibroblasts were seaded as follows: 1250 cells, 2500 cells, 5000 cells

Figure 9. Fv1 treatment does not lead to acute cytotoxicity but effects rapidly dividing non-malignant cells. (**A**) Freshly isolated red blood cells were seeded in 96 well plates and treated with different concentrations of Fv1. Absorbance of hemoglobin was measured in the supernatant at the given time points. 0.5% Triton X100 was used as maximum release control. Raw data are shown in Supplementary Table S2. Four technical replicates are shown; (**B**) Peripheral blood mononuclear cells (PBMCs) were isolated from freshly drawn human blood and activated. Resting or activated cells were treated with Fv1 or DMSO as solvent control. After 72 h, the viability was measured with an MTT assay. Data show raw OD-values. Data are presented as mean values ± standard deviation (SD) from three independent experiments; (**C**) For measurement of acute cytotoxicity, lactate dehydrogenase (LDH) release was measured in Panc89 cells after 1 and 24 h. Experiment performed at least twice with 4 technical replicates each; (**D**) Three non-malignant (HUVEC, NHDF, KIF5eGFP, HPDE) and two PDAC cell lines (Panc89, A818-4) were seeded at different densities. After 24 h, they were treated with Fv1 for 72 h. Dose response curves and EC50 values were calculated using nonlinear regression (curve fit) with Prism (GraphPad). Experiments were performed at least twice with 4 technical replicates each.

To characterize the anti-proliferative activity in more detail, we measured acute cytotoxicity by a lactatdehydrogenase (LDH) release assay (Figure 9D). Cancer cell lines did not release LDH after 1 h of treatment with Fv1, but after 24 h we detected a dose-dependent high LDH release (Figure 9C). This indicates a cytotoxic effect of Fv1 after 24 h, but argues against acute cytotoxicity.

To test whether inhibition of proliferation was restricted to cancer cell lines, we tested the effects of Fv1 on different non-malignant cell lines and primary cells (human pancreatic ductal epithelial/HPDE cells, the fibroblast cell lines KIF5 and NHDF and freshly isolated endothelial HUVEC cells). Since these cells were rapidly dividing, we observed similar anti-proliferative effects as in cancer cell lines (Figure 9D).

3. Discussion

In this paper, we describe the anticancer effects of a Baltic brown seaweed extract. Fv1 inhibits proliferating cells and does not affect resting cells. This effect is comparable to clinically used chemotherapeutic drugs. Our findings show that the cell line A818-4 was only inhibited by Fv1 when proliferating. In other proliferating cells like Panc89 or Colo357, Fv1 led to an S/G2-phase arrest and to

an increase of the cell cycle inhibitors p21, p27 and p57. These findings were supported by the gene expression experiments. Large scale array experiments showed particularly regulation of genes involved in cell cycle regulation. Cell cycle inhibitors were upregulated after Fv1 treatment whereas the expression of downstream targets was decreased. Normally, this enforced form of cell cycle inhibition leads to apoptosis, necroptosis or other forms of programmed cell death [19,20]. Analyses of apoptosis via PARP cleavage showed, that in later stages of Fv1 treatment, a PARP-cleavage occurred, so eventually the cells undergo apoptosis. This hypothesis was supported by Annexin V/PI staining where events of early and late apoptosis/necrosis were observed. However, the cell death was not blocked by the caspase inhibitor zVAD-fmk. Therefore, we assume that it might only be a secondary effect of Fv1 treatment. In addition, Fv1 did not cause mitochondrial swelling or destruction, thus Fv1 did not induce cell death by the mitochondrial pathways. Interestingly, Fv1 seems to be counteracted by autophagy mechanisms. Studies show that autophagy is not only involved in cell death [21,22]. Autophagy pathways also provide a rescue mechanism by stabilizing the cell metabolism [22]. A connection between cell cycle or DNA damage and autophagy is discussed in literature, but not fully understood, yet [23–25]. Further *in vivo* experiments with Fv1 could include the combination with inhibitors of autophagy.

Interestingly, some of the described outcomes in the various test systems occur also when cells were treated with Gemcitabine. Gemcitabine is often described to induce apoptosis [26,27] but there is evidence that this could only be a side effect. Studies suggest that the effect of Gemcitabine alone is not influenced by inhibition of caspases [27,28]. This means, that Gemcitabine, Fv1 and other chemotherapeutics induce cell death, but the apoptotic pathway involving caspase activation and PARP cleavage only plays a secondary role.

This supports the hypothesis that Fv1 is a strong inhibitor of the cell cycle like, e.g., Gemcitabine. Indeed, Fv1 led to a cell cycle arrest in G2 phase. This is in line with the microscopic observation that many cells entered the process of mitosis and duplicated their nuclei, but did not finish cytokinesis. The question is how this cell cycle arrest and cell death is mediated. The up-regulated proteins p21, p27 and p57 are all under the control of p53 [19]. Our experiment with p53 knockout cells showed, that there is an influence of p53 on the Fv1 effect. The difference we observed between p53 wild-type and deficient cells was comparable to the one observed for 5-FU. For this DNA-damaging chemotherapeutic agent, the p53 dependency has been described in literature [29]. However, in our other studied cancer cell lines except HCT116 and Colo357, p53 is mutated [18,30]. This is interesting, as Colo357 cells were more resistant to Fv1 than other PDAC cell lines. A connection might be the tumor protein 53 inducible protein 1 (TP53INP1). TP53INP1 is strongly induced by Fv1 on the gene expression level and it is able to play an autonomous role in cell cycle regulation and mediates several of its functions independently of p53 [31]. Another player might be CDC20. This gene was down-regulated by Fv1. It plays an important role in the spindle checkpoint. Eichhorn *et al*. showed that knockdown of CDC20 in HeLa cells induced mitotic arrest, similar to our observations [32]. Moreover, in Western blots, we observed a strong decrease of tubulin at later time points and higher Fv1 concentrations (data shown in Supplementary Figures S2 and S3). This might lead to a destruction of the spindle apparatus and activation of the spindle checkpoint.

Combination experiments with chemotherapeutic drugs indicated that extracts of *Fucus vesiculosus* share completely additive effects with gemcitabine, paclitaxel and cisplatin (Supplementary Figure S10).

They neither inhibited nor synergistically enhanced the effects of the other drug. These findings support the assumption that a combination of chemotherapeutic drugs and Fv1 may be effective *in vivo*.

Fv1 is a potent compound with strong anti-cancer activity as shown here under *in vitro* conditions. Subsequently, *in vivo* experiments in mice would be necessary to confirm the promising *in vitro* data and to assess potential side effects such as hepatotoxicity and nephrotoxicity of Fv1. Other compounds like fucoxanthin also show toxic effects on non-malignant cells in cell culture, but have no toxic effect *in vivo* [7]. Experiments in laboratory rodents would also reveal the uptake and bioavailability of Fv1 when applied to complex organisms. Another way of further application would be the use of Fv1 for targeted therapy of cancer. To do so, Fv1 could be conjugated to cancer-specific target molecules or be wrapped by liposomes that can release their content specifically to cancer cells. However, structure and other chemical characteristics of Fv1 need to be elucidated prior clinical trials. In conclusion, Fv1 is a potent inhibitor of cancer cell growth. It does not induce apoptosis or necroptosis, nor does it induce mitochondrial swelling. However, Fv1 efficiently kills pancreatic cancer cells by inducing a cell cycle arrest by the induction of cell cycle inhibitors involving TP53INP1.

4. Material and Methods

4.1. Algae Extraction and Fractioning

Freshly frozen parts of the central thallus of the alga *Fucus vesiculosus*, which were collected at spring time from coastal areas of Bülk, Kiel Fjord, Western Baltic Sea, were thawed and extracted with acetone at the rate of 1:2 (*w/v*). After further processing and drying, the extract was re-dissolved in dimethyl sulfoxide (DMSO) as preparation for normal phase high performance liquid chromatography (HPLC) on a Pharmprep60CC SiO_2 column, followed by reversed-phase HPLC on an Amberlite® XAD7HP column. 67 fractions were generated, dried and dissolved in DMSO D6.

Fv1 is represented by a pool of three successively eluted fractions within the hydrophilic sector of the applied gradient. According to their similar and most efficient anti-proliferative activity in the sequence of seven tested neighboring fractions and according to their characteristic ^{1}H-NMR-profile showing four signals each at 5.82, 6.63, 7.89 and 8.98 ppm, the three nearby fractions were pooled to Fv1 in a concentration of 42 mg/mL in DMSO and stored at −60 °C for subsequent testing.

4.2. Cell Lines, Cell Culture Maintenance and General Experiment Procedure

PancTu1 cells were a kind gift of Dr. M. von Bülow (Mainz, Germany), Panc89 cells of Dr. T. Okabe (Tokyo, Japan), and Colo357 cells of Dr. R. Morgan (Denver, CO, USA) [33]. Panc1 cells were obtained from ATCC (LGC Standards, Wesel, Germany). These four pancreatic cancer cell lines were chosen in order to not depend too much on the particular genetic outfit of the cell lines. Most experiments have been done with 2 or more of the cell lines and representative experiments are shown. The E6/E7-HPV16-immortalized human pancreatic ductal epithelial cell line HPDE was a gift of Dr. M. Tsao (MD, FRCPC, University Health Network, Toronto, ON, Canada) [34,35]. NHDF cells were purchased from Promocell (Heidelberg, Germany). Cell culture maintenance and experiments were performed in an incubator at 37 °C with a 5% CO_2 atmosphere and 5% humidity. HPDE cells were routinely cultured in HPDE medium (RPMI 1640 medium (Life Technologies, Darmstadt, Germany) supplemented with 10% FBS

(PAN Biotech, Aidenbach, Germany), 1% Glutamax (Life Technologies, Darmstadt, Germany) and mixed immediately before use 1:1 with keratinocyte medium SFM (Life Technologies, Darmstadt, Germany) supplemented with 0.025% bovine pituitary extract/2.5 µg/L epidermal growth factor (Life Technologies, Darmstadt, Germany)). NHDF cells were cultivated in fibroblast growth medium supplemented with supplement pack 2 (Promocell, Heidelberg, Germany). All other cell lines were cultured in RPMI 1640 medium (Life Technologies, Darmstadt, Germany) supplemented with 10% FBS (PAN Biotech, Aidenbach, Germany), 1% Glutamax and 1% sodium pyruvate (both Life Technologies, Darmstadt, Germany). Red blood cells were isolated directly from fresh blood from healthy donors by centrifugation and maintained in PBS. Peripheral blood mononuclear cells (PBMC) were isolated and activated with a T cell activation/expansion kit (130-091-441, Miltenyi Biotec, Bergisch-Gladbach, Germany).

4.3. Proliferation and Viability Experiments

For proliferation experiments, cells were seeded in 96 well plates (5×10^3 cells per well if not noted otherwise) and treated after 24 h with serial dilutions of extracts premixed in cell culture medium. The algae extract stocks (42 mg/mL in DMSO) were thawed directly before use. Serial dilutions were done in DMSO to ensure a constant DMSO concentration of 0.15% in cell culture medium for each treatment. A DMSO concentration of 0.15% in cell culture medium was used as solvent control. TRAIL (PeproTech, Hamburg, Germany) was dissolved in PBS (0.5 µg/µL) and diluted in cell culture medium in a concentration of 200 ng/mL. zVAD-fmk (Promega, Mannheim, Germany) was dissolved in DMSO and diluted in cell culture medium using a concentration of 20 µM. After the indicated time points, the proliferation tests were performed as described below. Dose response curves were produced and EC50 values calculated with Prism (GraphPad).

4.4. Alamar Blue

Ten microliters of AlamarBlue (Invitrogen, Carlsbad, CA, USA) reagent was added to each 96 well containing cells in 100 µL of medium and incubated for 4 h. Fluorescence of AlamarBlue was measured using an excitation wavelength of 545 nm and an emission wavelength of 595 nm (Tecan Spectrafluor Plus, Tecan, Maennedorf, Switzerland).

4.5. BrdU ELISA

For A818-4 cells, a BrdU ELISA was used to determine the optimal cell seeding concentration for contact-inhibited cell growth. Experiments were performed as described before and for the last 5 h, the BrdU labelling reagent was added to the cell culture at a final concentration of 10 µM. The following BrdU-staining was performed according to the manual (Roche, Cat. No. 11647229001). The BrdU-reaction was stopped with 25 µL 1 M H_2SO_4. Absorbance was measured using the Tecan Sunrise Reader (Tecan, Maennedorf, Germany) with a wavelength of 450 nm (Reference: 600 nm).

4.6. XCelligence Proliferation Measurement

Cells were seeded in XCelligence CIM-plate 16 (AceaBio, San Diego, CA, USA) according to the manufacturer's instructions in 10% FCS containing RPMI medium. After 24 h, cells were treated as described in the general experiment section for 96 well plates. Proliferation activity was measured every 15 min for 72 h in a RTCA DP system (AceaBio, San Diego, CA, USA).

4.7. Cytotoxicity LDH-Release

LDH-release assays were performed using RPMI medium with 1% FCS, 0.5% GlutaMAX and 0.5% sodium-pyruvate for treatment, because these substances can interfere with the assay reagents. 1×10^4 cells per well were seeded in 200 µL cell culture medium. After 24 h attachment, the cells were treated with extracts as described above. For each treatment, half of the wells were also treated with Triton-X100 (1% final concentration in medium) as 100% control. After 1 or 24 h, LDH release was tested according to the manual (Takara Bio, Saint-Germain-en-Laye, France) and absorbance was measured in a Sunrise plate reader at 492 nm with a reference wavelength of 650 nm (Tecan, Maennedorf, Switzerland).

4.8. Gene Expression Analysis

For Agilent gene chip expression analysis, 1.07×10^6 cells were grown in 12 mL cell culture medium in T75 flasks for 24 h before treatment. Cells were treated with 30 µg/mL Fv1 or 0.15% DMSO as control. After an incubation time of 6 or 24 h, the supernatant was removed, the cells were washed with PBS and detached with Accutase and frozen at −80 °C. Then the RNA was extracted with the RNeasy Plus Mini Kit (Qiagen, Hilde, Germany), according to the manual. Quantity of the RNA was measured using NanoDrop (PeqLab). Experiments were performed in three independent replicates. RNA quality was controlled using a BioAnalyzer. Gene expression was measured using the "Sureprint G3 Human GE 8 × 60K" (Agilent, Santa Clara, CA, USA) array which was processed according to the manufacturer's instructions. For analysis, only genes were included that showed a p-value < 0.05 and a log fold change (lfc) >1 or <−1 and that were changed on at least three pancreatic cancer cell lines (Panc1, Panc89, PancTU1). The experiments were performed as three biological replicates with each cell line.

4.9. Preparation of Cell Lysates and Western Blotting

Cells were lysed with RIPA buffer and ultrasound. Protein concentration was measured with DC reagent (Bio-Rad Laboratories, Munich, Germany). Equal amounts of protein were loaded on a 4%–20% tris-glycine gel (Novex, Life Technologies, Carlsbad, CA, USA) and separated by SDS-PAGE. Proteins were transferred by semi dry blot on a PVDF membrane (Immobilon-FL; Millipore/Merck, Darmstadt, Germany). For 2nd antibody, goat-anti-rabbit-IRDye800CW and goat-anti-mouse-IRDye680 (LI-COR, Bad Homburg, Germany) were used. Blots were dried and scanned using an Odyssey infrared imager (LI-COR, Bad Homburg, Germany). Used antibodies: β-Actin (CS, A5441), α-Tubulin (Epitomics, 1878-1), PARP (CS, 9542S), p21 (CS, 2946), p27 (CS, 2552), p15 (CS, 4822).

4.10. FACS Cell Cycle Profiling—Annexin V/PI Staining

For cell cycle profiling, experiments were performed as described above. Staining was performed in v-bottom shaped 96 well plates using a hypotonic propidium iodide (PI) staining solution (0.1% sodium citrate, 0.1% TritonX-100, 50 µg/mL PI, 5 µg/mL EDTA) [36]. Stained cells were measured immediately after staining using a FACS-Calibur (BD Biosciences, Heidelberg, Germany). Annexin V/PI staining was performed according to the manufacturer's instructions (Miltenyi Biotec; 130-092-052). Immediately after adding the PI solution, the cells were measured in FACS-Calibur (BD Biosciences, Heidelberg, Germany).

4.11. FACS PI Staining and Inhibitor Screening

One hundred thousand (1×10^5) Colo357 cells were seeded in 12 well cell culture plates in 0.5 mL cell culture medium. After 23 h they were pretreated with Bafilomycin (10 nM, 50 nM), Chloroquine (50 µM), 3-Methyadenine (0.5 mM, 5 mM) or cell culture medium (control). One hour later, 15 µg/mL Fv1 or cell culture medium (control) was added. After 24 h, the cells were detached with Accutase (PAA), stained with propidium iodide and measured with a FACS-Calibur (BD, Heidelberg, Germany). The percentage of PI positive cells was determined for each treatment.

4.12. Statistical Analysis

Statistics were performed with Prism (GraphPad) and Excel (Microsoft) unless indicated otherwise. Significance was tested using students *t*-test. Differences with *p*-values <0.05 (*), <0.01 (**) or <0.001 (***) were estimated as significant and indicated with asterisk.

Supplementary Materials

Table S1. Inhibition of cell viability by Fv1 in different cancer cell lines.
Figure S1. Genes involved in the cell cycle regulation pathway are regulated by Fv1.
Figure S2. Fv1 does not influence several proteins involved in cell cycle regulation.
Figure S3. Fv1 does not influence several proteins involved in cell cycle regulation and cell death.
Figure S4. Supplement to Figure 6. The effect of Fv1 on viability is not caspase dependent.
Figure S5. Mitosox ROS production of Colo357 cells treated with Fv1.
Figure S6. Mitosox ROS production of Colo357 cells treated with Antimycin as positive control.
Figure S7. TMRM membrane potential of Colo357 cells treated with Fv1.
Figure S8. TMRM membrane potential of Colo357 cells treated with FCCP as positive control.
Figure S9. Supplement to Figure 8. Fv1 preferentially inhibits proliferating cells.
Table S2. Fv1 does not induce hemolysis in fresh red blood cells.
Figure S10. Acetonic algae extracts show additive effects in combinations with different chemotherapeutics.
Figure S11. Cell cycle profile of Colo357 cells 4 h after treatment with Fv1.
Figure S12. Cell cycle profile of Panc89 cells 4 h after treatment with Fv1.
Figure S13. Cell cycle profile of Panc89 cells 24 h after treatment with Fv1.

Multimedia file S1. Life cell imaging Control.
Multimedia file S2. Life cell imaging Fv1.

Acknowledgments

This work was funded by the German "Bundesministerium für Bildung und Forschung" (BMBF-0315812) as a part of the "Algae against Cancer (AAC)"-project as well as by a grant from the Deutsche Krebshilfe (to D. A. and H. K., 110055). We thank Susanne Alban, Karina Ehrig, Christian Röder and Susanne Sebens for fruitful discussions and Nadine Genzel for excellent technical assistance. HUVEC cells were kindly provided by Stefanie Piegholdt.

Author Contributions

AAC-Project including development and production of the extract Fv1: L.P., M.Z., H.K., M.P., S.H., M.F., R.G., conceived and designed the project.

Mechanism elucidation: U.G., H.K., M.P (T-Cells), J.P. (Autophagy inhibitors) and D.A. (Autophagy inhibitors) conceived and designed the experiments; U.G., J.K., A.M. (Mitochondrial analyzes), M.P (T-Cells) and J.P. (Autophagy inhibitors) performed the experiments; U.G. analyzed the data; L.P., S.H., G.R., H.K., D.A. contributed reagents/materials/analysis tools; U.G., H.K. and G.R. wrote the paper.

Conflicts of Interest

The authors declare no conflicts of interest.

References

1. SEER Cancer Statistics Review, 1975–2011. National Cancer Institute Web site. Available online: http://seer.cancer.gov/csr/1975_2011/ (accessed on 7 November 2014).
2. Ferlay, J.; Soerjomataram, I.; Dikshit, R.; Eser, S.; Mathers, C.; Rebelo, M.; Parkin, D.M.; Forma, D.; Bray, F. Cancer incidence and mortality worldwide: Sources, methods and major patterns in GLOBOCAN 2012: Globocan 2012. *Int. J. Cancer* **2015**, *136*, E359–E386.
3. Rahib, L.; Smith, B.D.; Aizenberg, R.; Rosenzweig, A.B.; Fleshman, J.M.; Matrisian, L.M. Projecting cancer incidence and deaths to 2030: The unexpected burden of thyroid, liver, and pancreas cancers in the United States. *Cancer Res.* **2014**, *74*, 2913–2921.
4. Ale, M.T.; Maruyama, H.; Tamauchi, H.; Mikkelsen, J.D.; Meyer, A.S. Fucose-Containing Sulfated Polysaccharides from Brown Seaweeds iNhibit Proliferation of Melanoma Cells and Induce Apoptosis by Activation of Caspase-3 *in vitro*. *Mar. Drugs* **2011**, *9*, 2605–2621.
5. Kumar, S.R.; Hosokawa, M.; Miyashita, K. Fucoxanthin: A Marine Carotenoid Exerting Anti-Cancer Effects by Affecting Multiple Mechanisms. *Mar. Drugs* **2013**, *11*, 5130–5147.
6. Glombitza, K.W.; Hauperich, S.; Keusgen, M. Phlorotannins from the brown algae *Cystophora torulosa* and *Sargassum spinuligerum*. *Nat. Toxins* **1997**, *5*, 58–63.
7. Khotimchenko, Y.S. Antitumor properties of nonstarch polysaccharides: Fucoidans and chitosans. *Russ. J. Mar. Biol.* **2010**, *36*, 321–330.

8. Park, H.S.; Kim, G.-Y.; Nam, T.-J.; Deuk Kim, N.; Hyun Choi, Y. Antiproliferative Activity of Fucoidan Was Associated with the Induction of Apoptosis and Autophagy in AGS Human Gastric Cancer Cells. *J. Food Sci.* **2011**, *76*, T77–T83.
9. Ye, G.; Lu, Q.; Zhao, W.; Du, D.; Jin, L.; Liu, Y. Fucoxanthin induces apoptosis in human cervical cancer cell line HeLa via PI3K/Akt pathway. *Tumor Biol.* **2014**, *35*, 11261–11267.
10. Wang, S.K.; Li, Y.; White, W.L.; Lu, J. Extracts from New Zealand *Undaria pinnatifida* Containing Fucoxanthin as Potential Functional Biomaterials against Cancer *in vitro*. *J. Funct. Biomater.* **2014**, *5*, 29–42.
11. Ale, M.T.; Maruyama, H.; Tamauchi, H.; Mikkelsen, J.D.; Meyer, A.S. Fucoidan from *Sargassum* sp. and *Fucus vesiculosus* reduces cell viability of lung carcinoma and melanoma cells *in vitro* and activates natural killer cells in mice *in vivo*. *Int. J. Biol. Macromol*. **2011**, *49*, 331–336.
12. Athukorala, Y.; Ahn, G.N.; Jee, Y.-H.; Kim, G.-Y.; Kim, S.-H.; Ha, J.-H.; Ha, J.-H.; Kang, J.S.; Lee, K.-W.; Jeon, Y.-J. Antiproliferative activity of sulfated polysaccharide isolated from an enzymatic digest of *Ecklonia cava* on the U-937 cell line. *J. Appl. Phycol.* **2008**, *21*, 307–314.
13. Peng, J.; Yuan, J.-P.; Wu, C.-F.; Wang, J.-H. Fucoxanthin, a Marine Carotenoid Present in Brown Seaweeds and Diatoms: Metabolism and Bioactivities Relevant to Human Health. *Mar. Drugs* **2011**, *9*, 1806–1828.
14. Kang, H.S.; Chung, H.Y.; Kim, J.Y.; Son, B.W.; Jung, H.A.; Choi, J.S. Inhibitory phlorotannins from the edible brown alga *Ecklonia stolonifera* on total reactive oxygen species (ROS) generation. *Arch. Pharm. Res.* **2004**, *27*, 194–198.
15. Ahn, J.-H.; Yang, Y.-I.; Lee, K.-T.; Choi, J.-H.; Dieckol, isolated from the edible brown algae *Ecklonia cava*, induces apoptosis of ovarian cancer cells and inhibits tumor xenograft growth. *J. Cancer Res. Clin. Oncol.* **2015**, *141*, 255–268.
16. Yoon, J.-S.; Kasin Yadunandam, A.; Kim, S.-J.; Woo, H.-C.; Kim, H.-R.; Kim, G.-D. Dieckol, isolated from *Ecklonia stolonifera*, induces apoptosis in human hepatocellular carcinoma Hep3B cells. *J. Nat. Med.* **2013**, *67*, 519–527.
17. Shirayama, M.; Toth, A.; Galova, M.; Nasmyth, K. APC^{Cdc20} promotes exit from mitosis by destroying the anaphase inhibitor Pds1 and cyclin Clb5. *Nature* **1999**, *402*, 203–207.
18. Sipos, B.; Möser, S.; Kalthoff, H.; Török, V.; Löhr, M.; Klöppel, G. A comprehensive characterization of pancreatic ductal carcinoma cell lines: Towards the establishment of an *in vitro* research platform. *Virchows Arch.* **2003**, *442*, 444–452.
19. Weinberg, R. *The Biology of Cancer*, 2nd ed.; Garland Science: New York, NY, USA, 2013.
20. Ouyang, L.; Shi, Z.; Zhao, S.; Wang, F.-T.; Zhou, T.-T.; Liu, B.; Bao, J.K. Programmed cell death pathways in cancer: A review of apoptosis, autophagy and programmed necrosis. *Cell Prolif.* **2012**, *45*, 487–498.
21. Madeo, F.; Zimmermann, A.; Maiuri, M.C.; Kroemer, G. Essential role for autophagy in life span extension. *J. Clin. Invest.* **2015**, *125*, 85–93.
22. Czarny, P.; Pawlowska, E.; Bialkowska-Warzecha, J.; Kaarniranta, K.; Blasiak, J. Autophagy in DNA Damage Response. *Int. J. Mol. Sci.* **2015**, *16*, 2641–2662.
23. Hanahan, D.; Weinberg, R.A. Hallmarks of Cancer: The Next Generation. *Cell* **2011**, *144*, 646–674.

24. Zhang, D.; Tang, B.; Xie, X.; Xiao, Y.-F.; Yang, S.-M.; Zhang, J.-W. The Interplay Between DNA Repair and Autophagy in Cancer Therapy. *Cancer Biol. Ther.* **2015**, *16*, 1005–1013.
25. Wang, F.; Li, H.; Yan, X.-G.; Zhou, Z.-W.; Yi, Z.-G.; He, Z.-X.; Pan, X.T.; Yang, Y.X.; Wang, Z.Z.; Zhang, X.; *et al.* Alisertib induces cell cycle arrest and autophagy and suppresses epithelial-to-mesenchymal transition involving PI3K/Akt/mTOR and sirtuin 1-mediated signaling pathways in human pancreatic cancer cells. *Drug Des. Devel. Ther.* **2015**, *9*, 575–601.
26. Von Hoff, D.D.; Ervin, T.; Arena, F.P.; Chiorean, E.G.; Infante, J.; Moore, M.; Seay, T.; Tjulandin, S.A.; Ma, W.W.; Saleh, M.N.; *et al.* Increased Survival in Pancreatic Cancer with nab-Paclitaxel Plus Gem Citabine. *N. Engl. J. Med.* **2013**, *369*, 1691–1703.
27. Wei, W.-T.; Chen, H.; Wang, Z.-H.; Ni, Z.-L.; Liu, H.- B.; Tong, H.-F.; Guo, H.C.; Liu, D.L.; Lin, S.Z. Enhanced Antitumor Efficacy of Gemcitabine by Evodiamine on Pancreatic Cancer via Regulating PI3K/Akt Pathway. *Int. J. Biol. Sci.* **2012**, *8*, 1–14.
28. Stadel, D.; Cristofanon, S.; Abhari, B.A.; Deshayes, K.; Zobel, K.; Vucic, D.; Debatin, K.M.; Fulda, S. Requirement of Nuclear Factor κB for Smac Mimetic-Mediated Sensitization of Pancreatic Carcinoma Cells for Gemcitabine-Induced Apoptosis. *Neoplasia* **2011**, *13*, 1162–1170.
29. Sui, X.; Kong, N.; Wang, X.; Fang, Y.; Hu, X.; Xu, Y.; Chen, W.; Wang, K.; Li, D; Jin, W.; *et al*. JNK confers 5-fluorouracil resistance in p53-deficient and mutant p53-expressing colon cancer cells by inducing survival autophagy. *Sci. Rep.* **2014**, *4*, 4694.
30. Yoon, M.; Mitrea, D.M.; Ou, L.; Kriwacki, R.W. Cell cycle regulation by the intrinsically disordered proteins p21 and p27. *Biochem. Soc. Trans.* **2012**, *40*, 981–988.
31. Seillier, M.; Peuget, S.; Dusetti, N.J.; Carrier, A. Antioxidant Role of p53 and of Its Target TP53INP1. In *Antioxidant. Enzyme*; El-Missiry, M.A., Ed.; InTech Europe: Rijeka, Croatia, 2012.
32. Eichhorn, J.M.; Sakurikar, N.; Alford, S.E.; Chu, R.; Chambers, T.C. Critical role of anti-apoptotic Bcl-2 protein phosphorylation in mitotic death. *Cell Death Dis.* **2013**, *4*.
33. Morgan, R.T.; Woods, L.K.; Moore, G.E.; Quinn, L.A.; McGavran, L.; Gordon, S.G. Human cell line (COLO 357) of metastatic pancreatic adenocarcinoma. *Int. J. Cancer* **1980**, *25*, 591–598.
34. Furukawa, T.; Duguid, W.P.; Rosenberg, L.; Viallet, J.; Galloway, D.A.; Tsao, M.S. Long-term culture and immortalization of epithelial cells from normal adult human pancreatic ducts transfected by the E6E7 gene of human papilloma virus 16. *Am. J. Pathol.* **1996**, *148*, 1763–1770.
35. Ouyang, H.; Mou, L.; Luk, C.; Liu, N.; Karaskova, J.; Squire, J.; Tsao M.-S. Immortal Human Pancreatic Duct Epithelial Cell Lines with Near Normal Genotype and Phenotype. *Am. J. Pathol.* **2000**, *157*, 1623–1631.
36. Krishan, A. Rapid flow cytofluorometric analysis of mammalian cell cycle by propidium iodide staining. *J. Cell Biol.* **1975**, *66*, 188–193.

OPEN

Citation: Cell Death and Disease (2015) 6, e1930; doi:10.1038/cddis.2015.263

www.nature.com/cddis

Early effects of the antineoplastic agent salinomycin on mitochondrial function

A Managò[1], L Leanza[1], L Carraretto[1], N Sassi[1,2], S Grancara[2], R Quintana-Cabrera[1,3], V Trimarco[3], A Toninello[2], L Scorrano[1,3], L Trentin[3], G Semenzato[3], E Gulbins[4], M Zoratti[2,5] and I Szabò*[,1,5]

Salinomycin, isolated from *Streptomyces albus*, displays antimicrobial activity. Recently, a large-scale screening approach identified salinomycin and nigericin as selective apoptosis inducers of cancer stem cells. Growing evidence suggests that salinomycin is able to kill different types of non-stem tumor cells that usually display resistance to common therapeutic approaches, but the mechanism of action of this molecule is still poorly understood. Since salinomycin has been suggested to act as a K^+ ionophore, we explored its impact on mitochondrial bioenergetic performance at an early time point following drug application. In contrast to the K^+ ionophore valinomycin, salinomycin induced a rapid hyperpolarization. In addition, mitochondrial matrix acidification and a significant decrease of respiration were observed in intact mouse embryonic fibroblasts (MEFs) and in cancer stem cell-like HMLE cells within tens of minutes, while increased production of reactive oxygen species was not detected. By comparing the chemical structures and cellular effects of this drug with those of valinomycin (K^+ ionophore) and nigericin (K^+/H^+ exchanger), we conclude that salinomycin mediates K^+/H^+ exchange across the inner mitochondrial membrane. Compatible with its direct modulation of mitochondrial function, salinomycin was able to induce cell death also in Bax/Bak-less double-knockout MEF cells. Since at the concentration range used in most studies (around 10 μM) salinomycin exerts its effect at the level of mitochondria and alters bioenergetic performance, the specificity of its action on pathologic B cells isolated from patients with chronic lymphocytic leukemia (CLL) *versus* B cells from healthy subjects was investigated. Mesenchymal stromal cells (MSCs), proposed to mimic the tumor environment, attenuated the apoptotic effect of salinomycin on B-CLL cells. Apoptosis occurred to a significant extent in healthy B cells as well as in MSCs and human primary fibroblasts. The results indicate that salinomycin, when used above μM concentrations, exerts direct, mitochondrial effects, thus compromising cell survival.
Cell Death and Disease (2015) **6,** e1930; doi:10.1038/cddis.2015.263; published online 22 October 2015

Salinomycin (SAL), an antibiotic that belongs to a large group of polyether ionophores, is considered to be a potential anticancer drug for cancer chemoprevention and therapy. SAL has been proved to induce programmed cell death of cancer stem cells (CSCs)[1] as well as of various cancer cells including chronic lymphocytic leukemia (CLL) cells, human colon, breast, prostate, hepatocellular carcinoma and lung cancer cells.[2–4] On the other hand, the use of animal models revealed that SAL has a narrow therapeutic index and SAL-induced neuropathy occurs *in vivo* even at relatively low doses, which do not give rise to systemic toxicity.[5] Extensive research has been undertaken to clarify the general mechanism(s) by which SAL induces apoptosis and blocks tumor growth. Several independent ways of action have been proposed to account for the cancer cell-killing ability of SAL, including inhibition of proximal Wnt/β-catenin signaling[6] and induction of a marked increase in the expression of the pro-apoptotic protein NAG-1.[7] Recent results point to SAL as a strong mTORC1 signaling antagonist in breast and prostate cancer cells[8] and as an initiator of autophagy in tumor cells.[9,10] SAL however is also able to suppress late stages of autophagy, leading to accumulation of dysfunctional mitochondria with increased production of reactive oxygen species (ROS).[11]

SAL is expected to impact mitochondrial function thanks to its ability to act as an ionophore. However, only few early studies addressed the direct effect of SAL on isolated mitochondria;[12] later works generally interpreted mitochondria-related effects of SAL in intact cells presuming that SAL acts similarly to valinomycin (VAL), a potassium selective ionophore mediating potassium influx into the mitochondria according to the electrochemical driving force. For example, SAL-induced mitochondrial inner membrane (IMM) depolarization and mitochondrial ROS production have been proposed to be compatible with influx of positively charged potassium ions.[9,13,14] The chemical structure of SAL is however more similar to nigericin (NIG)

[1]Department of Biology, University of Padua, Padua, Italy; [2]Department of Biomedical Sciences, University of Padua, Padua, Italy; [3]Venetian Institute for Molecular Medicine, University of Padua, Padua, Italy; [4]Department of Molecular Biology, University of Duisburg-Essen, Essen, Germany and [5]CNR Institute of Neuroscience, Padua, Italy

*Corresponding author: I Szabò, Department of Biology, University of Padua, viale G. Colombo 3, Padua, 35121 PD, Italy. Tel: +39 049 827 6324; Fax: +39 049 827 6300; E-mail: ildi@civ.bio.unipd.it

Abbreviations: ATP, adenosine triphosphate; B-CLL, B-cell chronic lymphocytic leukemia; CSC, cancer stem cell; FCCP, carbonylcyanide-*p*-trifluoromethoxyphenylhydrazone; HMLE, human mammary epithelial cell line; IMM, mitochondrial inner membrane; MEF, mouse embryonic fibroblast; MSC, mesenchymal stromal cells; MTT, (3-(4,5-dimethylthiazol-2-yl)-2,5-diphenyltetrazolium bromide); NIG, nigericin; OxPhos, oxidative phosphorylation; PDAC, pancreatic ductal adenocarcinoma; PTP, permeability transition pore; ROS, reactive oxygen species; SAL, salinomycin; VAL, valinomycin

Received 04.5.15; revised 10.7.15; accepted 03.8.15; Edited by M Diederich

rather than to VAL (Supplementary Figure S1). We note the presence of a carboxyl group, which can act as the H^+ carrier. NIG, similarly to monensin, acts as an ionophore with a preference for potassium and mediates electroneutral exchange of potassium ions with protons at the level of the IMM. Notably, NIG and monensin have been shown to induce apoptosis in human lung cancer and lymphoma cells,[15,16] suggesting that the common mechanism of polyether ionophore antibiotics to altering potassium homeostasis in the cytoplasm and mitochondria contributes to the induction of apoptosis in cancer cells. In accordance, we have recently demonstrated that pharmacological inhibition of a mitochondrial potassium channel (whose expression is upregulated in many cancers[17]) and the consequent mitochondrial dysfunction might be exploited to selectively kill melanoma cells even *in vivo*, as well as in *ex vivo* human leukemic cells.[18,19]

The mitochondrial effects of SAL have generally been addressed 12–48 h following addition of the drug, even though it is expected to reach quickly the IMM, as VAL and NIG do when added to intact cells. The purpose of the present work therefore was to reveal the early effects of SAL on mitochondrial function as compared with VAL and NIG, in primary human healthy cells, in cancer stem cell-like immortalized human mammary epithelial cells expressing Twist[20] and in cancer cells. Our results reveal the short-term effects of SAL and thus contribute to the elucidation of its mechanism of action. In light of the fact that SAL is used in screening studies on a small group of patients with invasive carcinoma of the head, neck, breast and ovary,[4] this point is especially relevant.

Results

SAL affects the cell viability of many types of solid cancer and leukemic cells. First we focused our attention on T leukemic Jurkat cells, given that alteration of mitochondrial potassium influx in these cells significantly impacts cell survival.[21,22] Figure 1a shows a drastic reduction of cell survival, as assessed using MTT (3-(4,5-dimethylthiazol-2-yl)-2,5-diphenyltetrazolium bromide) assay, by addition of sub-μM concentration of NIG (IC_{50}: 0.33 μM). Similarly, Jurkat cells were sensitive to SAL and VAL in the μM range (IC_{50} SAL: 3.61 μM; IC_{50} VAL: 7.40 μM). Figure 1b proves, using Annexin binding assay, that the decreased cell viability was due to increased apoptosis. In all 10 μM of all three ionophores was sufficient to kill more than 80% of the cells, while at 1 μM NIG was most effective. Next, we tested the sensitivity of *ex vivo* human cells to the above three ionophores. Human pathologic B cells isolated from patients with CLL (B-CLL) have been reported to be efficiently killed by 1 μM SAL, in contrast to peripheral blood mononuclear cells from healthy subjects.[6] In accordance, 1 and 10 μM SAL induced 60% and 94% B-CLL death, respectively (Figure 1c). Similar data were obtained with NIG and with VAL (Figure 1c and Supplementary Figure S2).

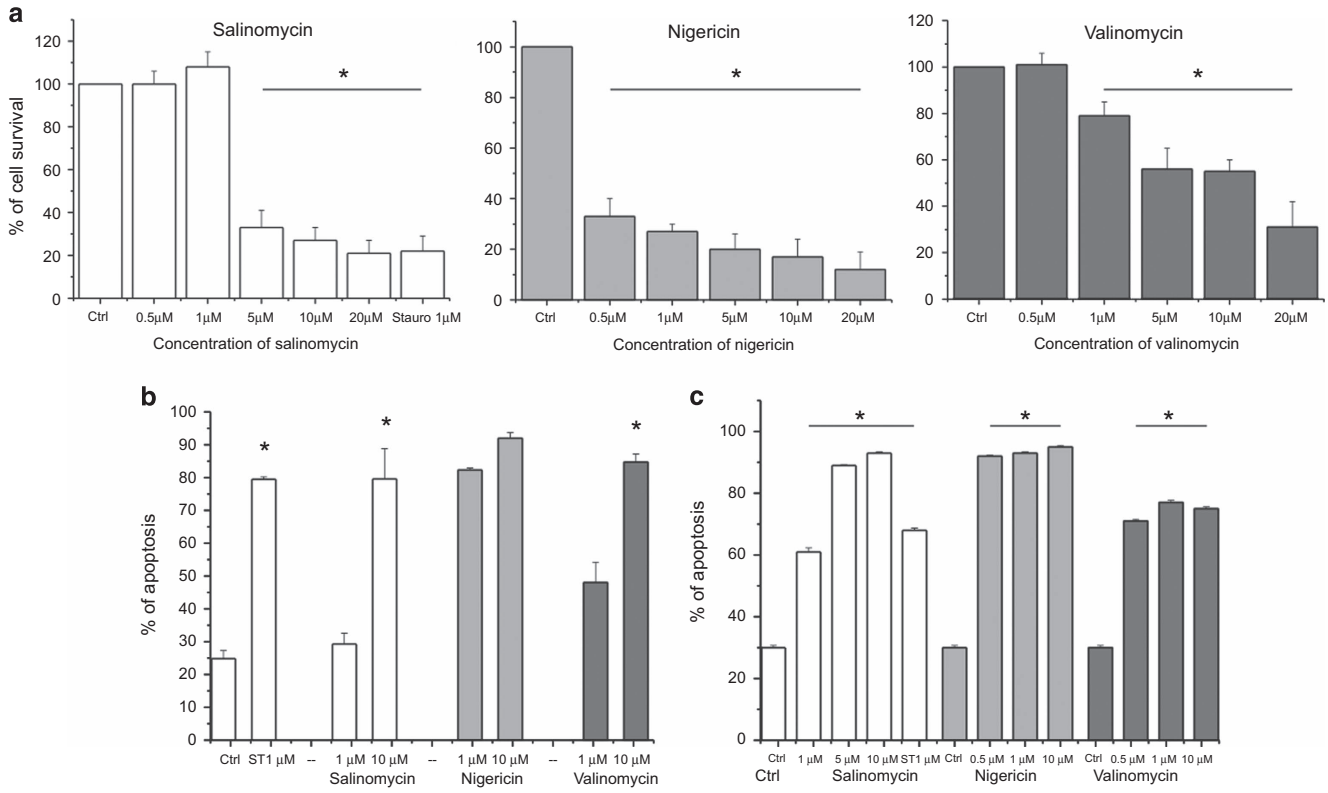

Figure 1 Effect of salinomycin, nigericin and valinomycin on lymphocytes. Jurkat leukemic T cells (**a** and **b**) and human primary B-CLL cells (**c**) were incubated for 24 h with different concentrations of the compounds, as indicated. Cell survival (**a**) was measured by MTT assay; values are expressed as the average percentage of cell survival compared with untreated cells $\pm$ S.E.M. ($n=5$). Cell death (**b** and **c**) was tested using FACS by the staining with FITC-Annexin V and propidium iodide. Staurosporine (Stauro or ST) was used as positive control. Indicated values refer to the percentage of dead cells $\pm$ S.E.M. ($n=14$). Statistically significant differences ($P<0.05$) are indicated by asterisks

The above results confirm the ability of SAL and the other two potassium ionophores to trigger apoptosis in lymphocytes. The property of these ionophores to accumulate in the mitochondria suggested that they might induce apoptosis by altering organellar potassium homeostasis via direct action at the level of the IMM. If this hypothesis were correct, death induced by these agents ought to be independent of Bax and Bak. These two pro-apoptotic proteins become inserted into the outer mitochondrial membrane during apoptosis and contribute to cytochrome *c* release from the intermembrane space, which however occurs also via other pathways.[23–25] Loss of cytochrome *c* has been shown to occur upon SAL treatment at later stages of apoptosis. We used WT and Bax/Bak double-knockout (DKO) mouse embryonic fibroblasts (MEFs) and observed that the absence of Bax and Bak did not confer protection against SAL, NIG and VAL (Figure 2a and Supplementary Figure S3). As expected, MEF DKO cells were instead more resistant to staurosporine.

Altogether these data suggested that apoptosis induced by these three ionophores might be, at least in part, due to their direct effect on mitochondria. Therefore, we measured acute changes of mitochondrial membrane potential ($\Delta\psi$), production of ROS, matrix pH, swelling, mitochondrial morphology and respiration upon addiction of SAL, NIG and VAL. First, we observed that addition of 1 μM SAL, similarly to NIG and in contrast to VAL, to isolated rat liver mitochondria (RLM) resulted in hyperpolarization (Figure 2b). Also in intact cells, only VAL caused depolarization (Figure 2c). Both depolarization and hyperpolarization might trigger ROS release (e.g. Zorov *et al.*[26]), and an increase in intracellular ROS 30 h after SAL addition to intact cells was observed.[13] In B-CLL cells, on a time scale of minutes, only VAL induced a significant mitochondrial ROS release measured by MitoSOX; even at 10 μM SAL, ROS production was comparable to that of untreated cells (Figure 2d). The same result was obtained in Jurkat lymphocytes (not shown), and in our study, preincubation with membrane-permeant ROS scavengers PEGylated catalase and PEGylated superoxide dismutase did not affect SAL-induced apoptosis, while it did reduce VAL-associated death (Supplementary Figure S4).

Given the similar consequences of NIG and SAL addition, we presumed that SAL mediates exchange of protons with potassium. To directly prove this point, matrix pH was measured in intact cells using mitochondria-targeted SypHer.[27] At 1 and 10 μM applied concentrations, both NIG and SAL triggered an immediate matrix acidification in MEF cells with a subsequent alkalinization that did not, however, re-establish the original pH value (Figure 3a). As mentioned above, SAL was shown to act on tumor stem cells as well, with a lower IC_{50} than the one found here for Jurkat, MEF or B-CLL cells.[1] In particular, Gupta *et al.*[1] showed (and we confirmed (not shown)) that immortalized human mammary epithelial cells (HMLE) ectopically expressing the transcription factor Twist and therefore forced to undergo epithelial–mesenchymal transition are sensitive to SAL, displaying an IC_{50} of around 1 μM regarding cell viability. Therefore, we asked whether SAL shows the same effect on the mitochondria of cells with stem cell-like features and used HMLE-Twist cells to measure mitochondrial function. As Figure 3b illustrates, sustained matrix acidification upon SAL and NIG addition could be observed also in these cells. ROS release and changes in membrane potential (Supplementary Figure S5 and S6) occurred similarly to the other cells described above.

Matrix acidification is due to the entry of protons in exchange for potassium ions leaving the matrix. VAL has also been shown to cause acidification to some extent in the absence of K^+/H^+ exchanger inhibitors.[28] Given that acidification is known to prevent activation of the permeability transition pore (PTP) (e.g. Szabo *et al.*[29] and Bernardi *et al.*[30]), which causes swelling and might contribute to cytochrome *c* release,[24] we tested whether SAL prevents calcium-induced PTP opening. A decrease of the absorbance, indicative of swelling, can be detected in isolated mitochondria upon addition of 140 μM calcium, sufficient to trigger the PTP opening (Figure 3c). In contrast, SAL and NIG, as expected, completely abolish the swelling due to calcium-induced PTP opening, at least on a relatively short time scale, even though mitochondria are able to take up calcium even in the presence of SAL as assessed by calcium retention assay (not shown). Addition of VAL results in incomplete swelling presumably due to entry of potassium and to the subsequent compensating activation of the K^+/H^+ antiporter.[31] Rapid changes in mitochondrial morphology upon addition of VAL were observed also in intact cells using mitochondria-targeted green fluorescence protein (Dimmer *et al.*[32] and Supplementary Figure S7). These experiments indicated that although SAL and NIG affect to a small extent the mitochondrial network, they do not have drastic early effects similar to those induced by VAL (massive swelling; Figure 3d and Supplementary Figure S7).

Although mitochondrial depolarization, ROS production and swelling do not take place in the early phases following SAL and NIG addition, the matrix acidification is expected to severely impact on mitochondrial bioenergetics. Adenosine triphosphate (ATP) depletion in cells upon SAL addition has been described after 24 h,[10] but whether it occurs as a direct consequence of SAL action on mitochondrial respiration or as a secondary independent effect is unclear. Figure 4 illustrates that already 1 μM SAL and NIG significantly reduced basal respiration in intact adherent MEFs as assessed by the extracellular flux analyzer using a previously established protocol.[33] This decrease in respiration was further accentuated by oligomycin, which blocks the ATP synthase. Subsequent addition of the uncoupler carbonylcyanide-*p*-trifluoromethoxyphenylhydrazone (FCCP) did not restore respiration, whereas the addition of antimycin A, an inhibitor of complex III, completely abolished oxygen consumption in both MEFs (Figure 4a) and HMLE-Twist cells (Figure 4b). Antimycin A inhibits the oxidation of ubiquinol in the electron transport chain of oxidative phosphorylation (OxPhos), preventing thereby the formation of the proton gradient across the IMM. In summary, SAL and NIG drastically reduced the respiratory response to the addition of FCCP. In contrast, VAL induced an immediate increase in respiration and a loss of response to oligomycin. When cellular respiration in MEFs was decreased by oligomycin, the addition of VAL but not of SAL and NIG induced a recovery of the respiratory rate (Figure 4c). This recovery is a reflection of the loss of $\Delta\psi$m induced by VAL. Subsequent addition of FCCP had no effect, whereas antimycin A reduced respiration (Figure 4c). Similar changes were observed in both settings with 10 μM SAL (Figure 4d),

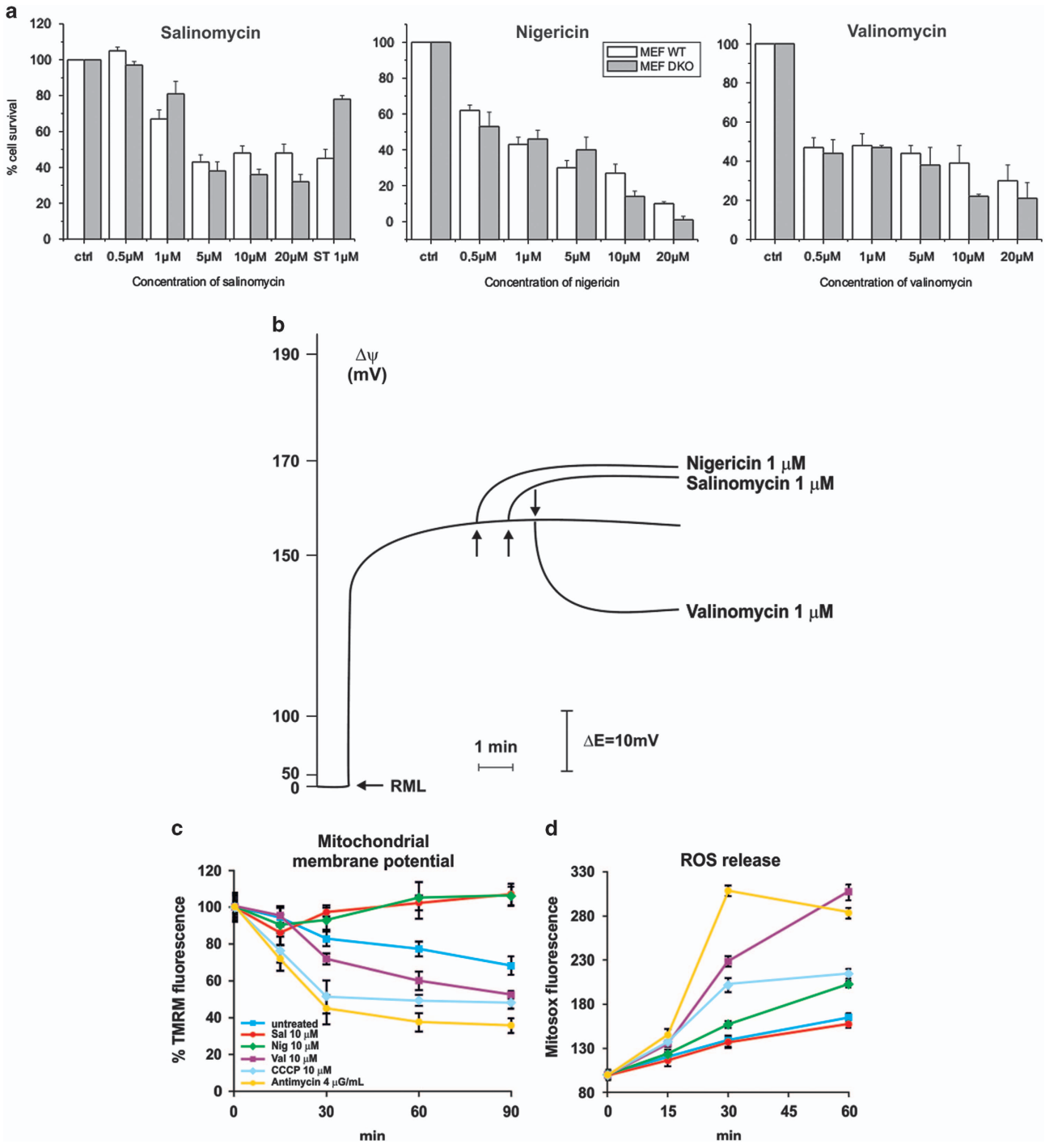

Figure 2 Salinomycin kills Bax/Bak-less mouse embryonic fibroblasts and alters mitochondrial membrane potential. (**a**) Cell survival in WT and Bax/Bak DKO MEFs was measured by MTT assay ($n=4$). Staurosporine was used as the classical apoptosis inducer. No significant differences were observed between WT and DKO cells. (**b**) Mitochondrial membrane potential determined on rat liver isolated mitochondria (RLM) by measuring the distribution of the TPP^+ ions across the mitochondrial membrane with a selective TPP^+ ion-sensitive electrode. Values are presented as variation of $\Delta\psi$ following addition of the indicated compounds. (**c** and **d**) Mitosox (**c**) and TMRM (**d**) fluorescence on B-CLL cells, measured by FACS analysis after treatment with salinomycin, nigericin and valinomycin at the indicated concentrations; CCCP, antimycin and staurosporine (ST) were used as positive controls. Average values ± S.D. are showed ($n=3$ independent experiments)

indicating that at least in MEF cells, 10 μM SAL was sufficient to drastically reduce bioenergetic efficiency. These results strongly suggest that matrix-pH-perturbing ionophores significantly reduce respiratory efficiency, contributing to the observed cell death.

In light of the above results we then compared B-CLL cells directly with B lymphocytes isolated from healthy subjects as previously described.[19] Under the experimental conditions used, SAL-induced apoptosis not only in B-CLL cells but also in healthy B cells, although to a statistically significantly less

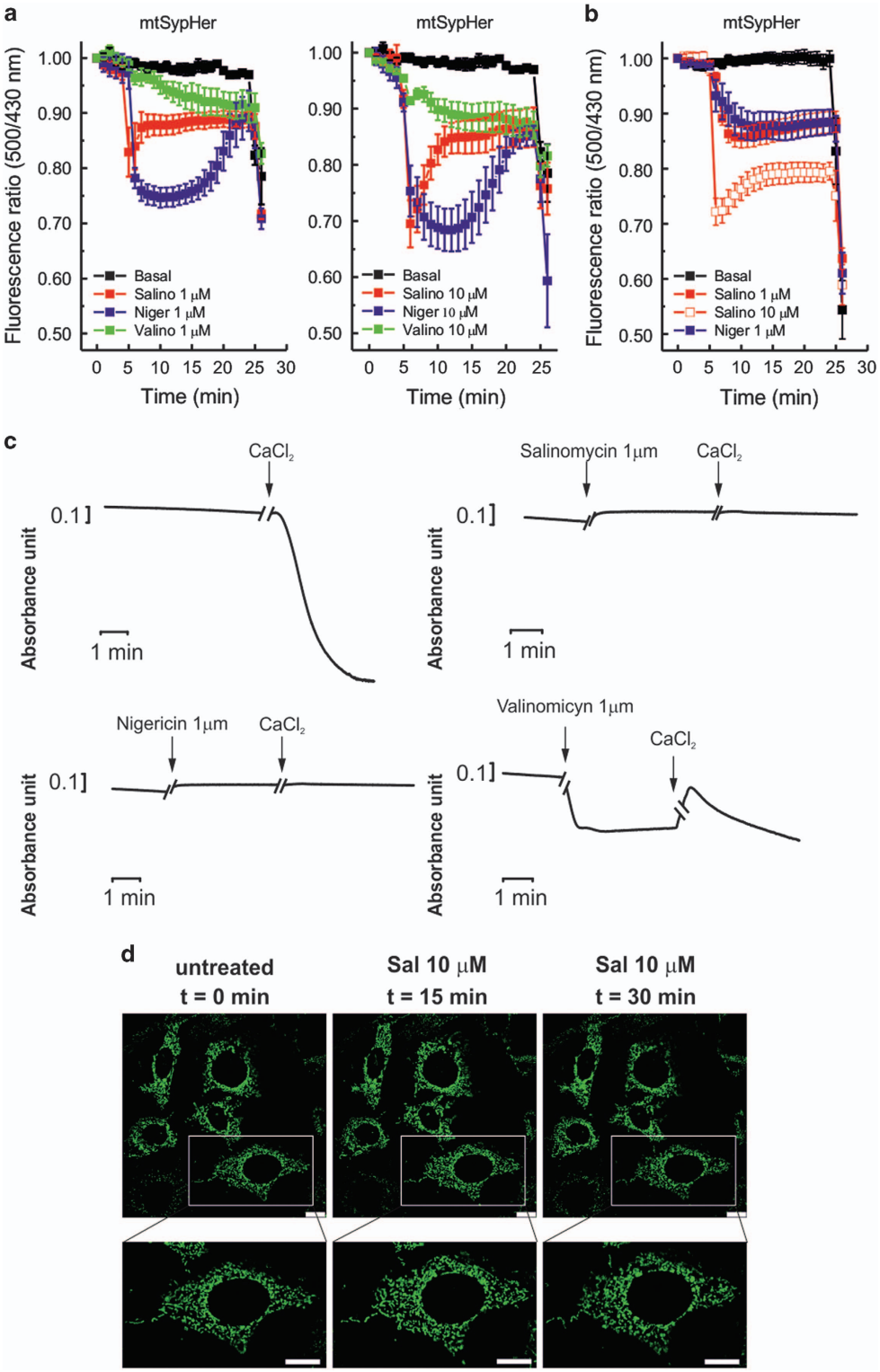

Figure 3 Salinomycin induces an instantaneous acidification of matrix pH in intact cells. (**a** and **b**) Measurement of transient variation of mitochondrial matrix pH in MEF WT cells (**a**) and in HMLE-Twist cells (**b**) expressing mito-SypHer; changes in pH correspond to variations in the 535-nm fluorescence emission after alternative excitation at 405 and 488 nm. Results are expressed as mean 500/430 nm ratios ± S.E.M. of four different experiments. Addition of drugs is indicated by red arrow, while Na-acetate (NaAc) was used as positive control (blue arrows). (**c**) Isolated rat liver mitochondria (RLM) swelling was measured as reduction of mitochondrial absorbance over time at 540 nm. $CaCl_2$ (140 μM) was used to induce PTP opening and swelling. (**d**) MEF WT cells expressing mito-YFP were treated with SAL at the indicated concentrations and live images were acquired over time to monitor changes in mitochondria morphology. Bars correspond to 25 μm. Magnified images are shown in the lower row. Results shown in (**a**)–(**d**) are representative of three independent experiments

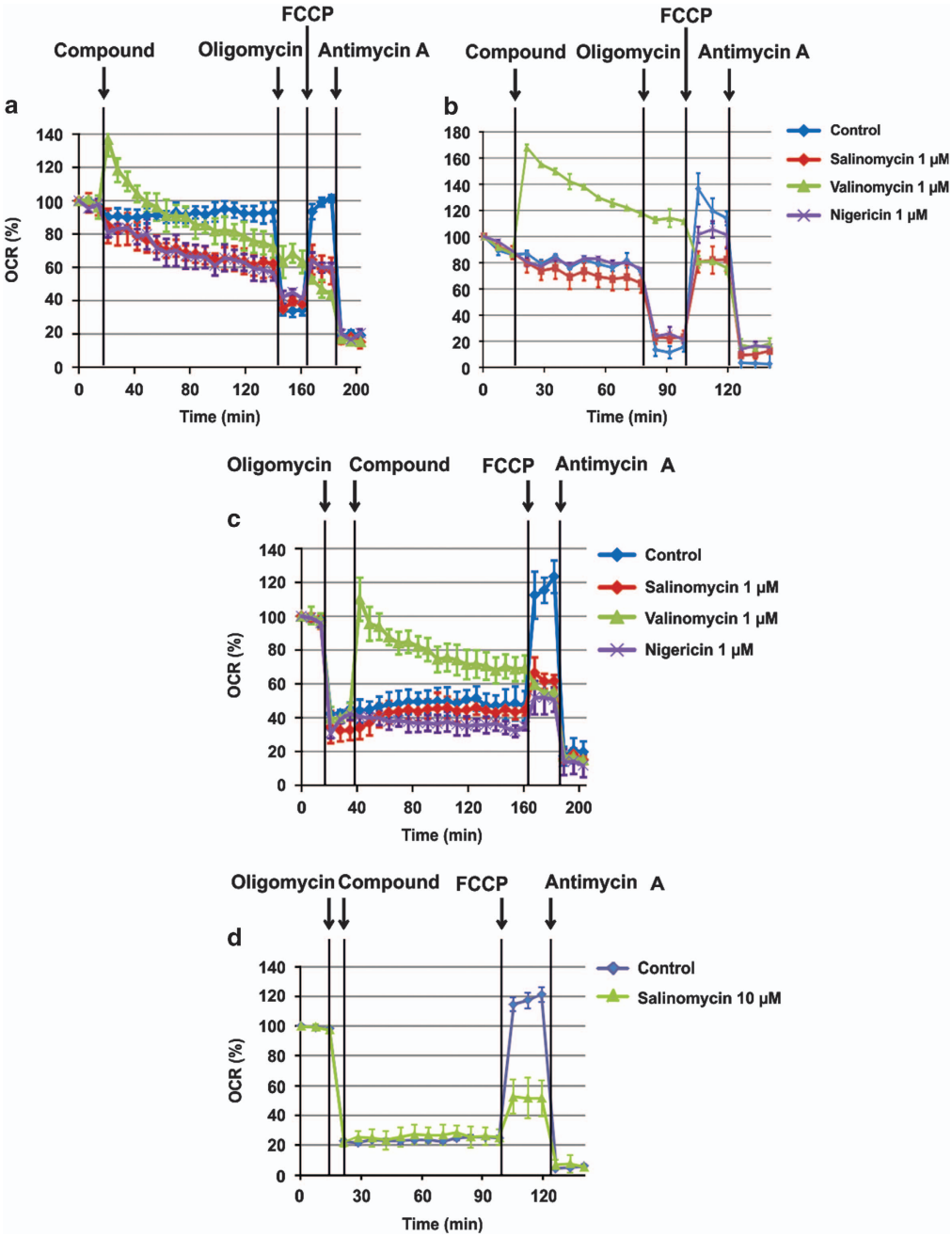

Figure 4 Salinomycin and nigericin affect respiration in a similar manner. (**a**–**d**) Oxygen consumption rate (OCR) of MEF WT cells (**a**, **c** and **d**) and of HMLE-Twist cells (**b**) was measured in the presence of 1 μM salinomycin, nigericin and valinomycin (compounds). Representative experiments are shown. The compounds were added to the cells either before (**a** and **b**) or after (**c** and **d**) inhibition of ATP synthase activity with oligomycin. The effect of 10 μM SAL in MEF cells was comparable to that of 1 μM, indicating that already the lower concentration exerts the maximal effect

extent than in pathologic cells (Figure 5a). The same experiments were performed on B-CLL cells co-cultured with mesenchymal stromal cells (MSCs) from healthy donors,[34] since MSCs of the bone marrow microenvironment have been reported to protect B-CLL cells from apoptosis induced by conventional chemotherapeutics.[35] The apoptosis-inducing effect of SAL was significantly reduced by the presence of MSCs both for pathologic (Figure 5b) and for healthy B cells (not shown) in agreement with the notion that adhesion of B-CLLs on MSC favors survival[36] and MSCs protect leukemia cells from apoptosis induced by chemotherapeutic drugs.[37] SAL was toxic to MSC after 24 h of treatment both when co-culturing B-CLL with MSC (Figure 5c and Supplementary Figure S8) and when culturing MSC alone (Supplementary Figure S9). In order to test also another non-tumoral system, cultured primary human skin fibroblasts were used (Figure 5d). Again, these cells were sensitive to SAL and were even more apoptotic with NIG applied at 10 μM concentration.

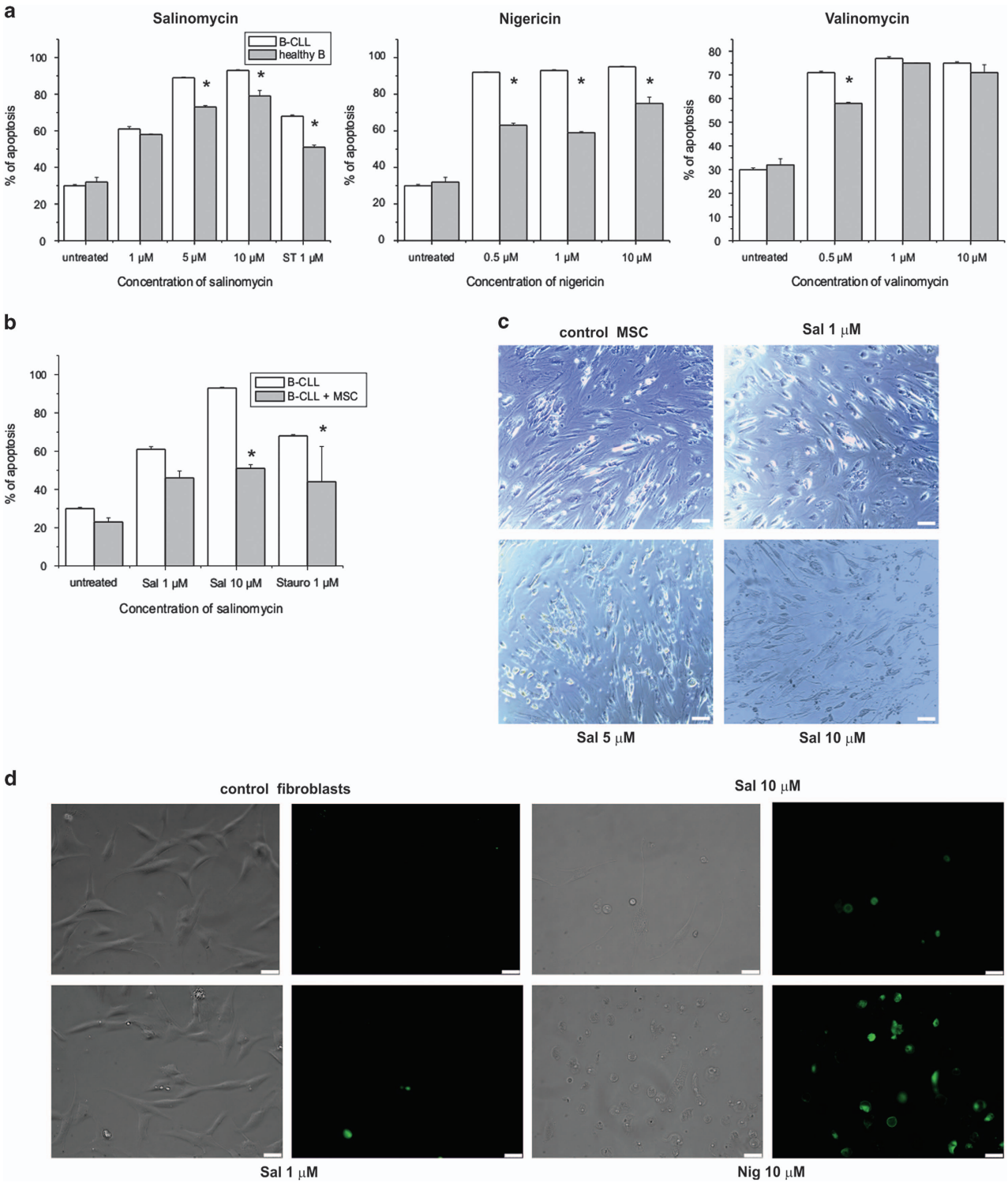

Figure 5 Salinomycin, nigericin and valinomycin affect survival of leukemic B cells, mesenchymal stromal cells and fibroblasts. (**a**) Comparison of apoptosis in pathologic B-CLL cells and B cells from healthy subjects (cells were incubated for 24 h in the presence of the indicated compounds and cell death was determined by FACS by staining with FITC-Annexin V and propidium iodide). Quantification of the cell death (all annexin-positive cells) ± S.E.M. ($n=14$ for B-CLL cells and $n=6$ for healthy B cells). (**b**) Apoptosis of B-CLL ($n=14$) cells compared with death occurring in the pathologic cells co-cultured with MSC ($n=4$). Apoptotic cells were identified by FACS as in (**a**). (**c**) Mesenchymal stromal cells were photographed after 24 h treatment with SAL and removal of co-cultured B-CLL cells by washing. Bars correspond to 75 μm. At higher concentrations of SAL the number of cells decreased and the cells showed significant morphological alterations. (**d**) Human primary fibroblasts treated with the indicated substances for 24 h. Annexin-FITC binding is shown. Results shown in (**c**) and (**d**) are representative of three independent experiments. Bars correspond to 50 μm

Discussion

In the present work, by comparing the effects of three K^+ ionophores on isolated mitochondria as well as in intact cells, we demonstrate that SAL and NIG, two drugs identified as promising chemotherapeutics, both act as K^+/H^+ exchangers at the level of the IMM and contribute to the loss of mitochondrial function in intact cells.

Our data clearly show that SAL action is comparable to that of NIG while being distinct from the effects of VAL, and demonstrates that in intact cells SAL mediates K^+/H^+ exchanger activity also at the level of the IMM. The measurements in cells indicating IMM hyperpolarization, mitochondrial matrix acidification and decrease of respiration leave no doubt that, similarly to NIG, SAL reaches the mitochondria within a few seconds upon addition. Indeed, NIG has been reported also by other groups to cause IMM hyperpolarization, without causing an acute effect on the cytosolic pH or on the plasma membrane potential,[38,39] and SAL was shown to cause extensive damage to the mitochondria of *Eimeria* sporozoites.[40] Our results suggest that the reported ATP depletion upon SAL addition is a result of the decreased respiration and that increase in mitochondrial ROS release and mitochondrial depolarization detected 24 h after addition are secondary effects occurring at a later time point. These ionophores impact also cellular ion homeostasis, that is, SAL suppresses autophagy flux and lysosomal proteolytic activity.[41] NIG and SAL may mediate the export of potassium through the plasma membrane down its concentration gradient in exchange for the uptake of protons, and as a consequence cause acidification of the cytosol. However, it has been shown that 0.5 μM NIG did not alter the cytosolic pH under conditions that caused a pronounced acidification of the mitochondrial matrix within 15 min.[38] On the other hand, on a longer time scale SAL treatment has been shown to cause membrane scrambling.[42]

In mitochondria, NIG and SAL cause hyperpolarization, that is, a shift of $\Delta\psi$ from the resting potential toward more negative values, since by acting as H^+/K^+ exchangers, they adjust ΔpH according to the K^+ gradient across the IMM (depletion of K^+ during organelle isolation does not occur (e.g. Szabo and Zoratti[25] and Bernardi[31]): the equilibrium condition for K^+/H^+ electroneutral exchange is $\Delta\mu_K = -\Delta\mu_H$. Since K^+ is by far more concentrated than H^+, upon addition of NIG or SAL the $\Delta\mu_H$ will essentially tend to the value set by the $\Delta\mu_K$ (with the opposite orientation). $\Delta\psi$ increases to maintain a constant $\Delta\tilde{\mu}_H$ in spite of the decrease (or inversion) of $\Delta\mu_H$.[38,43] In other words, proton influx being in exchange for K^+, that is, electroneutral, does not have by itself any effect on potential. Hyperpolarization derives from the collapse of ΔpH, which the mitochondrion compensates by increasing $\Delta\psi$ so as to keep the overall electrochemical potential nearly constant. Neither NIG nor SAL increases mitochondrial ROS production in intact cells, since these agents do not modify $\Delta\tilde{\mu}_H$ on short-term scale; instead, they cause matrix acidification. These results are in agreement with the study reporting that matrix alkalinization favors ROS generation, whereas matrix acidification induced by NIG strongly inhibits this process.[44] The data presented here on VAL are also in line with the findings described in the literature.[31]

Mitochondrial matrix pH is a factor that controls OxPhos in intact cells. Matrix pH ranges from 7.7 to 8.2 in different cell types, while the pH of the cytosol is around 7.0. This proton gradient significantly contributes to the driving force on the ATP synthase and impacts several transport processes responsible for exchanging metabolites (e.g. pyruvate, glutamate) or ions between mitochondria and the cytosol (e.g. Greenbaum and Wilson[45]). Using a mitochondrial pH-sensitive probe (mtAlpHi), Akhmedov *et al.*[38] observed in insulin-secreting cells a matrix acidification using 0.5 μM NIG, which was partially recovered over the following 15 min, similarly to our observations in MEF cells. Matrix realkalinization depends on the operation of the H^+ pumps and on the electrogenic influx of cations and efflux of anions,[46] but a ΔpH of 0.4 unit persisted after the partial recovery in Akhmedov *et al.*[38]. In addition, matrix acidification slowed down mitochondrial ATP synthesis by 20% over 20 min despite hyperpolarization of the IMM, by regulating OxPhos downstream of Complex II. In the present study, a sustained decrease of respiration by addition of NIG and SAL is observed. This process might be compensated for a while by ATP hydrolysis due to the ability of the ATP synthase to work in the reverse mode, which presumably contributes to the ATP depletion observed (after 24 h) in several studies. Sustained decrease of the respiration is expected to lead also to loss of $\Delta\Psi$m in the long term, which, in turn, might trigger autophagy, mitophagy and ROS release. Indeed, depolarization induced by FCCP leads to ROS release (e.g. Sassi *et al.*[47]) and is also known to trigger mitophagy (e.g. Lemasters[48]). Thus, the initial changes observed here upon SAL addition might well account for the published observations (mitochondrial depolarization, ATP depletion, ROS release and mitophagy[39]) occurring after >24 h. Caspase activation and cytochrome *c* release also occur at late time points.[9] Whether cytochrome *c* can be released upon depolarization-induced PTP opening or due to accumulation of dysfunctional mitochondria remains to be determined.

The relationship between mitochondrial respiratory inhibition, ATP depletion and cell death may be dependent on the cell type as well as on specific conditions (e.g. Poltl *et al.*[49]). Importantly, sensitivity of the cells to agents affecting mitochondrial respiration depends on the metabolic state of the cells, those relying mostly on mitochondrial respiration rather than on glycolysis are more sensitive. Growing evidence indicates that several types of cancer cells (e.g. CSC-like surviving pancreatic ductal adenocarcinoma cells (PDAC)[50] and both normal and leukemic stem cells[51]) are less glycolytic and more dependent on mitochondrial respiration than others. PDAC cells are unable to increase compensatory glycolytic fluxes following inhibition of OxPhos, thereby showing large sensitivity to inhibition of mitochondrial function. This may well explain the previously reported selectivity of SAL towards CSCs. Thus, differences in the sensitivity of the cell types used here and in other works towards SAL can likely be ascribed to differences in metabolic state. Healthy human fibroblasts and B lymphocytes have been shown to principally rely on OxPhos for their metabolism,[52] possibly accounting for the SAL effect observed here. In accordance with our findings, SAL was found to be cytotoxic to healthy human peripheral blood

lymphocytes at 10 μM concentration.[53] In general, induction of mitochondrial dysfunction and related energy metabolism[54–56] and/or of substantial ROS release[57,58] is considered a valid strategy to fight malignant diseases. The question also arises whether differences in sensitivity to SAL between CSCs and non-CSCs might be ascribed to differences in the mitochondrial response to SAL. Our data suggest that this is not the case, since the observed effects equally take place in the two cell types. Instead, it has been reported that autophagy flux is essential for maintaining proliferation of CSCs and that SAL reduces the activity of cathepsins resulting in the inhibition of lysosomal activity and autophagic flux to a greater extent in CSCs with respect to non-CSC cells.[41]

In summary, in the present work we provide evidence that SAL functions in intact cells as an K^+/H^+ antiporter and directly impacts mitochondrial function in a few minutes upon addition. Our findings contribute to the understanding of the mechanism of action of this promising anticancer drug. The results strengthen the hypothesis that polyether ionophore antibiotics contribute to apoptosis induction by a common mechanism and might explain toxicity upon SAL treatment (e.g. Boehmerle *et al.,*[5] Scherzad *et al.,*[53] and Ojo *et al.*[59]). Further studies will be necessary to exactly delineate the factors contributing to the moderate to high selectivity of SAL and NIG toward tumoral cells as observed in several cases, given that these ionophores *a priori* impact mitochondrial functions independently of differences in signaling pathways (e.g. Wnt) and in redox state and of the mitochondrial hyperpolarization typical of tumoral cells. Therefore, the hypothesis that the apoptotic effects of SAL and NIG depend on the ability of the cells to compensate mitochondrial dysfunction, deserves to be tested in future studies. For example, peroxisome proliferator-activated receptor gamma coactivator 1-*α*, an important regulator of mitochondrial biogenesis that is also involved in the regulation of several stress programs and might integrate mitochondrial biogenesis into cellular stress adaption, might be involved in compensatory mechanisms (e.g. Hofer *et al.*[60]).

Materials and Methods

Reagents and cell lines. SAL, NIG and VAL and other commercial chemicals were purchased from Sigma-Aldrich (Milan, Italy) unless otherwise specified.

Mouse embryonic fibroblast (MEF), MEF WT, BAX/BAK-less (DKO) and mito-YFP cells were grown in Dulbecco's modified Eagle's medium (DMEM) additionated with 10 mM HEPES buffer (pH 7.4), 10% (v/v) fetal bovine serum (FBS), 100 U/ml penicillin G, 0.1 mg/ml streptomycin and 1% non-essential amino acids (100 × solution; Life Technologies, Thermo Fisher Scientific Inc, Waltham, MA, USA), in a humidified atmosphere of 5% CO_2 at 37 °C. Jurkat T lymphocytes were grown in RPMI-1640 supplemented as above. B cells were isolated and maintained in culture on a MSC layer as previously reported.[34] Briefly, 2×10^5/well CLL MSCs were seeded and incubated for a few days before the experiment at 37 °C in 5% CO_2 up to confluence. Then purified B-CLL cells ($CD19^+/CD5^+$) were added to the MSC layer at a ratio of 2–5 : 1. Cells were then treated with SAL, NIG or VAL for 24 h to evaluate a possible resistance to this agent due to the co-culture. Human skin fibroblasts, kindly provided by Prof. V Bianchi (Padova), were cultured in DMEM supplemented with 10% FBS, L-glutamine and streptomycin.

HMLE TWIST cells were a kind gift of Prof. Weinberg and were grown in DMEM F1/2 supplemented with insulin, hydrocortisone, bovine pituitary extract and epidermal growth factor (all from Life Technologies, Thermo Fisher Scientific Inc). Cells were grown and cultured as reported in Cordenonsi *et al.*[61]

Proliferation and cell death assays. To determine cell viability, tetrazolium reduction (MTT) assay was used as reported previously.[18] Briefly, 0.005×10^6 MEF WT or DKO cells were seeded in standard 96-well plates in 200 μl of DMEM for 24 h. Then, the medium was replaced with DMEM without phenol red (PR) and FBS and cells were treated as indicated in the figure legends. Suspension cells were seeded and treated in DMEM without PR and FBS. After incubation, CellTiter 96 AQUEOUS One solution (Promega, Milan, Italy) was added to each well as indicated by the supplier. Absorbance at 490 nm to detect formazan formation was measured using a Packard Spectra Count 96-well plate reader (Life Technologies, Thermo Fisher Scientific Inc).

Apoptosis for B-CLL and healthy cells was determined by FACS analysis (FACS Canto II, BD BioSciences, Franklin Lakes, NJ, USA) using a double staining with Annexin V-FLUOS (Roche, Basel, Switzlerland) and propidium iodide (PI; Sigma Aldrich, St. Louis, MO, USA) as reported before.[19] After incubation with the different drugs, cells were incubated with PI (final concentration 1 μg/ml) and Annexin-V-FLUOS (0.6 μl/sample) for 20´ at 37 °C in the dark, and were analyzed by FACS. For human skin fibroblasts, cells were seeded in a 24-well plate and treated for 24 h as indicated in 1 ml of DMEM without PR and FBS. After incubation, 2 μl/well of Annexin V-FITC was added and cells were incubated for 20´ at 37 °C in the dark, and were analyzed by a Leica DMI 4000 fluorescence microscope (Leica Microsystems, Wetzlar, Germany).

Mitochondrial morphology. Mitochondrial network was studied by using MEF mito-YFP cells seeded directly onto glass coverslips in six-well plates (0.05×10^6) in DMEM. Then, coverslips were mounted onto holders, washed, filled with 1 ml of DMEM without PR and FBS and compounds were added directly onto the holder on the microscope stage of a Leica SP5 confocal system mounted on a Leica DMI6000 microscope.

Determination of mitochondrial matrix pH in live cells. MEF WT cells were seeded at a density of 50×10^3 cells/well onto glass coverslips. pH measurements were performed in Ca^{2+}/Mg^{2+} supplemented HEPES buffer (HBSS, Invitrogen, Milan, Italy) 24 h after transfection with a mtSypHer expression vector using Lipofectamine 2000 (Invitrogen). Coverslips were mounted onto the holder and the different compounds were added directly and analyzed by a Leica SP5 confocal system mounted on a Leica DMI6000 microscope. Ratiometric sequential images of the 535 nm emission fluorescence were acquired every 3 min during 30 min with a ×63 objective and the LAS-AF software after alternative excitation at 430 nm and 500 nm. As a control of acidification, cells were treated with 30 mM NaAc at the end of each experiment. The multi-measure plug-in of Image J software (NIH) was used to estimate mean fluorescence ratios of selected ROIs matching the mitochondria in at least four experiments following background subtraction; results are expressed as mtSypHer (500/430 nm) ratio.

Mitochondrial membrane potential and ROS production. Mitochondrial membrane potential (MMP) and ROS production were measured as in Leanza *et al.*[19] Briefly, MMP was monitored using tetramethylrhodamine methyl ester (TMRM; 20 nM), while ROS production was assayed using MitoSOX (1 μM). B cells either from CLL patients or from healthy subjects were incubated for 20 min at 37 °C. After incubation, the indicated compounds were added and the decrease in TMRM fluorescence or the increase in MitoSOX fluorescence was measured by FACS. HMLE TWIST cells (0.07×10^6 cells/well) were seeded in a 12-well plate in 1 ml of their culture medium. The day after, cells were incubated with TMRM 20 nM and MitoSOX 1μM in HBSS (Life Technologies, Thermo Fisher Scientific Inc) for 20 min at 37 °C in the dark. After incubation, compounds were added as indicated in the figure and the decrease in TMRM fluorescence or the increase in MitoSOX fluorescence was measured by a Leica DMI 4000 fluorescence microscope at the indicated time points.

Oxygen consumption assay. Oxygen consumption by adherent cells was measured using an XF24 Extracellular Flux Analyzer (Seahorse Bioscience, North Billerica, MA, USA) as reported before.[33,47] MEF WT cells were seeded at 3×10^4 cells/well in 200 μL of supplemented culture medium (DMEM; Sigma Aldrich). Oxygen consumption rate (OCR) was measured at preset time intervals while the instrument automatically carried out the preprogrammed additions of the various compounds (oligomycin final concentration 1 μg/ml, FCCP 400 nM, antimycin A 1 μM), added as a solution in 70 μL of DMEM. HMLE TWIST cells were seeded at 6×10^4 cells/well in 200 μL of supplemented culture medium. As for MEF WT, OCR was measured at preset time intervals upon the addition of the various compounds (oligomycin final concentration 0.5 μg/ml, FCCP 1 μM, antimycin A 1 μM), added as a solution in 70 μL of DMEM. A massive loss of cells because of death and

detachment was excluded by direct microscopic observation of the cells at the end of the experiments (not shown).

RLM isolation and determination of RLM membrane potential and swelling. Rats were killed and the liver was removed and immediately immerged in an ice-cold isolation medium (250 mM sucrose, 5 mM Hepes, 2 mM EGTA, pH 7.5). The liver tissue was minced, thoroughly rinsed several times with ice-cold medium and then homogenized in the same buffered solution using a glass/Teflon Potter homogenizer. Mitochondria were then isolated by conventional differential centrifugation and the protein content was measured by the biuret method with bovine serum albumin as a standard.

Experiments were carried out with 1 mg of mitochondrial protein/ml suspended in a standard incubation medium containing 200 mM sucrose, 10 mM HEPES (pH 7.4), 5 mM Na-succinate, 1.25 μM rotenone and 1 mM phosphate, additionated with 2 mM KCl.

Membrane potential ($\Delta\psi$) was determined on the basis of the distribution of lipid-soluble cation tetraphenylphosphonium (TPP^+) across the mitochondrial membrane, measured by a TPP^+-specific electrode, as in Kamo *et al.*[62]

Mitochondrial swelling was determined by measuring light scattering at 90° with a Perkin Elmer LS50B spectrofluorometer at 540 nm with a 5.5-nm slit width.

Conflict of Interest

The authors declare no conflict of interest.

Acknowledgements. We are grateful to the Italian Association for Cancer Research (AIRC grants to IG 11814, IS, GS, LT and LS) and to PRIN (MZ and IS) for financial support. LL is a recipient of a Young Investigator Grant of the University of Padova (GRIC12NN5G). The authors thank Luca Pellegrini for useful discussion and Prof. Weinberg and Prof. Piccolo for the HMLE-Twist cells. EG is grateful to DFG (GU 335/29-1).

1. Gupta PB, Onder TT, Jiang G, Tao K, Kuperwasser C, Weinberg RA *et al.* Identification of selective inhibitors of cancer stem cells by high-throughput screening. *Cell* 2009; **138**: 645–659.
2. Huczynski A. Salinomycin: a new cancer drug candidate. *Chem Biol Drug Des* 2012; **79**: 235–238.
3. Naujokat C, Fuchs D, Opelz G. Salinomycin in cancer: a new mission for an old agent. *Mol Med Rep* 2010; **3**: 555–559.
4. Antoszczak M, Huczynski A. Anticancer activity of polyether Ionophore - salinomycin. *Anticancer Agents Med Chem* 2015; **15**: 575–591.
5. Boehmerle W, Muenzfeld H, Springer A, Huehnchen P, Endres M. Specific targeting of neurotoxic side effects and pharmacological profile of the novel cancer stem cell drug salinomycin in mice. *J Mol Med (Berl)* 2014; **92**: 889–900.
6. Lu D, Choi MY, Yu J, Castro JE, Kipps TJ, Carson DA. Salinomycin inhibits Wnt signaling and selectively induces apoptosis in chronic lymphocytic leukemia cells. *Proc Natl Acad Sci USA* 2011; **108**: 13253–13257.
7. Arafat K, Iratni R, Takahashi T, Parekh K, Al Dhaheri Y, Adrian TE *et al.* Inhibitory effects of salinomycin on cell survival, colony growth, migration, and invasion of human non-small cell lung cancer A549 and LNM35: involvement of NAG-1. *PLoS One* 2013; **8**: e66931.
8. Lu W, Li Y. Salinomycin suppresses LRP6 expression and inhibits both Wnt/beta-catenin and mTORC1 signaling in breast and prostate cancer cells. *J Cell Biochem* 2014; **115**: 1799–1807.
9. Verdoodt B, Vogt M, Schmitz I, Liffers ST, Tannapfel A, Mirmohammadsadegh A. Salinomycin induces autophagy in colon and breast cancer cells with concomitant generation of reactive oxygen species. *PLoS One* 2012; **7**: e44132.
10. Jangamreddy JR, Ghavami S, Grabarek J, Kratz G, Wiechec E, Fredriksson BA *et al.* Salinomycin induces activation of autophagy, mitophagy and affects mitochondrial polarity: differences between primary and cancer cells. *Biochim Biophys Acta* 2013; **1833**: 2057–2069.
11. Klose J, Stankov MV, Kleine M, Ramackers W, Panayotova-Dimitrova D, Jager MD *et al.* Inhibition of autophagic flux by salinomycin results in anti-cancer effect in hepatocellular carcinoma cells. *PLoS One* 2014; **9**: e95970.
12. Mitani M, Yamanishi T, Miyazaki Y, Otake N. Salinomycin effects on mitochondrial ion translocation and respiration. *Antimicrob Agents Chemother* 1976; **9**: 655–660.
13. Kim KY, Yu SN, Lee SY, Chun SS, Choi YL, Park YM *et al.* Salinomycin-induced apoptosis of human prostate cancer cells due to accumulated reactive oxygen species and mitochondrial membrane depolarization. *Biochem Biophys Res Commun* 2011; **413**: 80–86.
14. Zhu LQ, Zhen YF, Zhang Y, Guo ZX, Dai J, Wang XD. Salinomycin activates AMP-activated protein kinase-dependent autophagy in cultured osteoblastoma cells: a negative regulator against cell apoptosis. *PLoS One* 2013; **8**: e84175.
15. Andersson B, Janson V, Behnam-Motlagh P, Henriksson R, Grankvist K. Induction of apoptosis by intracellular potassium ion depletion: using the fluorescent dye PBFI in a 96-well plate method in cultured lung cancer cells. *Toxicol In Vitro* 2006; **20**: 986–994.
16. Park WH, Seol JG, Kim ES, Kang WK, Im YH, Jung CW *et al.* Monensin-mediated growth inhibition in human lymphoma cells through cell cycle arrest and apoptosis. *Br J Haematol* 2002; **119**: 400–407.
17. Leanza L, O'Reilly P, Doyle A, Venturini E, Zoratti M, Szegezdi E *et al.* Correlation between potassium channel expression and sensitivity to drug-induced cell death in tumor cell lines. *Curr Pharm Des* 2014; **20**: 189–200.
18. Leanza L, Henry B, Sassi N, Zoratti M, Chandy KG, Gulbins E *et al.* Inhibitors of mitochondrial Kv1.3 channels induce Bax/Bak-independent death of cancer cells. *EMBO Mol Med* 2012; **4**: 577–593.
19. Leanza L, Trentin L, Becker KA, Frezzato F, Zoratti M, Semenzato G *et al.* Clofazimine, Psora-4 and PAP-1, inhibitors of the potassium channel Kv1.3, as a new and selective therapeutic strategy in chronic lymphocytic leukemia. *Leukemia* 2013; **27**: 1782–1785.
20. Mani SA, Guo W, Liao MJ, Eaton EN, Ayyanan A, Zhou AY *et al.* The epithelial-mesenchymal transition generates cells with properties of stem cells. *Cell* 2008; **133**: 704–715.
21. Szabo I, Bock J, Grassme H, Soddemann M, Wilker B, Lang F *et al.* Mitochondrial potassium channel Kv1.3 mediates Bax-induced apoptosis in lymphocytes. *Proc Natl Acad Sci USA* 2008; **105**: 14861–14866.
22. Gulbins E, Sassi N, Grassme H, Zoratti M, Szabo I. Role of Kv1.3 mitochondrial potassium channel in apoptotic signalling in lymphocytes. *Biochim Biophys Acta* 2010; **1797**: 1251–1259.
23. Kumarswamy R, Chandna S. Putative partners in Bax mediated cytochrome-c release: ANT, CypD, VDAC or none of them? *Mitochondrion* 2009; **9**: 1–8.
24. Scorrano L. Opening the doors to cytochrome c: changes in mitochondrial shape and apoptosis. *Int J Biochem Cell Biol* 2009; **41**: 1875–1883.
25. Szabo I, Zoratti M. Mitochondrial channels: ion fluxes and more. *Physiol Rev* 2014; **94**: 519–608.
26. Zorov DB, Juhaszova M, Sollott SJ. Mitochondrial reactive oxygen species (ROS) and ROS-induced ROS release. *Physiol Rev* 2014; **94**: 909–950.
27. Poburko D, Santo-Domingo J, Demaurex N. Dynamic regulation of the mitochondrial proton gradient during cytosolic calcium elevations. *J Biol Chem* 2011; **286**: 11672–11684.
28. Aldakkak M, Stowe DF, Cheng Q, Kwok WM, Camara AK. Mitochondrial matrix K+ flux independent of large-conductance Ca2+-activated K+ channel opening. *Am J Physiol Cell Physiol* 2010; **298**: C530–C541.
29. Szabo I, Bernardi P, Zoratti M. Modulation of the mitochondrial megachannel by divalent cations and protons. *J Biol Chem* 1992; **267**: 2940–2946.
30. Bernardi P, Vassanelli S, Veronese P, Colonna R, Szabo I, Zoratti M. Modulation of the mitochondrial permeability transition pore. Effect of protons and divalent cations. *J Biol Chem* 1992; **267**: 2934–2939.
31. Bernardi P. Mitochondrial transport of cations: channels, exchangers, and permeability transition. *Physiol Rev* 1999; **79**: 1127–1155.
32. Dimmer KS, Navoni F, Casarin A, Trevisson E, Endele S, Winterpacht A *et al.* LETM1, deleted in Wolf-Hirschhorn syndrome is required for normal mitochondrial morphology and cellular viability. *Hum Mol Genet* 2008; **17**: 201–214.
33. Manago A, Becker KA, Carpinteiro A, Wilker B, Soddemann M, Seitz AP *et al. Pseudomonas aeruginosa* pyocyanin induces neutrophil death via mitochondrial reactive oxygen species and mitochondrial acid sphingomyelinase. *Antioxid Redox Signal* 2015; **22**: 1097–1110.
34. Frezzato F, Trimarco V, Martini V, Gattazzo C, Ave E, Visentin A *et al.* Leukaemic cells from chronic lymphocytic leukaemia patients undergo apoptosis following microtubule depolymerization and Lyn inhibition by nocodazole. *Br J Haematol* 2014; **165**: 659–672.
35. Kurtova AV, Balakrishnan K, Chen R, Ding W, Schnabl S, Quiroga MP *et al.* Diverse marrow stromal cells protect CLL cells from spontaneous and drug-induced apoptosis: development of a reliable and reproducible system to assess stromal cell adhesion-mediated drug resistance. *Blood* 2009; **114**: 4441–4450.
36. Burger JA, Gribben JG. The microenvironment in chronic lymphocytic leukemia (CLL) and other B cell malignancies: insight into disease biology and new targeted therapies. *Sem Cancer Biol* 2014; **24**: 71–81.
37. Pillozzi S, Masselli M, De Lorenzo E, Accordi B, Cilia E, Crociani O *et al.* Chemotherapy resistance in acute lymphoblastic leukemia requires hERG1 channels and is overcome by hERG1 blockers. *Blood* 2011; **117**: 902–914.
38. Akhmedov D, Braun M, Mataki C, Park KS, Pozzan T, Schoonjans K *et al.* Mitochondrial matrix pH controls oxidative phosphorylation and metabolism-secretion coupling in INS-1E clonal beta cells. *FASEB J* 2010; **24**: 4613–4626.
39. Zhang H, Huang HM, Carson RC, Mahmood J, Thomas HM, Gibson GE. Assessment of membrane potentials of mitochondrial populations in living cells. *Anal Biochem* 2001; **298**: 170–180.
40. Fuller AL, Golden J, McDougald LR. Flow cytometric analysis of the response of Eimeria tenella (Coccidia) sporozoites to coccidiocidal effects of ionophores. *J Parasitol* 1995; **81**: 985–988.

41. Yue W, Hamai A, Tonelli G, Bauvy C, Nicolas V, Tharinger H *et al.* Inhibition of the autophagic flux by salinomycin in breast cancer stem-like/progenitor cells interferes with their maintenance. *Autophagy* 2013; **9**: 714–729.
42. Bissinger R, Malik A, Jilani K, Lang F. Triggering of erythrocyte cell membrane scrambling by salinomycin. *Basic Clin Pharmacol Toxicol* 2014; **115**: 396–402.
43. Nicholls DG. Simultaneous monitoring of ionophore- and inhibitor-mediated plasma and mitochondrial membrane potential changes in cultured neurons. *J Biol Chem* 2006; **281**: 14864–14874.
44. Selivanov VA, Zeak JA, Roca J, Cascante M, Trucco M, Votyakova TV. The role of external and matrix pH in mitochondrial reactive oxygen species generation. *J Biol Chem* 2008; **283**: 29292–29300.
45. Greenbaum NL, Wilson DF. The distribution of inorganic phosphate and malate between intra- and extramitochondrial spaces. Relationship with the transmembrane pH difference. *J Biol Chem* 1985; **260**: 873–879.
46. Zoratti M, Favaron M, Pietrobon D, Petronilli V. Nigericin-induced transient changes in rat-liver mitochondria. *Biochim Biophys Acta* 1984; **767**: 231–239.
47. Sassi N, Mattarei A, Azzolini M, Bernardi P, Szabo I, Paradisi C *et al.* Mitochondria-targeted resveratrol derivatives act as cytotoxic pro-oxidants. *Curr Pharm Des* 2014; **20**: 172–179.
48. Lemasters JJ. Variants of mitochondrial autophagy: Types 1 and 2 mitophagy and micromitophagy (Type 3). *Redox Biology* 2014; **2**: 749–754.
49. Poltl D, Schildknecht S, Karreman C, Leist M. Uncoupling of ATP-depletion and cell death in human dopaminergic neurons. *Neurotoxicology* 2012; **33**: 769–779.
50. Viale A, Pettazzoni P, Lyssiotis CA, Ying H, Sanchez N, Marchesini M *et al.* Oncogene ablation-resistant pancreatic cancer cells depend on mitochondrial function. *Nature* 2014; **514**: 628–632.
51. Lagadinou ED, Sach A, Callahan K, Rossi RM, Neering SJ, Minhajuddin M *et al.* BCL-2 inhibition targets oxidative phosphorylation and selectively eradicates quiescent human leukemia stem cells. *Cell Stem Cell* 2013; **12**: 329–341.
52. Lall R, Ganapathy S, Yang M, Xiao S, Xu T, Su H *et al.* Low-dose radiation exposure induces a HIF-1-mediated adaptive and protective metabolic response. *Cell Death Differ* 2014; **21**: 836–844.
53. Scherzad A, Hackenberg S, Schramm C, Froelich K, Ginzkey C, Hagen R *et al.* Geno- and cytotoxicity of salinomycin in human nasal mucosa and peripheral blood lymphocytes. *Toxicol In Vitro* 2015; **29**: 813–818.
54. Xiao Z, Sperl B, Ullrich A, Knyazev P. Metformin and salinomycin as the best combination for the eradication of NSCLC monolayer cells and their alveospheres (cancer stem cells) irrespective of EGFR, KRAS, EML4/ALK and LKB1 status. *Oncotarget* 2014; **5**: 12877–12890.
55. Fulda S, Galluzzi L, Kroemer G. Targeting mitochondria for cancer therapy. *Nat Rev Drug Discov* 2010; **9**: 447–464.
56. Rodriguez-Enriquez S, Gallardo-Perez JC, Hernandez-Resendiz I, Marin-Hernandez A, Pacheco-Velazquez SC, Lopez-Ramirez SY *et al.* Canonical and new generation anticancer drugs also target energy metabolism. *Arch Toxicol* 2014; **88**: 1327–1350.
57. Ralph SJ, Pritchard R, Rodriguez-Enriquez S, Moreno-Sanchez R, Ralph RK. Hitting the Bull's-Eye in Metastatic Cancers-NSAIDs Elevate ROS in Mitochondria, Inducing Malignant Cell Death. *Pharmaceuticals (Basel)* 2015; **8**: 62–106.
58. Gogvadze V. Targeting mitochondria in fighting cancer. *Curr Pharm Des* 2011; **17**: 4034–4046.
59. Ojo OO, Bhadauria S, Rath SK. Dose-dependent adverse effects of salinomycin on male reproductive organs and fertility in mice. *PLoS One* 2013; **8**: e69086.
60. Hofer A, Noe N, Tischner C, Kladt N, Lellek V, Schauss A *et al.* Defining the action spectrum of potential PGC-1alpha activators on a mitochondrial and cellular level in vivo. *Hum Mol Genet* 2014; **23**: 2400–2415.
61. Cordenonsi M, Zanconato F, Azzolin L, Forcato M, Rosato A, Frasson C *et al.* The Hippo transducer TAZ confers cancer stem cell-related traits on breast cancer cells. *Cell* 2011; **147**: 759–772.
62. Kamo N, Muratsugu M, Hongoh R, Kobatake Y. Membrane potential of mitochondria measured with an electrode sensitive to tetraphenyl phosphonium and relationship between proton electrochemical potential and phosphorylation potential in steady state. *J Membr Biol* 1979; **49**: 105–121.

Supplementary Information accompanies this paper on Cell Death and Disease website (http://www.nature.com/cddis)

Figure S1

Salinomycin

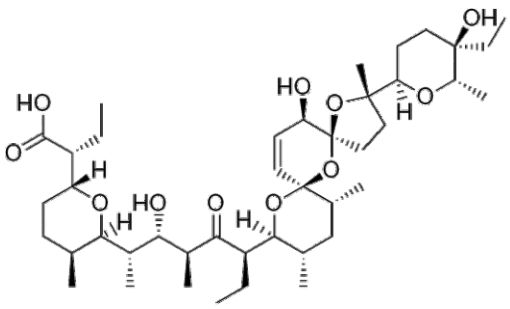

Valinomycin

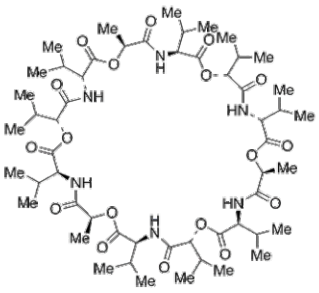

Nigericin

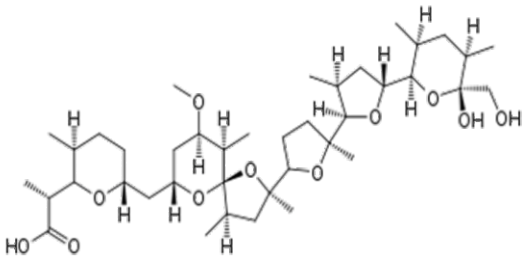

Figure S2

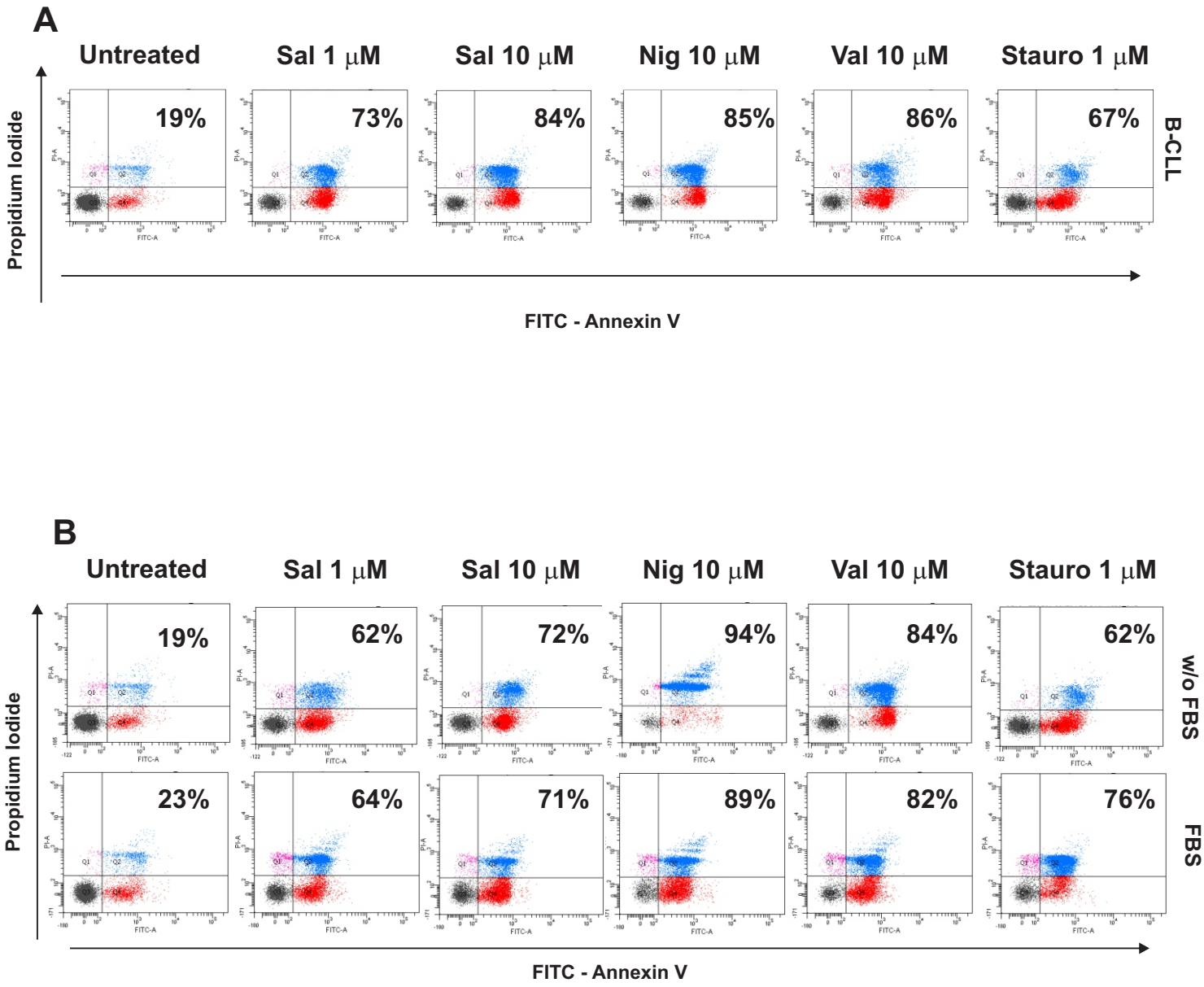
A
Untreated
Sal 1 μM
Sal 10 μM
Nig 10 μM
Val 10 μM
Stauro 1 μM
19%
73%
84%
85%
86%
67%
B-CLL
Propidium Iodide
FITC - Annexin V
B
Untreated
Sal 1 μM
Sal 10 μM
Nig 10 μM
Val 10 μM
Stauro 1 μM
19%
62%
72%
94%
84%
62%
w/o FBS
23%
64%
71%
89%
82%
76%
FBS
Propidium Iodide
FITC - Annexin V

Figure S3

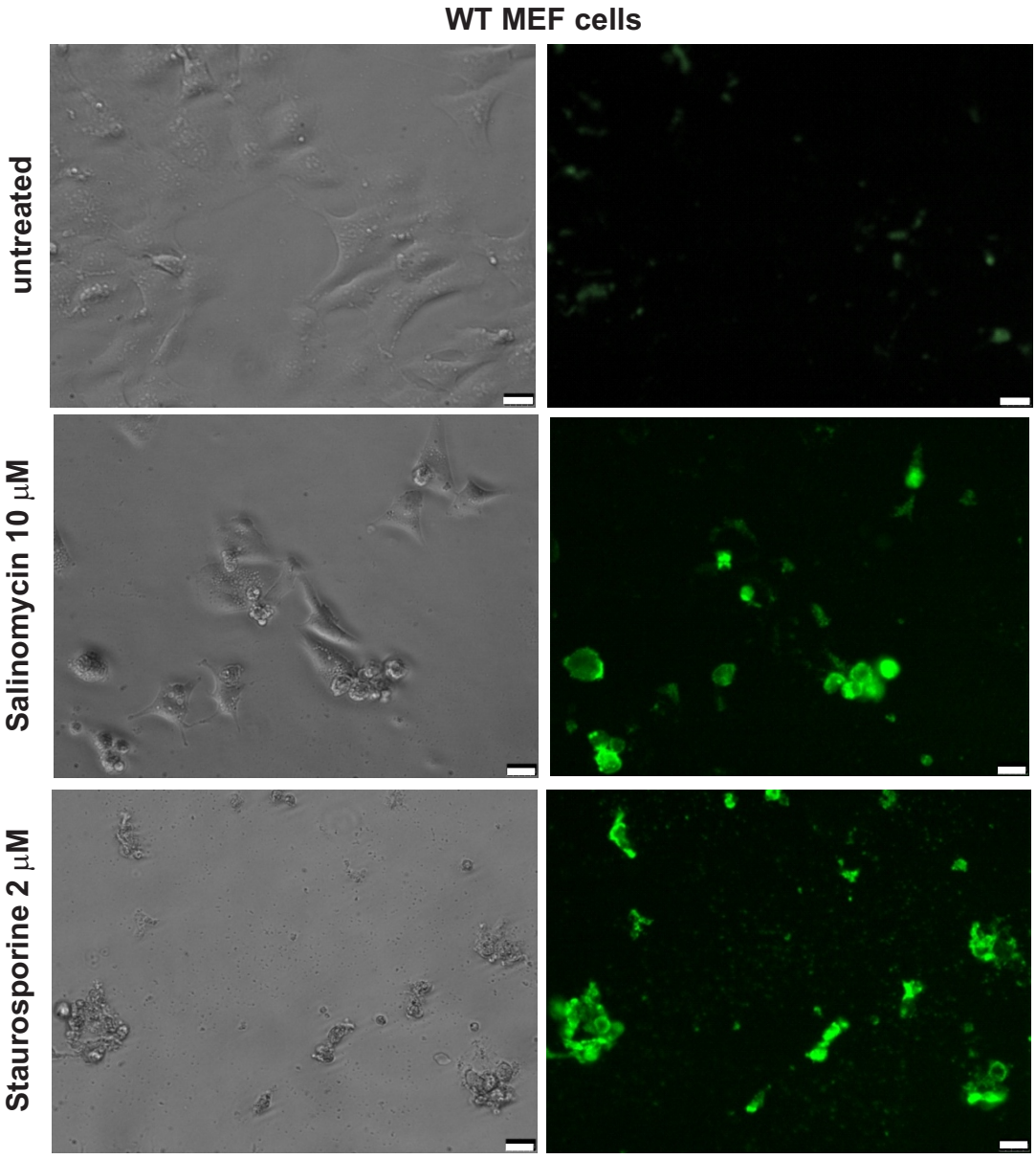
WT MEF cells
untreated
Salinomycin 10 μM
Staurosporine 2 μM

Figure S4

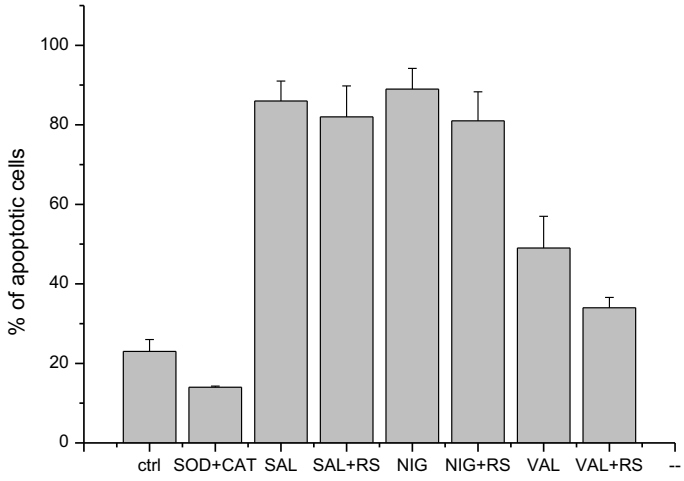
% of apoptotic cells
100
80
60
40
20
0
ctrl
SOD+CAT
SAL
SAL+RS
NIG
NIG+RS
VAL
VAL+RS
--

Figure S5

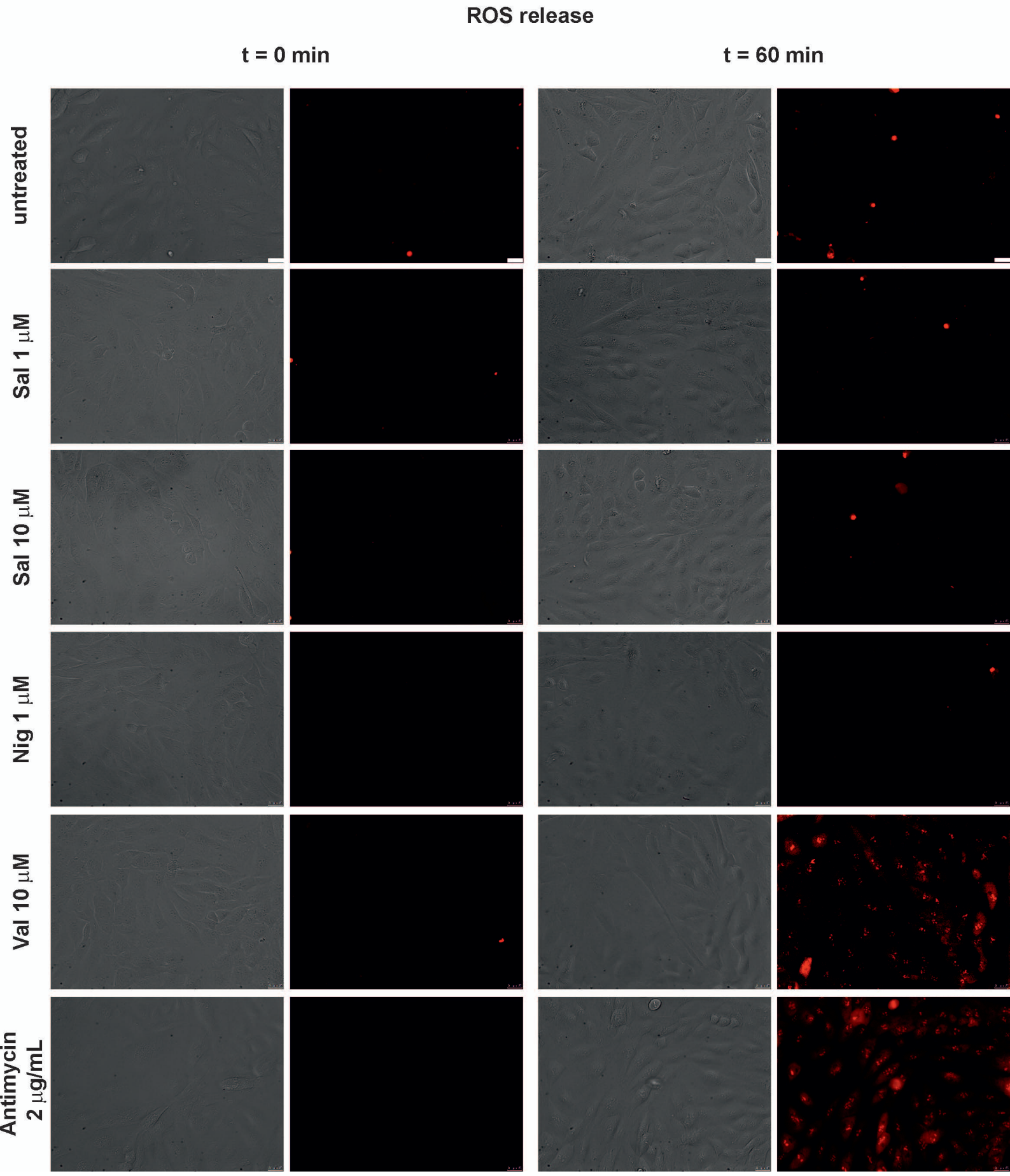
ROS release
t = 0 min
t = 60 min
untreated
Sal 1 μM
Sal 10 μM
Nig 1 μM
Val 10 μM
Antimycin 2 μg/mL

Figure S6

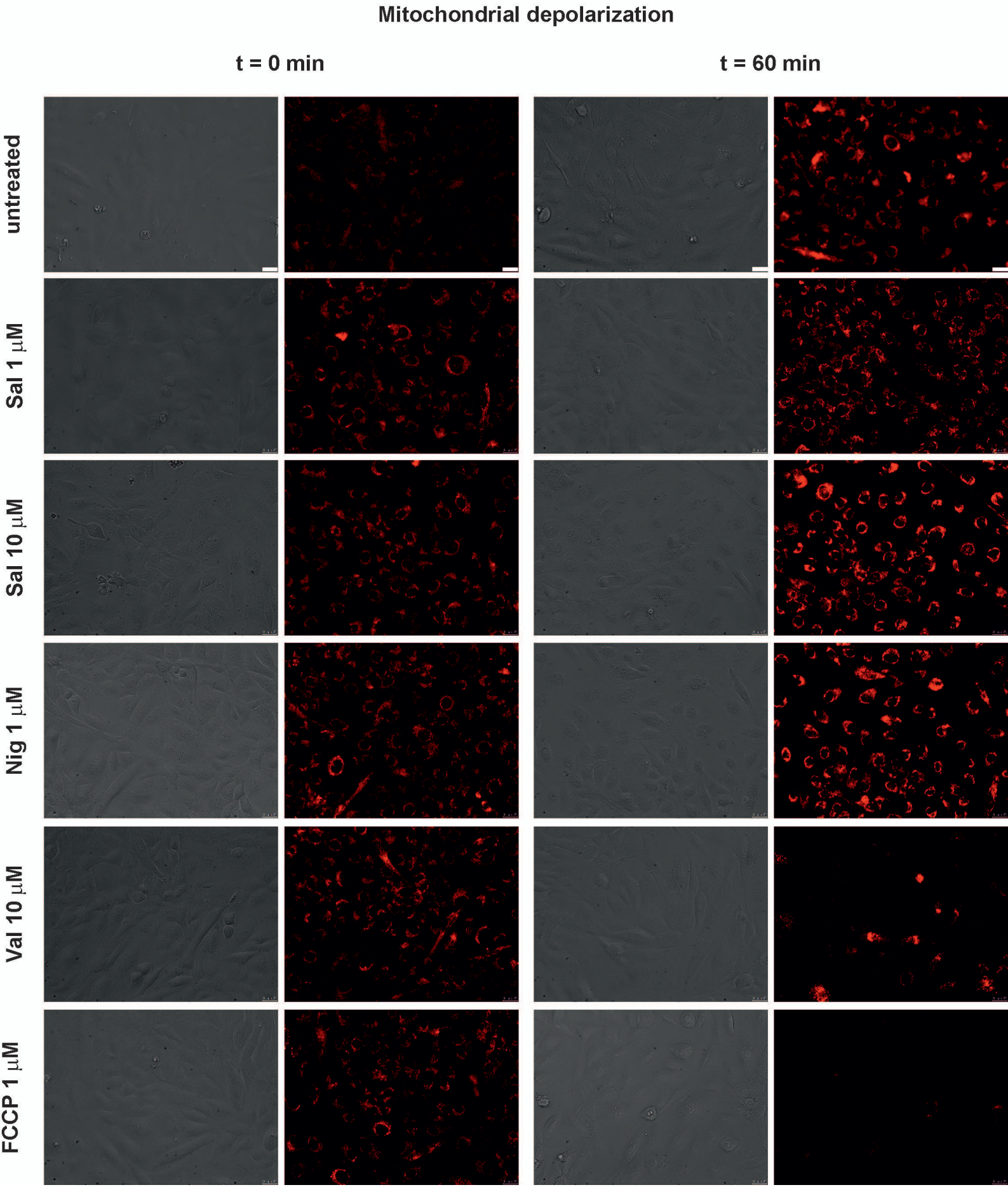
Mitochondrial depolarization
t = 0 min
t = 60 min
untreated
Sal 1 μM
Sal 10 μM
Nig 1 μM
Val 10 μM
FCCP 1 μM

Figure S7

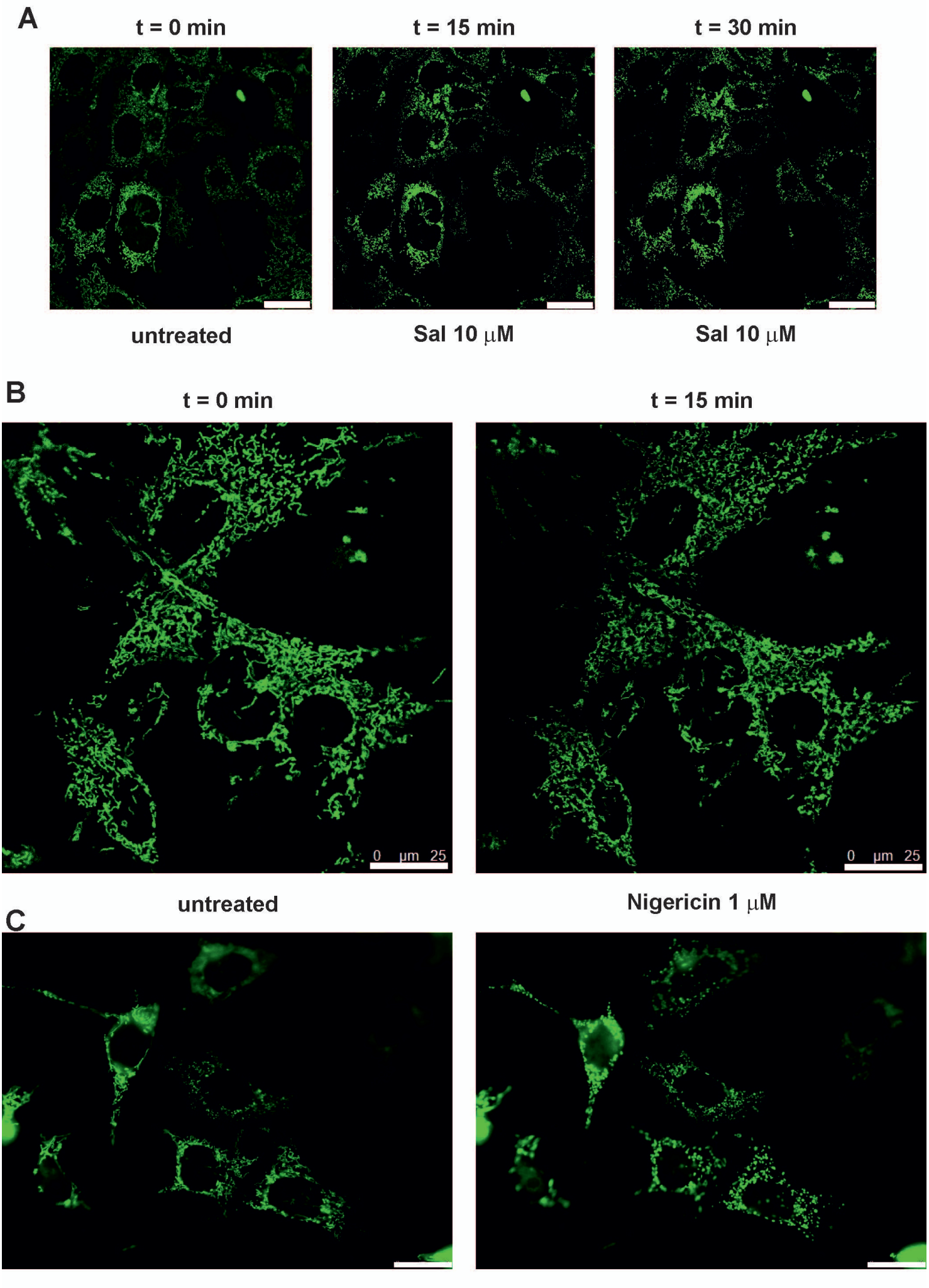
A
t = 0 min
t = 15 min
t = 30 min
untreated
Sal 10 μM
Sal 10 μM
B
t = 0 min
t = 15 min
0 μm 25
0 μm 25
untreated
Nigericin 1 μM
C
untreated
Valinomycin 10 μM

Figure S8

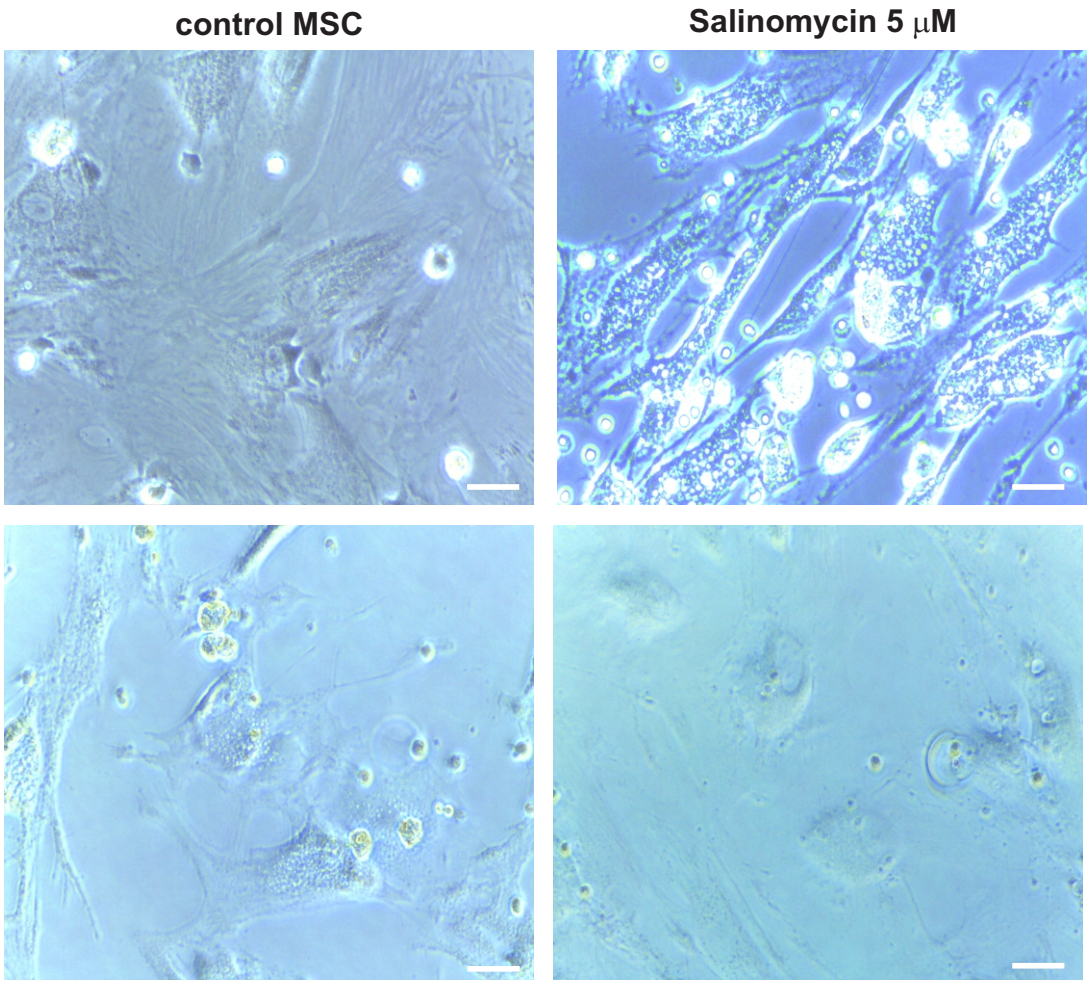
control MSC
Salinomycin 5 μM
Salinomycin 10 μM
Staurosporine 1 μM

Figure S9

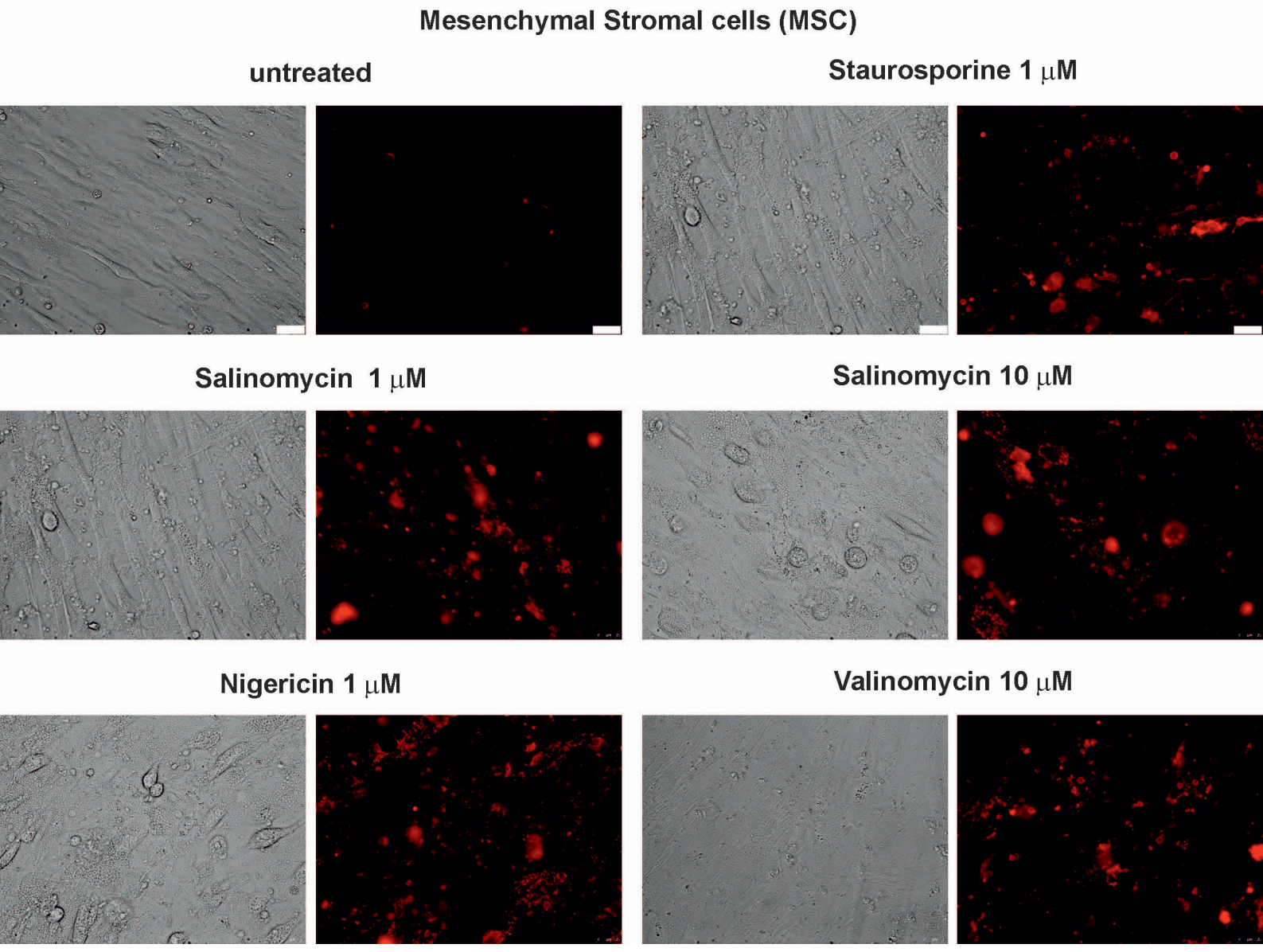
Mesenchymal Stromal cells (MSC)
untreated
Staurosporine 1 μM
Salinomycin 1 μM
Salinomycin 10 μM
Nigericin 1 μM
Valinomycin 10 μM

Biochimica et Biophysica Acta xxx (2015) xxx–xxx

Contents lists available at ScienceDirect

Biochimica et Biophysica Acta

journal homepage: www.elsevier.com/locate/bbamcr

Review

Pharmacological targeting of ion channels for cancer therapy: In vivo evidences

Luigi Leanza [a], Antonella Managò [a], Mario Zoratti [b,c], Erich Gulbins [d], Ildiko Szabo [a,c,*]

[a] Department of Biology, University of Padua, Padua, Italy
[b] Department of Biomedical Sciences, University of Padua, Padua, Italy
[c] CNR Institute of Neuroscience, Padua, Italy
[d] Department of Molecular Biology, University of Duisburg-Essen, Essen, Germany

ARTICLE INFO

Article history:
Received 2 October 2015
Received in revised form 25 November 2015
Accepted 26 November 2015
Available online xxxx

Keywords:
Calcium-permeable channels
Potassium channels
Sodium channels
Anion channels
In vivo cancer models
Pharmacological targeting

ABSTRACT

Since the discovery of the participation of various ion channels in the regulation of cell proliferation and programmed cell death two decades ago, the field exploring ion channel function in relation to cancer has undergone rapid development. Although the mechanisms accounting for the impact of ion channel modulators on cancer growth have not been fully clarified in all cases, numerous *in vivo* experiments targeting diverse ion channels in various cancer models illustrate the great potentiality of this approach and promote ion channels to the class of oncological targets. In the present review we give an updated overview of the field and critically discuss the promising results obtained in pre-clinical models using specific pharmacological modulators of calcium, sodium, potassium and anion-permeable ion channels, whose expression is often altered in tumor cells and tissues. The most, especially critical issues are specificity of action and side-effects. Interestingly, some of the most potent drugs are natural products, and several of the active compounds are already used in the clinic for other purposes. In these latter cases involving drug repositioning we may expect a faster progression from preclinical to clinical studies. This article is part of a Special Issue entitled: Calcium and Cell Fate. Guest Editors: Jacques Haiech, Claus Heizmann, Joachim Krebs, Thierry Capiod and Olivier Mignen.

1. Introduction

Plasma membrane ion channels are trans-membrane proteins that selectively facilitate the permeation of specific ions between intracellular and extracellular environments. By controlling ion fluxes at multiple sites within the cells and on multiple time scales, ion channels shape rapid cell signals in excitatory tissues but are involved also in slower processes, such as proliferation (e.g. [1–3]), volume regulation (e.g. [4,5]), apoptosis (e.g. [2,6–9]), migration (e.g. [10,11]) and cell adhesion (e.g. [12]) in non-excitable cells. Since the first reports linking ion channels to these processes (e.g. [13–18]) the field has undergone an exponential development and by now the scientific community accepted the idea that regulation of ion channel function during e.g. proliferation or apoptosis is not merely a "side-effect". Rather, channels play crucial modulating roles and are able to determine the fate of the cells. Indeed, a role of ion channels in cancer development has been hypothesized already two decades ago. Increasing evidence indicates that a variety of channel types not only in the plasma membrane but also in intracellular organelles are involved in neoplastic progression and importantly contribute to the acquisition of the main characteristics of the cancer cells [19], including metabolic re-programming [20,21], limitless proliferative potential [22,23], apoptosis-resistance [8,24], stimulation of neo-angiogenesis [25] as well as cell migration and invasiveness [12,26]. Thus, the channels impacting cancer development and progression have been defined as "oncogenic channels". Tumor progression leads to the acquisition of a specific molecular profile, giving rise to different malignant clones which display altered genotypic and phenotypic characteristics. In this respect, identification of the "channelome", i.e. of the type and expression level of a certain set of ion channels, of different cancer types is especially important, since ion channels not only contribute to malignant progression, but also offer a possibility of therapeutic intervention. Determination of the "channelome" in pathologic tissues might help to set up strategies to specifically target cancer cells but not healthy tissues, in contrast to the most widely used chemotherapeutics which affect the most rapidly proliferating cells.

Indeed, much convincing *in vitro* work by many different laboratories has established that modulation of ion channels in cancer cells by either altering their expression or using inhibitors/activators may impair the growth and/or migration of these cells. On the other hand efficacy against cultured cancer cells is not necessarily maintained when moving to more complex *in vivo* systems, since, for example pharmacokinetic properties of the anti-tumoral agents or effective drug delivery to tumor tissues in the case of solid tumors might not be satisfactory. Furthermore, the importance of the tumor microenvironment, with its immunomodulatory, pro-inflammatory and anti-apoptotic roles, is

* Corresponding author at: Department of Biology, University of Padua, Padua, Italy.
E-mail address: ildi@civ.bio.unipd.it (I. Szabo).

http://dx.doi.org/10.1016/j.bbamcr.2015.11.032
0167-4889/

coming into full focus (e.g. [27–29]). The tumor niche cannot be fully reconstituted *in vitro*. Nonetheless, recent *in vivo* studies demonstrate the efficacy of ion channel targeting, consecrating this class of proteins as promising pharmacological targets in oncology. Fig. 1. summarizes the various types of ion channels present in different tumor tissues, whose targeting yielded significant inhibition of tumor growth *in vivo* in animal models.

The primary scope of the present review is to give and updated overview of recent advances regarding pharmacological targeting; therefore, the specific mechanisms responsible for the tumor-reducing effects will be only briefly mentioned. For most of the channel proteins we discuss, evidence has been gained of their altered expression in tumor tissues with respect to healthy tissues, but for sake of simplicity we do not refer to these data. In general, while convincing cases of reduced tumor growth by application of channel inhibitors exist in the literature, in a few instances the mechanism is likely to be unrelated to their channel-inhibitory function, and/or, in several cases, the demonstration that the drugs inhibits proliferation via its action on ion channels is missing.

2. Calcium-permeable channels

Intracellular Ca^{2+} homeostasis impacts cell cycle checkpoints, apoptosis, autophagy, migration and release of soluble modulators such as neurotransmitters, hormones and growth factors in both normal and neoplastic cells [30–33]. Major Ca^{2+} influx pathways include voltage-gated Ca^{2+} channels (VCC; L-type: $Ca_V1.1$–1.4; N-type: $Ca_V2.2$; T-type: $Ca_V3.1$–3.3; R-type: $Ca_V2.3$; P/Q-type: $Ca_V2.1$), those mediated by the Ca^{2+} permeable ion channels of the transient receptor potential (TRP) family, purinergic receptors (e.g. P2X, forming Ca^{2+}- and Na^+-permeable pores), and the store-operated calcium entry (SOCE) pathway components Orai1 and STIM1 (or TRPC in combination with STIM1). In addition, the NMDA class glutamate receptors expressed in neurons and Piezo1 channels can also allow calcium influx being non-selective cation channels. At the intracellular level, activation of plasma membrane (PM) localized G protein-coupled receptors (GPCRs) leads to generation of inositol triphosphate (IP_3) and subsequent stimulation of IP3 receptors (IP_3Rs) located on the endoplasmic reticulum (ER), resulting in Ca^{2+} release from intracellular stores. Ca^{2+} from this compartment can be released also via the ryanodine receptors (RYR). Receptor-stimulated Ca^{2+} release from the ER stores serves as a signal to activate Ca^{2+} influx channels of the PM, the store-operated Ca^{2+} channels (SOCs). The two known SOCs are the Orai and TRPC channels. Orai must be activated by STIM1, an ER-resident multi-domain protein that functions as sensor of Ca^{2+} stored in the ER lumen and translocate into ER-PM junctions to tether and activate Orai channels when ER Ca^{2+} concentration decreases, while TRPC can function also independently of STIM1 [34,35]. The sarco/endoplasmic reticulum Ca^{2+} ATPase (SERCA), the secretory pathway Ca^{2+} ATPase (SPCA) and the mitochondrial calcium uniporter MCU which mediates uptake of this ion into mitochondria actively sequester cytosolic calcium. The plasma membrane Ca^{2+} ATPase (PMCA) and the PM-located Na^+/Ca^{2+} exchanger (NCX) also play

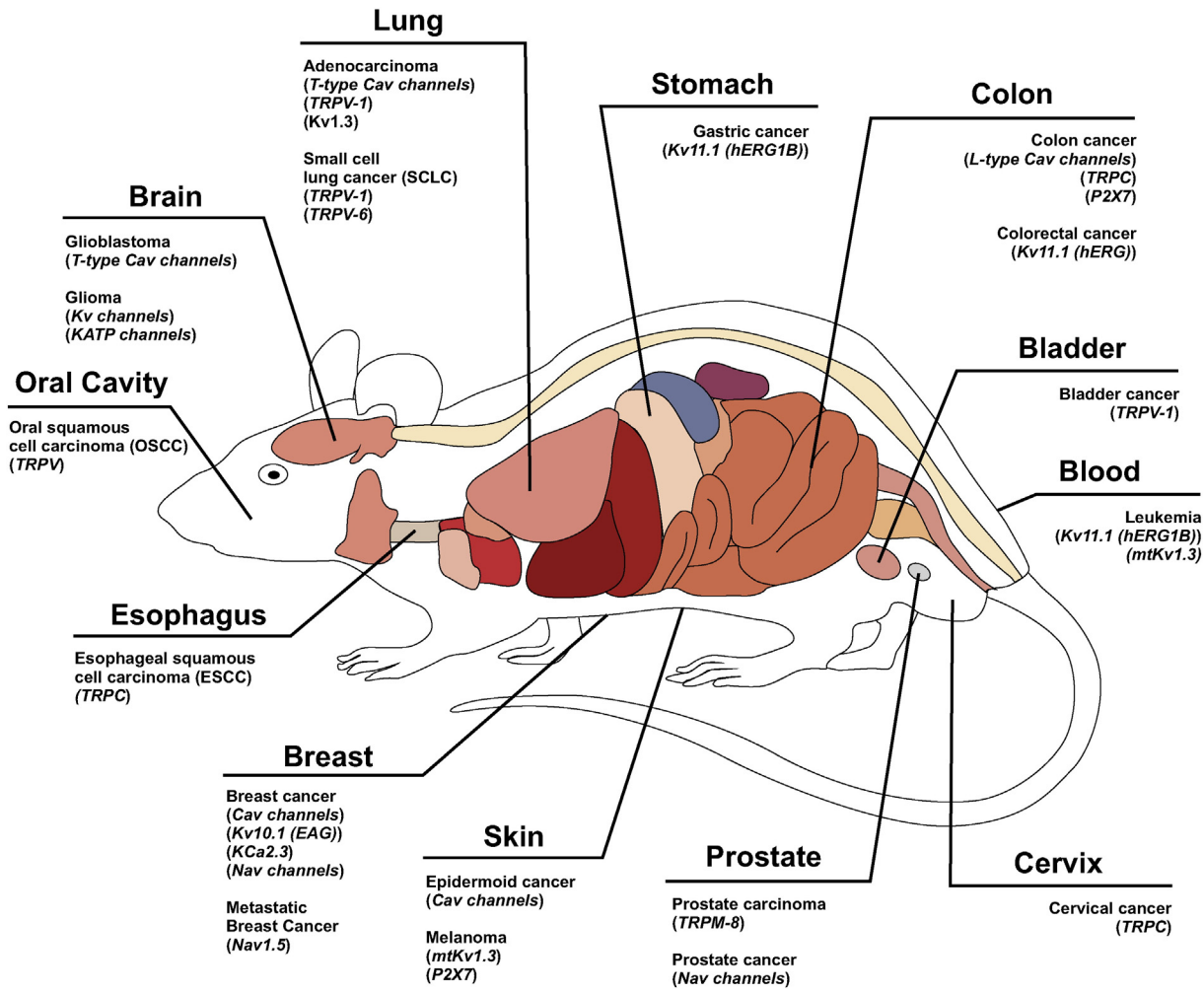

Fig. 1. *In vivo* targeting of ion channels for cancer therapy. The figure lists all channels expressed in different organs whose expression is altered in the corresponding tumor tissues and whose pharmacological targeting in vivo yielded significant result in relation to tumor size or metastasis. See text for further details.

Please cite this article as: L. Leanza, et al., Pharmacological targeting of ion channels for cancer therapy: In vivo evidences, Biochim. Biophys. Acta (2015), http://dx.doi.org/10.1016/j.bbamcr.2015.11.032

a role in restoring resting $Ca^{2+}{}_i$ by actively exporting calcium to the extracellular millieau (for recent reviews see e.g. [30,36]). In addition, acidic endogenous compartments such as lysosomes and lysosome-related organelles harbor functionally active Ca^{2+}-permeable TRP channels (the main type is TRPML, mucolipin) and TPC two pore channels as well as P2X receptors [37,38].

2.1. Voltage-gated calcium channels

Among the compounds targeting the $Ca^{2+}{}_{cyt}$-regulating systems mentioned above, some ion channel antagonists have been shown to impact on tumor size in various models. The expression of VCCs is a characteristic of excitable cells, but some members (especially of the Ca_V3 subfamily), are expressed in a number of cancer cell lines where they modulate proliferation [39]. One of the first *in vivo* studies has been performed in 1992 using structurally unrelated L-type voltage-gated calcium channel antagonists (CCA) amlodipine, diltiazem, and verapamil, all of which inhibit proliferation of HT-39 human breast cancer cells with IC_{50} values ranging from 1.5 μM (for the dihydropyridine amlodipine) to 10 μM (for the phenylalkylamine verapamil). Clinical studies in humans showed that verapamil acts as a chemo-sensitizer, overcoming multi-drug resistance (MDR) pump-mediated resistance to anthracycline and increasing survival of patients with metastatic breast carcinoma [40]. Its mechanism of action may thus be related more to its interaction with other channels, such as those selective for sodium (e.g. [41]) and potassium (e.g. [42,43], and with P-glycoprotein/MDR1 (e.g. [44]) than to Ca^{2+} channel inhibition. CCAs have been proposed to be tested in clinical trials in adjuvant therapy for recurrent or unresectable meningiomas [45,46]. *In vivo* in an animal model of breast cancer, oral administration of amlodipine (0.35 mg/day), diltiazem (3.5 mg/day) or verapamil (3.5 mg/day) for 10 days inhibited HT-39 breast tumor growth by 83.5 ± 20.1% (mean ± SE), 46.5 ± 6.6% and 68.2 ± 9.7%, respectively [47]. However, the mechanism responsible for the *in vitro* and *in vivo* effects could not be clarified, since HT39 cells were found not to express VCCs. Interestingly, the dihydropyridine (DHP) amlodipine proved to be the most efficient drug *in vivo* but not all compounds in this class display anti-proliferative effects *in vitro*. For example, while amlodipine, nicardipine and nimodipine, inhibited the growth and DNA synthesis of human epidermoid carcinoma A431 cells with IC_{50} values of 20–30 μM, the structurally related nifedipine did not exert such an effect [48]. In addition, the L-type voltage-gated calcium channel activator (F)-Bay K8644) did not prevent the anti-proliferative effect of the above DHP inhibitors, again pointing to a VCC-independent mechanism of action and in agreement with the finding that these cells do not express L-type VCC [49]. Daily intraperitoneal administration of amlodipine (10 mg/kg) for 20 days into mice bearing A431 xenografts, retarded tumor growth and prolonged the survival of mice: at day 23 post tumor inoculation, tumor size was reduced by more than 55%. Furthermore, clinical trials for the use of amlodipine in the treatment of hypertension suggest that long-term treatment with these agents (at concentrations comparable to those used in the above studies) does not cause significant toxicities. But what is the mechanism of action of amlodipine? In A431 cells amlodipine has been shown to attenuate capacitive Ca^{2+} entry via intracellular store-depletion activated calcium channels, I_{CRAC} [48]. Recently, the same group provided evidence that these cells express canonical transient receptor potential 1 (TRPC1) and TRPC5 which might mediate calcium influx and found that amlodipine arrested cell cycle progression at the G1 phase by inducing a cyclin-dependent kinase inhibitor [50]. Finally, amlodipine was found to inhibit tyrosine phosphorylation of EGFR both *in vitro* and *in vivo*, possibly by modulating cholesterol-rich, caveolin-1-containing membrane microdomains and thus impacting on EGFR-related mitogenic signaling [51]. At the same time, the effect of this drug on rafts might also have an impact on the SOC channels (especially TRPC) mediating I_{CRAC} (e.g. [52], which in turn seem to be essential components of a Ca^{2+}-dependent signal amplification required for EGF-dependent cell proliferation [53]. To our knowledge a systematic study unequivocally linking only the CCA drugs that inhibit cell proliferation to the above events has not been performed up to now. This would be important in order to generalize the observed effects and to confirm amlodipine as promising, lead compound for the development of derivatives as anti-tumor agents acting on mitogenic signaling.

Although in the above examples the CCA drugs presumably reduce tumor growth independently of their direct inhibitory effect on L-type calcium channels, targeting of the T-type VCCs by the selective inhibitor KYS05047 (a 3,4-dihydroquinazoline derivative; IC_{50} for T-type channels: ~0.2 μM) does so thanks to its ability to decrease intracellular calcium concentration [54,55]. Growth of human lung adenocarcinoma A549 cells was time and dose-dependently inhibited by KYS05047, 6–8 μM being the optimal, non-cytotoxic concentration. The authors provided *in vitro* evidence that these drug concentrations induced a reduction of the cyclin-dependent protein kinases cdk2 and cdk4, a reduction of the phosphorylation of the tumor suppressor protein RB (retinoblastoma) and of Akt and mTOR and as a consequence, an arrest of the cell cycle in G1 phase. The authors proposed that these events took place as a results of the reduction of cytosolic Ca^{2+} and of the activation of Ca^{2+}/calmodulin-dependent protein kinases (CaM-K), whose downstream effectors (e.g. Rb and the Akt pathway) play a role in the G1 to S transition [56]. Unfortunately, the specificity of the effect has not been investigated, e.g. by downregulation of the channel protein using siRNA, but oral administration of 10 mg/kg KYS05047 for 21 days in a BALB/cnu/nu mouse A549 xenograft model reduced tumor volume by approximately 50%. Whether this drug caused side effects and whether it prolonged animal survival has not been investigated. Another T-type calcium channel inhibitor, mibefradil, was also shown to impact *in vivo* on tumor growth in a glioblastoma model (C6 glioma). This compound, also known as Ro 40-5967, was approved by FDA for treating hypertension but it was then withdrawn by the producer (Roche) due to dangerous drug-drug interactions. It inhibits T-type channels with an IC_{50} of ~3 μM vs. ~18 μM for L-type channels [57]. The study involved administration of 30 mg/kg (intraperitoneally 3 times a day for 1 week) in combination with ionizing radiation [58]. The animals treated with mibefradil starting on postoperative day (POD) 15 followed by radiosurgery on POD 22, survived twice as much as the animals treated only with radiosurgery. In addition, mibefradil (45 mg/kg PO four times daily) in co-administration with temozolomide (an alkylating agent; 10 mg/kg/day IP) increased maximal survival from 20 days to 120 days in a D-54 MG xenograft model for glioblastoma multiformae [59]. A clinical trial is therefore underway to evaluate the effect of mibefradil in patients with progressive or recurrent glioblastoma following radiation therapy and the currently used chemotherapeutic temozolomide. As mentioned, CCAs have been proposed for testing in clinical trials as an adjuvant therapy for meningiomas [45,46]. Mibefradil, similarly to other VCC inhibitors, blocks cell cycle progression beyond the G1/S interphase, but also induces apoptosis by causing PM depolarization and by decreasing integrin expression and thus cell adhesion [60]. Interestingly, mibefradil and its derivative NNC 55-0396 were recently identified in a large-scale screening as down-regulators of mitochondrion-mediated hypoxia-inducible factor (HIF)-1α protein stability and angiogenesis inhibitors [61]. Ca^{2+} signaling has been shown to stimulate translation of HIF-1α during hypoxia [62]. The activity of this transcription factor is related to tumor cell survival, proliferation, and angiogenesis, but how exactly these drugs affect HIF-1α protein stability is still an open question. The finding that knockdown of T-type Ca^{2+} channel also suppressed hypoxia-induced HIF-1α protein stability specifically links this type of VCC to the effect of mibefradil and NNC 55-0396. The question arises whether any agent affecting intracellular Ca^{2+} homeostasis might affect HIF-1α stability. Calcium signaling has been shown to stimulate translation of HIF-alpha during hypoxia (e.g. [62]) and for example artemisinin and parthenolide, two SERCA inhibitors, induce phosphorylation of HIF-1α [63]. The L-type calcium channel blocker cilnidipine selectively suppressed HIF-1α activity in vascular cells [64] and expression of

Please cite this article as: L. Leanza, et al., Pharmacological targeting of ion channels for cancer therapy: In vivo evidences, Biochim. Biophys. Acta (2015), http://dx.doi.org/10.1016/j.bbamcr.2015.11.032

(HIF)-1/2α was significantly reduced in a neuroblastoma cell line expressing a dominant negative form of TRPM2 channel, the presence of which reduces calcium influx into these tumor cells in response to oxidative stress [65]. Using a mouse tumor xenograft model into which U87-MG human glioblastoma cells were injected, Kim and colleagues demonstrated that intraperitoneal administration of 10 or 20 mg/kg NNC 55-0396 was sufficient to reduce tumor volume by more than 60%, as well as angiogenesis, without inducing liver toxicity [61]. Finally, the case of simvastatin can be mentioned: this statin has been shown to reduce tumor growth in colitis-associated colon cancer (CAC) model *in vivo* by inducing apoptosis [66], and at the same time it has been recently suggested to inhibit calcium influx via L-type VCC [67]. However, simvastatin is likely to exert pleiotropic effect and the relevance of its action on L-type VCC *in vivo* has not been addressed up to now.

In summary, VCCs are potential oncological targets of demonstrated importance. The advantage of using drugs targeting VCCs is that most of these drugs have been approved by FDA for curing hypertension. The major shortcoming of this field is however that for most of the drugs the specificity of the effect via VCCs and the exact mechanism of action have not been fully demonstrated. As described above, some of the most promising drugs, like mibefradil, have multiple effects which impact tumor growth, therefore making these drugs good candidates for co-adjuvant therapies [68].

2.2. Transient receptor potential channels

Beside VCCs, TRP proteins are emerging as promising oncological targets [36,69]. TRP channels can be divided into subfamilies, namely TRPV (TRP vanilloid), TRPA (TRP ankyrin), TRPM (TRP melastatin), TRPC (TRP canonical) and TRPP (TRP polycystin). Mammalian TRP proteins form homo- or hetero tetrameric non-selective Ca^{2+}-permeable cation channels which can be stimulated by a variety of different factors, including change in temperature, mechanical stress, osmotic pressure, change in pO_2 and in pH, ROS, growth factors and cytokines. Therefore, they are expected to play a crucial role in the tumor-microenvironment cross-talk. TRPC channels are activated through pathways coupled to phospholipase C (PLC), and can support receptor-operated Ca^{2+} entry; TRPC1 and TRPC4 can also contribute to SOCE via relatively non-selective cation currents.

Several investigations found evidence for a role of TRPC channels in the regulation of hallmark cancer processes by using genetic modulation of their expression (e.g. [53]). Thus, knockdown of TRPC1 decreased tumor volume by 40% in a xenograft model using human grade IV glioma cell line D54MG [70]. However, a pharmacological agent that specifically targets a TRPC subtype became only recently available (e.g. [71,72]. A recent piece of work demonstrated that the sesquiterpene (−)–englerin A is a selective and potent activator of TRPC4 and 5 [73] and inhibits tumor cell growth by activating these ion channels, thereby inducing massive calcium influx and consequent cell death. Unfortunately, the concentrations at which englerin A activates a calcium influx (around 250 nM) are in the range in which englerin A was lethal within a few hours in rodents (132–544 nM) [74]. Interestingly, another natural compound, 20-O-β-D-glucopyranosyl-20(S)-protopanaxadiol (20-GPPD), a metabolite of ginseng saponin induced TRPC-mediated calcium influx into CT-26 colon cancer cells and AMPK kinase-dependent apoptosis *in vitro*. *In vivo*, daily injection of 20-GPPD (1 mg/kg) for 4 weeks reduced tumor weight by 75% [75]. However, which TRPC channel is targeted by this compound is unclear, as is the mechanism accounting for the selective effect of 20-GPPD on cancer cells.

Among TRPV channels, the highly calcium-selective channel TRPV6 (which allows however the passage of heavy metals zinc, manganese and cadmium as well [76]) has been found to be expressed in a variety of cancers including prostate and breast. Its expression correlates with cancer progression, suggesting that it drives cancer cell growth. TRPV6 indeed acts as oncogenic ion channels [77,78]. A few years ago, a synthesized derivative of TH-1177 was proven to be a specific inhibitor, capable of distinguishing between TRPV5 and TRPV6 and to block the proliferation of LNCaP human prostate cancer cells with and IC_{50} of 0.44 μM [79]. The same group has also achieved the synthesis of TRPV-inhibiting drugs starting from 2-Aminoethyl-diphenylborinate (2-APB), a known modulator of the IP3 receptor, of SERCA, of Orai and of TRP channels. One of the analogs is more efficient than 2-APB in blocking TRP channels, but it also blocks SERCA [80]. To our knowledge this study has not been followed up *in vivo* so far. Interestingly, two short peptides that derive from Soricidin, a novel paralytic peptide isolated from *Blarina brevicauda* were shown to bind TRPV6 in ovarian cancer cells with high affinity and can be exploited via conjugation with fluorescent dye for *in vivo* imaging of human ovarian tumors in a xenograft mouse model [81]. Whether these peptides show an anti-tumor activity *in vivo* is still to be tested. The prototypical vanilloid agonist capsaicin, the well-known ingredient of chili peppers, which activates both TRPV6 and TRPV1, was shown to induce apoptosis by its action on TRPV6 (as proven using siRNA) and downstream activation of calpains at 50 μM concentration in human small cell lung cancer cells (SCLC) *in vitro* while leaving unaffected normal human bronchial epithelial cells [82]. Importantly, *in vivo* dietary administration of capsaicin (50 mg capsaicin/kg food) almost completely blunted growth of DMS 53 human SCLC tumors xenografted in nude mice [82]. In T24 bladder cancer cells T24 200 μM Capsaicin caused significant TRPV1-dependent apoptosis by inducing ROS release and mitochondrial depolarization. *In vivo*, subcutaneous injection of 5 mg/kg capsaicin every 3 days for 4 weeks reduced the growth of T24 bladder cancer xenografts only slightly, by 15% [83]. Mitochondrial depolarization but not increased ROS release has been observed also in BON and QGP-1 NET pancreatic neuroendocrine tumor cells *in vitro* upon capsaicin treatment at high concentration [84]. In yet another study, the vanilloid receptor TRPV antagonist capsazepine (CPZ) proved to be more cytotoxic than capsaicin for some cell lines. ROS release by CPZ was related to apoptosis in oral squamous cell carcinoma cells (OSCC), but was found to be independent of TRPV1. Importantly, in three different OSCC xenograft models, intra-tumoral injection of max. 40 μg CPZ every other day for 18 days completely blunted tumor growth in two out of the three models used [85]. In addition, the authors also provided evidence that liver and kidney function had been preserved. Survival of immortalized normal oral keratinocytes was not affected. Mitochondrial $\Delta\psi$ loss and increased ROS release was associated with apoptosis in PC-3 prostate cancer cell line as well and subcutaneous injection of either capsaicin or capsazepine (5 mg/kg body weight) in nude mice significantly suppressed PC-3 tumor growth by inducing apoptosis of tumor cells [86]. Thus, capsaicinoids seem to have a very promising *in vivo* effect in various tumor models and most probably affect cell apoptosis via TRPV1 and/or TRPV6, in particular by inducing oxidative stress by still unknown mechanism. Most cancer cells display an increased metabolic activity and are therefore under oxidative stress. Increase in ROS by an external agent may disrupt this delicate balance between ROS levels and the anti-oxidant capabilities of the cancer cells thereby triggering ROS-induced apoptosis, without inducing the same impact on the healthy tissues [87].

Finally, it is of note that some cannabinoid compounds, in particular cannabidiol (CBD), stimulate TRPV1 while the non-psychotropic cannabigerol (CBG) is an antagonist of TRPM8 [88]. CBD displayed and anti-invasive action which depended on the effect of CBD cannabinoid receptor and TRPV1. *In vivo*, in a nude mice injected with human lung carcinoma A549 cells, intraperitoneal application of 5 mg/kg body weight CBD every 3 days for 28 days almost completely abolished the appearance of metastatic nodules [89,90]. CBD was employed also in a study with prostate carcinoma LNCaP cells, where the pro-apoptotic effect of CBD was interpreted as partly due to TRPM8 antagonism and was accompanied by ROS release and p53 activation. In this case, *in vivo*, application of 100 mg/kg CBD i.p. daily plus 5 mg/kg docetaxel, i.v. once a week reduced tumor volume by approximately 60% when compared to untreated animals [91]. Furthermore, CBG and other TRPM8 antagonists

Please cite this article as: L. Leanza, et al., Pharmacological targeting of ion channels for cancer therapy: In vivo evidences, Biochim. Biophys. Acta (2015), http://dx.doi.org/10.1016/j.bbamcr.2015.11.032

hampered colon cancer progression in xenograft tumors as well as chemically induced colon carcinogenesis [92].

Altogether, these results point to the relevance of TRP channel modulators for cancer treatment, especially in light of the fact that both capsaicinoids and cannabinoids are natural substances. However, given the pleiotropic effects of these drugs, a definitive proof demonstrating the requirement for channel activation or inhibition in relation to the anti-tumoral effects should ideally be provided for all cases.

2.3. Orai and STIM1

As mentioned above, SOCE, mediated by Orai and STIM1 proteins has been linked to the proliferative potential of various cell types [93–95] and to the resistance to apoptosis of cancer cells [96]. Ca^{2+} signaling mediated by TRP channels and by Orai/STIM1 directly or indirectly influences cancer and stroma cell migration [11]. In patients with esophageal squamous cell carcinoma (ESCC), high expression of Orai1 was associated with poor overall as well as recurrence-free survival [97]. Orai1 sustained cell proliferation, migration and invasion of KYSE-150 cells, an epithelial line derived from human ESCC tumor. In a mouse model, treatment (10 μg/g body weight, three times weekly i.p.) for four weeks with SKF96365, an inhibitor of SOCE (e.g. [98]), decreased tumor volume by approximately 50%. Although SKF96365, a phenylethylimidazole, is not very specific and inhibits TRPC and VCCs as well [71], an almost complete tumor-reducing effect was observed *in vivo* by silencing Orai1, indicating that indeed this SOCE component is fundamental for the development of ESCC [97]. In accordance with the fundamental role of SOCE in the above example, STIM1 expression was also found to be elevated in cervical cancer patient tissues and correlated with tumor size. Overexpression or knockdown of STIM1 in cervical cancer SiHa cells exacerbated or blunted tumor growth in SCID mice, respectively. I.p. injection of these mice bearing tumor xenograft of SiHa cells with SKF96365 (2.5 mg/kg), or 2-APB (2-aminoethoxydiphenyl borate; 50 μg/kg) from the sixth day post-inoculation for 9 days completely abolished tumor growth [99]. 2-APB not only is used as a modifier of SOCE but also acts on IP3Rs and TRPV and TRPC channels [100,101]. Chen and coworkers [99] however proved by genetic means that STIM1 overexpression enhanced invasive migration and VEGF secretion *in vitro* and, coherently, angiogenesis and local invasion. Thus, even though the pharmacological agents used are not specific, it seems clear that they targeted the STIM1/Orai1 complex. Hopefully, thanks to the resolved crystal structure of Orai1 [102], structure-based drug design strategy will provide more specific inhibitors [103]. However, since STIM and ORAi proteins are ubiquitously expressed, toxicity to normal cells should also be considered when SOCE inhibitors are applied systemically. In the above mentioned papers the question of toxicity has not been addressed in depth.

2.4. P2X receptors

The P2 family of receptors is comprised of P2Y metabotropic and P2X ionotropic receptors, the latter behaving as nonselective cation channels permeable to calcium, sodium, and potassium ions. ATP-mediated intercellular signaling is implicated in a wide range of physiological processes, including neurotransmission, neuromodulation, chemoattraction or chemotaxis, and pain. One of the first investigations linking P2X receptors to cancer reported that statins - shown to reduce the risk of pancreatic cancer by 80% in humans according to a case control study with half a million veterans [104] and to reduce pancreatic tumor growth in mouse models (see e.g. [105]) - probably act via P2X7 receptors [106]. In this *in vitro* work, the authors showed, using genetic tools that the decrease in pAkt level, the inhibition of cell proliferation and apoptosis induction by statins, in particular atorvastatin, was dependent on P2X7 expression. Following this lead, *in vivo* experiments in different tumor models have been conducted to support a role of P2X7 receptors in cancer progression. Tumor tissues contain much higher concentrations of extracellular ATP (hundreds μM range) than healthy tissues, [107,108]. ATP activates P2X receptors, among which P2X7 has been found to be highly overexpressed in several cancer types. In a zebrafish model using the highly metastatic cancer line MDA-MB-435, 10 μM A-438,079, a P2X7 antagonist halved the % of zebrafish with metastasis [109]. The same group later reported that emodin (1,3,8-trihydroxy-6-methylanthraquinone), an anthraquinone derivative *of Rheum officinale* with known anticancer properties, specifically inhibited P2X7-mediated currents with an IC_{50} of 3 μM [110]. In the same zebrafish model, *in vivo* invasiveness of the P2X7R-positive MDA-MB-435 cells was reduced by 50% using 10 μM emodin. Two other studies independently demonstrated that oxidized ATP (0.5 mg/mouse 3 times i.p.), a selective antagonist of P2X7, significantly reduced tumor volume in a B16 melanoma-bearing mice model [111] as well as in a colon cancer CT26 model (reduction by 90% with 3 intratumoral injections of oxATP (600 mmol/L) [112]. The same authors also showed that intratumoral injection of 300 nmol/L of the selective P2X7 inhibitor AZ10606120 caused a strong inhibition of melanoma B16 tumor growth as well. Interestingly, ATP was used also in a previous study against A375 melanoma cells and similarly to oxATP, an >50% reduction of tumor volume could be observed [113].

3. Potassium channels

As illustrated by the above examples, pharmacological targeting of different calcium-permeable channels may have a dramatic impact on tumor growth *in vivo*. Given the central role of calcium signaling in contributing basically to all aspects of the cancer hallmarks, these successful cases are not surprising. Beside calcium channels however, potassium sodium and chloride channels can also be successfully targeted and in some cases this strategy has already led to clinical trials in humans. Indeed, these channels are equally important for tumor development and progression as we know by now from numerous *in vitro* and some *in vivo* experiments. The first potassium channel with suggested oncogenic potential was a member of the voltage-gated Kv family, Kv11.1 (hERG) [114], shown to control the membrane resting-potential of neuroblastoma cells which was related to their proliferative abilities as described by Arcangeli and co-workers [115]. The first ion channel with proven oncogenic potential was Kv10.1 (EAG) [14], which can be detected in approximately 70% of human tumor biopsies of diverse origin [22]. In this seminal work, Stuhmer and colleagues proved that expression of both EAG and of the voltage-dependent Kv1.4 in non-tumoral Chinese hamster ovary cells conferred a transformed phenotype and *in vivo* both channel-transfected lines favored tumor progression when injected into the flank of immune-depressed mice. The size of the tumor obtained using the EAG-expressing line was twice as much as that observed with Kv1.4, indicating the expression of EAG (expressed only in the brain in healthy subjects but in different cancer cell types in cancer patients) gives rise to a more aggressive behavior. Soon after the discovery that this specific channel is so important for proliferation and tumor progression, several independent studies suggested that this is a general feature of potassium channels. Indeed, K^+ channels regulate cell cycle by affecting trans-membrane potential across the PM [22] since they set the resting membrane potential in both excitable and non-excitable cells: in general, the membrane potential varies during cell cycle (with hyperpolarized value and high permeability for K^+ at the G1 to S transition) [116] and cell types with a very hyperpolarized resting potential do not readily undergo mitotic division. Membrane potential in turn impacts on calcium entry and calcium signaling (for review see e.g. [23]). Furthermore, some K^+ channels proved to play an important role for angiogenesis: for example Eag1 was shown to increase HIF1α activity and angiogenesis [117]. Changes in channel expression, due to genomic, transcriptional, post-translational or epigenetic alterations, often occur in cancer cells (for recent review see e.g. [118]) and are correlated with increased proliferative potential and/or altered apoptosis resistance (for review see

Please cite this article as: L. Leanza, et al., Pharmacological targeting of ion channels for cancer therapy: In vivo evidences, Biochim. Biophys. Acta (2015), http://dx.doi.org/10.1016/j.bbamcr.2015.11.032

e.g. [6]. A variety of K^+ channels, such as voltage-gated K^+ channels (Kv), calcium-activated K^+ channels (K_{Ca}) and ATP-sensitive K^+ channels (K_{ATP}) show altered expression in tumor tissues (e.g. [118,119]).

Among the potassium channels, much attention has been dedicated to the pharmacological targeting of Kv10.1 (EAG), Kv11.1 (hERG) and the calcium-dependent potassium channel $K_{Ca}3.1$ for cancer treatment. A monoclonal antibody specifically produced against Kv10.1 inhibited the function of the channel, the colony forming ability of several different types of cancer lines and the *in vivo* tumor growth of the highly metastatic MDA-MB-435S cancer cells [120]. Furthermore, the open channel blocker astemizole (50 mg/kg, administered orally, daily), which does not cross the blood brain barrier and therefore does not affect neuronal EAG activity and is already used in the clinic, inhibited MDA-MB435S xenograft tumor growth by approximately 30% and growth of EAG-expressing CHO by 50% [117]. *In vivo* application of a combined therapy, using oral astemizole (50 mg/kg/day) and intraperitoneal injections of the active vitamin D calcitriol (0.03 μg/g body weight twice a week for 3 weeks), in mice xenografted with the human breast cancer cell line T-47D or with a primary breast cancer-derived cell culture (MBCDF), resulted in 85% inhibition of tumor volume. This treatment was more efficient than application of either drug alone [121].

Similarly to Kv10.1, Kv11.1 (hERG) is frequently overexpressed in cancer cells (e.g. [122]) and it is implicated in tumor progression and migration via regulation of HIF1α stability and of integrin function/adhesion-dependent signaling [123]. *In vivo* experiments using hERG1 blockers demonstrate the importance of hERG function in various systems: in a recent study, colorectal cancer cells (HCT116) were injected into nude mice that were then treated with specific Kv11.1 inhibitors WAY123,398 and E4031 (both substances at 20 mg/kg, i.p. for two weeks daily). An approximately 50% reduction of the tumor volume has been detected, but most importantly these drugs were very effective also using the same line that lacked p53 and inhibited both angiogenesis and metastasis [124]. Similar results were obtained in azoxymethane-induced colorectal carcinoma [125] and in a gastric cancer model [126]: in the former case i.p. injections of E-4031 for 3 months caused an 80% reduction in the number of colonic polyps, while in the latter study combined application of 20 mg/kg E-4301 and of the anti-VEGF-A antibody bevacizumab almost completely abolished tumor growth. In addition, block of hERG in immune-deficient mice decreased the bone marrow engraftment and peripheral blood invasion of myeloid/lymphoblastic leukemia cells and could overcome mesenchymal stroma cell (MSC)-induced chemoresistance *in vivo* in leukemia mouse models (E4031 administered daily at 20 mg/kg for max. 4 weeks) [127]. However, most of the drugs that modulate Kv11.1 function are associated with cardiotoxicity, either the long QT syndrome or fatal arrhythmias which can be triggered by class III antiarrhythmic drugs such as E4031 and Way 123,398. Given that tumor cells seem to preferentially express a different splice variant of Kv11.1, i.e. hERG1B (e.g. [128]) with respect to the cardiac tissue, drugs acting exclusively on the tumor-associated variant might be of great therapeutic utility. In this respect, it is interesting to note, that ZC88, a novel 4-amino piperidine analog inhibited the tumor growth in nude mice engrafted with SH-SY5Y neuroblastoma cells by 60% at a dosage (50 mg/kg, i.p. application every 4 d for 16 days) that only slightly influenced the cardiac QT interval. A previous study identified ZC88 as blocker of the N-type calcium channel (IC_{50} value of 0.45 μM), although the ZC88-mediated anti-proliferative effect was not correlated with its effect on the calcium channel activity [129]. Recently, another, very promising molecule which is specific for the hERG1B variant has been identified: CD-160,130, a novel pyrimido-indole compound block this isoform with an IC_{50} value (1.8 μM) that is ten-fold less with respect to that obtained for hERG1A. This drug caused apoptosis in vitro and in vivo (10 mg/kg) reduced leukemia burden by 90% in a preclinical SCID leukemia model using HL60 cells. As expected, this compound did not induce any cardiotoxicity and enhanced long-term survival [130].

Thus, numerous *in vivo* models illustrate very convincingly that both EAG and hERG are especially promising oncological targets. *In vivo* studies targeting other K^+ channels also point to an important role of K^+ channels in general to the tumor progression. As to other Kv channels, recent *in vitro* data pointed out that selective blockers of voltage-gated K^+ (Kv) channels or ATP-sensitive K^+ (KATP) channels significantly inhibited the proliferation of U87-MG human glioma cells, blocked the cell cycle at the G0/G1 phase and induced apoptosis. In the U87-MG xenograft model in nude mice, suspensions of the cells treated with 4-AP (5 mmol/l), TEA (20 mmol/l) or glibenclamide (200 μmol/l) were injected. The growth of the K^+ channel inhibitor-treated cells was reduced by 50%, but the specificity of the effect has not been demonstrated nor the specific Kv channel responsible was identified [131].

In vivo evidence for the involvement of Kv1.3 in tumor growth has been obtained in an A549 human lung adenocarcinoma model: margatoxin (Mgtx), a selective blocker of Kv1.3 (IC_{50} 2 nM) or short hairpin RNA (shRNA) against Kv1.3, significantly blocked cell proliferation and intra-tumoral injection of 1 nM Mgtx for seven days reduced tumor volume *in vivo* by 75% [132]. Inhibition of Kv1.3 significantly increased expression level of $p21^{Waf1/Cip1}$ and decreased the expression level of Cdk4 and cyclin D3, altogether inhibiting G1 to S transition. The *in vivo* anti-proliferative effect of Mgtx was confirmed also in an independent work, in an orthotopic melanoma model using B16F10 cells [133]. Furthermore, this study revealed for the first time, that membrane-permeant Kv1.3 inhibitors such as Psora-4, PAP-1 and clofazimine, were able to induce apoptosis of different cancer cell lines, via their action on the mitochondrial counterpart (mtKv1.3) of the plasma membrane-located Kv1.3 [134]. Importantly, this effect was observed exclusively with the membrane-permeant inhibitors and genetic deficiency or siRNA-mediated downregulation of Kv1.3 abrogated the effects of these drugs, which also killed cells in the absence of Bax and Bak, in agreement with the following, experiment-based model: block of mtKv1.3 inhibits depolarizing influx into the mitochondrial matrix with consequent hyperpolarization. This alteration leads to significant ROS production by mitochondria which in turn opens the permeability transition pore (PTP), induce cytochrome c release independently of the pro-apoptotic Bax and Bak molecules and finally triggers apoptosis [21,135]. Since hyperpolarization also provides an increased driving force for the mitochondrial calcium uptake system, the calcium uniplex (MCU) [136,137] and a matrix calcium overload is known to trigger opening of the PTP, we checked whether knockdown of the channel forming MCU protein impacts signaling in the above system. MCU itself might become a good oncological target, similarly to other intracellular channels and to PTP [20,21], once specific activators will be identified. As Fig. 2 illustrates, the mtKv1.3 inhibitors exerted the apoptosis-inducing effect to the same extent, suggesting that an interplay between mtKv1.3 and MCU does not play a role in our experimental model. *In vivo*, intraperitoneal injection of clofazimine in an orthotopic melanoma B16F10 mouse model reduced tumor size by 90%, without causing visible side-effects as assessed by histology [133]. Expression of Kv1.3 in different cancer lines correlated with the sensitivity of the cells toward the above inhibitors [138]. In accordance, primary B cells obtained from patients suffering of chronic lymphocytic leukemia that expressed high level of Kv1.3 also in their mitochondria, readily underwent apoptosis upon treatment with the above Kv1.3 inhibitors while T cells from the same patients were resistant [139]. Co-culturing with MSC did not reduce the ability of these drugs to kill the pathologic B cells [140]. Using primary B cells from patients or healthy subjects, it was possible to provide evidence that the selective cancer cell-killing action of mtKv1.3 inhibitors can be ascribed to a synergistic effect between altered redox state of cancer cells and the ability of these drugs to induce drastic ROS increase, thereby forcing the cell to cross the critical ROS threshold (see above). Because clofazimine is already used clinically to treat some autoimmune diseases and leprosy and shows an excellent safety profile [141], targeting mtKv1.3 is a feasible cancer therapy for at least some cancer types. In general, targeting of

Please cite this article as: L. Leanza, et al., Pharmacological targeting of ion channels for cancer therapy: In vivo evidences, Biochim. Biophys. Acta (2015), http://dx.doi.org/10.1016/j.bbamcr.2015.11.032

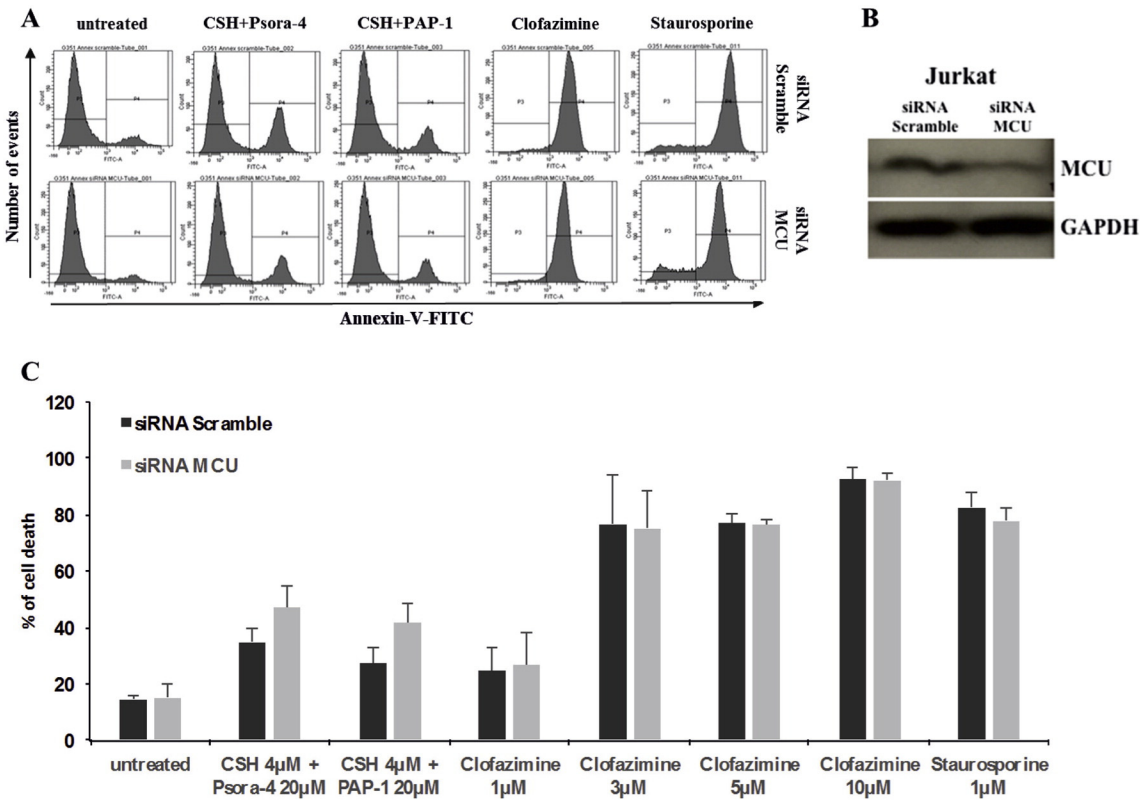

Fig. 2. Membrane-permeant inhibitors of the potassium channel Kv1.3 induce apoptosis independently of MCU (mitochondrial calcium uniporter) activity. A) Cell death of Jurkat lymphocytes expressing Kv1.3 either expressing control scramble siRNA or siRNA against MCU, following 24 h-incubation with the indicated inhibitors. Concentrations were applied as indicated in C). B) Western blot is shown to evaluate protein expression following transfection with siRNA (100 μg/lane of total extract). Kv1.3 migrates at 65 kDa. Anti-GAPDH was used as loading control. C) Cell death was analyzed as in A); values reported in the bar-graph indicate the mean percentage ± SD of dead cells calculated taking into account all annexin positive cells ($n \geq 3$). Differences between control and MCU-silenced cells are not statistically significant.

mitochondrial channels represents and interesting strategy since alteration of mitochondrial bioenergetic efficiency and function which may be achieved by changing ion channel function [142] can have a dramatic consequence on cell fate (see e.g. [21,143–145].

In addition to Kv potassium channels, calcium-dependent potassium channels and the two pore TASK-3 channel have been identified as oncological targets e.g. [146,147], but *in vivo* evidence by specific pharmacological targeting of TASK is still missing to our knowledge. As to $K_{Ca}3.1$, an important role for this channel in natural killer lymphocytes (NK), known to participate in the killing of cancerous cells. TRAM-34 and NS6180, two specific inhibitors of $K_{Ca}3.1$ increased proliferation of the NK cells as well as their ability to reduce *in vivo* tumor growth of the leukemic K562 cells [148]. Block of PM-located $K_{Ca}2.3$ (SK channel) has an impact on the migration of tumor cells: the edelfosine-like alkyl-lipid inhibitor named Ohmline ((1-O-hexadecyl- 2-O-methyl-sn-glycero-3-lactose) was shown to block SK channel with and IC_{50} of 300 nM [149] and was able to prevent bone metastasis of the highly metastatic MDA-MB-435 cells [150]. Intravenous application of 15 mg/kg Ohmline 3 times a week for 15 weeks reduced by 50% lung metastasis and completely blocked bone metastasis without impacting on the primary tumor volume. Interestingly, the authors provided evidence that Ohmline acted as a disrupting agent for lipid raft localization of the SK3–Orai1 complex, this way the SK3–Orai1 complex moved away from lipid rafts, and SK3-dependent Ca^{2+} entry, migration, and bone metastases were impaired.

In this respect it is interesting to note that several studies demonstrated that sphingolipids are involved in the regulation of SOCs [151–153]. These studies focused in particular on ceramide and sphingosine. Cellular ceramide is either *de novo* synthesized or released from sphingomyelin by the activity of neutral or acid sphingomyelinases. Ceramide is then converted by acid or neutral ceramidase to sphingosine, which can be phosphorylated to sphingosine 1-phosphate by the activity of sphingosine kinase 1 and 2 [154]. Ceramide molecules dramatically alter the biophysical properties of cell membranes, since they spontaneously associate with each other to form small, relatively rigid, gel-like ceramide-enriched membrane domains. These small domains spontaneously fuse to highly hydrophobic, tightly packed, and gel-like large ceramide-enriched membrane domains, also termed platforms, that serve the organization of membranes and proteins within membranes [155–157]. Ceramide molecules also exclude cholesterol from membrane domains further promoting the unique properties of ceramide-enriched membrane domains. Ceramide-enriched membrane platforms serve to bind, trap and reorganize receptors, ion channels and intracellular signaling molecules and, thus, facilitate signal transduction. Consistent with this notion are the results of studies showing that receptors such as CD95 [156], CD40 [157], DR5 [158], and CFTR [159], or signaling molecules such as NADPH-oxidase [160], caspase 8 [161], and Kv1.3 [162], are concentrated and clustered within ceramide-enriched membrane domains, a process that is crucial for signal transduction via these molecules.

This change of membrane properties might be also the mechanism how ceramide acts on ion channel such as SOCs. Thus, it was shown that overexpression of the acid sphingomyelinase releasing ceramide from sphingomyelin or the addition of exogenous ceramide blocks the activity of SOCs. Moreover, receptors such as CD95 that release ceramide by activation of the acid sphingomyelinase also blocked SOCs via this pathway as evidenced in experiments using acid sphingomyelinase-deficient cells that failed to inhibit SOCs after CD95 ligation [152]. However, ceramide can be converted to sphingosine that also inhibits SOCs and triggers an increase of the membrane capacitance. Similar to CD95, the p75 Nerve growth factor receptor that activates the acid sphingomyelinase/ceramide also inhibited SOCs [151]. The cellular effectors of sphingosine and the mechanisms how this lipid acts are

Please cite this article as: L. Leanza, et al., Pharmacological targeting of ion channels for cancer therapy: In vivo evidences, Biochim. Biophys. Acta (2015), http://dx.doi.org/10.1016/j.bbamcr.2015.11.032

presently unknown. It might be possible that both lipids alter membrane biophysics that result in inhibition of SOCs.

Consistent with the trapping model of ceramide functions described above, ceramide was shown to also recruit TRPC6 channels to caveolae [153]. However, in contrast to the inhibition of store-operated calcium channels by ceramide, TRPC6 channels in endothelial cells were not inhibited by ceramide and Ca^{2+}-influx even increased. This suggests that the membrane composition, in particular an increase of ceramide in membranes may have very different effects on different ion channels depending on the interaction of the particular ion channel with the membrane environment. Ceramide and sphingosine are very hydrophobic molecules and it seems highly unlikely that these lipids leave the membrane to directly interact with the acqueous pore of an ion channel. Ceramide has been shown to form small ceramide enriched-membrane domains that spontaneously fuse to large ceramide-enriched membrane platforms [156]. These domains and platforms were shown to trap receptor and signaling molecules [163–165] and it might be possible that these domains cluster Ca^{2+} channels. These domains differ from other parts of the plasma membrane and it is very likely that the rigidity and the hydrophobicity of ceramide-enriched membrane domains is higher than that of other domains. Further, the transmembrane diameter might be altered in these domains compared to other parts of the membrane. The trapping of channels in such a domain may result in a conformational change of the protein to provide an energetically more stable status. This conformational change then may regulate the channels. Alternatively, it might be possible that ceramide-enriched membrane domains cluster signaling molecules that are integrated into the membrane via lipid anchors, for instance Src-like tyrosine kinase [166]. Clustering of such kinases may result in a transactivation of previously almost inactive kinases that then directly or indirectly phosphorylate intracellular residues in ion channels and thereby regulate these channels. This mechanisms was observed for Kv1.3 channels, although these studies employed short chain ceramides [166] and studies with physiologically more-relevant long chain ceramides are not available at present to our knowledge.

4. Sodium channels

The expression of voltage-gated Na+ channels (VGSCs), especially of $Na_v1.5$, $Na_v1.6$ and $Na_v1.7$ and of their splicing variants was found to be increased in many cancer types, including breast, prostate, lung (both small-cell, SCLC, and non-small-cell, NSCLC), cervical cancer, leukemia (for recent review see [167]). In breast cancer, the neonatal isoform of $Na_v1.5$ ($nNa_v1.5$) would allow greater Na^+ entry into the cell, compared with the adult splice variant, with consequences of calcium homeostasis and of the regulation of intra- and extracellular pH [167]. In breast, prostate and NSCLC tumor cells, VGSC activity was shown to increase invasiveness by stimulating cysteine cathepsin activity [168]. Several independent preclinical studies demonstrated that pharmacological targeting of VGSC inhibits breast tumor growth and metastasis formation. α-Hydroxy-α-phenylamides, a new class of small molecules have potent inhibitory effect on voltage-gated sodium channels. Intraperitoneal injection of 10 mg/kg (every day for 24 days) of newly synthesized enantiomers of 3-chlorophenyl-α-hydroxyamide into mice bearing prostate cancer line PC3 xenografts resulted in a 60% decrease in tumor volume [169]. Importantly, the inhibitory effect on hERG was relatively small, up to 16% at the lowest dose used. In another study, administration of the VGSC inhibitor RS100642 (intravenously 0.25 mg/kg for 4 weeks) to mice developing 7,12-dimethylbenz(a)anthracene (DMBA)-induced breast cancer increased the survival of the animals by 50 days [170]. In a prostate cancer model using Mat-LyLu cells, injection of the general VGSC blocker tetrodotoxin at 200 nM concentration decreased metastasis and prolonged survival [171]. Tumor growth of orthotopic xenografts using the breast cancer line MDA-MB-231 expressing $Na_v1.5$ could be reduced by 30% applying 60 mg/kg (daily for four weeks) phenytoin, without affecting animal weight. Phenytoin reduced cancer cell proliferation *in vivo* and metastasis to the liver, lungs and spleen [172]. The important aspect of this study is that it identifies a drug that is already used at similar doses in the clinic to treat epilepsy which is also able to reduce breast cancer growth, although only partially. Another clinically used drug with metastasis-inhibitory effect of breast cancer cells is ranolazine: when injected into mice bearing MDA-MB-231 xenograft (50 mg/kg/day for 8 weeks), it significantly reduced lung colonization by these $Na_v1.5$-expressing human breast cancer cells [173]. Importantly, both the tumor volume, as assessed by bioluminescent imaging, and the number of lung metastasis were reduced to a similar extent to what has been obtained using the same cell line in which $Na_v1.5$ expression was abolished. Ranolazine is already used in the clinic as antianginal agent with antiarrhythmic properties [174,175].

5. Anionic channels

A strategy involving anion channels that was recently applied with success is targeting the ClC-3 channels, shown to be implicated in human glioma spread [176]. Chlorotoxin, (ChlTx) purified from the venom of the scorpion *Leiurus quinquestriatus* binds to matrix metalloproteinase-2 (MMP-2), a key factor involved in the process of tumor metastasis [177] and is also able to inhibit a voltage gated chloride channel that is specifically expressed on human astrocytoma and glioma cells [178]. This chloride channel was then identified as ClC-3, a type of Cl^-/H^+ exchanger mainly expressed in endosomal/lysosomal compartments (>95%). ChlTx has been reported to inhibit the migration and invasion of glioma cells [179,180]. The facts that these ClC-3 channels are highly expressed in glioblastoma and ChlTx binds them as well as the observation that ChlTx preferentially binds to a variety of human malignancies, but shows little or no binding to normal human tissues that has allowed to exploit Chltx as a diagnostic agent or as a vehicle for drug delivery [181]. Indeed, a synthetic version of ChlTx, covalently linked to iodine 131 (^{131}I-TM-601) was used in Phase I clinical in patients with recurrent glioma [182]. TM601 has been also shown to reduce angiogenesis *in vivo* [183]. Furthermore, a liposome system containing doxorubicin and modified with chlorotoxin inhibited the growth of metastatic tumor by 85% and prevented the incidence of lung metastasis in mice bearing 4T1 tumors, displaying only low systemic toxicity [184].

ANO1/TMEM16A, initially identified from airway epithelial cells, is a member of Ca^{2+}-activated Cl^- channels (CaCCs) that function to regulate epithelial secretion and cell volume for maintenance of ion and tissue homeostasis. ANO1/TMEM16A has recently been shown to be highly expressed in several epithelium originated carcinomas, gastrointestinal stromal tumor, ESCC and pancreatic cancer. Knockdown of ANO1 breast cancer cell lines and other cancers inhibited proliferation, induced apoptosis, and reduced tumor growth in established cancer xenografts [185–187]. Compared with primary tumors, ANO1 expression decreases in metastatic lymph nodes of patients with squamous cell carcinoma of the head and neck. Stable reduction of ANO1 expression enhanced cell motility and increased metastases while decreasing tumor proliferation in an orthotopic mouse model [188]. The calcium-activated chloride channel inhibitor (CaCCinh)-A01, a low molecular weight inhibitor of ANO1 activity [189] and the recently identified ANO1 inhibitors idebenone (short-chain analog of CoQ10), miconazole and plumbagin [190] will hopefully be soon exploited for *in vivo* studies.

6. Conclusion and future direction

As illustrated in the above examples and in the summarizing Table 1, this relatively new field has already importantly contributed to the identification of possible therapeutic agents for several different cancer types demonstrating the significant efficacy of ion-channel targeting drugs mostly in preclinical models. Now, knowing the set of the channels that contribute to the tumor development in a given tissue, a

Please cite this article as: L. Leanza, et al., Pharmacological targeting of ion channels for cancer therapy: In vivo evidences, Biochim. Biophys. Acta (2015), http://dx.doi.org/10.1016/j.bbamcr.2015.11.032

Table 1
Drugs targeting ion channels *in vivo* in cancer models. Please note that proof of specificity refers to evidence obtained by the lack of the observed pharmacological effect either *in vitro* or *in vivo* following knockdown of the ion channel expression. Therefore we do not considered as proof of specificity for this table the well-demonstrated specific effect of the different drugs/molecules on channel proteins (e.g. the actions of TTX as well as that of anti-Kv10.1 antibodies are specific on the respective target proteins). For side-effects "n.d." stays for not determined, while "NO" refers to studies where the occurrence of side-effects was investigated at organ/tissue level or to the absence of apparent toxic effect. Please see for further details in the text.

Target channel	Channel modulator	Proof of specificity	Type of cancer; % of reduction of tumor size	Side effects	References
Voltage-gated calcium channels					
Cav channels	Amlodipine, diltiazem, verapamil	NO	Breast cancer; 83.5 ± 20.1% (mean ± SE), 46.5 ± 6.6% and 68.2 ± 9.7%, respectively	NO; n.d.	[40,47]
	Amlodipine	NO	Epidermoid carcinoma; 55%	n.d.	[48]
T-type Cav channels	KYS05047	NO	Lung adenocarcinoma; 50%	n.d.	[54]
	Mibefradil	NO	Glioblastoma; Reduction followed by radiosurgery	n.d.	[58,59]
	NNC 55-0396	NO	Glioblastoma; 60%	n.d.	[61]
L-type Cav channels	Simvastatin	NO	Colon cancer; 57%	n.d.	[66].
TRP channels					
TRPC	20-GPPD	NO	Colon cancer; 75%	n.d.	[75]
	SKF96365	NO	Esophageal squamous cell carcinoma (ESCC); 50%	n.d.	[71]
	SKF96365	NO	Cervical cancer;	n.d.	[99]
TRPV	Capsazepine (CPZ)	NO	Oral squamous cell carcinoma cells (OSCC) 98,4%	NO	[85]
TRPV1	Capsaicin	NO	Bladder; 15%	NO	[83]
	Cannabidiol	NO	Lung carcinoma; 83% (metastatic lesions)	n.d.	[89,90]
TRPV6-TRPV1	Capsaicin	siRNA *vs* TRPV6	Small cell lung cancer (SCLC); 91%	n.d.	[82]
TRPM8	Cannabidiol	NO	Prostate carcinoma; 34%	n.d.	[91]
P2X7 receptors					
P2X7	Oxidized ATP	NO	Melanoma; 69%	n.d.	[111]
	Oxidized ATP	NO	Colon cancer; 90%	n.d.	[112]
	AZ10606120	NO	Melanoma; 58%	n.d.	[112]
	ATP	NO	Melanoma; 50%	n.d.	[113]
Potassium channels					
Kv10.1 (EAG)	mAb56 (anti-EAG antibody)	NO	Breast cancer; 50%	n.d.	[120]
	Astemizole	siRNA *vs* EAG1	Breast cancer; 30%	n.d.	[117]
	Astemizole + vitamin D calcitriol	NO	Breast cancer; 85%	NO	[121]
Kv11.1 (hERG)	WAY123,398 and E4031	siRNA *vs* hERG1	Colorectal cancer; 50%	n.d.	[124]
	E4031	NO	Gastric cancer; 80%	n.d.	[126]
Kv11.1 (hERG1B)	CD-160,130	NO	Leukemia; 90%	NO	[130]
Kv channels and KATP channels	4-AP, TEA and glibenclamide	NO	Glioma; 50%	NO	[131]
Kv1.3	Margatoxin	shRNA *vs* Kv1.3	Lung adenocarcinoma; 75%	n.d.; NO	[132]
			Melanoma; 30%		[133]
mtKv1.3	Clofazimine	siRNA *vs* Kv1.3	Melanoma; 90%	NO	[133]
KCa2.3	Ohmline	NO	Metastatic breast cancer; 50% reduction of lung metastasis, total block of bone metastasis	n.d.	[150]
Sodium channels					
Nav channels	3-Chlorophenyl-α-hydroxyamide	NO	Prostate cancer; 60%	n.d.	[169]
	RS100642	NO	Breast cancer; Survival increased by 50 days	n.d.	[170]
	Tetrodotoxin	NO	Prostate cancer; 45% reduction of metastasis	n.d.	[171]
Nav1.5	Phenytoin		Breast cancer; 36%	NO	[172]
	Ranolazine	shRNA *vs* Nav1.5	Metastatic breast cancer;	NO	[173]

Please cite this article as: L. Leanza, et al., Pharmacological targeting of ion channels for cancer therapy: In vivo evidences, Biochim. Biophys. Acta (2015), http://dx.doi.org/10.1016/j.bbamcr.2015.11.032

combined therapy either using more than one channel inhibitors together or employing the drugs together with chemotherapeutics seems to be a possible future therapeutic approach. However, the main issue remains that in most cases the specificity of ion-channel targeting drugs for the observed anti-proliferative, pro-apoptotic, anti-angiogenic or anti-metastatic effects has not been proven using genetic tools. While in several cases knock-down of the channel protein brings to a similar behavior of the cancer cells to that observed upon inhibition of the channels by pharmacological means, a clear-cut demonstration of possible pleiotropic effects should be performed by proving that a certain drug is not efficient anymore when the channel is not expressed. For example, the natural compound curcumin with potent anti-tumoral activity against various types of cancer (also *in vivo*), although widely considered as safe, is not selective, as it acts by multiple mechanisms. In fact, it inhibits $K_V11.1$ (hERG1) in human leukemic cell lines THP-1 [191] but also other channels, including Ora1 (I_{CRAC}) [192]. Therefore it would be mandatory to perform an in-depth study to understand whether its inhibitory effect of cancer growth is related to ion channel inhibition and if yes, to which one.

Another main issue to be addressed in this field is the question of the possible side-effects. In many studied, this important point is not addresses at all. Independently of these issues, the reported studies point to the possibility of repositioning already approved drugs (for recent review see e.g. [193]), such as ranolazine, clofazimine, astemizole, phenytoin, mibefradil, for which Phase II clinical trials for cancer studies can be directly undertaken. This is an important achievement, and hopefully future large-sale studies will clarify whether the use of these drugs in patients confer any protective effect on long-term scale for the respective tumors.

Finally, it would be desirable to exploit the novel techniques that might help drug delivery also for the modulators that target ion channels. Indeed, tumor-specific delivery of anticancer therapeutics could enhance the efficacy of anticancer drugs and could limit side effects associated with traditional chemotherapy. Various strategies including employment of pro-apoptotic peptides, oligonucleotides, liposomes, nanoparticles, radionuclides for delivery to the tumor site might be useful in this respect [194–196]. In addition, application of tumor-homing peptides is a very promising possibility, based also on numerous preclinical and clinical trials [194]. The so-far most successful strategy applies tumor-penetrating peptides like iRGD, iNGR and tLyp-1, which activate a transport pathway leading to the deep penetration of peptide/drug complex into the tumor tissue. These peptides have a consensus motif termed CendR which permits their binding to neurophilin-1 (NRP-1) receptors, shown to be over expressed in tumor tissues and to allow entrance of the drugs to endothelial cells (for recent review see [194]). This strategy thus helps to overcome the limitation given by the fact that most of the drugs do not penetrate the tumor tissue effectively.

Declaration of conflict of interest

The authors declare that they have no conflict of interest.

Acknowledgments

We are grateful to the Italian Association for Cancer Research (AIRC grant IG 11814 to IS) and to the Italian Ministry of Education (PRIN project 2010CSJX4F to I.S., PRIN n. 20107Z8XBW_004 to M.Z.) for financial support. E.G. is grateful to DFG (GU 335/29-1) and I.S. to Iontrac Marie-Curie Training Network (FP7-PEOPLE-2011-ITN Grant Agreement No. 289648). The authors are grateful to Dr. Marzia Tavernese for contribution to the experiment shown and to Dr. Anna Raffaello for providing siRNA against MCU.

References

[1] E.K. Hoffmann, N.B. Holm, I.H. Lambert, Functions of volume-sensitive and calcium-activated chloride channels, IUBMB Life 66 (4) (2014) 257–267.
[2] F. Lang, et al., Cell volume in the regulation of cell proliferation and apoptotic cell death, Cell. Physiol. Biochem. 10 (5–6) (2000) 417–428.
[3] V.R. Rao, et al., Voltage-gated ion channels in cancer cell proliferation, Cancers (Basel) 7 (2) (2015) 849–875.
[4] F. Lang, et al., The biological significance of cell volume, Ren. Physiol. Biochem. 16 (1–2) (1993) 48–65.
[5] N.A. McCarty, R.G. O'Neil, Calcium signaling in cell volume regulation, Physiol. Rev. 72 (4) (1992) 1037–1061.
[6] I. Szabo, M. Zoratti, E. Gulbins, Contribution of voltage-gated potassium channels to the regulation of apoptosis, FEBS Lett. 584 (10) (2010) 2049–2056.
[7] A. Kondratskyi, et al., Ion channels in the regulation of apoptosis, Biochim. Biophys. Acta 1848 (10 Pt B) (2015) 2532–2546.
[8] C.D. Bortner, J.A. Cidlowski, Ion channels and apoptosis in cancer, Philos. Trans. R. Soc. Lond. Ser. B Biol. Sci. 369 (1638) (2014) 20130104.
[9] Z. Wang, Roles of K+ channels in regulating tumour cell proliferation and apoptosis, Pflugers Arch. 448 (3) (2004) 274–286.
[10] A. Schwab, et al., Role of ion channels and transporters in cell migration, Physiol. Rev. 92 (4) (2012) 1865–1913.
[11] A. Schwab, C. Stock, Ion channels and transporters in tumour cell migration and invasion, Philos. Trans. R. Soc. Lond. Ser. B Biol. Sci. 369 (1638) (2014) 20130102.
[12] A. Litan, S.A. Langhans, Cancer as a channelopathy: ion channels and pumps in tumor development and progression, Front. Cell. Neurosci. 9 (2015) 86.
[13] L.A. Pardo, et al., Cell cycle-related changes in the conducting properties of r-eag K+ channels, J. Cell Biol. 143 (3) (1998) 767–775.
[14] L.A. Pardo, et al., Oncogenic potential of EAG K(+) channels, Embo j 18 (20) (1999) 5540–5547.
[15] A. Arcangeli, et al., Integrin-mediated neurite outgrowth in neuroblastoma cells depends on the activation of potassium channels, J. Cell Biol. 122 (5) (1993) 1131–1143.
[16] I. Szabo, et al., Tyrosine phosphorylation-dependent suppression of a voltage-gated K+ channel in T lymphocytes upon Fas stimulation, J. Biolumin. Chemilumin. 271 (34) (1996) 20465–20469.
[17] I. Szabo, et al., Tyrosine kinase-dependent activation of a chloride channel in CD95-induced apoptosis in T lymphocytes, Proc. Natl. Acad. Sci. U. S. A. 95 (11) (1998) 6169–6174.
[18] J.A. Grimes, et al., Differential expression of voltage-activated Na+ currents in two prostatic tumour cell lines: contribution to invasiveness in vitro, FEBS Lett. 369 (2–3) (1995) 290–294.
[19] D. Hanahan, R.A. Weinberg, Hallmarks of cancer: the next generation, Cell 144 (5) (2011) 646–674.
[20] L. Leanza, et al., Intracellular ion channels and cancer, Front. Physiol. 4 (2013) 227.
[21] L. Leanza, et al., Mitochondrial ion channels as oncological targets, Oncogene 33 (49) (2014) 5569–5581.
[22] D. Urrego, et al., Potassium channels in cell cycle and cell proliferation, Philos. Trans. R. Soc. Lond. Ser. B Biol. Sci. 369 (1638) (2014) 20130094.
[23] L.A. Pardo, W. Stuhmer, The roles of K(+) channels in cancer, Nat. Rev. Cancer 14 (1) (2014) 39–48.
[24] E.K. Hoffmann, I.H. Lambert, Ion channels and transporters in the development of drug resistance in cancer cells, Philos. Trans. R. Soc. Lond. Ser. B Biol. Sci. 369 (1638) (2014) 20130109.
[25] L. Munaron, Systems biology of ion channels and transporters in tumor angiogenesis: An omics view, Biochim. Biophys. Acta 1848 (10 Pt B) (2015) 2647–2656.
[26] M.B. Djamgoz, R. Onkal, Persistent current blockers of voltage-gated sodium channels: a clinical opportunity for controlling metastatic disease, Recent Pat Anticancer Drug Discov 8 (1) (2013) 66–84.
[27] J.A. Burger, J.G. Gribben, The microenvironment in chronic lymphocytic leukemia (CLL) and other B cell malignancies: insight into disease biology and new targeted therapies, Semin. Cancer Biol. 24 (2014) 71–81.
[28] M.P. Lisanti, et al., Understanding the "lethal" drivers of tumor-stroma co-evolution: emerging role(s) for hypoxia, oxidative stress and autophagy/mitophagy in the tumor micro-environment, Cancer Biol. Ther. 10 (6) (2010) 537–542.
[29] B.L. Brucher, I.S. Jamall, Cell-cell communication in the tumor microenvironment, carcinogenesis, and anticancer treatment, Cell. Physiol. Biochem. 34 (2) (2014) 213–243.
[30] T.A. Stewart, K.T. Yapa, G.R. Monteith, Altered calcium signaling in cancer cells, Biochim. Biophys. Acta 1848 (10 Pt B) (2015) 2502–2511.
[31] R. Rizzuto, et al., Mitochondria as sensors and regulators of calcium signalling, Nat. Rev. Mol. Cell Biol. 13 (9) (2012) 566–578.
[32] A. Kondratskyi, et al., Calcium-permeable ion channels in control of autophagy and cancer, Front. Physiol. 4 (2013) 272.
[33] T.J. Shuttleworth, Intracellular Ca^{2+} signalling in secretory cells, J Exp Biol 200 (Pt 2) (1997) 303–314.
[34] S. Choi, et al., The TRPCs–STIM1–Orai interaction, Handb. Exp. Pharmacol. 223 (2014) 1035–1054.
[35] K.T. Cheng, et al., Contribution and regulation of TRPC channels in store-operated Ca^{2+} entry, Curr. Top. Membr. 71 (2013) 149–179.
[36] I. Azimi, S.J. Roberts-Thomson, G.R. Monteith, Calcium influx pathways in breast cancer: opportunities for pharmacological intervention, Br. J. Pharmacol. 171 (4) (2014) 945–960.
[37] H. Xu, E. Martinoia, I. Szabo, Organellar channels and transporters, Cell Calcium 58 (1) (2015) 1–10.

Please cite this article as: L. Leanza, et al., Pharmacological targeting of ion channels for cancer therapy: In vivo evidences, Biochim. Biophys. Acta (2015), http://dx.doi.org/10.1016/j.bbamcr.2015.11.032

[38] S. Patel, X. Cai, Evolution of acidic Ca(2)(+) stores and their resident Ca(2)(+)-permeable channels, Cell Calcium 57 (3) (2015) 222–230.
[39] N. Prevarskaya, R. Skryma, Y. Shuba, Ion channels and the hallmarks of cancer, Trends Mol. Med. 16 (3) (2010) 107–121.
[40] D. Belpomme, et al., Verapamil increases the survival of patients with anthracycline-resistant metastatic breast carcinoma, Ann. Oncol. 11 (11) (2000) 1471–1476.
[41] A.S. Segal, J.P. Hayslett, G.V. Desir, On the natriuretic effect of verapamil: *inhibition of ENaC and transepithelial sodium transport*, Am. J. Physiol. Ren. Physiol. 283 (4) (2002) F765–F770.
[42] J.J. Duan, et al., Verapamil blocks HERG channel by the helix residue Y652 and F656 in the S6 transmembrane domain, Acta Pharmacol. Sin. 28 (7) (2007) 959–967.
[43] T. Ninomiya, et al., Verapamil, a Ca^{2+} entry blocker, targets the pore-forming subunit of cardiac type KATP channel (Kir6.2), J. Cardiovasc. Pharmacol. 42 (2) (2003) 161–168.
[44] X.D. Qian, W.T. Beck, *Binding* of an optically pure photoaffinity analogue of verapamil, LU-49888, to P-glycoprotein from multidrug-resistant human leukemic cell lines, Cancer Res. 50 (4) (1990) 1132–1137.
[45] B.T. Ragel, et al., Calcium channel antagonists augment hydroxyurea- and ru486-induced inhibition of meningioma growth in vivo and in vitro, Neurosurgery 59 (5) (2006) 1109–1120 discussion 1120-1.
[46] B.T. Ragel, et al., Chronic suppressive therapy with calcium channel antagonists for refractory meningiomas, Neurosurg. Focus. 23 (4) (2007) E10.
[47] J.M. Taylor, R.U. Simpson, Inhibition of cancer cell growth by calcium channel antagonists in the athymic mouse, Cancer Res. 52 (9) (1992) 2413–2418.
[48] J. Yoshida, T. Ishibashi, M. Nishio, Antiproliferative effect of Ca^{2+} channel blockers on human epidermoid carcinoma A431 cells, Eur. J. Pharmacol. 472 (1–2) (2003) 23–31.
[49] W.H. Moolenaar, et al., The epidermal growth factor-induced calcium signal in A431 cells, J. Biolumin. Chemilumin. 261 (1) (1986) 279–284.
[50] J. Yoshida, T. Ishibashi, M. Nishio, G1 cell cycle arrest by amlodipine, *a dihydropyridine Ca^{2+} channel blocker, in human epidermoid carcinoma A431 cells*, Biochem. Pharmacol. 73 (7) (2007) 943–953.
[51] J. Yoshida, et al., Amlodipine, a Ca^{2+} channel blocker, suppresses phosphorylation of epidermal growth factor receptor in human epidermoid carcinoma A431 cells, Life Sci. 86 (3–4) (2010) 124–132.
[52] S.C. Brazer, et al., Caveolin-1 contributes to assembly of store-operated Ca^{2+} influx channels by regulating plasma membrane localization of TRPC1, J. Biolumin. Chemilumin. 278 (29) (2003) 27208–27215.
[53] N. Tajeddine, P. Gailly, TRPC1 protein channel is major regulator of epidermal growth factor receptor signaling, J. Biolumin. Chemilumin. 287 (20) (2012) 16146–16157.
[54] H.K. Rim, et al., T-type Ca2+ channel blocker, KYS05047 induces G1 phase cell cycle arrest by decreasing intracellular Ca2+ levels in human lung adenocarcinoma A549 cells, Bioorg. Med. Chem. Lett. 22 (23) (2012) 7123–7126.
[55] H. Rhim, et al., Synthesis and biological activity of 3,4-dihydroquinazolines for selective T-type Ca^{2+} channel blockers, Bioorg. Med. Chem. Lett. 15 (2) (2005) 283–286.
[56] O.G. Rodriguez-Mora, et al., Calcium/calmodulin-dependent kinase I and calcium/calmodulin-dependent kinase kinase participate in the control of cell cycle progression in MCF-7 human breast cancer cells, Cancer Res. 65 (12) (2005) 5408–5416.
[57] G. Mehrke, et al., The Ca(++)-channel blocker Ro 40-5967 blocks differently T-type and L-type Ca++ channels, J Pharmacol Exp Ther 271 (3) (1994) 1483–1488.
[58] J.P. Sheehan, et al., Inhibition of glioblastoma and enhancement of survival via the use of mibefradil in conjunction with radiosurgery, J. Neurosurg. 118 (4) (2013) 830–837.
[59] S.T. Keir, et al., Mibefradil, a novel therapy for glioblastoma multiforme: cell cycle synchronization and interlaced therapy in a murine model, J. Neuro-Oncol. 111 (2) (2013) 97–102.
[60] B. Nebe, et al., Induction of apoptosis by the calcium antagonist mibefradil correlates with depolarization of the membrane potential and decreased integrin expression in human lens epithelial cells, Graefes Arch. Clin. Exp. Ophthalmol. 242 (7) (2004) 597–604.
[61] K.H. Kim, et al., NNC 55-0396, a T-type Ca^{2+} channel inhibitor, inhibits angiogenesis via suppression of hypoxia-inducible factor-1alpha signal transduction, J Mol Med (Berl) 93 (5) (2015) 499–509.
[62] A.S. Hui, et al., Calcium signaling stimulates translation of HIF-alpha during hypoxia, FASEB J. 20 (3) (2006) 466–475.
[63] C. Riganti, et al., Artemisinin induces doxorubicin resistance in human colon cancer cells via calcium-dependent activation of HIF-1alpha and P-glycoprotein overexpression, Br. J. Pharmacol. 156 (7) (2009) 1054–1066.
[64] S. Oda, et al., The calcium channel blocker cilnidipine selectively suppresses hypoxia-inducible factor 1 activity in vascular cells, Eur. J. Pharmacol. 606 (1–3) (2009) 130–136.
[65] S.J. Chen, et al., A splice variant of the human ion channel TRPM2 modulates neuroblastoma tumor growth through hypoxia-inducible factor (HIF)-1/2alpha, J. Biolumin. Chemilumin. 289 (52) (2014) 36284–36302.
[66] S.J. Cho, et al., Simvastatin induces apoptosis in human colon cancer cells and in tumor xenografts, and attenuates colitis-associated colon cancer in mice, Int. J. Cancer 123 (4) (2008) 951–957.
[67] M.A. Borahay, et al., Simvastatin potently induces calcium-dependent apoptosis of human leiomyoma cells, J. Biolumin. Chemilumin. 289 (51) (2014) 35075–35086.
[68] B. Dziegielewska, L.S. Gray, J. Dziegielewski, T-type calcium channels blockers as new tools in cancer therapies, Pflugers Arch. 466 (4) (2014) 801–810.
[69] N. Deliot, B. Constantin, Plasma membrane calcium channels in cancer: alterations and consequences for cell proliferation and migration, Biochim. Biophys. Acta 1848 (10 Pt B) (2015) 2512–2522.
[70] V.C. Bomben, H. Sontheimer, Disruption of transient receptor potential canonical channel 1 causes incomplete cytokinesis and slows the growth of human malignant gliomas, Glia 58 (10) (2010) 1145–1156.
[71] M. Gautier, et al., New insights into pharmacological tools to TR(i)P cancer up, Br. J. Pharmacol. 171 (10) (2014) 2582–2592.
[72] R.S. Bon, D.J. Beech, In pursuit of small molecule chemistry for calcium-permeable non-selective TRPC channels — mirage or pot of gold? Br. J. Pharmacol. 170 (3) (2013) 459–474.
[73] Y. Akbulut, et al., (−)-Englerin A is a potent and selective activator of TRPC4 and TRPC5 calcium channels, Angew Chem Int Ed Engl 54 (12) (2015) 3787–3791.
[74] C. Carson, et al., Englerin A agonizes the TRPC4/C5 cation channels to inhibit tumor cell line proliferation, PLoS One 10 (6) (2015), e0127498.
[75] J.A. Hwang, et al., 20-O-beta-d-glucopyranosyl-20(S)-protopanaxadiol, a metabolite of ginseng, inhibits colon cancer growth by targeting TRPC channel-mediated calcium influx, J. Nutr. Biochem. 24 (6) (2013) 1096–1104.
[76] G. Kovacs, et al., Heavy metal cations permeate the TRPV6 epithelial cation channel, Cell Calcium 49 (1) (2011) 43–55.
[77] M. Raphael, et al., TRPV6 calcium channel translocates to the plasma membrane via Orai1-mediated mechanism and controls cancer cell survival, Proc. Natl. Acad. Sci. U. S. A. 111 (37) (2014) E3870–E3879.
[78] V. Lehen'kyi, N. Prevarskaya, Oncogenic TRP channels, Adv. Exp. Med. Biol. 704 (2011) 929–945.
[79] C.P. Landowski, et al., Chemical inhibitors of the calcium entry channel TRPV6, Pharm. Res. 28 (2) (2011) 322–330.
[80] A. Hofer, et al., Design, synthesis and pharmacological characterization of analogs of 2-aminoethyl diphenylborinate (2-APB), a known store-operated calcium channel blocker, for inhibition of TRPV6-mediated calcium transport, Bioorg. Med. Chem. 21 (11) (2013) 3202–3213.
[81] C.V. Bowen, et al., In vivo detection of human TRPV6-rich tumors with anti-cancer peptides derived from soricidin, PLoS One 8 (3) (2013), e58866.
[82] J.K. Lau, et al., Capsaicin induces apoptosis in human small cell lung cancer via the TRPV6 receptor and the calpain pathway, Apoptosis 19 (8) (2014) 1190–1201.
[83] Z.H. Yang, et al., Capsaicin mediates cell death in bladder cancer T24 cells through reactive oxygen species production and mitochondrial depolarization, Urology 75 (3) (2010) 735–741.
[84] M. Skrzypski, et al., Capsaicin induces cytotoxicity in pancreatic neuroendocrine tumor cells via mitochondrial action, Cell. Signal. 26 (1) (2014) 41–48.
[85] C.B. Gonzales, et al., Vanilloids induce oral cancer apoptosis independent of TRPV1, Oral Oncol. 50 (5) (2014) 437–447.
[86] A.M. Sanchez, et al., Induction of apoptosis in prostate tumor PC-3 cells and inhibition of xenograft prostate tumor growth by the vanilloid capsaicin, Apoptosis 11 (1) (2006) 89–99.
[87] D. Trachootham, J. Alexandre, P. Huang, Targeting cancer cells by ROS-mediated mechanisms: a radical therapeutic approach? Nat. Rev. Drug Discov. 8 (7) (2009) 579–591.
[88] L. De Petrocellis, et al., Effects of cannabinoids and cannabinoid-enriched *Cannabis* extracts on TRP channels and endocannabinoid metabolic enzymes, Br. J. Pharmacol. 163 (7) (2011) 1479–1494.
[89] R. Ramer, et al., Cannabidiol inhibits cancer cell invasion via upregulation of tissue inhibitor of matrix metalloproteinases-1, Biochem. Pharmacol. 79 (7) (2010) 955–966.
[90] R. Ramer, et al., Cannabidiol inhibits lung cancer cell invasion and metastasis via intercellular adhesion molecule-1, FASEB J. 26 (4) (2012) 1535–1548.
[91] L. De Petrocellis, et al., Non-THC cannabinoids inhibit prostate carcinoma growth in vitro and in vivo: pro-apoptotic effects and underlying mechanisms, Br. J. Pharmacol. 168 (1) (2013) 79–102.
[92] F. Borrelli, et al., Colon carcinogenesis is inhibited by the TRPM8 antagonist cannabigerol, a *Cannabis*-derived non-psychotropic cannabinoid, Carcinogenesis 35 (12) (2014) 2787–2797.
[93] C. El Boustany, et al., Differential roles of STIM1, STIM2 and Orai1 in the control of cell proliferation and SOCE amplitude in HEK293 cells, Cell Calcium 47 (4) (2010) 350–359.
[94] C. Dubois, et al., Remodeling of channel-forming ORAI proteins determines an oncogenic switch in prostate cancer, Cancer Cell 26 (1) (2014) 19–32.
[95] M. Vandenberghe, et al., ORAI1 calcium channel orchestrates skin homeostasis, Proc. Natl. Acad. Sci. U. S. A. 110 (50) (2013) E4839–E4848.
[96] M. Flourakis, et al., Orai1 contributes to the establishment of an apoptosis-resistant phenotype in prostate cancer cells, Cell Death Dis 1 (2010) e75.
[97] H. Zhu, et al., Elevated Orai1 expression mediates tumor-promoting intracellular Ca^{2+} oscillations in human esophageal squamous cell carcinoma, Oncotarget 5 (11) (2014) 3455–3471.
[98] Y.M. Leung, C.Y. Kwan, Current perspectives in the pharmacological studies of store-operated Ca^{2+} entry blockers, Jpn. J. Pharmacol. 81 (3) (1999) 253–258.
[99] Y.F. Chen, et al., Calcium store sensor stromal-interaction molecule 1-dependent signaling plays an important role in cervical cancer growth, migration, and angiogenesis, Proc. Natl. Acad. Sci. U. S. A. 108 (37) (2011) 15225–15230.
[100] M.D. Bootman, et al., 2-aminoethoxydiphenyl borate (2-APB) is a reliable blocker of store-operated Ca^{2+} entry but an inconsistent inhibitor of InsP3-induced Ca^{2+} release, FASEB J. 16 (10) (2002) 1145–1150.
[101] C.K. Colton, M.X. Zhu, 2-Aminoethoxydiphenyl borate as a common activator of TRPV1, TRPV2, and TRPV3 channels, Handb. Exp. Pharmacol. 179 (2007) 173–187.
[102] X. Hou, et al., Crystal structure of the calcium release-activated calcium channel Orai, Science 338 (6112) (2012) 1308–1313.

Please cite this article as: L. Leanza, et al., Pharmacological targeting of ion channels for cancer therapy: In vivo evidences, Biochim. Biophys. Acta (2015), http://dx.doi.org/10.1016/j.bbamcr.2015.11.032

[103] J. Xie, et al., SOCE and cancer: recent progress and new perspectives, Int. J. Cancer (2015).
[104] V. Khurana, et al., Statins reduce the risk of pancreatic cancer in humans: a case–control study of half a million veterans, Pancreas 34 (2) (2007) 260–265.
[105] T. Kusama, et al., 3-Hydroxy-3-methylglutaryl-coenzyme a reductase inhibitors reduce human pancreatic cancer cell invasion and metastasis, Gastroenterology 122 (2) (2002) 308–317.
[106] O. Mistafa, U. Stenius, Statins inhibit Akt/PKB signaling via P2X7 receptor in pancreatic cancer cells, Biochem. Pharmacol. 78 (9) (2009) 1115–1126.
[107] S. Roger, et al., Understanding the roles of the P2X7 receptor in solid tumour progression and therapeutic perspectives, Biochim. Biophys. Acta 1848 (10 Pt B) (2015) 2584–2602.
[108] P. Pellegatti, et al., Increased level of extracellular ATP at tumor sites: in vivo imaging with plasma membrane luciferase, PLoS One 3 (7) (2008), e2599.
[109] B. Jelassi, et al., P2X(7) receptor activation enhances SK3 channels- and cystein cathepsin-dependent cancer cells invasiveness, Oncogene 30 (18) (2011) 2108–2122.
[110] B. Jelassi, et al., Anthraquinone emodin inhibits human cancer cell invasiveness by antagonizing P2X7 receptors, Carcinogenesis 34 (7) (2013) 1487–1496.
[111] F. Hattori, et al., Feasibility study of B16 melanoma therapy using oxidized ATP to target purinergic receptor P2X7, Eur. J. Pharmacol. 695 (1–3) (2012) 20–26.
[112] E. Adinolfi, et al., Expression of P2X7 receptor increases in vivo tumor growth, Cancer Res. 72 (12) (2012) 2957–2969.
[113] N. White, et al., An in vivo model of melanoma: treatment with ATP, Purinergic Signal 5 (3) (2009) 327–333.
[114] J.I. Vandenberg, et al., hERG K(+) channels: structure, function, and clinical significance, Physiol. Rev. 92 (3) (2012) 1393–1478.
[115] A. Arcangeli, et al., A novel inward-rectifying K+ current with a cell-cycle dependence governs the resting potential of mammalian neuroblastoma cells, J. Physiol. 489 (Pt 2) (1995) 455–471.
[116] P.J. Stambrook, H.G. Sachs, J.D. Ebert, The effect of potassium on the cell membrane potential and the passage of synchronized cells through the cell cycle, J. Cell. Physiol. 85 (2 Pt 1) (1975) 283–291.
[117] B.R. Downie, et al., Eag1 expression interferes with hypoxia homeostasis and induces angiogenesis in tumors, J. Biolumin. Chemilumin. 283 (52) (2008) 36234–36240.
[118] N. Comes, et al., Involvement of potassium channels in the progression of cancer to a more malignant phenotype, Biochim. Biophys. Acta 1848 (10 Pt B) (2015) 2477–2492.
[119] J. Bielanska, et al., Voltage-dependent potassium channels Kv1.3 and Kv1.5 in human cancer, Curr. Cancer Drug Targets 9 (8) (2009) 904–914.
[120] D. Gomez-Varela, et al., Monoclonal antibody blockade of the human Eag1 potassium channel function exerts antitumor activity, Cancer Res. 67 (15) (2007) 7343–7349.
[121] J. Garcia-Quiroz, et al., In vivo dual targeting of the oncogenic Ether-a-go-go-1 potassium channel by calcitriol and astemizole results in enhanced antineoplastic effects in breast tumors, BMC Cancer 14 (2014) 745.
[122] E. Lastraioli, et al., hERG1 channels drive tumour malignancy and may serve as prognostic factor in pancreatic ductal adenocarcinoma, Br. J. Cancer 112 (6) (2015) 1076–1087.
[123] A. Cherubini, et al., Human ether-a-go-go-related gene 1 channels are physically linked to beta1 integrins and modulate adhesion-dependent signaling, Mol. Biol. Cell 16 (6) (2005) 2972–2983.
[124] O. Crociani, et al., hERG1 channels modulate integrin signaling to trigger angiogenesis and tumor progression in colorectal cancer, Sci. Rep. 3 (2013) 3308.
[125] A. Fiore, et al., Characterization of hERG1 channel role in mouse colorectal carcinogenesis, Cancer Med 2 (5) (2013) 583–594.
[126] O. Crociani, et al., hERG1 channels regulate VEGF-A secretion in human gastric cancer: clinicopathological correlations and therapeutical implications, Clin. Cancer Res. 20 (6) (2014) 1502–1512.
[127] S. Pillozzi, et al., Chemotherapy resistance in acute lymphoblastic leukemia requires hERG1 channels and is overcome by hERG1 blockers, Blood 117 (3) (2011) 902–914.
[128] S. Pillozzi, et al., Differential expression of hERG1A and hERG1B genes in pediatric acute lymphoblastic leukemia identifies different prognostic subgroups, Leukemia 28 (6) (2014) 1352–1355.
[129] X. Wei, et al., ZC88, a novel 4-amino piperidine analog, inhibits the growth of neuroblastoma cells through blocking hERG potassium channel, Cancer Biol. Ther. 14 (5) (2013) 450–457.
[130] L. Gasparoli, et al., New pyrimido-indole compound CD-160130 preferentially inhibits the KV11.1B isoform and produces antileukemic effects without cardiotoxicity, Mol. Pharmacol. 87 (2) (2015) 183–196.
[131] Q. Ru, et al., Voltage-gated and ATP-sensitive K+ channels are associated with cell proliferation and tumorigenesis of human glioma, Oncol. Rep. 31 (2) (2014) 842–848.
[132] S.H. Jang, et al., Anti-proliferative effect of Kv1.3 blockers in A549 human lung adenocarcinoma in vitro and in vivo, Eur. J. Pharmacol. 651 (1–3) (2011) 26–32.
[133] L. Leanza, et al., Inhibitors of mitochondrial Kv1.3 channels induce Bax/Bak-independent death of cancer cells, EMBO Mol Med 4 (7) (2012) 577–593.
[134] I. Szabo, et al., A novel potassium channel in lymphocyte mitochondria, J. Biolumin. Chemilumin. 280 (13) (2005) 12790–12798.
[135] L. Leanza, et al., Targeting a mitochondrial potassium channel to fight cancer, Cell Calcium (2014).
[136] D. De Stefani, et al., A forty-kilodalton protein of the inner membrane is the mitochondrial calcium uniporter, Nature 476 (7360) (2011) 336–340.
[137] D. De Stefani, M. Patron, R. Rizzuto, Structure and function of the mitochondrial calcium uniporter complex, Biochim. Biophys. Acta (2015).
[138] L. Leanza, et al., Correlation between potassium channel expression and sensitivity to drug-induced cell death in tumor cell lines, Curr. Pharm. Des. 20 (2) (2014) 189–200.
[139] L. Leanza, et al., Clofazimine, Psora-4 and PAP-1, inhibitors of the potassium channel Kv1.3, as a new and selective therapeutic strategy in chronic lymphocytic leukemia, Leukemia 27 (8) (2013) 1782–1785.
[140] I. Szabo, et al., Biophysical characterization and expression analysis of Kv1.3 potassium channel in primary human leukemic B cells, Cell. Physiol. Biochem. 37 (3) (2015) 965–978.
[141] M.C. Cholo, et al., Clofazimine: current status and future prospects, J Antimicrob Chemother 67 (2) (2012) 290–298.
[142] I. Szabo, M. Zoratti, Mitochondrial channels: ion fluxes and more, Physiol. Rev. 94 (2) (2014) 519–608.
[143] A. Manago, et al., *Pseudomonas aeruginosa* pyocyanin induces neutrophil death via mitochondrial reactive oxygen species and mitochondrial acid sphingomyelinase, Antioxid. Redox Signal. (2015).
[144] L. Huang, et al., A new fungal diterpene induces VDAC1-dependent apoptosis in Bax/Bak-deficient cells, J. Biolumin. Chemilumin. 290 (39) (2015) 23563–23578.
[145] V. Shoshan-Barmatz, et al., The mitochondrial voltage-dependent anion channel 1 in tumor cells, Biochim. Biophys. Acta 1848 (10 Pt B) (2015) 2547–2575.
[146] A.J. Patel, M. Lazdunski, The 2P-domain K+ channels: role in apoptosis and tumorigenesis, Pflugers Arch. 448 (3) (2004) 261–273.
[147] L. Pei, et al., Oncogenic potential of TASK3 (Kcnk9) depends on K+ channel function, Proc. Natl. Acad. Sci. U. S. A. 100 (13) (2003) 7803–7807.
[148] S. Koshy, et al., Blocking KCa3.1 channels increases tumor cell killing by a subpopulation of human natural killer lymphocytes, PLoS One 8 (10) (2013), e76740.
[149] A. Girault, et al., New alkyl-lipid blockers of SK3 channels reduce cancer cell migration and occurrence of metastasis, Curr. Cancer Drug Targets 11 (9) (2011) 1111–1125.
[150] A. Chantome, et al., Pivotal role of the lipid Raft SK3–Orai1 complex in human cancer cell migration and bone metastases, Cancer Res. 73 (15) (2013) 4852–4861.
[151] C. Mathes, A. Fleig, R. Penner, Calcium release-activated calcium current (ICRAC) is a direct target for sphingosine, J. Biolumin. Chemilumin. 273 (39) (1998) 25020–25030.
[152] A. Lepple-Wienhues, et al., Stimulation of CD95 (Fas) blocks T lymphocyte calcium channels through sphingomyelinase and sphingolipids, Proc. Natl. Acad. Sci. U. S. A. 96 (24) (1999) 13795–13800.
[153] R. Samapati, et al., Lung endothelial Ca^{2+} and permeability response to platelet-activating factor is mediated by acid sphingomyelinase and transient receptor potential classical 6, Am. J. Respir. Crit. Care Med. 185 (2) (2012) 160–170.
[154] Y.A. Hannun, L.M. Obeid, Principles of bioactive lipid signalling: lessons from sphingolipids, Nat. Rev. Mol. Cell Biol. 9 (2) (2008) 139–150.
[155] X. Xu, et al., Effect of the structure of natural sterols and sphingolipids on the formation of ordered sphingolipid/sterol domains (rafts). Comparison of cholesterol to plant, fungal, and disease-associated sterols and comparison of sphingomyelin, cerebrosides, and ceramide, J. Biolumin. Chemilumin. 276 (36) (2001) 33540–33546.
[156] H. Grassme, et al., CD95 signaling via ceramide-rich membrane rafts, J. Biolumin. Chemilumin. 276 (23) (2001) 20589–20596.
[157] H. Grassme, et al., Ceramide-rich membrane rafts mediate CD40 clustering, J. Immunol. 168 (1) (2002) 298–307.
[158] C.A. Dumitru, E. Gulbins, TRAIL activates acid sphingomyelinase via a redox mechanism and releases ceramide to trigger apoptosis, Oncogene 25 (41) (2006) 5612–5625.
[159] M.P. Kowalski, G.B. Pier, Localization of cystic fibrosis transmembrane conductance regulator to lipid rafts of epithelial cells is required for *Pseudomonas aeruginosa*-induced cellular activation, J. Immunol. 172 (1) (2004) 418–425.
[160] D.X. Zhang, A.P. Zou, P.L. Li, Ceramide-induced activation of NADPH oxidase and endothelial dysfunction in small coronary arteries, Am J Physiol Heart Circ Physiol 284 (2) (2003) H605–H612.
[161] A. Eramo, et al., CD95 death-inducing signaling complex formation and internalization occur in lipid rafts of type I and type II cells, Eur. J. Immunol. 34 (7) (2004) 1930–1940.
[162] J. Bock, et al., Ceramide inhibits the potassium channel Kv1.3 by the formation of membrane platforms, Biochem. Biophys. Res. Commun. 305 (4) (2003) 890–897.
[163] H. Grassme, et al., Ceramide-mediated clustering is required for CD95-DISC formation, Oncogene 22 (35) (2003) 5457–5470.
[164] H. Grassme, et al., Host defense against *Pseudomonas aeruginosa* requires ceramide-rich membrane rafts, Nat. Med. 9 (3) (2003) 322–330.
[165] H. Grassme, H. Schwarz, E. Gulbins, Molecular mechanisms of ceramide-mediated CD95 clustering, Biochem. Biophys. Res. Commun. 284 (4) (2001) 1016–1030.
[166] E. Gulbins, et al., Ceramide-induced inhibition of T lymphocyte voltage-gated potassium channel is mediated by tyrosine kinases, Proc. Natl. Acad. Sci. U. S. A. 94 (14) (1997) 7661–7666.
[167] S.P. Fraser, et al., Regulation of voltage-gated sodium channel expression in cancer: hormones, growth factors and auto-regulation, Philos. Trans. R. Soc. Lond. Ser. B Biol. Sci. 369 (1638) (2014) 20130105.
[168] L. Gillet, et al., Voltage-gated sodium channel activity promotes cysteine cathepsin-dependent invasiveness and colony growth of human cancer cells, J. Biolumin. Chemilumin. 284 (13) (2009) 8680–8691.
[169] G.C. Davis, et al., Asymmetric synthesis and evaluation of a hydroxyphenylamide voltage-gated sodium channel blocker in human prostate cancer xenografts, Bioorg. Med. Chem. 20 (6) (2012) 2180–2188.

Please cite this article as: L. Leanza, et al., Pharmacological targeting of ion channels for cancer therapy: In vivo evidences, Biochim. Biophys. Acta (2015), http://dx.doi.org/10.1016/j.bbamcr.2015.11.032

[170] K. Batcioglu, et al., Oxidative stress in the in vivo DMBA rat model of breast cancer: suppression by a voltage-gated sodium channel inhibitor (RS100642), Basic Clin. Pharmacol. Toxicol. 111 (2) (2012) 137–141.
[171] S. Yildirim, et al., Voltage-gated sodium channel activity promotes prostate cancer metastasis in vivo, Cancer Lett. 323 (1) (2012) 58–61.
[172] M. Nelson, et al., The sodium channel-blocking antiepileptic drug phenytoin inhibits breast tumour growth and metastasis, Mol. Cancer 14 (2015) 13.
[173] V. Driffort, et al., Ranolazine inhibits NaV1.5-mediated breast cancer cell invasiveness and lung colonization, Mol. Cancer 13 (2014) 264.
[174] C. Antzelevitch, et al., Electrophysiological effects of ranolazine, a novel antianginal agent with antiarrhythmic properties, Circulation 110 (8) (2004) 904–910.
[175] T. Gupta, et al., Antiarrhythmic properties of ranolazine: a review of the current evidence, Int. J. Cardiol. 187 (2015) 66–74.
[176] H. Sontheimer, An unexpected role for ion channels in brain tumor metastasis, Exp Biol Med (Maywood) 233 (7) (2008) 779–791.
[177] J. Deshane, C.C. Garner, H. Sontheimer, Chlorotoxin inhibits glioma cell invasion via matrix metalloproteinase-2, J. Biolumin. Chemilumin. 278 (6) (2003) 4135–4144.
[178] N. Ullrich, et al., Expression of voltage-activated chloride currents in acute slices of human gliomas, Neuroscience 83 (4) (1998) 1161–1173.
[179] M.B. McFerrin, H. Sontheimer, A role for ion channels in glioma cell invasion, Neuron Glia Biol. 2 (1) (2006) 39–49.
[180] O. Veiseh, et al., Inhibition of tumor-cell invasion with chlorotoxin-bound superparamagnetic nanoparticles, Small 5 (2) (2009) 256–264.
[181] S.A. Lyons, J. O'Neal, H. Sontheimer, Chlorotoxin, a scorpion-derived peptide, specifically binds to gliomas and tumors of neuroectodermal origin, Glia 39 (2) (2002) 162–173.
[182] A.N. Mamelak, D.B. Jacoby, Targeted delivery of antitumoral therapy to glioma and other malignancies with synthetic chlorotoxin (TM-601), Expert Opin Drug Deliv 4 (2) (2007) 175–186.
[183] D.B. Jacoby, et al., Potent pleiotropic anti-angiogenic effects of TM601, a synthetic chlorotoxin peptide, Anticancer Res. 30 (1) (2010) 39–46.
[184] C. Qin, et al., Inhibition of metastatic tumor growth and metastasis via targeting metastatic breast cancer by chlorotoxin-modified liposomes, Mol. Pharm. 11 (10) (2014) 3233–3241.
[185] U. Duvvuri, et al., TMEM16A induces MAPK and contributes directly to tumorigenesis and cancer progression, Cancer Res. 72 (13) (2012) 3270–3281.
[186] L. Jia, et al., Inhibition of calcium-activated chloride channel ANO1/TMEM16A suppresses tumor growth and invasion in human lung cancer, PLoS One 10 (8) (2015), e0136584.
[187] A. Britschgi, et al., Calcium-activated chloride channel ANO1 promotes breast cancer progression by activating EGFR and CAMK signaling, Proc. Natl. Acad. Sci. U. S. A. 110 (11) (2013) E1026–E1034.
[188] D.J. Shiwarski, et al., To "grow" or "go": TMEM16A expression as a switch between tumor growth and metastasis in SCCHN, Clin. Cancer Res. 20 (17) (2014) 4673–4688.
[189] R. De La Fuente, et al., Small-molecule screen identifies inhibitors of a human intestinal calcium-activated chloride channel, Mol. Pharmacol. 73 (3) (2008) 758–768.
[190] Y. Seo, et al., Inhibition of ANO1/TMEM16A chloride channel by idebenone and Its cytotoxicity to cancer cell lines, PLoS One 10 (7) (2015) e0133656.
[191] U. Banderali, et al., Curcumin blocks Kv11.1 (erg) potassium current and slows proliferation in the infant acute monocytic leukemia cell line THP-1, Cell. Physiol. Biochem. 28 (6) (2011) 1169–1180.
[192] X. Zhang, et al., Effects of curcumin on ion channels and transporters, Front. Physiol. 5 (2014) 94.
[193] V.P. Kale, S.G. Amin, M.K. Pandey, Targeting ion channels for cancer therapy by repurposing the approved drugs, Biochim. Biophys. Acta 1848 (10 Pt B) (2015) 2747–2755.
[194] A. Gautam, et al., Tumor homing peptides as molecular probes for cancer therapeutics, diagnostics and theranostics, Curr. Med. Chem. 21 (21) (2014) 2367–2391.
[195] U.K. Marelli, et al., Tumor targeting via integrin ligands, Front Oncol 3 (2013) 222.
[196] R. Tietze, et al., Magnetic nanoparticle-based drug delivery for cancer therapy, Biochem. Biophys. Res. Commun. (2015).

Please cite this article as: L. Leanza, et al., Pharmacological targeting of ion channels for cancer therapy: In vivo evidences, Biochim. Biophys. Acta (2015), http://dx.doi.org/10.1016/j.bbamcr.2015.11.032

Tumor-reducing effect of the clinically used clofazimine in a SCID mouse model of pancreatic ductal adenocarcinoma

Angela Zaccagnino[1]*, Antonella Managò[2]* Luigi Leanza[2]§, , Artur Gontarewitz[1], Bernhard Linder[1], Michele Azzolini[3], Mario Zoratti[3,4], Anna Trauzold[1], Holger Kalthoff[1]^ and Ildiko Szabo[2,4]^§

* the first two authors contributed equally to this work

^ the last two authors contributed equally to this work

[1]Institut für Experimentelle Tumorforschung (IET) Sektion für Molekulare Onkologie UKSH, Campus Kiel, Arnold-Heller-Strasse 3 (Haus 17) D-24105 Kiel

[2]Department of Biology, University of Padova, viale G. Colombo 3. Padova, I-35121 Italy

[3]Department of Biomedical Sciences, University of Padova, I-35121 Italy

[4] CNR Institute of Neuroscience, Padova, Italy

Correspondence should be addressed to: I. Szabo (ildi@civ.bio.unipd.it) or L. Leanza (luigi.leanza@unipd.it)

Abstract

Pancreatic ductal adenocarcinoma (PDAC) represents the most common form of pancreatic cancer with rising incidence in developing countries. Unfortunately, the overall 5-year survival rate is less than 5%. The most frequent oncogenic mutations in PDAC are loss-of function mutations in p53 and gain-of-function mutations in KRAS. Here we show that clofazimine (Lamprene), a drug already used in the clinic for autoimmune diseases and leprosy, is able to efficiently kill *in vitro* five different PDAC cell lines harboring p53 mutations. We provide evidence using siRNA, that clofazimine induces apoptosis in PDAC cells with an IC_{50} in the μM range via its specific inhibitory action on the potassium channel Kv1.3, known to regulate both proliferation and apoptosis in various cell types. We show that intraperitoneal injection of clofazimine results in accumulation of the substance in the pancreas of mice 8 hours after injection. In an orthotopic PDAC model employing SCID beige mouse clofazimine reduces the tumor weight by 50% while does not significantly alter histology regarding tumor structure and angiogenesis and does not affect the number of liver metastases. In summary, our work identifies clofazimine as a promising therapeutic agent against PDAC and further highlights ion channels as possible oncological targets.

Introduction

Pancreatic ductal adenocarcinoma (PDAC) is one of the most aggressive types of tumors, being the fourth leading cause of cancer mortality. Due to the poor prognostic factors, patients are diagnosed at a rather late stage of disease and their life expectancy is at most five years after diagnosis. In most cases, the only valid therapeutic approach is the radical surgical resection of the tumor, which however is feasible only in 20% of the cases, but recurrence of cancer lesions often occurs. Some other patients (30-40%) show unresectable locally advanced pancreatic cancer (LAPC) with a median survival of one year [1]. For the rest of the patients, who manifest metastasis at diagnosis, six months is the expected survival period (for a detailed review see e.g. [2]). Usually, in all cases palliative or curative systemic chemotherapy, sometimes associated to radiotherapy, is administered but unfortunately, a positive outcome cannot be guaranteed.

For about 20 years, the only therapeutic option considered valid for the treatment of PDAC has been 5-fluorouracile (5-FU). Nowadays, FOLFIRINOX (5-fluorouracil, leucovorin, irinotecan and oxaliplatin) has become a promising first line therapy in patients [3], albeit the most diffused chemotherapy drug in clinical use is gemcitabine, administered alone or in combination with other chemotherapeutics such as 5-fluorouracile, capecitabine, platinum analogues and taxane [4]. The mechanism of action by which the cytotoxic effect is exerted by these molecules is the block of DNA synthesis; therefore considerable side effects occur in the healthy tissues by these therapies. Only recently, new molecules with aberrant expression in PDAC tissues have emerged as possible alternative targets in pancreatic tumor treatment. Among these are the epidermal growth factor receptor (EGFR)[5], human epidermal growth factor receptor type 2 (HER2) [6] and vascular endothelial growth factor (VEGF) [7]. For all of them a phase II or III clinical trial has been conducted but the improvement of outcome for PDAC patients is not satisfactory. Therefore, new therapeutic approaches are necessary.

During the last decade, ion channels emerged as possible prognostic markers and therapeutic targets against various types of cancer as indicated also by *in vivo* studies in preclinical models [8, 9]. In particular, potassium (K^+) channels have been shown to be crucially involved in many important physiological processes such as proliferation, migration, angiogenesis, cell volume regulation and apoptosis [10, 11] and to contribute to cancer progression [12]. The voltage-gated potassium channel Kv1.3 belongs to the *Shaker* family and is expressed in different tissues, such as brain, kidney, olfactory bulb, lymphocytes, skeletal muscle, adipose tissue [13]. Prevalent expression in healthy individuals occurs mainly in tissues of CNS and immune cells [14], but several types of cancer cells also display an altered expression of the protein [13]. Aberrant expression of Kv1.3 has indeed been observed in different types of tumors [15], such as melanoma [16], prostate [17], breast [18], B-cell lymphoma [19], chronic lymphocytic leukemia (B-CLL) [20, 21] gastric [22], pancreatic tumor [23] and in lung cancer [24]. Overexpression of Kv1.3 in cancer cells could give an advantage to cancer cells enhancing tumorigenic processes such as proliferation, cell migration and metastasis [10].

Kv1.3 is expressed and active both in plasma membrane (PM) and in the inner mitochondrial membrane (IMM) of lymphocytes (mtKv1.3) [25], hippocampal neurons [26] and in various tumor cells [27, 28]. Expression of

Kv1.3 in the IMM seems to correlate with that in the PM e.g. [27]. Kv1.3 was located to cis-Golgi membranes as well [29] and, recently, to nuclear membrane [30] where it seems to be involved in regulation of transcription. While the plasma membrane Kv1.3 is required for cell proliferation, the mitochondrial channel regulates apoptosis. At the molecular level, mtKv1.3 is a target of the pro-apoptotic protein Bax, which inhibits the channel via a conserved positive amino acid residue, lysine 128, with a Kv1.3-inhibiting toxin like mechanism [31, 32]. Bax, or membrane permeant Kv1.3 inhibitors which can reach the mitochondrial channel, block the positive inward (toward the mitochondrial matrix) potassium current, thereby determining a transient hyperpolarization followed by the release of reactive oxygen species, the opening of the permeability transition pore with consequent loss of mitochondrial membrane potential and release of cytochrome c, finally leading to the activation of apoptotic cascade.

We have previously shown that *in vitro* inhibition of mtKv1.3 using membrane-permeant Kv1.3 inhibitors such as Psora-4, PAP-1 and clofazimine results in apoptosis of various Kv1.3-expressing tumor cells [20, 28, 33]. These drugs were efficient even in the case of poor-prognosis tumors lacking Bax/Bak and bearing p53 mutations. Importantly, this effect was observed exclusively with the membrane-permeant inhibitors indicating the importance of the mtKv1.3 versus PM Kv1.3. Genetic deficiency or siRNA-mediated downregulation of Kv1.3 abrogated the effects of these drugs. The specific drugs, targeting mtKv1.3, were able to reduce tumor volume *in vivo* by 90% in a preclinical model of melanoma, without side effects [28] as well as to kill primary pathologic B cells from chronic lymphocytic leukemia patients, without affecting survival of healthy T cells of the same individual [20]. The mechanism of action has been clarified, pointing to a synergistic effect between the altered redox state, characteristic of tumor cells and the ability of these drugs to induce production of significant oxidative stress by inhibiting mtKv1.3, leading finally to ROS-induced cell death in the cancer cells, while leaving healthy cells alive.

Clofazimine blocks Kv1.3 with an IC_{50} of 300 nM, while it is much less effective on other potassium channels of the same family [34]. Clofazimine is a lipophilic riminophenazine antibiotic approved by the FDA and already in clinical use in human to treat pathologies like leprosy and psoriasis; its antibiotic, immunomodulatory and anti-inflammatory properties make it a versatile drug [35]. In light of the results obtained with clofazimine on B-CLL cells and in the orthotopic melanoma model, and of indication about expression of Kv1.3 in pancreatic tissues, we investigated whether this drug can be used against PDAC in an orthotopic xenograft model.

Results

Kv1.3 is expressed in different human PDAC cell lines

Since our purpose was to understand whether clofazimine might be useful to induce apoptosis in PDAC cell lines via inhibition of the mitochondrial Kv1.3 channel, first we checked whether the widely used human PDAC lines of various origin express Kv1.3. To this end, we extracted information available in a previously reported Affymetrix U133 GeneChip set [36, 37]. Analysis of the microarray data shows that in 5 out of 8 lines expression of the *KcnA* gene encoding for Kv1.3 channel was relatively high (Figure 1A). To confirm these data in the cell lines used in our laboratories and to compare Kv1.3 expression with that of a non-tumoral pancreatic ductal epithelial line, we performed quantitative real time PCR using multiple reference genes of the non-tumoral HPDE line for normalization (Figure 1B). HPDE6-E6E7 (H6C7) is a non-tumoral, immortalized human pancreatic ductal epithelial cell line, generated by transformation with human papilloma virus 16 (HPV-16). Cultured HPDE cells express low levels of epidermal growth factor receptor (EGFR), erbB2, transforming growth factor (TGF)-alpha, Met/hepatocyte growth factor receptor (HGFR), vascular endothelial growth factor (VEGF), and keratinocyte growth factor (KGF). HPDE was shown to be non-tumorigenic when transplanted into SCID mice [38].

The human tumor lines that were used have different origin and characteristics. All these lines have been characterized in detail in several previous works [39-41] and were found to be mutated in p53 and most of them, except BxPC3 are mutated also in K-RAS [41]. It is of note, that these cell lines, harboring mutation in p53, have been tested previously to be largely resistant to standard chemotherapeutics. Mutations in the p53 gene have been described in more than 50% of the patient samples and there is evidence that the p53 network is genetically altered in an even much higher proportion. AsPC1 is a human pancreatic tumor cell line that was derived from the metastatic site, an ascites, of a patient with adenocarcinoma in the head of the pancreas. Nude mice tumor model of AsPC1 shows the similar characteristics of human PDAC with abundant mucin production and granular differentiation. BxPC3 is a primary human pancreatic tumor cells line from the body of the pancreas of a patient with adenocarcinoma. These cells are not prone to give metastasis and they are poorly differentiated. Nude mice tumor model of BxPC3 shows the similar characteristics of human PDAC with mucin production and displaying moderately differentiated adenocarcinomas with occasional lymphocytic infiltrations at the tumor peripheries. Colo357 cells originate from lymph node metastasis from a PDAC patient. They express low levels of Bcl-xL, are highly metastatic and are moderately differentiated. Capan1 PDAC line, originally obtained from liver metastasis, is highly resistant to different chemotherapeutic drugs, in particular to 5-FU. Tumor models using Capan1 show a well-differentiated adenocarcinoma with abundant mucin production. The poorly differentiated MiaPaCa2 cell line was initially delivered from the body and tail of the pancreas of a PDAC patient, while the metastatic Panc1 line was isolated from the head of the pancreas which invaded duodenal wall from a patient and expresses a high level of the anti-apoptotic Bcl-xL [42]. The relative quantity of Kv1.3 expression was higher in all these PDAC lines with respect to HPDE. To confirm that Kv1.3 was expressed also at protein level, we performed Western blot analysis on whole-cell extracts (Figure 1C), revealing a similar level of expression in all cell lines (but it is to note that HPDE does not form tumors and thus does not have the typical characteristics of pathologic cells). Finally, in one of these lines, namely in Colo357 which was used for the *in vivo* studies in this paper (see below), we assessed mitochondrial expression of Kv1.3. The intensity of the channel protein band in progressively purer mitochondrial fractions was comparable, while the intensity of PM (PMCA) and ER (SERCA) markers decreased in contrast to the mitochondrial marker Bak (Figure 1D). Altogether, these results indicate the presence of Kv1.3 in different PDAC cell lines.

Clofazimine decreases cell survival in PDAC lines harbouring p53 mutations but spares non-tumoral lines

Next, we studied the effect of clofazimine in the above PDAC lines in a previously used setting to induce apoptosis. Figure 2A shows that while HPDE and the epithelial cell line HUVEC were resistant to 10 µM clofazimine, basically all PDAC lines, even those that are resistant to 4 µM Staurosporine (PANC1, AsPC-1, Capan-1 and

MiaPaCa2), responded to this concentration of clofazimine with a significant reduction of cell survival. The efficiency of clofazimine, in accordance with data obtained with other cell lines [43], further increased when the drug was applied together with 4 µM Cyclosporin H, an inhibitor of multidrug resistance pumps, that is expected to decrease the export of clofazimine from the cells. EC_{50} was 1.5 µM for wt Colo357 cells. Although this value increased to 6 µM in Bcl-xL-overexpressing cells [44], there was still a significant impairment of cell survival at the highest concentration of clofazimine (Figure 2B). This result is in agreement with the action of clofazimine on the IMM-located mtKv1.3, i.e. downstream and independent of the OMM-located Bcl-2 family members.

In order to prove that reduction of cell survival correlated with cell death and that clofazimine induced apoptosis via its action on Kv1.3, we followed Annexin binding in BxPC3 and AsPC1 cells transiently transfected either with scrambled RNA or with siRNA against Kv1.3 (Figure 2C-D). In both cell lines clofazimine-induced apoptosis and Annexin binding is evident after treatment with 10 µM clofazimine, even without addition of MDR inhibitors (in agreement with Fig 2A) when Kv1.3 is expressed, but upon silencing of the channel expression the drug is not effective anymore. Staurosporine was used as positive control, and in agreement with data of Fig 2A, this assay confirmed the resistance of AsPC-1 cells to this classical apoptosis-inducer, as well as the sensitivity of BxPC-3 cells. PAP-1 without MDRi acts prevalently on the PMKv1.3 and was indeed unable to trigger apoptosis. Similar results were obtained also with Colo357 cells (Figure 2E).

Clofazimine reduces tumor weight *in vivo*

To further prove the relevance of our findings *in vivo*, we treated severe combined immunodeficient (SCID) beige mice bearing orthotopically xenotransplanted human Colo357 cells with intraperitoneally (i.p) injected clofazimine ten times, starting 10 days after tumor cell inoculation and continued every second day (Figure 3A). For the treatment regimen we followed a previously established inoculation protocol for Colo357 [45] and then analyzed tumor growth and metastasis. A statistically significant reduction of tumor weight occurred in the clofazimine-treated mice by more than 50% with respect to the control group treated with the same protocol but using only the solvent (Figure 3B). Instead, no difference in the number of liver metastasis occurred in the clofazimine-treated animals with respect to controls (Figure 3C). In order to prove that indeed clofazimine can reach the pancreatic tissue, we determined the clofazimine concentration in various tissues. Following i.p. administration of a single dose of clofazimine, it was found readily absorbed and metabolized. Low concentrations of the drug were detected in blood. HPLC–UV–ESI/MS analysis of whole tissues showed that clofazimine was basically absent in the brain indicating that it does not cross the blood brain barrier and was accumulated only to low extent in the heart. In the pancreas, kidney, liver and spleen, relatively high concentrations of clofazimine were found (Figure 4D).

Next, we performed an immunohistochemical staining in order to characterize the orthotopic tumor tissues. We analysed the tumor area, proliferation and angiogenesis via staining with antibodies against KL1, Ki67 and CD31, respectively. The anti-KL1 antibody recognizes keratin and binds to cells with epithelial origin. Therefore, it stains neoplastic cells of epithelial origin and permits the detection of tumor area. Anti-Ki67 is against a nuclear protein which is highly expressed in proliferating cells, in particular during late G1-S-M and G2 phases of the cell cycle. Quiescent cells (G0 phase) are negative for this protein. Finally, anti CD31 or anti-PECAM-1 is against a protein which is constitutively expressed on the surface of embryonic and endothelial cells (also monocytes and neutrophils) and represents a marker of angiogenesis. Evaluation of the marker Ki67 showed a reduction in proliferation by 13% in the Clofazimine treated group. The other markers highlighted the presence of larger mucinous lobules in the clofazimine-treated pancreas tissues, but only minor differences regarding the tumor structure and the angiogenesis were observed between the control and drug-treated groups.

Discussion

In the present paper we report for the first time that clofazimine, a drug already used in the clinic is able to substantially reduce tumor weight in an orthotopic ductal pancreas adenocarcinoma model. Clofazimine is an FDA-approved anti-mycobacterial agent recommended by the World Health Organization as part of the standard treatment of leprosy [35]. It has been in clinical use since the 1960s and is well-tolerated, although bioaccumulation of the drug can lead to visible (but reversible) changes in skin pigmentation. CFZ possesses anti-inflammatory and immunosuppressive activities, therefore it is used in various cutaneous, non-microbial, and chronic inflammatory disorders. In addition, clofazimine has recently been reported to exert potent antifungal activity by inducing a PKC1-dependent stress [46]. More recent studies suggested an expansion of the clinical use of CFZ to noncutaneous inflammatory disorders such as multiple sclerosis, rheumatoid arthritis, and type I diabetes mellitus [35]. Despite this known anti-inflammatory activity, the molecular and cellular mechanisms that underlie this property of CFZ have not been elucidated, but modulation of inflammation by clofazimine via its apoptosis-inducing effect on macrophages is a possibility [47, 48]. Indeed, clofazimine has been shown to cause mitochondrial membrane destabilization and activation of apoptosis in macrophages, at least *in vitro* [21, 49].

We have previously shown that clofazimine is able to induce apoptosis in a cancer cell-selective way both in primary human tumor cells and *in vivo* in an orthotopic melanoma model by inducing ROS release from mitochondria due to its inhibitory effect on mtKv1.3. Experiments employing sub-lethal concentrations of a mitochondria-targeted pro-oxidant suggested a synergistic action between mtKv1.3-inhibition induced ROS release in mtKv1.3-expressing cancer cells and the elevated basal ROS level typical of cancer cells [50, 51] that drives prevalently the cancer cells to bypass a critical threshold of oxidative stress causing cells death [52, 53]. In addition, clofazimine might also act on the PM Kv1.3, known to be an important regulator of cell proliferation at least in some cell types [14, 24], and reduce tumor progression by decreasing proliferation. However the slight reduction of the Ki67 index indicative of proliferation and, in contrast, a larger reduction of the tumor weight suggests that the apoptosis-inducing effect of the applied drug was prevalent in the case of PDAC. Although in our studies, including the present work with PDAC cells, we obtained evidence using siRNA against Kv1.3 that this drug induced apoptosis prevalently due to its action on the channel, it must be mentioned that clofazimine is a drug with multiple targets and additional mechanisms accounting for its anti-tumoral effect have to be taken into account. For example, clofazimine has recently been identified in a large-scale screening as an inhibitor of Wnt signaling [54] and Wnt/β-catenin signaling plays important roles in PDAC tumor initiation and progression as well [55, 56]. Clofazimine was shown to decrease proliferation of HTB19 triple-negative breast cancer cells whose growth is Wnt pathway-dependent. The

authors also reported that clofazimine exerted a significantly smaller effect on non-cancerous mammary epithelial cells (HMEC) than on HTB19 cells, providing thus a further case of selective action on tumoral versus non-tumoral cells [54]. In addition, clofazimine has been shown to exert an inhibitory action on ABCB1/MDR1/P-glycoproteins (Pgp)[57], although this aspect is particularly relevant when applied together with chemotherapeutics to chemo-resistant cells (e.g. [58]). Finally, clofazimine has been shown via bioinformatic screening to have the potential to inhibit p53–MDM2 interaction leading in turn to stabilization and activation of the tumor suppressor p53 [59, 60]. However, in our experimental setting clofazimine induced cell death independently of the p53 status in several cell lines. This finding is particularly relevant given that most PDACs display p53 mutation.

Independently of the exact mechanism of action, in our experiments clofazimine reproducibly and substantially reduced PDAC tumor weight. This ability of clofazimine is in agreement with previous *in vivo* studies obtained in other type of cancers such as hepatocellular carcinoma [61] and melanoma [28]. In those works the effect of the drug on metastasis was not assessed, but the present report suggests that clofazimine might be taken into consideration for reduction of the primary tumor site only, since it did not reduce liver metastasis. The question arises why clofazimine was less effective in the PDAC model with respect to e.g. the melanoma model. We hypothesize that this result may reflect the well-known difficulty of drugs in general to reach PDAC tissues due to the stromal barrier, i.e. a dense extracellular matrix composed of hyaluronic acid, smooth muscle actin and collagen fibers [62, 63]. At the dosages used for the leprosy treatment, with oral administration, the plasma concentrations of the drug reaches 0.5–1 μM [64]. However, a study on tissue concentrations found clofazimine ranging from 0.2 mg/g to 1.5 mg/g (approximately up to 500 μM) in the different organs of a human patient (a value of 0.4mg/g was obtained for pancreas) [65], which is in agreement with the finding that the drug is generally harmless for normal tissues of the organism. While in the present study a relatively high concentration of clofazimine was found in the pancreas of control animals, it is plausible to suppose that such high concentration could not be reached in PDAC pancreas because of the stromal barrier. Furthermore, clofazimine is a rather insoluble molecule: indeed it has been shown to form crystals in the kidney and to massively accumulate in macrophages during long-term oral dosing, where it forms insoluble, intracellular crystal-like drug inclusions (CLDIs). Recently, it has been reported that *in vitro*, soluble CFZ was cytotoxic because it depolarized mitochondria and induced apoptosis in macrophages [47] while *in vivo*, CLDIs did not induce macrophage apoptosis. Instead, CLDIs altered immune signaling response pathways downstream of Toll-like receptor (TLR) ligation, leading to decreased NF-κB activation and tissue necrosis factor alpha (TNFα) production and to enhanced interleukin-1 receptor antagonist (IL-1RA) production. Thus, the authors concluded that *in vivo*, macrophages detoxify soluble clofazimine by sequestering it in a biocompatible, insoluble form and this may contribute to the anti-inflammatory activity of the drug. Interestingly, we have recently demonstrated that the major pro-inflammatory cytokine tumor necrosis factor TNFα plays a major role in the malignancy of PDAC cells *in vitro* and *in vivo*. *In vitro*, TNFα strongly increased invasiveness of Colo357 cells while *in vivo*, TNFα treatment led to dramatically enhanced tumor growth and metastasis [66]. Furthermore, in severe combined immunodeficient mice with orthotopically growing PDAC tumors, the human-specific anti-TNF antibody infliximab reduced tumor growth and metastasis by about 30% and 50%, respectively. Thus, it is tempting to hypothesize that the observed tumor-reducing effect of clofazimine is due to multiple factors, including apoptosis induction of PDAC cells but also to an indirect effect via modulation of macrophage function.

In conclusion, our work provides evidence that clofazimine might be a useful agent against PDAC, possibly in combination with currently used chemotherapeutics or newly identified PDAC growth inhibitors such as infliximab. This possibility will have to be addressed in future studies. In addition, combination with other drugs targeting ion channels and/or ion transporters might be a strategy worthwhile to pursue. In fact, thanks to excellent recent works, several proteins mediating flux of ions have been identified as possible targets against PDAC. For example, hERG1 potassium channels have been shown to drive PDAC tumor malignancy [67], the neurotransmitter GABA was identified as a promising agent for the prevention of PDAC in individuals at risk due to chronic alcohol consumption [68], the transient receptor potential melastatin-related 7 channel was found to regulate tumor migration [69], the store-operated calcium channels (SOCs) were shown to contribute to PDAC apoptosis resistance [70] while the P2X7 receptor regulates cell survival, migration and invasion [71]. Ion transporters which regulate pH are also relevant in this context [72, 73] - e.g. we have recently shown that the specific sodium-proton exchanger NHE1 inhibitor cariporide reduced both three-dimensional growth and invasion and synergistically sensitized these behaviours to low doses of erlotinib [74]. Thus, in an ideal situation, a combined therapy bypassing basic mechanisms responsible for cancer progression and chemoresistance e.g. [75] might be particularly useful.

Materials & Methods

Cell lines and cell culture

A panel of pancreatic cancer cell lines representing different phases of tumor progression were used. AsPC-1, BxPC3, Capan-1, MIA PaCa-2 and PANC-1 were provided by ATCC. AsPC1 and BxPC3 were cultured in RPMI-1640 (Gibco/Life Technologies, Darmstadt, Germany) supplemented with 10% fetal bovine serum “GOLD” (FBS “GOLD”, PAA Laboratories/GE Healthcare Life Sciences), 1mM GlutaMAX and 1 mM sodium pyruvate (LifeTechnologies, Darmstadt, Germany). MIA PaCa-2 and PANC-1 were cultured in DMEM (4.5 g/l D-glucose) supplemented with 10% FBS “GOLD”, 1mM GlutaMAX and 1 mM sodium pyruvate. Capan-1 cells were grown in IMEM supplemented with 20% FBS “GOLD”, 1mM GlutaMAX and 1 mM sodium pyruvate. Human cell line of metastatic pancreas adenocarcinoma, Colo357, was obtained from Dr. R. Morgan (Denver, CO) [76]. The cells were cultured in a complete growth medium composed of RPMI-1640, 10% FCS (PAN-Biotech, Aidenbach, Germany), 1mM GlutaMAX and 1 mM sodium pyruvate. The HPV16-E6E7 - immortalized human pancreatic duct epithelial cells (HPDE), kindly provided by Dr. Ming-Sound Tsao (Ontario Cancer Institute, Toronto, Ontario, Canada) [77] were used as a model for benign pancreatic ductal epithelium. The complete growth HPDE-medium was mixed with 50% RPMI 1640, supplemented with 10% FCS and 1mM GlutaMAX and 50% keratinocyte medium SFM (Gibco) supplemented with 0.025% bovine pituitary extract, 2.5 μg l^{-1} epidermal growth factor (Gibco). All cells were cultivated and maintained at 37°C in a humid atmosphere with 5% CO_2.

Western blot
Membrane enriched fraction proteins from different Pancreatic cell lines were obtained as previously reported [43]. Briefly, cells were washed in PBS and then resuspended in 300 µL of TES buffer (100 mM TES + 1 M sucrose, 100 mM EGTA, 1X cocktail protease inhibitors) and lysed by an electronic pestle (Kontes, Sigma Aldrich) for 2 min on ice. Unbroken cells were separated by centrifugation at 500 g for 10 min at 4°C. The soluble cytosolic fraction was separated from the membrane-enriched fraction by centrifugation at 19,000 g for 10 min at 4°C. The pelleted membranes were suspended in TES buffer and separated by SDS-PAGE in a 10% polyacrylamide gel containing 6 M Urea. To enhance protein separation, samples were solubilized for 1 h at RT in Sample Buffer (30% Glycerol + 125 mM Tris/HCl pH 6.8 + 9% SDS + 0.1 M DTT+ Bromophenol blue). Protein concentration was determined using the BCA method in a 96 well plate (200 µL total volume for each well) incubating at 37°C in the dark for 30 min. Absorbance at 540 nm was measured by a Packard Spectra Count 96 well plate reader. After separation by electrophoresis, gels were blotted overnight at 4°C onto Polyvinylidene fluoride (PVDF) membranes. After blocking with a 10% solution of defatted milk, the membranes were incubated with the following primary antibodies overnight at 4°C: anti-Kv1.3 (1:200, rabbit polyclonal, Alamone Labs APC-101); anti-GAPDH (1:1000, mouse monoclonal, Millipore MAB374). After washing, the membranes were developed using corresponding anti-mouse or anti-rabbit secondary antibodies (Calbiochem). Antibody signal was detected with enhanced chemiluminescence substrate (SuperSignal West Pico Chemiluminescent Substrate, Thermo Scientific).

MTT assay
To determine cell growth/viability in PDAC cells, we employed the tetrazolium reduction (MTT) assay. To this end, 10,000/well PDAC cells were seeded in standard 96-well plates and allowed to grow in the normally used medium for each line (200ml) for 24 h. The growth medium was then replaced with new fresh phenol red-free medium. Four wells were used for each condition. After 24 h incubation with the indicated drugs 10% CellTiter 96 AQUEOUS One solution (Promega) was added to each well. After 1-3 h of colour development at 37°C, absorbance at 490nm was measured using a Packard Spectra Count 96-well plate reader as in [78].

siRNA
The sequences for the siRNA targeting human Kv1.3 were coupled to Alexa Fluo 555 (Qiagen). 80,000 cells/well (Colo357, BxPC-3, AsPC-1) were seeded into a 12 well plate in 1 mL of the growing medium. After 24 h cells were transiently transfected with 2 µg siRNA/well by Lipofectamine 2000, as suggested by the supplier. After 48 h from transfection, cells were treated for more 24 h with the different drugs as indicated. Cell death, evaluated by the binding of a FITC-labelled Annexin V, as well as siRNA transfection were determined using a DMI4000 Leica fluorescence microscope.

Purification of mitochondria
Mitochondria from Colo357 cells were purified by differential centrifugation as in [28]. Briefly, approximately 80% confluent cells from eight 150-cm2 flasks were washed once with PBS, detached by gentle scraping and spun down in a table centrifuge at room temperature. The pellet was resuspended in sucrose/N-[79]-2-aminoethanesulfonic acid (TES) buffer (300 mM sucrose, 10 mM TES, 0.5 mM EGTA, pH 7.4). After standing for 30 min on ice, cells were lysed in a Dounce homogenizer, and the lysate was centrifuged at 600 x g for 10min at 4°C. The pellet was again processed in the same way to maximize recovery. The combined supernatants were centrifuged once at 600 x g, and the pellet was discarded. The mitochondria-containing supernatant from the last step was centrifuged at 8000 x g for 10 min at 4°C. The pellet was gently homogenized and suspended in a small volume of TES buffer. A further purification was obtained by centrifugation (8500 x g, 10min, 4°C) on a discontinuous Percoll gradient (60, 30 and 18% Percoll in TES buffer). The floating material was discarded, and the fraction at the lower interface was collected and washed three times by centrifugation at 19,000 x g for 5 min. The final pellet was resuspended in TES buffer.

Gene expression analysis
Kv1.3 gene expression (KCNA3) was analyzed in a transcriptome microarray U133 A/B Affimetrix GeneChip set, including microdissected freshly frozen tissues specimen from pancreatic cancer and normal pancreatic tissue, a collection malignant pancreatic and benign stromal cell lines [37].

Quantitative Real time PCR
Total RNA was isolated from culture cells 24 hours after seeding. The total RNA was purified using peqGOLD Total RNA kit and treated with DNase I (PEQLAB Biotechnology GmbH) for removing residual DNA. RNA concentration was measured using Nanodrop spectrophotometer (PEQLAB Biotechnology GmbH) and the RNA-extracted quality was checked on 1% agarose gel. 1µg of RNA was reverse transcribed into cDNA with Maxima First Strand cDNA Synthesis kit (Thermo Fisher Scientific). Real- time PCR was performed in a total volume of 20µl using 50ng of the first-strand cDNA synthesis mixture as template. The assay was done with Double-dye (Taqman technology) probes; the exon-exon spanning primers sequence for *kcnA3* (Kv1.3) was supplied by Primerdesign Ltd (Southampton, United Kingdom). The amplification reaction was run in StepOnePlus Real-time machine according to the follow conditions: Taqman enzyme activation at 95°, 10 min; denaturation at 95°, 15 sec, annealing at 50°C, 30 sec; extension at 72°C, 15 sec (50 cycles). The relative quantification of gene expression was calculated by the help of qBase Browser (Biogazelle NV, Zwijnaarde, Belgium) by applying the comparative C_T methods with a multiple reference gene normalization. *Actb* and *Ywhaz* were set as reference genes to normalize the gene expression; HPDE were used as reference sample to determine *KcnA3* relative expression (fold change) in the panel of pancreatic cancer cell lines.

Laboratory animals
Four weeks old females SCID beige (C.B.-17.Cg-Prkdcscid Lystbb/Crl) mice weighting 14-19 g were obtained from Charles River (Sulzfeld, Germany). They were housed in a sterile environment and allowed to acclimatize for one week. The animal experiment and care were carried out in accordance with the guidelines of institutional authorities

and approved by local authorities (number V312-7224.121-7(123-10/11)).

Orthotopic xenograft of human adenocarcinoma cells and treatment in a palliative setting
The orthotopic injection was performed as previously described [80]. Human metastatic pancreas adenocarcinoma cells Colo357 were detached with Accutase solution (PAA Laboratories GmbH), resuspended at the concentration of 10^6 cells ml^{-1} in 25 µl of Matrigel (BD-Biosciences) and stored on ice. After median laparotomy, 25µl of cell suspension were injected in tail of pancreas. For the palliative therapy, the animals were randomly designated to the treatment procedure: (1) no treatment, (2) Clofazimine treatment. The therapy was initiated ten days after the tumor inoculation and spanned over 20 days. Clofazimine was freshly dissolved at [2.5mM] in DMSO and sterile water for injection (Ampuwa, Fresenius-Kabi, Germany). For the therapy, it was administered in a dose of 5µl/g intraperitoneally. The control group was treated with a solution containing DMSO and physiological saline buffer. All animals were examined daily for general signs of distress and complications; tumor growth was monitored by ultrasound imaging. Thirty days after cell inoculation, the animals were sacrificed and tumor weight was determined after blood removal. Furthermore, several organs have been embedded in paraffin for histological staining and analysis.

Immunohistochemistry
Primary tumor samples from paraffin-embedded tissue were cut in 2µm sections and mounted onto slides. The specimen were tested for pan-cytokeratin (KL1, Beckman Coulter, mouse monoclonal 1:1500), Ki-67(SP6, ThermoScientific, rabbit monoclonal 1:300) and CD31 (SZ31, Dianova, rat monoclonal 1:30). The immunohistochemistry (IHC) was carried out according the following procedure: de-paraffinization with xylene, rehydration in descending concentrations of ethanol, followed by heat-induced epitope retrieval with sodium citrate buffer (pH 6.0). Washing steps were performed at room temperature with tris-buffered saline (TBS); to avoid non-specific binding of the antibody to the tissues, all specimen were incubated with POD (Peroxidase-blocking solution, Dako) for fifteen minutes. The primary diluted antibodies (antibody diluent, DCS LabLine, Hamburg, Germany) were applied and the samples were kept in a humidified chamber for one hour. For the detection, the tissues were incubate with HPR-conjugate anti-rabbit/mouse (Dako) and Mouse-PO anti-rat for thirty minutes; subsequently, the substrate chromogen-DAB (Dako) was added and the staining developed for five minutes. Finally, the samples were counterstained with Hematoxylin (Dako) and dehydrated with ascending concentrations of ethanol and rinsed in xylene.

Determination of clofazimine concentration in tissues
Clofazimine (10 nmol/g) was injected into control mice every two days four times and after treatment the various tissues were collected, 100 mg were weighed, PBS (1 vol) was added, and the mixture containing tissues cut into small pieces was homogenized by use of electric pestle. The samples were vortexed (2 min) and then stabilized and extracted adding 0.43 M acetic acid (0.1 vol) + 100 uM 5-MOP as internal reference (0.1 vol) and acetone (10 vol), vortexed (2 min), sonicated (2 min), and centrifuged (12,000 g, 7 min, 4°C); the supernatant was collected, concentrated, and finally analyzed via HPLC-UV and LC-ESI/MS. according to previously established protocols for other drugs [81]. Blood samples were obtained by the tail bleeding technique: before drug administration, mice were anesthetized with isoflurane and the tip of the tail was cut off; blood samples (80−100 µL each) were then taken from the tail tip after 8 hours of drug administration. Blood was collected in heparinized tubes, kept in ice, and treated as described below within 10 min.

Figure legends

Figure 1. Expression of Kv1.3 potassium channel in different pancreatic ductal adenocarcinoma cell lines. A) Histogram of the distribution of KcnA3 gene expression in a panel of pancreatic cancer cell lines from Affymetrix U133 Gene Chip. Arbitrary intensity units of the probe ID (207237_at) for Kcna3; the intensity values were normalized with dCHIP2006 software (www.dchip.org) **B)** The Relative quantity of the gene expression as determined by quantitative RT-PCR was calculated by using qBase_Biogazelle software, which allows a multiple reference genes-normalization and performs inter-run calibration. *Actb* and *Ywhaz* of non-tumoral HPDE cells were set as reference genes (value 1) to normalize the gene expression. **C)** Whole cell extracts (50 µg/lane) from different PDAC cell lines were loaded on SDS-PAGE. Western blot revealed Kv1.3 bands (multiple bands are presumably due to glycosylation according to manufacturer or to degradation products) at around 65 kDa. These bands correlated with Kv1.3 expression since none of the bands were present in a cell line silenced for Kv1.3 (not shown). The same blot was developed with the antibody against GAPDH (45 kDa) as loading control. **D)** Whole cell extract (Tot ext), enriched membranous fraction (Memb) and Percoll-purified mitochondria (Mito) fractions obtained from Colo357 were loaded at equal protein concentration (40 µg/lane). Enrichment in the mitochondrial marker Bak and decrease of the intensity of SERCA (ER marker) and PMCA (PM marker) indicates progressive purity during mitochondria isolation.

Figure 2 Clofazimine induces apoptosis in PDAC lines with p53 mutation in a Kv1.3-dependent manner. A) MTT assay indicates decrease of cell survival at the higher concentration applied in seven independent PDAC lines, while two non-tumoral lines were largely resistant to clofazimine treatment. Staurosporine was used as positive control. **B)** Dose-response curve of the effect of clofazimine in wt Colo357 cells and in those stably overexpressing anti-apoptotic Bcl-xL. Higher than 10 µM clofazimine was not used due to the known crystal-forming ability of the drug above this concentration. **C)** - **E)** Effect of clofazimine on the indicated PDAC lines following transfection with scrambled RNA or siRNA against Kv1.3. Transfection efficiency is indicated by the red signal, since the siRNAs were labeled with Alexa568. Apoptotic cells are visualized by binding of FITC-labeled Annexin to phosphatidylserine, known to be translocated to the outer leaflet of the PM only during apoptosis. Staurosporine was used as positive control, while PAP-1 without MDRi as negative control.

Figure 3 Reduction of tumor weight by clofazimine treatment in a SCID orthotopic PDAC model. A) SCID beige mice were treated with 5 µg/g body weight using the protocol indicated in the scheme. **B)** Tumor weight was determined for 6 mice each group at the end of the treatment as in (A). Statistical analysis shows significant difference ($p<0.05$) between the two groups. **C)** mean number of liver metastasis ± SD. Difference is not statistically significant ($p>0.05$). **D)** Tissue accumulation of clofazimine determined as described in the materials and methods section. **E)** Percentage of Ki67 positive cells indicate the proliferative capacity of the cells. Samples from all six mice/group were evaluated revealing non-statistically significant difference (p-value=0.1433).

Figure 4 Immunohistochemical analysis of PDAC tissues reveal no gross alterations regarding tumor structure and angiogenesis upon clofazimine treatment. Representative slides show tumoral tissues from control-treated group (left panels) and from the clofazimine-treated groups (right panels) stained with the indicated markers for proliferation (Ki67), epithelial cells (KL-1) angiogenesis marker (CD31) and with hematoxylin/eosin. Experiments are representative of three independent staining for each group of animals. notevole non varrebbe la pena di mostrare solo quella???

References:

1. Peixoto, R.D., et al., *Prognostic factors and sites of metastasis in unresectable locally advanced pancreatic cancer.* Cancer Med, 2015. **4**(8): p. 1171-7.
2. Vincent, A., et al., *Pancreatic cancer.* Lancet, 2011. **378**(9791): p. 607-20.
3. Nagrial, A.M., et al., *Second-line treatment in inoperable pancreatic adenocarcinoma: A systematic review and synthesis of all clinical trials.* Crit Rev Oncol Hematol, 2015. **96**(3): p. 483-97.
4. Herreros-Villanueva, M., et al., *Adjuvant and neoadjuvant treatment in pancreatic cancer.* World J Gastroenterol, 2012. **18**(14): p. 1565-72.
5. Philip, P.A. and M.P. Lutz, *Targeting Epidermal Growth Factor Receptor-Related Signaling Pathways in Pancreatic Cancer.* Pancreas, 2015. **44**(7): p. 1046-52.
6. Safran, H., et al., *Lapatinib and gemcitabine for metastatic pancreatic cancer. A phase II study.* Am J Clin Oncol, 2011. **34**(1): p. 50-2.
7. Ko, A.H., et al., *A phase II randomized study of cetuximab and bevacizumab alone or in combination with gemcitabine as first-line therapy for metastatic pancreatic adenocarcinoma.* Invest New Drugs, 2012. **30**(4): p. 1597-606.
8. Leanza, L., et al., *Pharmacological targeting of ion channels for cancer therapy: in vivo evidences.* Biochim Biophys Acta, 2015.
9. Fraser, S.P., et al., *Regulation of voltage-gated sodium channel expression in cancer: hormones, growth factors and auto-regulation.* Philos Trans R Soc Lond B Biol Sci, 2014. **369**(1638): p. 20130105.
10. Pardo, L.A. and W. Stuhmer, *The roles of K(+) channels in cancer.* Nat Rev Cancer, 2014. **14**(1): p. 39-48.
11. Huang, X. and L.Y. Jan, *Targeting potassium channels in cancer.* J Cell Biol, 2014. **206**(2): p. 151-62.
12. Comes, N., et al., *Involvement of potassium channels in the progression of cancer to a more malignant phenotype.* Biochim Biophys Acta, 2015. **1848**(10 Pt B): p. 2477-92.
13. Comes, N., et al., *The voltage-dependent K(+) channels Kv1.3 and Kv1.5 in human cancer.* Front Physiol, 2013. **4**: p. 283.
14. Cahalan, M.D. and K.G. Chandy, *The functional network of ion channels in T lymphocytes.* Immunol Rev, 2009. **231**(1): p. 59-87.
15. Arcangeli, A., et al., *Targeting ion channels in cancer: a novel frontier in antineoplastic therapy.* Curr Med Chem, 2009. **16**(1): p. 66-93.
16. Artym, V.V. and H.R. Petty, *Molecular proximity of Kv1.3 voltage-gated potassium channels and beta(1)-integrins on the plasma membrane of melanoma cells: effects of cell adherence and channel blockers.* J Gen Physiol, 2002. **120**(1): p. 29-37.
17. Abdul, M. and N. Hoosein, *Reduced Kv1.3 potassium channel expression in human prostate cancer.* J Membr Biol, 2006. **214**(2): p. 99-102.
18. Abdul, M., A. Santo, and N. Hoosein, *Activity of potassium channel-blockers in breast cancer.* Anticancer Res, 2003. **23**(4): p. 3347-51.
19. Alizadeh, A.A., et al., *Distinct types of diffuse large B-cell lymphoma identified by gene expression profiling.* Nature, 2000. **403**(6769): p. 503-11.
20. Leanza, L., et al., *Clofazimine, Psora-4 and PAP-1, inhibitors of the potassium channel Kv1.3, as a new and selective therapeutic strategy in chronic lymphocytic leukemia.* Leukemia, 2013. **27**(8): p. 1782-5.
21. Szabo, I., et al., *Biophysical Characterization and Expression Analysis of Kv1.3 Potassium Channel in Primary Human Leukemic B Cells.* Cell Physiol Biochem, 2015. **37**(3): p. 965-978.

22. Lan, M., et al., *Expression of delayed rectifier potassium channels and their possible roles in proliferation of human gastric cancer cells.* Cancer Biol Ther, 2005. **4**(12): p. 1342-7.
23. Brevet, M., et al., *Deregulation of 2 potassium channels in pancreas adenocarcinomas: implication of KV1.3 gene promoter methylation.* Pancreas, 2009. **38**(6): p. 649-54.
24. Jang, S.H., et al., *Anti-proliferative effect of Kv1.3 blockers in A549 human lung adenocarcinoma in vitro and in vivo.* Eur J Pharmacol, 2011. **651**(1-3): p. 26-32.
25. Szabo, I., et al., *A novel potassium channel in lymphocyte mitochondria.* J Biol Chem, 2005. **280**(13): p. 12790-8.
26. Bednarczyk, P., et al., *Identification of a voltage-gated potassium channel in gerbil hippocampal mitochondria.* Biochem Biophys Res Commun, 2010. **397**(3): p. 614-20.
27. Gulbins, E., et al., *Role of Kv1.3 mitochondrial potassium channel in apoptotic signalling in lymphocytes.* Biochim Biophys Acta, 2010. **1797**(6-7): p. 1251-9.
28. Leanza, L., et al., *Inhibitors of mitochondrial Kv1.3 channels induce Bax/Bak-independent death of cancer cells.* EMBO Mol Med, 2012. **4**(7): p. 577-93.
29. Zhu, J., J. Yan, and W.B. Thornhill, *The Kv1.3 potassium channel is localized to the cis-Golgi and Kv1.6 is localized to the endoplasmic reticulum in rat astrocytes.* Febs j, 2014. **281**(15): p. 3433-45.
30. Jang, S.H., et al., *Nuclear localization and functional characteristics of voltage-gated potassium channel Kv1.3.* J Biol Chem, 2015. **290**(20): p. 12547-57.
31. Szabo, I., et al., *Mitochondrial potassium channel Kv1.3 mediates Bax-induced apoptosis in lymphocytes.* Proc Natl Acad Sci U S A, 2008. **105**(39): p. 14861-6.
32. Szabo, I., et al., *Single-point mutations of a lysine residue change function of Bax and Bcl-xL expressed in Bax- and Bak-less mouse embryonic fibroblasts: novel insights into the molecular mechanisms of Bax-induced apoptosis.* Cell Death Differ, 2011. **18**(3): p. 427-38.
33. Leanza, L., et al., *Targeting a mitochondrial potassium channel to fight cancer.* Cell Calcium, 2014.
34. Ren, Y.R., et al., *Clofazimine inhibits human Kv1.3 potassium channel by perturbing calcium oscillation in T lymphocytes.* PLoS One, 2008. **3**(12): p. e4009.
35. Cholo, M.C., et al., *Clofazimine: current status and future prospects.* J Antimicrob Chemother, 2012. **67**(2): p. 290-8.
36. Pilarsky, C., et al., *Identification and validation of commonly overexpressed genes in solid tumors by comparison of microarray data.* Neoplasia, 2004. **6**(6): p. 744-50.
37. Grutzmann, R., et al., *Gene expression profiling of microdissected pancreatic ductal carcinomas using high-density DNA microarrays.* Neoplasia, 2004. **6**(5): p. 611-22.
38. Liu, N., et al., *Comparative phenotypic studies of duct epithelial cell lines derived from normal human pancreas and pancreatic carcinoma.* Am J Pathol, 1998. **153**(1): p. 263-9.
39. Ungefroren, H., et al., *Human pancreatic adenocarcinomas express Fas and Fas ligand yet are resistant to Fas-mediated apoptosis.* Cancer Res, 1998. **58**(8): p. 1741-9.
40. Sipos, B., et al., *A comprehensive characterization of pancreatic ductal carcinoma cell lines: towards the establishment of an in vitro research platform.* Virchows Arch, 2003. **442**(5): p. 444-52.
41. Monti, P., et al., *A comprehensive in vitro characterization of pancreatic ductal carcinoma cell line biological behavior and its correlation with the structural and genetic profile.* Virchows Arch, 2004. **445**(3): p. 236-47.
42. Hinz, S., et al., *Bcl-XL protects pancreatic adenocarcinoma cells against CD95- and TRAIL-receptor-mediated apoptosis.* Oncogene, 2000. **19**(48): p. 5477-86.
43. Leanza, L., et al., *Correlation between potassium channel expression and sensitivity to drug-induced cell death in tumor cell lines.* Curr Pharm Des, 2014. **20**(2): p. 189-200.
44. Zhou, D.H., et al., *TRAIL-induced expression of uPA and IL-8 strongly enhanced by overexpression of TRAF2 and Bcl-xL in pancreatic ductal adenocarcinoma cells.* Hepatobiliary Pancreat Dis Int, 2013. **12**(1): p. 94-8.
45. Egberts, J.H., et al., *Anti-tumor necrosis factor therapy inhibits pancreatic tumor growth and metastasis.* Cancer Res, 2008. **68**(5): p. 1443-50.
46. Robbins, N., et al., *An Antifungal Combination Matrix Identifies a Rich Pool of Adjuvant Molecules that Enhance Drug Activity against Diverse Fungal Pathogens.* Cell Rep, 2015. **13**(7): p. 1481-92.
47. Yoon, G.S., et al., *Phagocytosed Clofazimine Biocrystals Can Modulate Innate Immune Signaling by Inhibiting TNFalpha and Boosting IL-1RA Secretion.* Mol Pharm, 2015. **12**(7): p. 2517-27.
48. Henson, P.M. and D.L. Bratton, *Antiinflammatory effects of apoptotic cells.* J Clin Invest, 2013. **123**(7): p. 2773-4.
49. Fukutomi, Y., Y. Maeda, and M. Makino, *Apoptosis-inducing activity of clofazimine in macrophages.* Antimicrob Agents Chemother, 2011. **55**(9): p. 4000-5.
50. Gogvadze, V., B. Zhivotovsky, and S. Orrenius, *The Warburg effect and mitochondrial stability in cancer cells.* Mol Aspects Med, 2010. **31**(1): p. 60-74.
51. Gogvadze, V., *Targeting mitochondria in fighting cancer.* Curr Pharm Des, 2011. **17**(36): p. 4034-46.
52. Liu, J. and Z. Wang, *Increased Oxidative Stress as a Selective Anticancer Therapy.* Oxid Med Cell Longev, 2015. **2015**: p. 294303.
53. Gorrini, C., I.S. Harris, and T.W. Mak, *Modulation of oxidative stress as an anticancer strategy.* Nat Rev Drug Discov, 2013. **12**(12): p. 931-47.
54. Koval, A.V., et al., *Anti-leprosy drug clofazimine inhibits growth of triple-negative breast cancer cells via inhibition of canonical Wnt signaling.* Biochem Pharmacol, 2014. **87**(4): p. 571-8.
55. Arensman, M.D., et al., *Calcipotriol Targets LRP6 to Inhibit Wnt Signaling in Pancreatic Cancer.* Mol Cancer Res, 2015. **13**(11): p. 1509-19.
56. Morris, J.P.t., S.C. Wang, and M. Hebrok, *KRAS, Hedgehog, Wnt and the twisted developmental biology of pancreatic ductal adenocarcinoma.* Nat Rev Cancer, 2010. **10**(10): p. 683-95.
57. Van Rensburg, C.E., et al., *The riminophenazine agents clofazimine and B669 reverse acquired multidrug resistance in a human lung cancer cell line.* Cancer Lett, 1994. **85**(1): p. 59-63.
58. Koot, D. and D. Cromarty, *Anticancer efficacy and toxicokinetics of a novel paclitaxel-clofazimine nanoparticulate co-formulation.* Drug Deliv Transl Res, 2015. **5**(3): p. 257-67.

59. Patil, S.P., *FOLICation: engineering approved drugs as potential p53-MDM2 interaction inhibitors for cancer therapy.* Med Hypotheses, 2013. **81**(6): p. 1104-7.
60. Casey, F.P., E. Pihan, and D.C. Shields, *Discovery of small molecule inhibitors of protein-protein interactions using combined ligand and target score normalization.* J Chem Inf Model, 2009. **49**(12): p. 2708-17.
61. Ruff, P., et al., *A phase II study of oral clofazimine in unresectable and metastatic hepatocellular carcinoma.* Ann Oncol, 1998. **9**(2): p. 217-9.
62. Buckway, B., et al., *Overcoming the stromal barrier for targeted delivery of HPMA copolymers to pancreatic tumors.* Int J Pharm, 2013. **456**(1): p. 202-11.
63. Feig, C., et al., *The pancreas cancer microenvironment.* Clin Cancer Res, 2012. **18**(16): p. 4266-76.
64. Nix, D.E., et al., *Pharmacokinetics and relative bioavailability of clofazimine in relation to food, orange juice and antacid.* Tuberculosis (Edinb), 2004. **84**(6): p. 365-73.
65. Jadhav, M.V., et al., *Tissue concentration, systemic distribution and toxicity of clofazimine--an autopsy study.* Indian J Pathol Microbiol, 2004. **47**(2): p. 281-3.
66. Goumas, F.A., et al., *Inhibition of IL-6 signaling significantly reduces primary tumor growth and recurrencies in orthotopic xenograft models of pancreatic cancer.* Int J Cancer, 2015. **137**(5): p. 1035-46.
67. Lastraioli, E., et al., *hERG1 channels drive tumour malignancy and may serve as prognostic factor in pancreatic ductal adenocarcinoma.* Br J Cancer, 2015. **112**(6): p. 1076-87.
68. Al-Wadei, M.H., H.A. Al-Wadei, and H.M. Schuller, *Gamma-amino butyric acid (GABA) prevents the induction of nicotinic receptor-regulated signaling by chronic ethanol in pancreatic cancer cells and normal duct epithelia.* Cancer Prev Res (Phila), 2013. **6**(2): p. 139-48.
69. Rybarczyk, P., et al., *Transient receptor potential melastatin-related 7 channel is overexpressed in human pancreatic ductal adenocarcinomas and regulates human pancreatic cancer cell migration.* Int J Cancer, 2012. **131**(6): p. E851-61.
70. Kondratska, K., et al., *Orai1 and STIM1 mediate SOCE and contribute to apoptotic resistance of pancreatic adenocarcinoma.* Biochim Biophys Acta, 2014. **1843**(10): p. 2263-9.
71. Giannuzzo, A., S.F. Pedersen, and I. Novak, *The P2X7 receptor regulates cell survival, migration and invasion of pancreatic ductal adenocarcinoma cells.* Mol Cancer, 2015. **14**(1): p. 203.
72. Kong, S.C., et al., *Acid-base transport in pancreatic cancer: molecular mechanisms and clinical potential.* Biochem Cell Biol, 2014. **92**(6): p. 449-59.
73. Hoffmann, E.K. and I.H. Lambert, *Ion channels and transporters in the development of drug resistance in cancer cells.* Philos Trans R Soc Lond B Biol Sci, 2014. **369**(1638): p. 20130109.
74. Cardone, R.A., et al., *A novel NHE1-centered signaling cassette drives epidermal growth factor receptor-dependent pancreatic tumor metastasis and is a target for combination therapy.* Neoplasia, 2015. **17**(2): p. 155-66.
75. Zheng, X., et al., *Epithelial-to-mesenchymal transition is dispensable for metastasis but induces chemoresistance in pancreatic cancer.* Nature, 2015. **527**(7579): p. 525-30.
76. Morgan, R.T., et al., *Human cell line (COLO 357) of metastatic pancreatic adenocarcinoma.* Int J Cancer, 1980. **25**(5): p. 591-8.
77. Ouyang, H., et al., *Immortal human pancreatic duct epithelial cell lines with near normal genotype and phenotype.* Am J Pathol, 2000. **157**(5): p. 1623-31.
78. Manago, A., et al., *Early effects of the antineoplastic agent salinomycin on mitochondrial function.* Cell Death Dis, 2015. **6**: p. e1930.
79. Leanza, L., et al., *Induction of apoptosis in macrophages via Kv1.3 and Kv1.5 potassium channels.* Curr Med Chem, 2012. **19**(31): p. 5394-404.
80. Tepel, J., et al., *Significant growth inhibition of orthotopic pancreatic ductal adenocarcinoma by CpG oligonucleotides in immunodeficient mice.* Int J Colorectal Dis, 2006. **21**(4): p. 365-72.
81. Azzolini, M., et al., *Synthesis and Evaluation as Prodrugs of Hydrophilic Carbamate Ester Analogues of Resveratrol.* Mol Pharm, 2015. **12**(9): p. 3441-54.

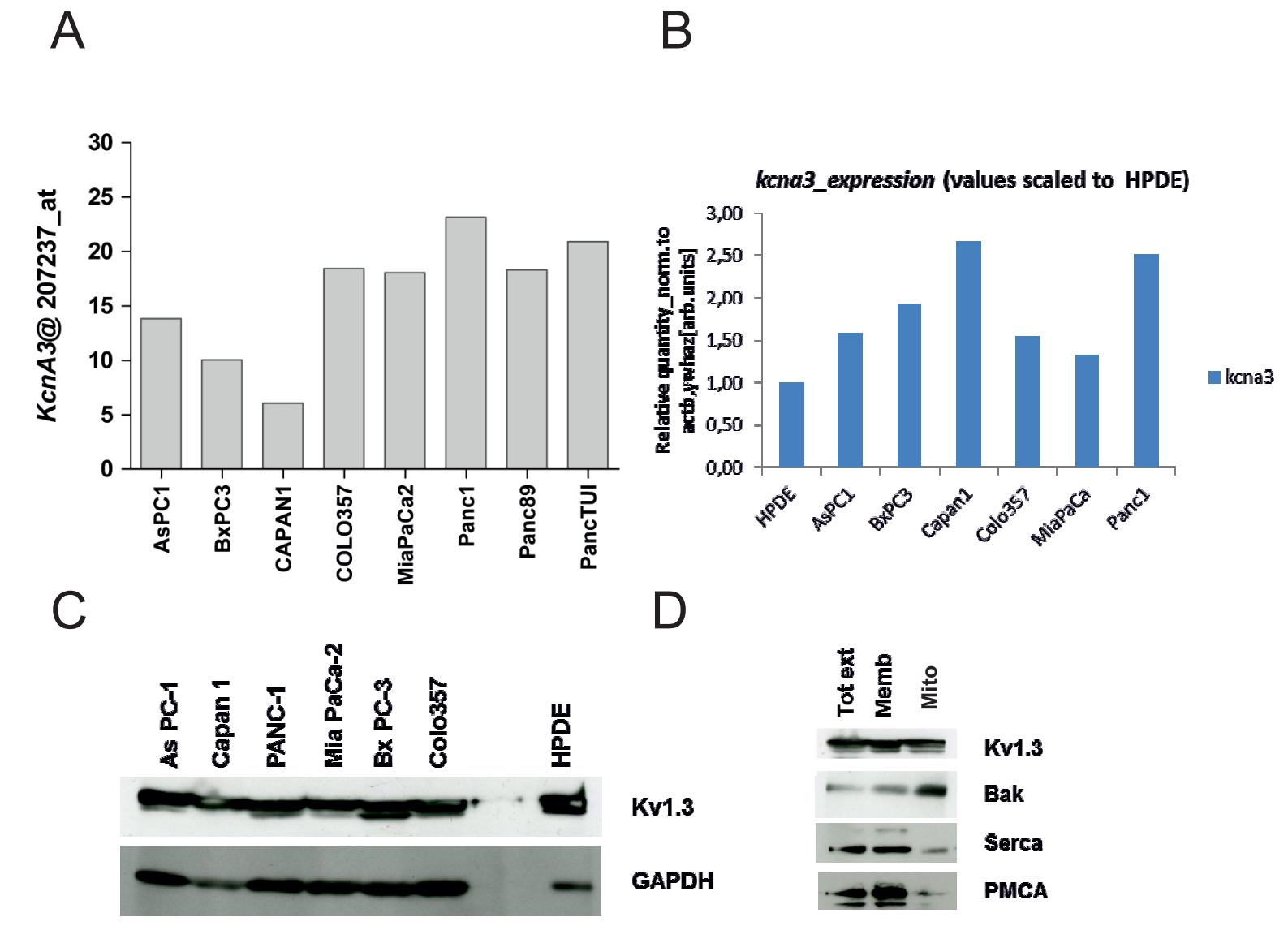
A
B
KcnA3@ 207237_at
30
25
20
15
10
5
0
AsPC1
BxPC3
CAPAN1
COLO357
MiaPaCa2
Panc1
Panc89
PancTUI
kcna3_expression (values scaled to HPDE)
Relative quantity_norm.to actb,ywhaz[arb.units]
3,00
2,50
2,00
1,50
1,00
0,50
0,00
HPDE
AsPC1
BxPC3
Capan1
Colo357
MiaPaCa
Panc1
kcna3

C
D
As PC-1
Capan 1
PANC-1
Mia PaCa-2
Bx PC-3
Colo357
HPDE
Kv1.3
GAPDH
Tot ext
Memb
Mito
Kv1.3
Bak
Serca
PMCA

Figure 1.

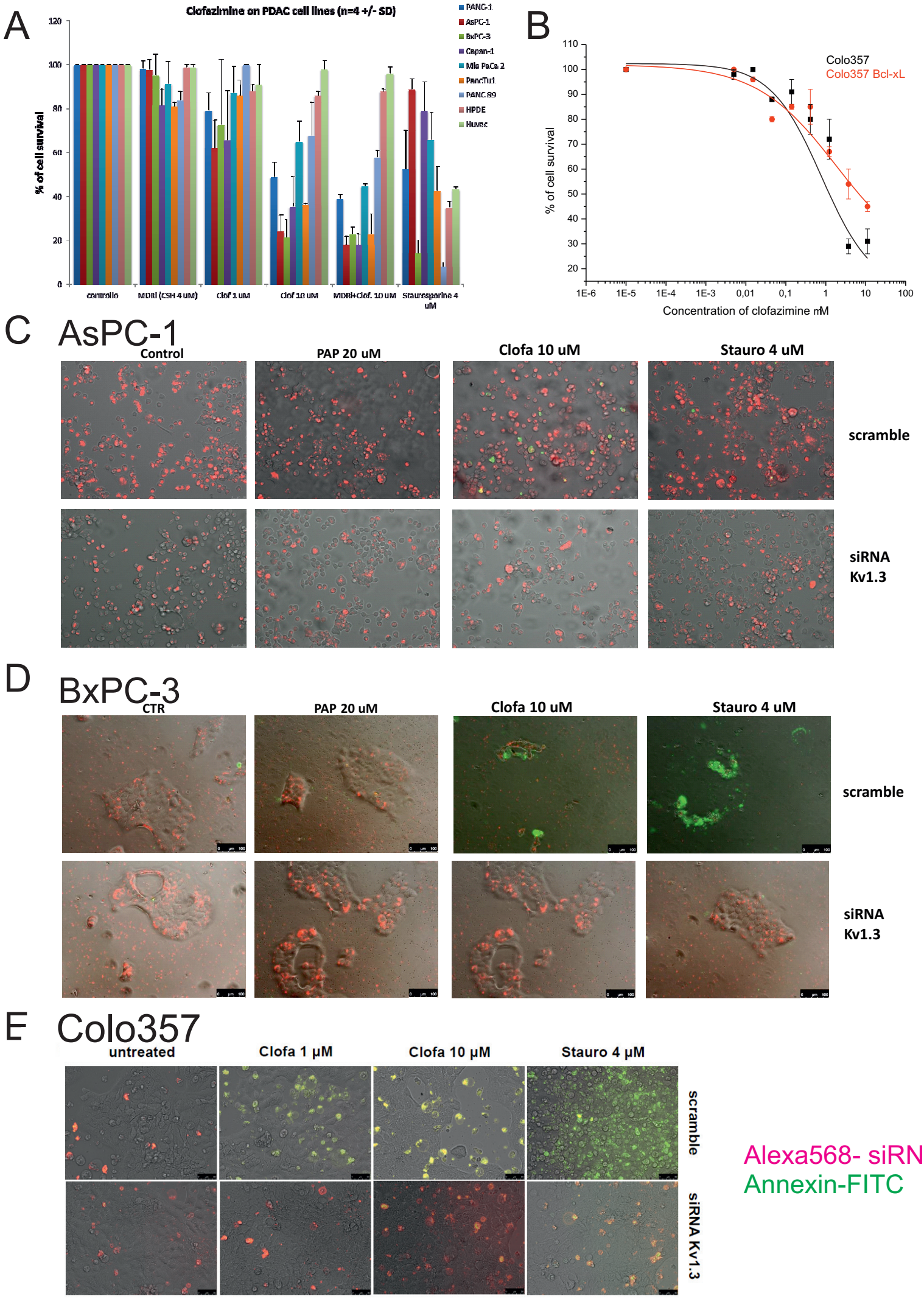
A
Clofazimine on PDAC cell lines (n=4 +/- SD)
% of cell survival
PANC-1
AsPC-1
BxPC-3
Capan-1
Mia PaCa 2
PancTu1
PANC 89
HPDE
Huvec
controllo
MDRI (CSH 4 uM)
Clof 1 uM
Clof 10 uM
MDRI+Clof. 10 uM
Staurosporine 4 uM
B
Colo357
Colo357 Bcl-xL
% of cell survival
Concentration of clofazimine mM
C
AsPC-1
Control
PAP 20 uM
Clofa 10 uM
Stauro 4 uM
scramble
siRNA Kv1.3
D
BxPC-3
CTR
PAP 20 uM
Clofa 10 uM
Stauro 4 uM
scramble
siRNA Kv1.3
E
Colo357
untreated
Clofa 1 µM
Clofa 10 µM
Stauro 4 µM
scramble
siRNA Kv1.3
Alexa568- siRNA
Annexin-FITC

Figure 2.

A

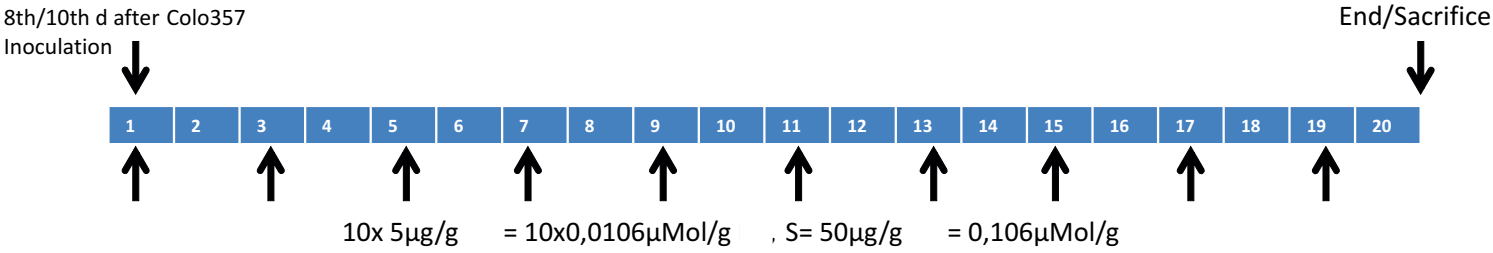

B

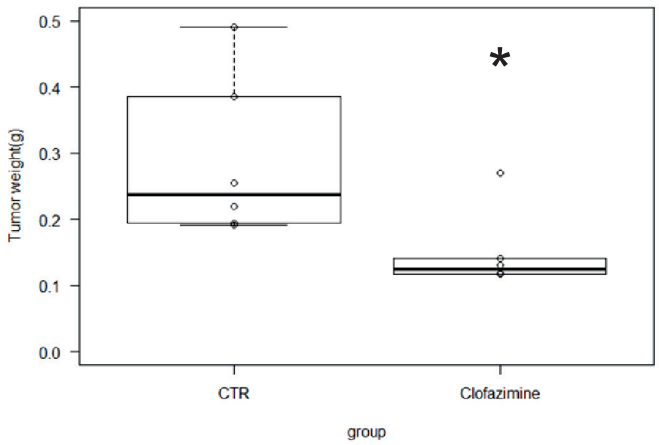

C

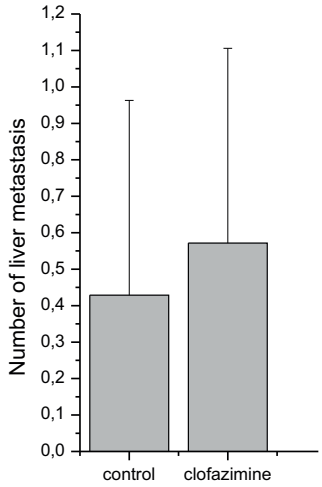

D

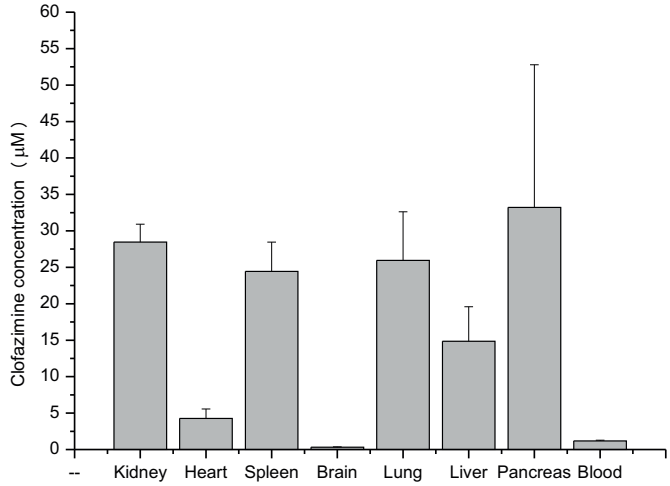

E

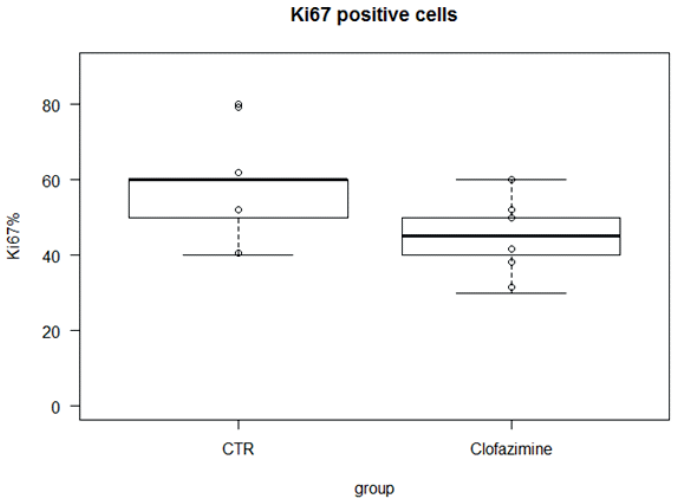

Figure 3.

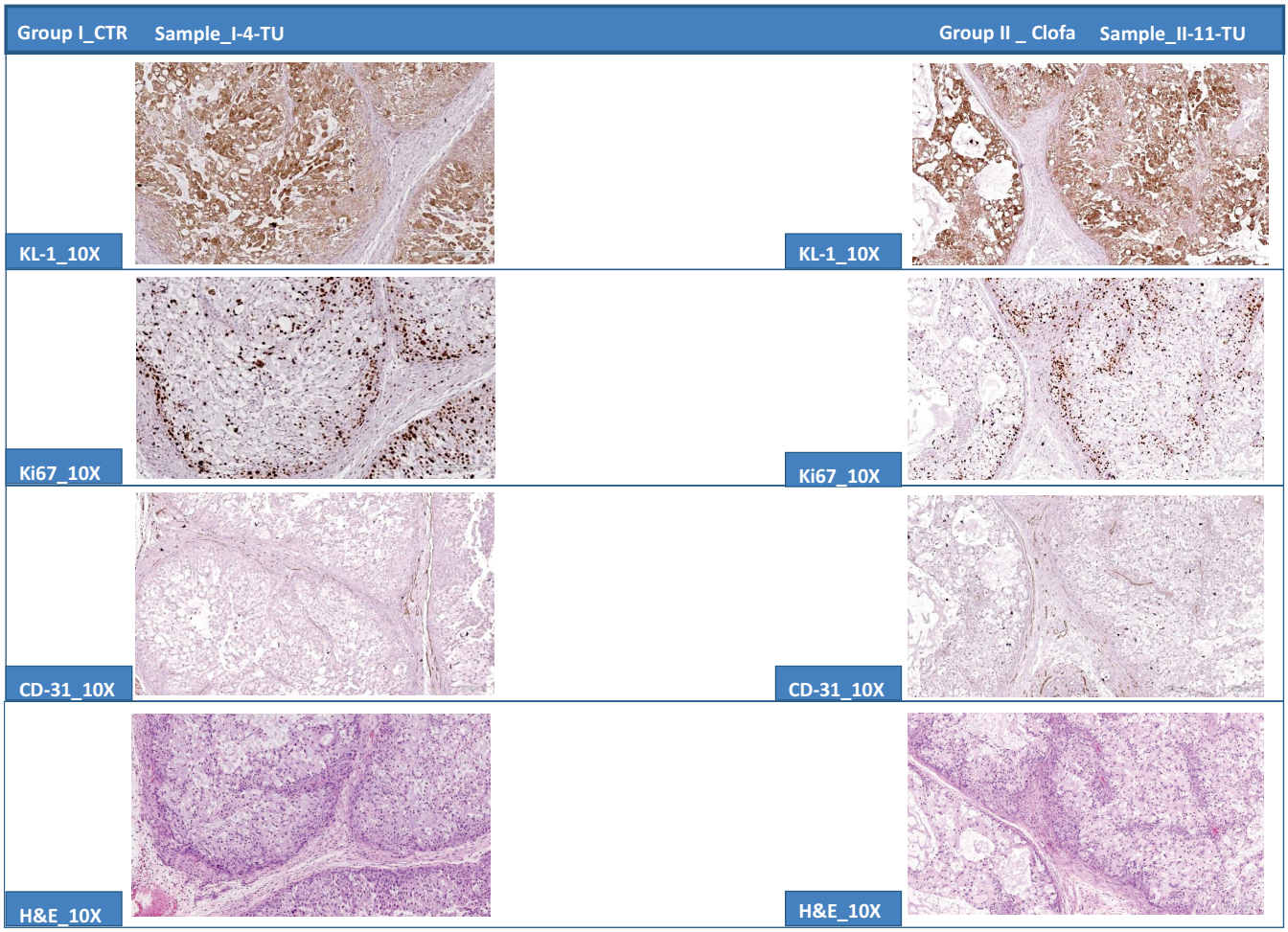
Group I_CTR
Sample_I-4-TU
Group II _ Clofa
Sample_II-11-TU
KL-1_10X
KL-1_10X
Ki67_10X
Ki67_10X
CD-31_10X
CD-31_10X
H&E_10X
H&E_10X

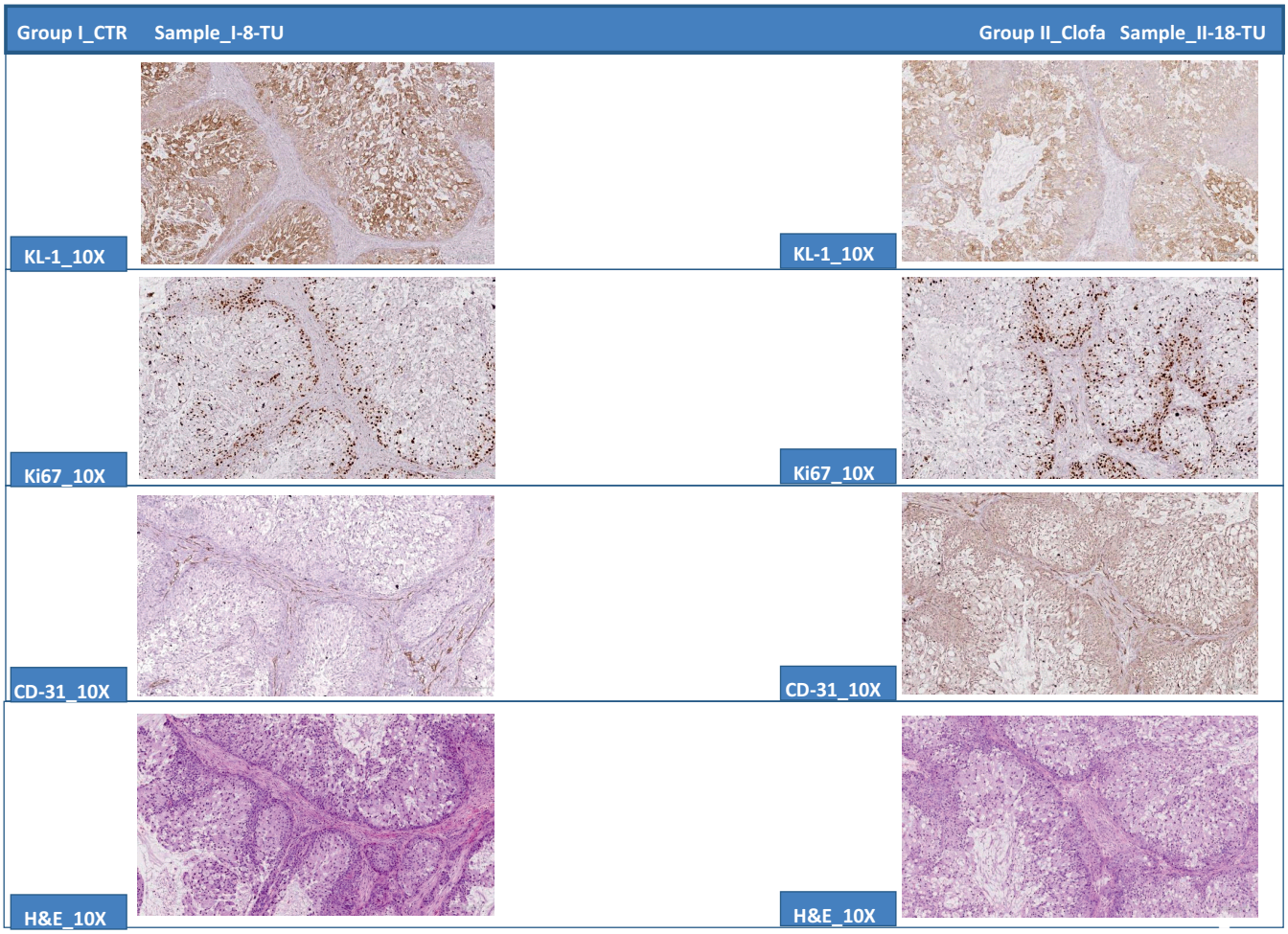
Group I_CTR
Sample_I-8-TU
Group II_Clofa
Sample_II-18-TU
KL-1_10X
KL-1_10X
Ki67_10X
Ki67_10X
CD-31_10X
CD-31_10X
H&E_10X
H&E_10X

Figure 4.